

THERAPEUTIC PROTEIN PRODUCTION AND ITS SEPARATION BY  
ZEOLITIC IMIDAZOLATE FRAMEWORK – 8 ADSORBENT

A THESIS SUBMITTED TO  
THE GRADUATE SCHOOL OF NATURAL AND APPLIED SCIENCES  
OF  
MIDDLE EAST TECHNICAL UNIVERSITY

BY

YİĞİT AKGÜN

IN PARTIAL FULFILLMENT OF THE REQUIREMENTS  
FOR  
THE DEGREE OF MASTER OF SCIENCE  
IN  
CHEMICAL ENGINEERING

JANUARY 2018



Approval of the thesis:

**THERAPEUTIC PROTEIN PRODUCTION AND ITS SEPARATION BY  
ZEOLITIC IMIDAZOLATE FRAMEWORK – 8 ADSORBENT**

submitted by **YİĞİT AKGÜN** in partial fulfillment of the requirements for the degree of **Master of Science in Chemical Engineering, Middle East Technical University** by,

Prof. Dr. Gülbin Dural Ünver  
Dean, **Graduate School of Natural and Applied Sciences** \_\_\_\_\_

Prof. Dr. Halil Kalıpçılar  
Head of Department, **Chemical Engineering** \_\_\_\_\_

Prof. Dr. Pınar Çalık  
Supervisor, **Chemical Engineering Dept., METU** \_\_\_\_\_

Prof. Dr. Halil Kalıpçılar  
Co-supervisor, **Chemical Engineering Dept., METU** \_\_\_\_\_

**Examining Committee Members:**

Prof. Dr. Halil Kalıpçılar  
Chemical Engineering Dept., METU \_\_\_\_\_

Prof. Dr. Pınar Çalık  
Chemical Engineering Dept., METU \_\_\_\_\_

Assoc. Prof. Dr. Zeynep Çulfaz Emecen  
Chemical Engineering Dept., METU \_\_\_\_\_

Assist. Prof. Dr. Salih Özçubukçu  
Chemistry Dept., METU \_\_\_\_\_

Assist. Prof. Dr. Eda Çelik Akdur  
Chemical Engineering Dept., Hacettepe University \_\_\_\_\_

**Date:** \_\_\_\_\_ 29.01.2018

**I hereby declare that all information in this document has been obtained and presented in accordance with academic rules and ethical conduct. I also declare that, as required by these rules and conduct, I have fully cited and referenced all material and results that are not original to this work.**

Name, Last name: Yiğit AKGÜN

Signature:

## ABSTRACT

### THERAPEUTIC PROTEIN PRODUCTION AND ITS SEPARATION BY ZEOLITIC IMIDAZOLATE FRAMEWORK – 8 ADSORBENT

Akgün, Yiğit

M.Sc., Department of Chemical Engineering

Supervisor: Prof. Dr. Pınar Çalık

Co-Supervisor: Prof. Dr. Halil Kalıpçılar

January 2018, 194 pages

The objectives of this thesis are investigation of the effects of oxygen transfer conditions on the recombinant human growth hormone (rhGH) production by *Pichia pastoris* under glyceraldehyde-3-phosphate dehydrogenase promoter ( $P_{GAP}$ ); and, separation and purification of the synthesized and secreted rhGH by zeolitic imidazolate framework-8 adsorbent (ZIF-8). The effects of the oxygen transfer were studied at three conditions at constant dissolved oxygen concentrations ( $C_{DO}$ ) of  $C_{DO} = 1\%$ ,  $5\%$ , and  $15\%$ . The highest cell and rhGH concentrations were obtained at  $C_{DO} = 15\%$  condition, respectively as,  $177.3 \text{ g/L}$  and  $40.5 \text{ mg/L}$ . The cell concentration at  $C_{DO} = 15\%$  condition was 1.7- and 3.4-fold higher; whereas,  $C_{rhGH}$  was 2.04- and 2.64-fold higher, than those obtained at  $C_{DO} = 5\%$  and  $C_{DO} = 1\%$  conditions, respectively. For the separation and purification of rhGH, ZIF-8 was synthesized. Besides rhGH, recombinant granulocyte colony-stimulating factor (rGCSF) was used as the second model

protein to be separated for comparison. Although ZIF-8 has high adsorption performance, was not selective in the separation of the r-proteins. Thus, metal and ligand addition-based modifications, such as nickel impregnation, bimetallic Ni/ZIF-8 syntheses, addition of a terminating ligand (1-methylimidazole), and surface ligand exchange reaction with histamine dihydrochloride, were applied separately. Amongst, the last two were used to create a specific molecular-separation-arm (spacer) in ZIF-8. ZIF-8 was synthesized by the solvothermal/hydrothermal method with a yield of  $37\pm 0.5\%$ . ZIF-8 synthesis yield decreased to  $9\pm 0.5\%$  by the addition of 1-methylimidazole (1-MI) into the reaction mixture. NaOH was used to increase the syntheses yields of ZIF-8 and 1-MI-ZIF-8; thus, ZIF-8 and 1-MI-ZIF-8 were synthesized, respectively, with  $99\pm 0.5\%$  and  $41\pm 0.5\%$  yields. The highest protein adsorption attained at pH = 5.0, and the elution at T = 35 °C were determined as the optimum separation conditions. Although the eluents glycerol and L-histidine showed better performance than those of NaCl, NTA, Na<sub>2</sub>HPO<sub>4</sub>, and MgCl<sub>2</sub>.6H<sub>2</sub>O; they also did not provide a selective separation and purification. Thus, ZIF-8 needs to be modified with further modifications to create a selective resin for the IMAC process.

**Keywords:** Oxygen transfer condition, recombinant human growth hormone, granulocyte colony stimulating factor, *Pichia pastoris*, immobilized metal affinity chromatography, separation and purification, ZIF-8

## ÖZ

### TERAPÖTİK PROTEİN ÜRETİMİ VE ZEOLİTİK İMİDAZOL KAFES - 8 YAPILI ADSORBAN İLE AYIRILMASI

Akgün, Yiğit

Yüksek Lisans, Kimya Mühendisliği Bölümü

Tez Yöneticisi : Prof. Dr. Pınar Çalık

Ortak Tez Yöneticisi : Prof. Dr. Halil Kalıpçılar

Ocak 2018, 194 Sayfa

*Pichia pastoris*'te glyceraldehit-3-fosfat promotörü ( $P_{GAP}$ ) altında rekombinant rekombinant insan büyüme hormonu (rhGH) üretimine düşük- ile orta- oksijen aktarım koşulları arasında oksijen aktarımının etkilerinin, ve üretilen rhGH'nin ZIF-8 temelli adsorban ile ayrılması, tezin amaçlarıdır. Oksijen aktarım koşullarının etkisi çözünen sabit-oksijen derişimlerinde ( $C_{DO}$ ):  $C_{DO} = \%1, \%5, ve \%15$ 'te, üç oksijen aktarım koşulunda araştırılmıştır. En yüksek hücre ve rhGH derişimleri,  $C_{DO} = \%15$  oksijen aktarım koşulu için, sırasıyla,  $C_x = 177.3 \text{ g L}^{-1}$   $C_{rhGH} = 40.5 \text{ mg L}^{-1}$  olarak elde edilmiştir. Hücre konstantrasyonu,  $C_{DO} = 5\%$  ve  $C_{DO} = 1\%$  oksijen aktarım koşullarından 1.7- ve 3.4-kat daha yüksekken, rhGH derişimleri  $C_{DO} = 5\%$  ve  $C_{DO} = 1\%$  koşullarından 2.04- ve 2.64-kat daha yüksek bulunmuştur. Araştırmanın ikinci programında, rhGH'nin ayrılıp saflaştırılması için ZIF-8 sentezlenmiştir. Rekombinant protein rGCSF, rhGH ile karşılaştırma

yapmak için ikinci model protein olarak kullanılmıştır. ZIF-8, yüksek protein tutma performansı göstermesine rağmen seçimli ayırma yapamadığı için ZIF-8 modifiye edilmiştir. ZIF-8'e yapılan modifikasyonlar: a) nikel emdirilmesi, b) sonlandırıcı ligand (1-metilimidazol) eklenmesi, ZIF-8 c) iki-metalli (Ni/ZIF-8) sentez, ve d) histamin dihidroklorid ile ZIF-8'in yüzeyinde ligand değişimi, oluşturulmasıdır. Sonlandırıcı ligand (1-metilimidazol) eklenmiş ZIF-8 ve ZIF-8'in yüzeyinde ligand değişimi yapılmış modifikasyonlar, ZIF-8'e moleküler-ayırma-uzantısı (kol) eklemek amacıyla yapılmıştır. ZIF-8'in üretim verimi solvotermal/hidrotermal sentez yöntemiyle % 37±0.5 olarak bulunmuştur. ZIF-8 sentezinde 1-metilimidazol (1-MI) eklenmesi verimi % 9±0.5'a düşürmüştür. Verimi yükseltmek için NaOH kullanılmış; ZIF-8 ve 1-MI-ZIF-8 için, sırasıyla, % 99±0.5 ve % 41±0.5 verim elde edilmiştir. pH = 5.0'te en yüksek protein adsorpsiyonu, T = 35°C'ta elüsyon, en uygun ayırma koşulları olarak bulunmuştur. Elüsyon işlemi için farklı hareketli fazlar denenmiş; içlerinden gliserol ve L-histidin; NaCl, NTA, Na<sub>2</sub>HPO<sub>4</sub> ve MgCl<sub>2</sub>.6H<sub>2</sub>O göre daha iyi performans göstermiştir, ancak seçici bir ayırma ve saflaştırma sağlanamamıştır. Metal şelat afinite kromatografisi için ZIF-8'in türevleri geliştirilmelidir.

**Anahtar Kelimeler:** Çözünmüş oksijen etkisi, rekombinant insan büyüme hormonu, granülosit-koloni uyarıcı faktör, *Pichia pastoris*, metal şelat afinite kromatografisi, ayırma ve saflaştırma, ZIF-8



*To my beloved family*

## ACKNOWLEDGMENTS

First and foremost, I wish to express my sincere gratitude to my supervisor Prof. Dr. Pınar Çalık for her generous advice, continuous support, guidance, and help, in all the possible way, throughout this study.

I would like to thank my co-supervisor, Prof. Dr. Halil Kalıpçılar for his thoughtful advice and critics. I am also thankful to Assist. Prof. Dr. Salih Özçubukçu for his invaluable advice.

There have been many people who have walked alongside me during the last three years. My sincere thanks go to all my labmates in my research group Industrial Biotechnology and Metabolic Engineering Laboratory Özge Kalender, Damla Hücetoğulları, Duygu Yalçinkaya Yavuz, Sibel Öztürk, Aslan Massahi, Özge Ata Akyol, Bebeta Hoxha, Burcu Gündüz Ergün, Onur Ersoy, Erdem Boy, Abdullah Keskin, İrem Demir, Omar Wehbe Masri, and Ekin Artan I would like to especially thank Özge Kalender and Başak Kütükcü for their friendship and for helping me collect unforgettable memories.

I would like to express my thanks to Özçubukçu laboratory group members, especially Tuğçe Yılmaz, for their help. It was a great pleasure to work with them.

Middle East Technical University Research Fund Project and the Scientific and Technical Research Council of Turkey (Project no: 114R091) are greatly acknowledged.

I would also like to thank all academic, administrative and technical staff of Department of Chemical Engineering, METU, for their support through my education.

Above all, I am thankful with all my heart to my family, Coşkun Akgün, Hatice Akgün, Yalın Akgün and Eylem Akgün who always believed in me and courage me to follow my dreams. Thanks to their love and support, I am here today.

## TABLE OF CONTENTS

|  |      |
|--|------|
| ABSTRACT .....   | v    |
| ÖZ.....  | vii  |
| ACKNOWLEDGMENTS.....   | x    |
| TABLE OF CONTENTS .....  | xii  |
| LIST OF TABLES .....   | xvii |
| LIST OF FIGURES.....   | xix  |
| NOMENCLATURE.....  | xxiv |
| CHAPTERS   |      |
| 1. INTRODUCTION.....   | 1    |
| 2. LITERATURE SURVEY .....   | 5    |
| 2.1. Production, separation and purification of human growth hormone ..... | 5    |
| 2.2. Second model protein; granulocyte colony-stimulating factor.....      | 6    |
| 2.3. Microorganism; <i>Pichia pastoris</i> .....                           | 7    |
| 2.4. Promoter; Glyceraldehyde-3-phosphate dehydrogenase (GAP) .....        | 8    |
| 2.5. Production strategies for recombinant human growth hormone (rhGH)11   |      |
| 2.5.1. The effect of oxygen transfer on production of rhGH.....            | 12   |
| 2.5.2. Temperature.....  | 17   |
| 2.5.3. pH .....  | 17   |
| 2.6. Computational equations and parameters for bioprocess .....           | 18   |
| 2.6.1. Mass conservation equation for the cell growth.....                 | 19   |

|            |  |    |
|------------|--|----|
| 2.6.2.     | Mass conservation equation for the substrate.....                            | 20 |
| 2.6.3.     | Mass conservation equation for the product.....                              | 20 |
| 2.6.4.     | Mathematical model for fed-batch bioreactor with continuous feed stream..... | 21 |
| 2.6.5.     | Overall yield coefficients .....   | 22 |
| 2.7.       | Protein separation and purification methods .....                            | 23 |
| 2.7.1.     | Chromatographic Separation Methods.....                                      | 26 |
| 2.7.1.1.   | Affinity chromatography .....  | 26 |
| 2.7.1.1.1. | Protein location in microorganism .....                                      | 26 |
| 2.7.1.1.2. | Affinity chromatography separation steps .....                               | 27 |
| 2.8.       | Surface adsorption phenomena.....  | 29 |
| 2.9.       | Parameters controlling adsorption .....                                      | 31 |
| 2.9.1.     | Effects of protein properties on adsorption .....                            | 32 |
| 2.9.2.     | Effects of surface properties of adsorbent on adsorption.....                | 33 |
| 2.9.3.     | Vroman effect.....   | 33 |
| 2.9.4.     | Effect of IMAC components .....  | 34 |
| 2.9.4.1.   | Influences of affinity tags on protein separation.....                       | 35 |
| 2.9.4.2.   | Influences of spacer arms on protein separation.....                         | 37 |
| 2.9.4.3.   | Influences of chelate on protein separation.....                             | 38 |
| 2.9.4.4.   | Influences of support for protein separation .....                           | 41 |
| 2.10.      | IMAC .....   | 42 |
| 2.11.      | Metal-organic frameworks (MOFs).....   | 46 |
| 2.11.1.    | Zeolitic imidazolate frameworks (ZIFs).....                                  | 46 |
| 2.11.1.1.  | Zeolitic imidazolate framework-8 (ZIF-8).....                                | 49 |

|  |    |
|--|----|
| 2.11.1.2. ZIF-8 synthesis.....   | 53 |
| 3. MATERIALS AND METHODS .....   | 61 |
| 3.1. Chemicals .....   | 61 |
| 3.2. Microorganism and Plasmid .....   | 61 |
| 3.3. Growth Media.....   | 61 |
| 3.3.1. Solid Media .....   | 61 |
| 3.3.2. Pre-cultivation Media .....   | 62 |
| 3.3.3. Carbon Source Starvation Media (Synchronization).....                   | 62 |
| 3.3.4. Production media.....   | 63 |
| 3.4. Recombinant human growth hormone production .....                         | 64 |
| 3.4.1. Organic acid analysis.....  | 67 |
| 3.4.2. Glucose analysis .....  | 68 |
| 3.4.3. Ethanol analysis.....   | 69 |
| 3.4.4. Homogenization and preparation of rGCSF medium.....                     | 69 |
| 3.5. ZIF-8 Synthesis.....  | 70 |
| 3.5.1. Procedure of ZIF-8 synthesis .....                                      | 70 |
| 3.5.2. Procedure of bimetallic ZIF-8 synthesis (Ni/ZIF-8) .....                | 71 |
| 3.5.3. Nickel impregnation on ZIF-8 (Ni-ZIF-8) .....                           | 72 |
| 3.5.4. Synthesis of ZIF-8 with modulating ligand 1-methylimidazole ....        | 73 |
| 3.5.5. Surface modifications .....   | 73 |
| 3.6. Characterization of ZIF-8 .....   | 75 |
| 3.7. Incubation, separation and purification procedure for rhGH and rGCSF..... | 75 |
| 3.8. Bradford Analyse.....   | 77 |

|  |     |
|--|-----|
| 3.9. Sodium dodecyl sulfate polyacrylamide gel electrophoresis (SDS-PAGE).....                             | 77  |
| 3.9.1. Gel Preparation.....  | 77  |
| 3.9.2. Silver Staining.....  | 78  |
| 3.9.3. Coomassie Blue Staining.....  | 78  |
| 4. RESULTS AND DISCUSSION.....   | 81  |
| 4.1. Parameters of bioreactor conditions.....  | 81  |
| 4.2. Effect of oxygen transfer conditions on cell generation and rhGH production.....                      | 82  |
| 4.3. Effect oxygen transfer condition on the yield coefficients and the specific rates.....                | 88  |
| 4.4. Effect of oxygen transfer condition on organic acid concentrations.....                               | 90  |
| 4.5. Characterization of ZIF-8 synthesis.....  | 92  |
| 4.5.1. Effect of Hmim/ $Zn^{2+}$ ratio on ZIF-8.....   | 95  |
| 4.5.2. Effect of NaOH on ZIF-8 production.....   | 97  |
| 4.5.3. Effect of modifications on ZIF-8.....   | 99  |
| 4.5.3.1. Effect of Hmim/1-MI ratio.....  | 102 |
| 4.6. Separation and Purification Experiments.....  | 105 |
| 4.6.1. Separation and purification performance of ZIF-8 on rhGH.....                                       | 105 |
| 4.6.2. Modification of ZIF-8 with nickel metal.....  | 107 |
| 4.6.3. Comparison of Ni/ZIF-8 and Ni impregnated ZIF-8 resins for separation and purification of rhGH..... | 108 |
| 4.6.4. Comparison of ZIF-8 and bimetallic Ni/ZIF-8 particles.....  | 109 |
| 4.6.5. Temperature effects on elution step.....  | 110 |

|   |     |
|---|-----|
| 4.6.6. Determination of the suitable washing and elution composition for ZIF-8 adsorbent.....                           | 110 |
| 4.6.7. Time optimization for rGCSF .....  | 114 |
| 4.6.8. Comparison of Ni-ZIF-8 and Ni impregnated ZIF-8 resin for separation and purification of recombinant rGCSF ..... | 115 |
| 4.6.9. Adsorption equilibrium of rGCSF on ZIF-8 .....   | 116 |
| 4.6.10. Investigation of pH effect on adsorption and elution steps .....  | 119 |
| 4.6.11. Performance of different solvents for elution step .....  | 121 |
| 4.6.12. Surface ligand exchange of ZIF-8 for further modifications .....  | 128 |
| 5. CONCLUSIONS .....  | 131 |
| REFERENCES .....  | 137 |
| APPENDICES  |     |
| A. SDS-PAGE BUFFER SOLUTIONS AND REQUIRED COMPONENT INFORMATION.....  | 165 |
| B. CALIBRATION CURVES AND NUMERICAL DATA OF ORGANIC ACIDS FOR HPLC .....  | 167 |
| C. NUMERICAL DATA OF ZIF-8 FOR ADSORPTION EQUILIBRIUM ....  | 173 |
| D. ZINC-BASED YIELD CALCULATION OF ZIF-8 .....  | 175 |
| E. SELECTIVITY AND YIELD CALCULATIONS OF VARIOUS ELUENTS WITH RESULTS .....   | 177 |
| F. SEM MICROGRAPHS OF ZIF-8 SYNTHESSES AND MODIFICATIONS  | 183 |
| G. SEPARATION AND PURIFICATION CALCULATIONS .....   | 191 |
| H. FTIR COMPARISON OF ZIF-8 AND NH <sub>2</sub> -ZIF-8 .....  | 193 |



## LIST OF TABLES

### TABLES

|   |    |
|---|----|
| <b>Table 2. 1</b> Studies for rhGH production with <i>P. pastoris</i> .....                                     | 12 |
| <b>Table 2. 2</b> Studies related to oxygen transfer condition and other parameters on <i>P. pastoris</i> ..... | 13 |
| <b>Table 2. 3</b> Yield demonstration with unit and definition for a system .....                               | 23 |
| <b>Table 2. 4</b> Categorization of proteins by structural characteristics .....                                | 23 |
| <b>Table 2. 5</b> Categorization of proteins by function .....  | 24 |
| <b>Table 2. 6</b> Timeline of protein purification .....  | 25 |
| <b>Table 2. 7</b> Common separation methods by physicochemical basis .....                                      | 25 |
| <b>Table 2. 8</b> Chromatographic techniques with their separation basis .....                                  | 26 |
| <b>Table 2. 9</b> Linear forms of Langmuir isotherm .....   | 30 |
| <b>Table 2. 10</b> Linear form of Freundlich isotherm .....   | 31 |
| <b>Table 2. 11</b> The most used affinity tags and properties.....  | 36 |
| <b>Table 2. 12</b> Structure of ligands.....  | 39 |
| <b>Table 2. 13</b> Studies of ZIF-8 synthesis .....   | 55 |
| <b>Table 3. 1</b> Solid YPD medium composition.....   | 62 |
| <b>Table 3. 2</b> BMGY composition .....  | 62 |
| <b>Table 3. 3</b> Composition of carbon source starvation medium.....   | 63 |
| <b>Table 3. 4</b> Composition of production medium, BSM .....   | 63 |
| <b>Table 3. 5</b> Composition of trace salt solution, PTM1 .....  | 64 |
| <b>Table 3. 6</b> Organic acid measurement parameters for HPLC system.....                                      | 68 |
| <b>Table 4. 1</b> System parameters for each experiment.....  | 82 |
| <b>Table 4. 2</b> Total substrate fed into the bioreactor related to the highest rhGH concentration .....       | 88 |

|  |     |
|--|-----|
| <b>Table 4. 3</b> Variations in the fermentation characteristics with the cultivation time and oxygen transfer conditions in fed-batch bioreactor experiments..... | 89  |
| <b>Table 4. 4</b> Overall yield coefficient of oxygen transfer conditions .....  | 90  |
| <b>Table 4. 5</b> Experimental components of synthesis .....   | 95  |
| <b>Table 4. 6</b> Experimental design of Hmim/1-MI experiments.....  | 102 |
| <b>Table 4. 7</b> Composition of Nickel impregnation on ZIF-8 and synthesis of bimetallic ZIF-8.....   | 107 |
| <b>Table B. 1</b> HPLC values of organic acids.....  | 171 |
| <b>Table C. 1</b> Values of $q_e$ and $C_e$ data for each amount of ZIF-8.....   | 173 |
| <b>Table C. 2</b> $\log(q_e)$ versus $\log(C_e)$ .....   | 173 |
| <b>Table E. 1</b> SDS-PAGE results of different eluents.....   | 178 |
| <b>Table E. 2</b> SDS-PAGE results of promising eluents .....  | 180 |
| <b>Table E. 3</b> SDS-PAGE results of glycerol and L-histidine with respect to elution time and concentration .....  | 181 |
| <b>Table E. 4</b> SDS-PAGE results for increasing elution number.....  | 182 |

## LIST OF FIGURES

### FIGURES

|  |    |
|--|----|
| <b>Figure 2. 1</b> Amino acid sequence of hGH .....  | 6  |
| <b>Figure 2. 2</b> Amino acid sequence of GCSF .....   | 7  |
| <b>Figure 2. 3</b> <i>P. pastoris</i> central carbon metabolism.....   | 10 |
| <b>Figure 2. 4 (a)</b> Transfer steps of oxygen from gas bubble into the cell <b>(b)</b> Dissolved oxygen concentration profile through the oxygen transfer process .....  | 13 |
| <b>Figure 2. 5</b> Affinity chromatography matrix .....  | 27 |
| <b>Figure 2. 6</b> Illustration of selective binding.....  | 28 |
| <b>Figure 2. 7</b> Elution of target protein .....   | 28 |
| <b>Figure 2. 8</b> Re-equilibration of matrix.....   | 29 |
| <b>Figure 2. 9</b> The illustration presents three different processes with respect to change at the surface during adsorption. (A) First adsorbed protein 1 (blue) desorbs in order to protein 2 (red) adsorption. (B) While protein 2 is attaching strongly, protein 1 desorbs. (C) Protein 2 anchors on the pre-adsorbed protein 1 and causes position change and desorption of protein 1 ..... | 34 |
| <b>Figure 2. 10</b> IMAC process steps from preparation of resin to adsorption of protein .....  | 35 |
| <b>Figure 2. 11</b> Mainly used purification systems with fundamental cloning .....  | 37 |
| <b>Figure 2. 12</b> Chromatogram indicates spacer arm effect between matrix and biomolecule during ligation and elution phases .....   | 38 |
| <b>Figure 2. 13</b> Comparison of adsorption and specificity .....   | 40 |
| <b>Figure 2. 14</b> Possible binding problems of ligand a) multi-site attachment, b) improper orientation, and c) steric hindrance.....  | 41 |
| <b>Figure 2. 15</b> Bond angle between metal ions and silicones.....   | 46 |

|  |    |
|--|----|
| <b>Figure 2. 16</b> Imidazole ligands .....  | 47 |
| <b>Figure 2. 17</b> Crystal structures given and categorized based on topologies (three-letter symbol). ZnN <sub>4</sub> (blue) is the largest cage for all ZIFs, CoN <sub>4</sub> in pink polyhedral. Space in the cage is shown in yellow. H atoms are excluded to provide clear presentation (C, black; N, green; O, red; Cl, pink) ..... | 48 |
| <b>Figure 2. 18</b> Possible functionality of external surface structure of ZIF-8. Color of atoms are presented in; Zn (green), C (grey), N (blue), H (white), O (red) .....   | 49 |
| <b>Figure 2. 19</b> Structural evolution of crystal morphology with time a) cube, b) cube with truncated edges, c) and d) rhombic dodecahedron with truncated corners (truncated rhombic dodecahedron) and e) rhombic dodecahedron .....   | 50 |
| <b>Figure 2. 20</b> Formation of ZIF-8 crystals with time .....  | 50 |
| <b>Figure 2. 21</b> Conventional synthesis and synthesis with modulating ligand.....   | 52 |
| <b>Figure 2. 22</b> Composition and temperature effect on nucleation step of ZIF-8 synthesis (2-methylimidazole is shown in 2-MeIM abbreviation).....  | 53 |
| <b>Figure 2. 23</b> Synthesis methods; a) solvothermal, b) microwave, c) sonochemical, d) mechanochemical, e) dry-gel conversion, f) microfluidic, and g) electrochemical method .....   | 54 |
| <b>Figure 3. 1</b> BIOSTAT Cplus bioreactor overview .....   | 67 |
| <b>Figure 3. 2</b> Procedure of ZIF-8 synthesis .....  | 71 |
| <b>Figure 3. 3</b> Procedure of Ni/ZIF-8 synthesis .....   | 72 |
| <b>Figure 3. 4</b> Nickel impregnation on ZIF-8 (Ni-ZIF-8) .....   | 73 |
| <b>Figure 3. 5</b> Mechanism of the surface ligand exchange on 1-MI-ZIF-8 .....  | 74 |
| <b>Figure 3. 6</b> Mechanism of the surface ligand exchange on ZIF-8.....  | 74 |
| <b>Figure 3. 7</b> Separation and purification process .....   | 76 |
| <b>Figure 4. 1</b> Variations in cell generation with the oxygen transfer condition and cultivation time.....  | 83 |
| <b>Figure 4. 2</b> Variations in rhGH concentration with the oxygen transfer condition and cultivation time .....  | 84 |

|   |     |
|---|-----|
| <b>Figure 4. 3</b> Variations in glucose concentration with the oxygen transfer condition and cultivation time .....                                  | 86  |
| <b>Figure 4. 4</b> Variations in ethanol concentration with the cultivation time at $C_{DO} = 15\%$ .....   | 87  |
| <b>Figure 4. 5</b> Variations of organic acid concentrations with cultivation time for $C_{DO} = 15\%$ .....  | 92  |
| <b>Figure 4. 6</b> XRD pattern of ZIF-8 .....   | 93  |
| <b>Figure 4. 7</b> FTIR spectrum of ZIF-8.....  | 94  |
| <b>Figure 4. 8</b> TGA thermogram of ZIF-8 .....  | 94  |
| <b>Figure 4. 9</b> XRD patterns of various Hmim/ $Zn^{2+}$ experiments of ZIF-8.....  | 97  |
| <b>Figure 4. 10</b> Yield percentage of various Hmim/ $Zn^{2+}$ experiments of ZIF-8 .....  | 97  |
| <b>Figure 4. 11</b> XRD patterns of NaOH added experiments into the ZIF-8 synthesis .....   | 98  |
| <b>Figure 4. 12</b> Effect of NaOH addition on yield percentage of ZIF-8 .....  | 99  |
| <b>Figure 4. 13</b> XRD pattern of 1-MI-ZIF-8 modification .....  | 100 |
| <b>Figure 4. 14</b> Yield percentage change of 1-MI-ZIF-8 with time.....  | 101 |
| <b>Figure 4. 15</b> Variation of crystal structure of 1-MI-ZIF-8 with time .....  | 101 |
| <b>Figure 4. 16</b> XRD patterns of various Hmim/1-MI experiments of 1-MI-ZIF-8 .....   | 102 |
| <b>Figure 4. 17</b> Yield percentage of various Hmim/1-MI experiments of 1-MI-ZIF-8 .....   | 103 |
| <b>Figure 4. 18</b> XRD patterns of NaOH added experiments into the 1-MI-ZIF-8 synthesis .....  | 104 |
| <b>Figure 4. 19</b> Yield of 1-MI-ZIF-8 syntheses with addition time of NaOH .....  | 104 |
| <b>Figure 4. 20</b> rhGH separation by ZIF-8 (Std, standard; PM, production medium; RM, remained medium after adsorption; W, wash; E, elution). ..... | 106 |
| <b>Figure 4. 21</b> Comparison of Ni-ZIF-8 and Ni/ZIF-8 crystals.....   | 108 |
| <b>Figure 4. 22</b> Comparison of ZIF-8 and Ni/ZIF-8 .....  | 109 |

|  |     |
|--|-----|
| <b>Figure 4. 23</b> Effect of temperature on elution (M, marker; hGH standard with lysozyme and hGH standard; PM, production medium x10 diluted; RM, supernatant after adsorption; W, wash; E1, elution at 25 °C; E2, elution at 35 °C; elution at 40 °C)..... | 110 |
| <b>Figure 4. 24</b> Eluent concentration effect on elution step.....   | 111 |
| <b>Figure 4. 25</b> Color change of Ni/ZIF-8 structure at elution step.....  | 111 |
| <b>Figure 4. 26</b> SEM micrographs of Ni/ZIF-8 crystals during separation and purification process (A, Ni/ZIF-8 crystals; B, after washing; C, after elution) .   | 113 |
| <b>Figure 4. 27</b> Time optimization of rGCSF for SDS-PAGE (A, 0-1 minute; B, 1-2 minutes; C, 2-3 minutes) .....  | 114 |
| <b>Figure 4. 28</b> Comparison of ZIF-8 and Ni/ZIF-8 separation and purification performance.....  | 115 |
| <b>Figure 4. 29</b> Adsorption performance of various amount of ZIF-8.....   | 116 |
| <b>Figure 4. 30</b> Adsorbed rGCSF amount versus ZIF-8 amount .....  | 117 |
| <b>Figure 4. 31</b> $q_e$ (mg/g) versus $C_e$ (mg/L) .....   | 117 |
| <b>Figure 4. 32</b> Langmuir isotherm of rGCSF .....   | 118 |
| <b>Figure 4. 33</b> Freundlich isotherm of rGCSF.....  | 118 |
| <b>Figure 4. 34</b> 2D Electrophoresis of rGCSF .....  | 119 |
| <b>Figure 4. 35</b> Effect of production medium pH on adsorption .....   | 121 |
| <b>Figure 4. 36</b> Elution step with different eluents .....  | 122 |
| <b>Figure 4. 37</b> Elution steps of promising eluents.....  | 123 |
| <b>Figure 4. 38</b> Variation in elution performance with elution time.....  | 126 |
| <b>Figure 4. 39</b> Variation in eluate with increasing elution number .....   | 127 |
| <b>Figure 4. 40</b> TGA thermogram of NH <sub>2</sub> -ZIF-8 (SLER) .....  | 129 |
| <b>Figure 4. 41</b> XRD pattern of SLER.....   | 130 |
| <b>Figure A. 1</b> Band profile of the PageRuler Prestained Protein Ladder for SDS-PAGE.....   | 165 |
| <b>Figure B. 1</b> Bovine serum albumin (BSA) standard curve.....  | 167 |
| <b>Figure B. 2</b> Calibration curve of oxalic acid .....  | 167 |

|  |     |
|--|-----|
| <b>Figure B. 3</b> Calibration curve of formic acid .....  | 168 |
| <b>Figure B. 4</b> Calibration curve of pyruvic acid.....  | 168 |
| <b>Figure B. 5</b> Calibration curve of malic acid .....   | 169 |
| <b>Figure B. 6</b> Calibration curve of acetic acid.....   | 169 |
| <b>Figure B. 7</b> Calibration curve of fumaric acid.....  | 170 |
| <b>Figure B. 8</b> Calibration curve of succinic acid .....  | 170 |
| <b>Figure B. 9</b> Calibration curve of citric acid.....   | 171 |
| <b>Figure F. 1</b> SEM micrographs of ZIF-8 .....  | 184 |
| <b>Figure F. 2</b> SEM micrographs of Ni/ZIF-8-4.....  | 185 |
| <b>Figure F. 3</b> XRD pattern of Ni/ZIF-8-5 .....   | 186 |
| <b>Figure F. 4</b> SEM micrographs for 30 min. later NaOH added ZIF-8.....                                     | 187 |
| <b>Figure F. 5</b> SEM micrographs for 1-MI-ZIF-8 .....  | 188 |
| <b>Figure F. 6</b> SEM micrographs for 1-hour later NaOH added 1-MI-ZIF-8.....                                 | 189 |
| <b>Figure F. 7</b> SEM micrographs for NH <sub>2</sub> -ZIF-8 .....  | 183 |
| <b>Figure H. 1</b> FTIR comparison of ZIF-8 and NH <sub>2</sub> -ZIF-8.....                                    | 193 |
| <b>Figure H. 2</b> FTIR comparison between 600-900 cm <sup>-1</sup> of ZIF-8 and NH <sub>2</sub> -ZIF-8.....   | 193 |
| <b>Figure H. 3</b> FTIR comparison between 1000-1300 cm <sup>-1</sup> of ZIF-8 and NH <sub>2</sub> -ZIF-8..... | 194 |
| <b>Figure H. 4</b> FTIR comparison between 3200-3500 cm <sup>-1</sup> of ZIF-8 and NH <sub>2</sub> -ZIF-8..... | 194 |

## NOMENCLATURE

|       |   |   |
|-------|---|---|
| C     | Concentration   | $\text{g L}^{-1}$   |
| $C_e$ | The equilibrium concentration of adsorbate                              | $\text{mg L}^{-1}$  |
| DO    | Dissolved oxygen  | %   |
| $K_f$ | Freundlich isotherm constant  | $\text{mg g}^{-1}$  |
| $K_L$ | Langmuir isotherm constant  | $\text{L mg}^{-1}$  |
| n     | Adsorption intensity  |   |
| N     | Agitation rate  | $\text{min}^{-1}$   |
| q     | The specific rate for formation or consumption                          | $\text{g g}^{-1} \text{h}^{-1}$ or $\text{mg g}^{-1} \text{h}^{-1}$ |
| $q_e$ | The amount of protein adsorbed per gram of the adsorbent at equilibrium | $\text{mg g}^{-1}$  |
| Q     | Volumetric flow rate  | $\text{L h}^{-1}$   |
| $Q_o$ | Maximum monolayer coverage capacity                                     | $\text{mg g}^{-1}$  |
| t     | Time  | h   |
| V     | Fermentation Volume   | L   |
| Y     | Yield   | $\text{g g}^{-1}$ or $\text{mg g}^{-1}$                             |



### **Greek Letters**

|         |                                  |                 |
|---------|----------------------------------|-----------------|
| $\mu$   | The specific growth rate         | $\text{h}^{-1}$ |
| $\mu_0$ | The pre-determined specific rate | $\text{h}^{-1}$ |

### **Subscripts**

|    |                   |
|----|-------------------|
| 0  | Initial condition |
| i  | Eluent type       |
| c  | Constant          |
| P  | Product           |
| S  | Substrate         |
| TP | Total protein     |
| X  | Cell              |

### **Abbreviations**

|      |                                  |
|------|----------------------------------|
| AOX1 | Alcohol oxidase 1                |
| BET  | Brunauer–Emmett–Teller           |
| BMGY | Buffered glycerol complex medium |
| BR   | Bioreactor                       |

|          |   |
|----------|---|
| BSM      | Basal Salt Medium   |
| DF       | Dilution factor   |
| E        | Elution Step  |
| EDX      | Energy-dispersive X-ray spectroscopy                      |
| FTIR     | Fourier Transform Infrared Spectroscopy                   |
| GAP      | Glyceraldehyde-3 phosphate dehydrogenase                  |
| GCSF     | Granulocyte colony-stimulating factor                     |
| hGH      | Human growth hormone                                      |
| Hmim     | 2-Methylimidazole   |
| HPLC     | High-performance liquid chromatography                    |
| IDA      | Iminodiacetic acid  |
| IMAC     | Immobilized metal affinity chromatography                 |
| M        | Marker  |
| MOF      | Metal-organic framework                                   |
| PM       | Production medium   |
| RM       | Remained in the medium                                    |
| SDS-PAGE | Sodium dodecyl sulfate polyacrylamide gel electrophoresis |

|      |                                  |
|------|----------------------------------|
| SEM  | Scanning electron microscopy     |
| SLER | Surface ligand exchange reaction |
| SOD  | Sodalite structure               |
| Std. | Standard                         |
| TCA  | Tricarboxylic acid               |
| TGA  | Thermogravimetric analysis       |
| W    | Washing step                     |
| XRD  | X-ray diffraction                |
| YPD  | Yeast extract-peptone-dextrose   |
| ZIF  | Zeolitic imidazolate framework   |



## CHAPTER 1

### INTRODUCTION

As a result of the population increase in the world, biology-based technologies have begun to play a vital role in humanity in order to meet the diverse needs in different areas such as health, environment, and food. Biotechnology is an important research area, especially to overcome faced problems such as tackling disease, environmental pollution, harnessing natural sources, and feeding next generations. Biotechnology has been defined “The application of science and technology to living organisms, as well as parts, products and models thereof, to alter living or non-living materials for the production of knowledge, goods, and services.” by Organization for Economic Co-operation and Development (OECD) since 2005. From ancient times to nowadays, usage of biotechnology has been attractive on various products and industries such as wine making, beer brewing, penicillin, DNA technology, cloning, and others.

Production of proteins from various mammalian or microorganisms (bacteria or yeasts) cells has been increasing with the development of genetic applications. There are 400 recombinant proteins (r-proteins) that have been approved by the United States Food and Drug Administration (FDA) and by European Medicines Agency (EMA) for pharmaceutical use and this number is expected to reach over 200 in the next few years. 45% of the r-proteins are produced in mammalian cell hosts, 39% in bacterium *Escherichia coli* and 15% in the yeast *Saccharomyces cerevisiae* (Sanchez-Garcia *et al.*, 2016).

Production of especially human hormones by microorganisms provides high yield, simple and cheaper production conditions for the industry so r-protein technology becomes more popular.

The yeast *Pichia pastoris* (*Komagataella phaffii*), one of the famous host microorganisms, has been in the spotlight in the last decade due to its hybrid characteristics of both bacteria and yeasts, with its well-established expression systems for extracellular- and intracellular- r-protein production with high expression levels. The reasons for this popularity are ease of genetic modification, similarity to *S. cerevisiae* which is the model yeast, and the ability of post-translational modifications.

Glyceraldehyde-3-phosphate dehydrogenase (GAPDH) is a key enzyme in the glycolysis and gluconeogenesis pathways. Its promoter,  $P_{GAP}$ , is a constitutive promoter providing high expression with genetic modifications and optimization of fermentation strategies. Especially, selection of carbon source is one of the most important optimization parameters affecting the strength of the expression system. For the production of r-proteins, high expression levels can be reached on glucose medium. Also, glycerol can be used as another carbon source to provide production relatively (Çalık et al., 2015).

Inducible systems are limited for practical applications because of the transcriptional heterogeneity at the single cell level, inducer toxicity, and inducer-mediated pleiotropic effects (Khlebnikov, Artem, et al., 2000, Qin, Xiulin, et al., 2011). Methanol is not required particularly for  $P_{GAP}$  induction when the compared with  $P_{AOX}$  which is well-known methanol inducible promoter. So,  $P_{GAP}$ , a constitutive promoter, provides a benefit for industrial fermentation to eliminate hazardous effects and transportation and storage problems of methanol.

Furthermore, one of the most important steps of recombinant protein production is downstream processes. Up to now, different separation and purification methods have been used with various resins such as anion exchange (AEX), and cation exchange (CEX) resins for ion exchange purification; Avidin and Streptavidin for biotin affinity purification; agarose, Co/Ni-NTA, Co/Ni-IDA, magnetic beads for fusion protein purification; bio-beads and bio-gels for size exclusion method. For this purpose, a lot of chromatographic methods have been used regarding the properties of proteins. For example, hydrophobic interaction chromatography is based on surface properties of protein; size exclusion chromatography is based on size and shape of protein; ion exchange chromatography is based on the charge of protein, and affinity chromatography is based on the biospecific interaction of the protein with resin. When the methods are compared to each other, purification yield and capacity were considered, affinity chromatography performance is more effective than the others.

In affinity chromatography, the interaction between the tagged recombinant protein and resin which is designed based on the properties of the target protein is the prominent step. For proteins, various tags can be used namely His-tag, FLAG, Strep-tag II, S-tag, and NusA (Arnau, Lauritzen, Petersen, & Pedersen, 2006). His-tag is one of the most popular tags due to its low molecular weight, usually, 6 residues of histidine is used. 6xHis-tag provides ease for genetic modification of the recombinant protein. His-tag is particularly used for immobilized metal affinity chromatography. The main mechanism of immobilized metal affinity chromatography (IMAC) occurs between the interaction of His-tag and metal ions which are bounded by a ligand. The interaction provides high selectivity and yield also chromatography steps are easy, cheap and time-consuming. Various ligands have been used like nitrilotriacetic acid (NTA), iminodiacetic acid (IDA), carboxymethyl aspartate (CM-Asp), Tris-carboxy-methylated ethylenediamine (TED), etc. According to the used ligand, performance of the chromatographic

method can change because of the ability of coordination binding. Also used metal ions show different performance with ligands. Especially, divalent metal ions,  $\text{Cu}^{2+}$ ,  $\text{Ni}^{2+}$ ,  $\text{Zn}^{2+}$ ,  $\text{Co}^{2+}$ , are used.

For the immobilization of these ions, different supports are utilized. As an adsorbent, silica has been used, but, to increase separation capacity, to overcome non-specific adsorption and to provide simplicity at the separation steps, the usage of different materials is increasing. Composite and magnetic materials as well as nanomaterials are examples to materials worked in the literature.

Zeolitic imidazolate framework, ZIF, is a subunit of the metal-organic framework. ZIF-8, a member of ZIF class, can be described structurally as bridging of 2-methylimidazole which is an imidazole-based linker between Zn metal centers. ZIF-8 presents high porosity, surface area, crystallinity, thermal, and chemical stability. When all of these properties are considered, ZIF-8 provides availability in different areas like gas separation and storage, drug delivery, and sensing.

In this study, the aim is the investigation of the effect of oxygen transfer condition in recombinant hGH, rhGH, production under GAP promoter by *P. pastoris*, as well as separation and purification of rhGH with modified ZIF-8 by IMAC. For the comparison of the performance of separation process, in addition to rhGH, rGCSF was also considered as a second model protein. Initially, effects of oxygen on cell growth and rhGH production were investigated at three different oxygen transfer conditions. Then, ZIF-8 was synthesized by the developed modified method to overcome non-specific interaction r-protein and ZIF-8. Thereafter, separation and purification conditions were optimized for the ZIF-8-based resins.



## CHAPTER 2

### LITERATURE SURVEY

#### **2.1. Production, separation and purification of human growth hormone**

Studies on growth hormone (GH) were started at the beginning of the 1900s. In 1944, the first bovine GH isolation had been succeeded by Li and Evans (C. H. Li & Evans, 1944). In 1956, isolation of GH was achieved from the pituitary gland (C. H. Li & Papkoff, 1956). After some studies, human growth hormone has become one of the most popular pharmaceutical proteins. Application areas in clinic treatment increased with scientific research. Growth hormone therapy was used to treat several illness such as growth hormone deficiency (1985), chronic renal insufficiency (1993), Turner syndrome (1997), Prader–Willi syndrome (2000), small for gestational age (2001), idiopathic short stature (2003), short stature homeobox-containing gene deficiency (2006), Noonan syndrome (2007) (Ayyar, 2011).

Growth hormone also called somatotropin, is a globular protein produced by the anterior pituitary and consists of 191 amino acid sequences and 21,700 Da (~ 22 kDa) molecular weight (Cogan & John A. Phillips, 2014; TANNER, 1972). Also, the pituitary gland has four GH variants each with 45 kDa, 24 kDa, 24 kDa, and 20 kDa molecular weight (Chawla, Parks, & Rudman, 1983). The smallest one is approximately 20 kDa and constitutes approximately 10% of GH (Norman & Litwack, 1997). In addition, hGH includes two disulfide bridges between four cysteine residues locating at 53th, 165th, 182th, 189th positions in amino acid sequence (Brems, Brown, & Becker, 1990). A consequence of disulfide bonds, protein structure gains a tertiary structure.

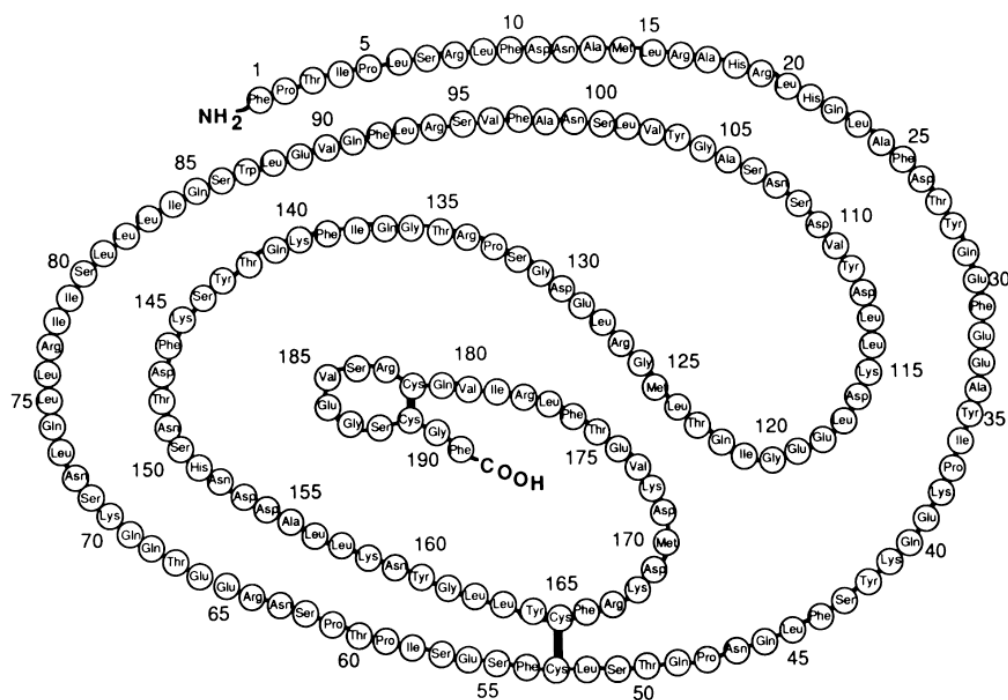


**Figure 2. 1** Amino acid sequence of hGH (Cogan & John A. Phillips, 2014)

## 2.2. Second model protein; granulocyte colony-stimulating factor

Granulocyte colony-stimulating factor, GCSF, was used as a second model protein to compare the separation and purification efficiency with that of hGH. GCSF is one of the secreted glycoproteins coordinating the proliferation, survival, differentiation, and function of hematopoietic cells (S. Xu, Höglund, Håkansson, & Venge, 2000). In 1979, the purification, cloning, evaluation in clinical trials and licensing to use on patients who suffer from hematopoietic disorders and deadly illness had been completed and used (Garland, Quesenberry, & Hilton, 1997). There are two forms of GCSF, glycosylated (Nagata et al., 1986) and non-glycosylated (Souza et al., 1986). The highly purified protein, as called Filgrastim, consists of 175 amino acid sequences which have ~18.8 kDa molecular weight (Walsh, 2007).

GCSF is mostly produced by hematopoietic cells which are activated by tumor necrosis factor  $\alpha$  (TNF- $\alpha$ ), interferon  $\gamma$  (IFN- $\gamma$ ) and lipopolysaccharide (LPS)

(Sallerfors & Olofsson, 1992). Also, GCSF can be produced by bone marrow stromal cells, endothelial cells, fibroblasts, and astrocytes with same activation (S. Xu et al., 2000). GCSF also includes two disulfide bonds that consist of between two cysteine pairs located in 37<sup>th</sup>-43<sup>th</sup> and 55<sup>th</sup> – 75<sup>th</sup> positions. In this study, a modified GCSF was used.

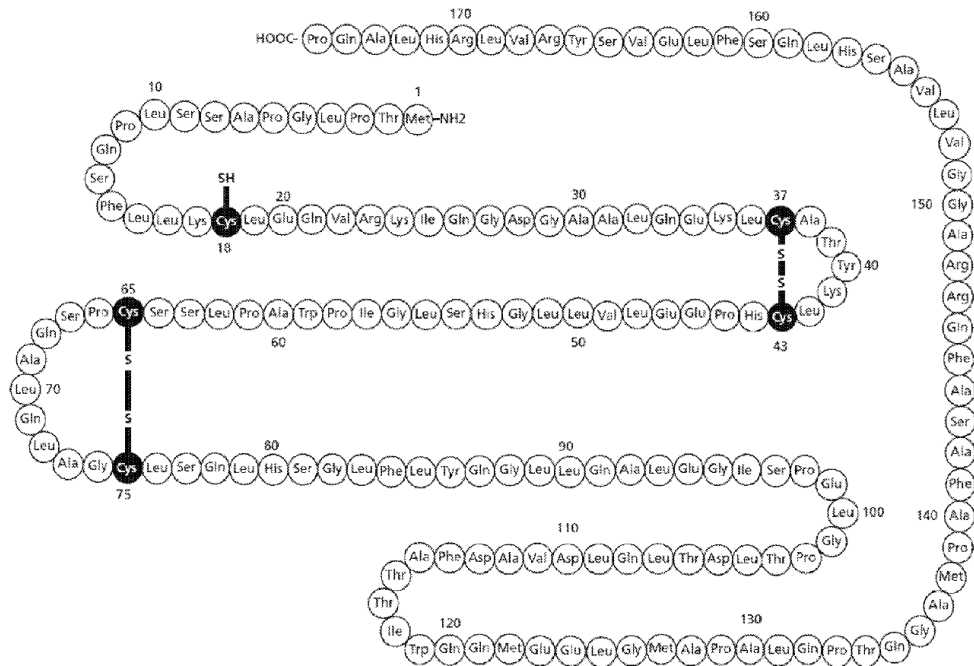


**Figure 2. 2** Amino acid sequence of GCSF (Toksöz, Yenice, Üzgün, & Öner, 2011)

### 2.3. Microorganism; *Pichia pastoris*

Yeasts became a promising host for eukaryotic heterologous proteins production (Romanos, Scorer, & Clare, 1992) because of the availability to genetic modification and the specific growth (Cregg, Vedvick, & Raschke, 1993). For these reasons and in the light of the information about the structure and genetic of *Saccharomyces cerevisiae* which was the first yeast studied (Hitzeman et al., 1981).

*P. pastoris*, methylotrophic yeast, showed popularity in the production area of different heterologous proteins (J. L. Cereghino & Cregg, 2000). The reasons for this popularity can be listed in;

1. Molecular genetic modification simplicity
2. Similarity of *Pichia pastoris* to *Saccharomyces cerevisiae* which is one of the most investigated yeast
3. Production availability on both of the intracellular and extracellular proteins
4. Performance availability under the post-translational modifications which are disulfide bond formation, glycosylation, and proteolytic processing.

Furthermore, physiology of *P. pastoris* is another reason for the popularity of usage as a host. *P. pastoris* chooses respiratory type growth rather than fermentative type growth. Fermentation causes side products like ethanol and acetic acid which can be toxic at high-level cell density (G. P. L. Cereghino, Cereghino, Ilgen, & Cregg, 2002).

Moreover, *P. pastoris* has methanol utilization pathway so it can utilize methanol as a carbon source. *P. pastoris* expression system having an AOX1 promoter that is robust and inducible at methanol existence in the medium, but the presence of different carbon sources like glycerol or glucose repress the AOX1 promoter (Byrne, 2015) and various proteins has been produced with this system (Romanos et al., 1992; Sreekrishna et al., 1997; Sreekrishna & Kropp, 1996).

#### **2.4. Promoter; Glyceraldehyde-3-phosphate dehydrogenase (GAP)**

Inducible promoters like  $P_{AOX1}$  provide control on gene expression but application area is restricted because of the transcriptional heterogeneity at single cell level (Khlebnikov et al., 2000), inducer toxicity and pleiotropic effects. Given these issues, a constitutive promoter is used allowing continuous and steady-state gene expression control and transcriptional homogeneity (Qin et al., 2011).

Glyceraldehyde-3-phosphate dehydrogenase promoter ( $P_{GAP}$ ) is a constitutive promoter.  $P_{GAP}$  was first isolated in 1997 (Waterham, Digan, Koutz, Lair, & Cregg, 1997).  $P_{AOXI}$  is stronger than the other promoters for expression of any protein but  $P_{GAP}$  is more safety than  $P_{AOXI}$  in industries because of the toxic inducer absence in the medium. However, the specific growth rate of host and carbon source are effective on the expression on  $P_{GAP}$  (Çalık et al., 2015; Müller, Bruhn, Flaschel, Friehs, & Risse, 2016). The expression level of  $P_{GAP}$  is considered, glycerol and glucose are more efficient than methanol (Waterham et al., 1997; A. L. Zhang et al., 2009).

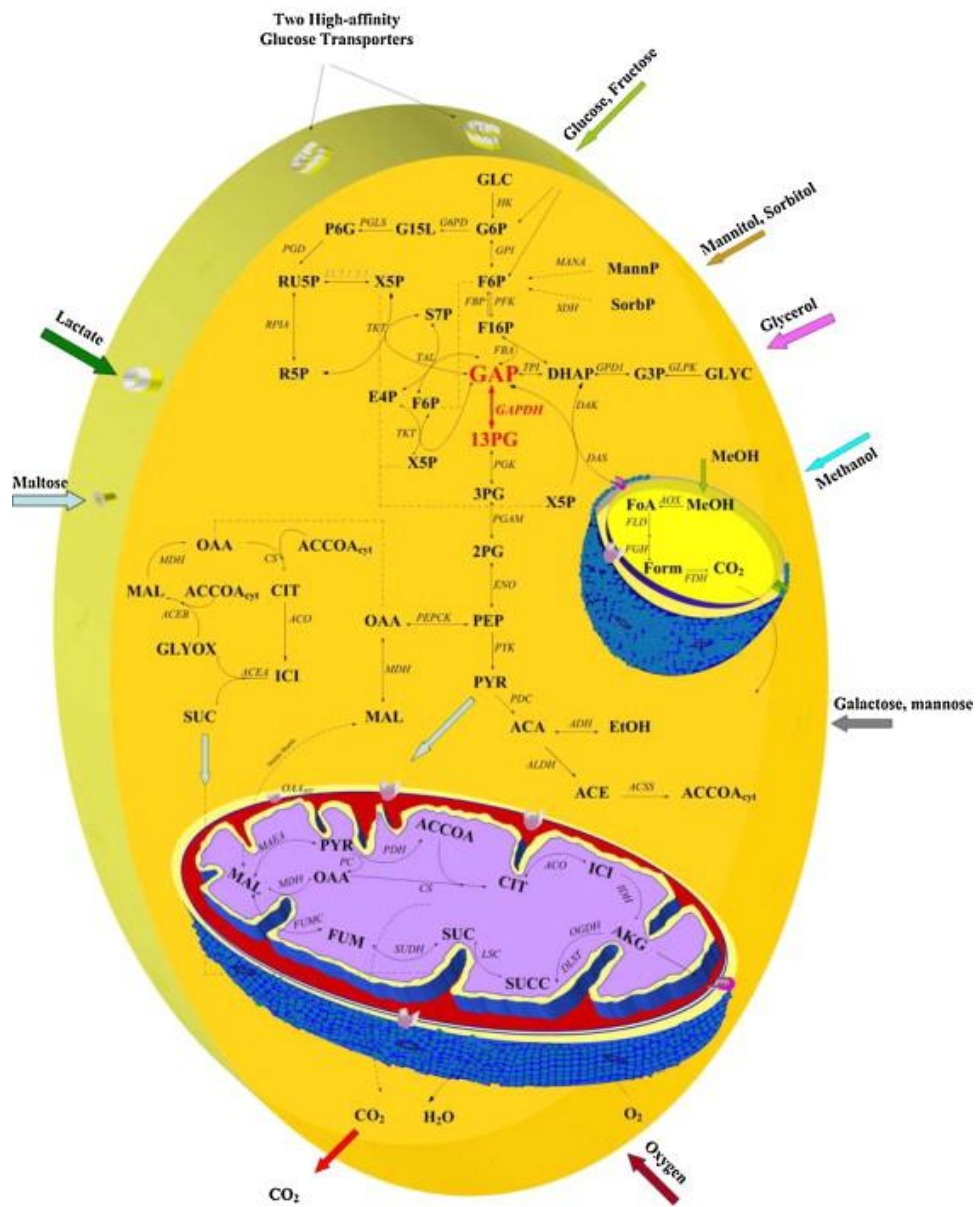


Figure 2. 3 *P. pastoris* central carbon metabolism (Çalık et al., 2015)

## **2.5. Production strategies for recombinant human growth hormone (rhGH)**

Through the recombinant DNA technology, several proteins became producible in mammalian, bacterial or yeast cells to reach high production and high protein activity in the production processes.

For the optimization of recombinant protein production required steps can be listed like that;

1. The host strain selection providing post-translational modifications and folding,
2. Selection of vector, promoter, and marker,
3. Codon-optimization the gene,
4. Combining of the gene with a tag for purification or detection of recombinant protein,
5. A specific signal sequence selection for recombinant protein within extracellular or intracellular conditions,
6. Preventing the proteolytic cleavage of the product,
7. Fermentation medium optimization
8. Designing of bioreactor conditions (temperature, pH, agitation, and oxygen transfer) (Çelik & Çalık, 2012).

For recombinant protein production, generally, the production medium consists of trace salt solution, basalt salt medium, ammonium hydroxide (nitrogen source and pH regulator), and glucose, glycerol or methanol as a carbon source.

Mostly, the bioprocess temperature of *P. pastoris* was set to 30 °C for growth. In addition, pH value of the medium has prominent effects on the enzyme activity, cell growth and, proteolytic degradation (Çelik & Çalık, 2012). Different pH conditions were determined as an optimum value for the production of various

recombinant proteins (Macauley-Patrick, Fazenda, McNeil, & Harvey, 2005). Studies related to the rhGH production were listed in Table 2.1

**Table 2. 1** Studies for rhGH production with *P. pastoris*

| Host               | Strain           | Promoter | Temp. (°C) | pH      | Carbon Source                    | Agitation Speed (rpm) | Dissolved Oxygen | hGH (mg/L) | Reference                          |
|--------------------|------------------|----------|------------|---------|----------------------------------|-----------------------|------------------|------------|------------------------------------|
| <i>P. pastoris</i> | GS115            | AOX1     | 30         | 5.8     | Glycerol                         | -                     | 30%              | 500        | (Apte-Deshpande et al., 2009)      |
|                    | X-33             | -        | 30         | 6       | Methanol                         | -                     | -                | 790        | (Lee et al., 2015)                 |
|                    | GS115            | AOX1     | 30         | 5.8     | Glycerol                         | 700                   | >20%             | 49         | (Ecamilla et al., 2000)            |
|                    | Mut <sup>+</sup> | AOX1     | 30         | 5       | Glycerol                         | 900                   | >20%             | 270        | (Çalık et al., 2010)               |
|                    | KM71             | AOX1     | 30         | 4.5     | Glycerol                         | 400-1200              | >20%             | 300        | (Yardlung Suwannarat et al., 2013) |
|                    | Mut <sup>+</sup> | AOX1     | 30         | 5.5-5.0 | Glycerol<br>Methanol<br>Sorbitol | 900                   | 20%              | 640        | (Çalık et al., 2013)               |

### 2.5.1. The effect of oxygen transfer on production of rhGH

In this study, oxygen transfer conditions effects were investigated for rhGH production and the related studies are given in Table 2.2. Performance of the bioreactor can be evaluated regarding the conversion of biochemical components and transport process (Lübbert & Bay Jorgensen, 2001). Oxygen is one of the key parameters because of its low solubility and high requirement of bioprocess (Garcia-Ochoa & Gomez, 2009). Bioreactors are as an example to the multiphase reactors. For oxygen transportation, oxygen (gas phase) transport should be considered to cells (solid phase) in broth (liquid phase). The transportation is explained by two film theory which is divided into nine steps.

1. Transfer of the bubble from bulk gas to the gas-liquid interface,
2. Transportation through the gas-liquid interface,
3. Diffusion of gas into the liquid film which covered the bubble,
4. Movement along the bulk liquid,



5. Diffusion to the stagnant liquid film which covers the cell,
6. Movement through the liquid-cell interface (If cells make cluster, initially gas diffuse into solid and after that diffuse to the individual cell,
7. Transfer into the cytoplasm,
8. Oxygen is consumed and CO<sub>2</sub> is produced as a result of reactions in cytoplasm,
9. Movement of produced gases in the reverse direction.

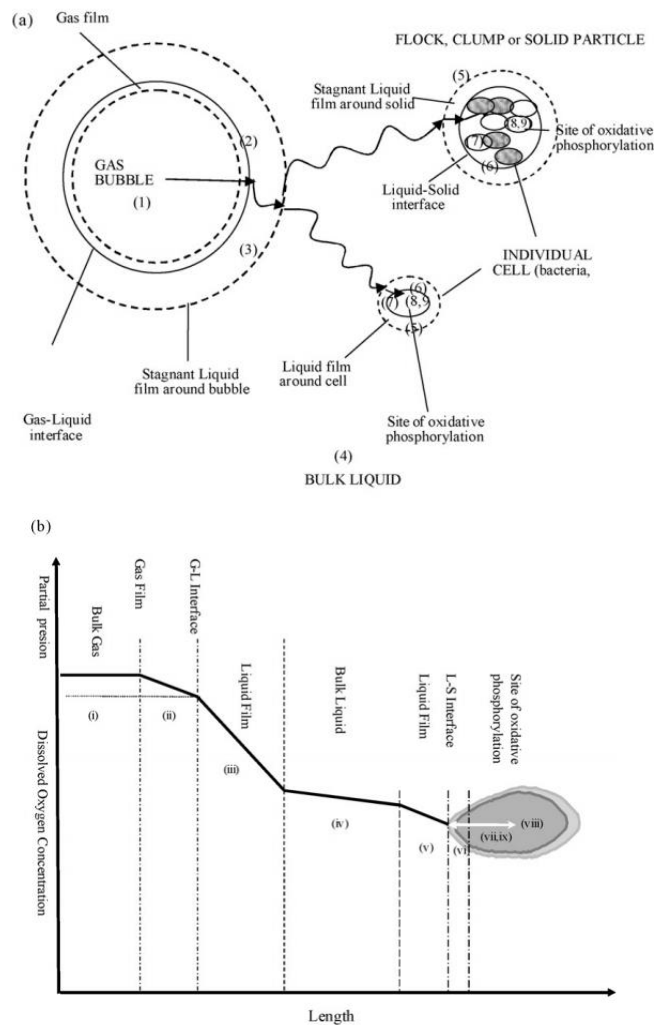


**Figure 2. 4 (a)** Transfer steps of oxygen from gas bubble into the cell **(b)** Dissolved oxygen concentration profile through the oxygen transfer process (Garcia-Ochoa, Gomez, Santos, & Merchuk, 2010)

**Table 2. 2** Studies related to oxygen transfer condition and other parameters on *P. pastoris*

| Strain | Plasmid | Promoter            | Recombinant protein (rP)           | Operation strategy in production phase (PP)             | C <sub>rP</sub>   | C <sub>DO</sub> | Aeration Rate (vvm) | N (rpm)    | T (°C) | pH <sub>0,PP</sub> (L) | V <sub>0,PP</sub> (L) | C <sub>X0,PP</sub> (OD <sub>600</sub> ) | References                 |          |
|--------|---------|---------------------|------------------------------------|---|-------------------|-----------------|---------------------|------------|--------|------------------------|-----------------------|---|----------------------------|----------|
| X-33   | pGAPZαA | GAP                 | Human antibody fragment 2F5 Fab    | Chemostat   | 8 µg/L            | >20%            | 0.8                 | 700        | 25     | 5                      | 1                     | -                                       | García-Ortega et al., 2017 |          |
|        |         |                     |                                    | Dilution rate of D=0.1 h <sup>-1</sup>                  | 12 µg/L           | 0%              |                     |            |        |                        |                       |   |                            |          |
| X-33   | pPICZα  | (Mut <sup>-</sup> ) | <i>e.c.-Rhizopus oryzae</i> lipase | Methanol Non-limited Fed-Batch (C <sub>M</sub> = 3 g/L) | 127 mg/L          | 5% (~7%)        | -                   | -          | -      | -                      | -                     | -                                       | -                          |          |
|        |         |                     |                                    | Batch   | 166 mg/L          | 10%             | -                   | 800 – 1000 | 30     | 5.5                    | 2                     | 2.5                                     | Ponte et al., 2016         |          |
|        |         |                     |                                    |   | 174 mg/L          | 25%             | -                   | -          | -      | -                      | -                     | -                                       | -                          |          |
|        |         |                     |                                    |   | 158 mg/L          | 50% (~45%)      | -                   | -          | -      | -                      | -                     | -                                       | -                          |          |
| X-33   | pGAPαA  | GAP                 | Antibody fragment, Fab             | Chemostat µ = 0.1 h <sup>-1</sup>                       | ~50 extracellular | 21%             | 1.5                 | 700        | 25     | 5                      | 2                     | 1                                       | Camiceo et al. 2009        |          |
|        |         |                     |                                    | 10> intracellular (µgFab/gDWht)                         | ~40-50            | 11%             |                     |            |        |                        |                       |   |                            | (25 g/L) |
|        |         |                     |                                    | ~10 intracellular (µgFab/gDWht)                         | ~80 extracellular | 8%              |                     |            |        |                        |                       |   |                            |          |
|        |         |                     |                                    | ~10 intracellular (µgFab/gDWht)                         | ~80 extracellular |                 |                     |            |        |                        |                       |   |                            |          |

**Table 2. 2** Studies related to oxygen transfer condition and other parameters on *P. pastoris* (cont'd.)

| Strain                      | Plasmid | Promoter | Recombinant protein (rP) | Operation strategy in production phase (PP)                | C <sub>RP</sub> | C <sub>DO</sub> | Aeration Rate (vvm) | N (rpm) | T (°C) | pH <sub>out,PP</sub> | V <sub>out,PP</sub> (L) | C <sub>X<sub>out,PP</sub></sub> (OD <sub>600</sub> ) | References           |                     |
|-----------------------------|---------|----------|--------------------------|--|-----------------|-----------------|---------------------|---------|--------|----------------------|-------------------------|--|----------------------|---------------------|
| GS115                       | -       | GAP      | S-adenosyl-L-methionine  | Glycerol Fed-Batch   | 3.45 g/L        | 50%             | 0.2-1.4             | 800     | 30     | 6                    | 7.5                     | (20 g/L)   | Hu et al. 2008       |                     |
|                             |         |          |                          |  | 4.14 g/L        | 25%             |                     |         |        |                      |                         |  |                      |                     |
|                             |         |          |                          |  | 5.22 g/L        | 0%              |                     |         |        |                      |                         |  |                      |                     |
| GS115                       | pPIC9   | PGK      | L-lactic acid            | Batch<br>C <sub>GLY</sub> = 40 g/L                         | 10 g/L          | 3%              | 0.05                | 350     | 30     | 5                    | 0.5                     | 2  | de Lima et al., 2016 |                     |
|                             |         |          |                          |  | 8 g/L           | 5%              |                     |         |        |                      |                         |  |                      |                     |
|                             |         |          |                          |  | 22 g/L          | 30%             |                     |         |        |                      |                         |  |                      |                     |
| CBS7435 MutS strain (Aoch1) | -       | -        | Horsradish peroxidase    | Exponential Glycerol Fed-Batch<br>μ = 0.08 h <sup>-1</sup> | 22 g/L          | 30%             | -                   | 500     | 30     | 5                    | 0.5                     | 2  | (20 g/L)             | Gmeiner et al. 2015 |
|                             |         |          |                          |  | 56.5 U/mg       |                 |                     |         |        |                      |                         |  |                      |                     |
|                             |         |          |                          |  | 0.54 U/mg       | 10%             |                     |         |        |                      |                         |  |                      |                     |
|                             |         |          |                          |  | 47.2 U/mg       |                 |                     |         |        |                      |                         |  |                      |                     |
|                             |         |          |                          |  | 0.29 U/mg       |                 |                     |         |        |                      |                         |  |                      |                     |
|                             |         |          |                          |  | 7.41 U/mg       | 20%             |                     |         |        |                      |                         |  |                      |                     |
|                             |         |          |                          |  | 15.9 U/mg       |                 |                     |         |        |                      |                         |  |                      |                     |
|                             |         |          |                          |  | 61.7 U/mg       |                 |                     |         |        |                      |                         |  |                      |                     |
|                             |         |          |                          |  | 0.21 U/mg       | 30%             |                     |         |        |                      |                         |  |                      |                     |
|                             |         |          |                          |  | 38.7 U/mg       |                 |                     |         |        |                      |                         |  |                      |                     |
|                             |         |          |                          |  | 0.2 U/mg        |                 |                     |         |        |                      |                         |  |                      |                     |
|                             |         |          |                          |  |                 |                 |                     |         |        |                      |                         |  |                      |                     |

**Table 2. 2** Studies related to oxygen transfer condition and other parameters on *P. pastoris* (cont'd.)

| Strain | Plasmid | Promoter | Recombinant protein (rP)                   | Operation strategy in production phase (PP)     | $C_{-rP}$                                 | $C_{DO}$ | Aeration Rate (vvm) | N (rpm)  | T (°C) | pH <sub>0,PP</sub> | V <sub>0,PP</sub> (L) | C <sub>X<sub>0,PP</sub></sub> (OD <sub>600</sub> ) | References          |           |
|--------|---------|----------|--|---|---|----------|---------------------|----------|--------|--------------------|-----------------------|--|---------------------|-----------|
|        | pGAPZαA |          | Human monoclonal antibody 3H6 Fab fragment | Chemostat Dilution Rate D = 0.1 h <sup>-1</sup> | ~0.023 mg g <sup>-1</sup> h <sup>-1</sup> | 20.97%   | 1.5                 | 700      | 25     | 5                  | 1                     | 1  |                     |           |
|        |         |          |  |   | ~0.035 mg g <sup>-1</sup> h <sup>-1</sup> | 10.91%   |                     |          |        |                    |                       |  |                     |           |
|        |         |          |  |   | ~0.05 mg g <sup>-1</sup> h <sup>-1</sup>  | 8.39%    |                     |          |        |                    |                       |  |                     |           |
|        |         |          |  |   | ~0.069 mg g <sup>-1</sup> h <sup>-1</sup> | 5.87%    |                     |          |        |                    |                       |  |                     |           |
| X-33   | pPICZαB | GAP      | Human monoclonal antibody 3H6 Fab fragment | Glucose Fed-Batch F = 161.7 g/h                 | 46.85 mg/L                                | >20%     |                     |          |        |                    |                       |  | Baumann et al. 2008 |           |
|        |         |          |  |   | Human trypsinogen                         |          |                     |          |        |                    |                       |  |                     | 20.08 U/L |
|        |         |          |  |   | Porcine trypsinogen                       |          |                     |          |        |                    |                       |  |                     | 79.2 U/L  |
|        | pGAPZαA |          | Human monoclonal antibody 3H6 Fab fragment | Glucose Fed-Batch μ = 0.2 h <sup>-1</sup>       | 52.75 mg/L                                | 5.87%    | 1                   | 600-1200 | 25     | 5                  | 17                    | 1  |                     |           |
|        |         |          |  |   | Human trypsinogen                         |          |                     |          |        |                    |                       |  |                     | 22.34 U/L |
|        |         |          |  |   | Porcine trypsinogen                       |          |                     |          |        |                    |                       |  |                     | 86.95 U/L |
|        |         |          |  |   |   |          |                     |          |        |                    |                       |  |                     |           |

Different proteins were produced under various oxygen transfer conditions from low to moderate. Güneş and Çalık conducted experiments to investigate the oxygen transfer effect on protein production by *Pichia pastoris* under glyceraldehyde-3-phosphate dehydrogenase promoter. Two kinds of strategies were applied. One of them kept at constant oxygen transfer rate and the other one was kept at constant  $C_{DO}$  which are  $C_{DO} = 5, 10, 15, 20,$  and  $40\%$ . At  $C_{DO} = 20\%$ , the highest cell concentration was succeeded. On the other hand, the highest enzyme and volumetric activities were reached at  $C_{DO} = 15\%$  condition (Güneş & Çalık, 2016).

### **2.5.2. Temperature**

For determination the stability of microorganism and protein, temperature optimization is one of the critical parameters. The optimum growth and production temperature is  $30\text{ }^{\circ}\text{C}$  for *P. pastoris* (Cos, Ramón, Montesinos, & Valero, 2006). Above  $32\text{ }^{\circ}\text{C}$ , expression of the protein halts and deterioration occurs on growth (Invitrogen, 2002).

In the literature, different studies were worked at different temperatures on various proteins produced by *P. pastoris* to understand the effect of temperature. Hong and friends stated that laccase specific activity increases with decreasing of temperature from  $30\text{ }^{\circ}\text{C}$  to  $20\text{ }^{\circ}\text{C}$  and reasons of this result were associated with instability of target protein, folding problems of the protein and coming up of protease from dead cells at high temperature (Hong, Meinander, & Jönsson, 2002). Moreover, at low temperature, higher yield for Herring antifreeze protein (Z. Li et al., 2001), low folding stress (Dragosits et al., 2009), high volumetric activity and productivity with specific activity for galactose oxidase (Anasontzis, Penã, Spadiut, Brumer, & Olsson, 2014) were achieved.

### **2.5.3. pH**

Commonly pH in various studies is between 5 and 6 yet, *P. pastoris* shows growth ability in a broad range from  $\text{pH}=3$  to 7 (Jahic, Gustavsson, Jansen, Martinelle, & Enfors, 2003). Additionally, pH should be adjusted to an optimum value where the

protease influence is low (Cregg et al., 1993). On the other hand, X. Shi and colleagues indicate a relationship between pH, protease activity, and accumulation of single-chain antibody (X. Shi et al., 2003). Çalık and colleagues (P. Çalık et al., 2010) studied the effect of pH on rhGH production by *Pichia pastoris* with four pH values which are pH=4.2, 5.0, 5.5, and 6.0. As a result of this research, the highest protein concentration was obtained at pH=5.0. Also, increases were achieved at protease secretion and oxygen uptake rate with increase in pH (P. Çalık et al., 2010).

## 2.6. Computational equations and parameters for bioprocess

The bioprocess parameters including cell formation rate, the specific growth rate, production formation rate, and substrate consumption rate should be defined to understand the response of a bioprocess. Mathematical notifications and formulations gain a significant importance for the representation of the bioprocess.

For bioreactor, mass conversation equations are written according to the verbal equation, like that;

$$\text{Input} - \text{Output} + \text{Generation} = \text{Accumulation} \quad (2.1)$$

Throughout the fed-batch process, perturbation effects of sampling on the cell generation can be held at the minimum level by holding sample volumes small during the process, and as a result of continuous feeding, fermentation volume (V) increases and the increase causes the positive values of the cultivation time derivative of the volume. That's why any change in the volume can be negligible related to base-, acid-, antifoam- additions, and sampling.

$$Q(t) \approx \frac{dV}{dt} \quad (2.2)$$

Also, the volume change for the batch process is shown as in equation 2.3.

$$\frac{dV}{dt} = 0 \quad (2.3)$$

### 2.6.1. Mass conservation equation for the cell growth

After the inoculation at  $t = 0$  h in batch of the process, any cell feeding is not applied to the cultivation medium so that mass conservation equations are same for the cell in batch and fed-batch operations (G. Çalık, Kocabaş, Afşar, Çalık, & Özdamar, 2016).

$$r_x V = \frac{d(C_x V)}{dt} \quad (2.4)$$

where  $r_x$ , cell (biomass) generation rate,  $C_x$  is the cell concentration,  $V$  is the bioreactor working volume,  $t$  is the cultivation or residence time. The cell generation rate can be shown in the production domain:

$$r_x = \mu C_x \quad (2.5)$$

From the combination of equations (2.4) and (2.5);

$$\frac{d(C_x V)}{dt} = \mu C_x V \quad (2.6)$$

The variables in the equation 2.6 were separated and integrated between the boundary conditions which are condition-1 ( $t = 0$ ,  $C_x = C_{x0}$ ) and condition-2 ( $t = t$ ,  $C_x = C_x$ ):

$$\int_0^t \mu dt = \int_{C_{x0}}^{C_x} \frac{dC_x}{C_x} \quad (2.7)$$

The equation 2.8 was derived for the specific growth rate under the constant fermentation medium density assumption and using the continuity equation for fed-batch operation having a continuous feed inlet stream with the flow rate  $Q(t)$ .

$$\mu = \frac{1}{C_x} \frac{dC_x}{dt} + \frac{Q(t)}{V} \quad (2.8)$$

For batch mode,  $Q(t) = 0$ , the specific growth rate can be written like that;

$$\mu = \frac{dC_x}{dt} \frac{1}{C_x} \quad (2.9)$$

### 2.6.2. Mass conservation equation for the substrate

The second equations group required for each continuously fed substrate in the fed-batch operation. For each continuously fed substrate with a time-varying feed stream flow rate of  $Q(t)$  without withdrawal of a corresponding effluent stream, is constructed as (G. Çalık et al., 2016);

$$Q(t)C_S^0 + r_S V = \frac{d(C_S V)}{dt} \quad (2.10)$$

where, substrate consumption rate,  $r_s$ , and  $C_S^0$  is the constant substrate feed concentration can be written in the product domain:

$$-r_s = q_s C_x \quad (2.11)$$

where,  $q_s$  is the specific substrate consumption rate. By substituting equation 2.11 into equation 2.10, the following is derived for  $q_s$ :

$$q_s = -\frac{1}{C_x} \left( \frac{dC_S}{dt} + \frac{C_S}{V} Q(t) - \frac{Q(t)}{V} C_S^0 \right) \quad (2.12)$$

### 2.6.3. Mass conservation equation for the product

The third equations group required in fed-batch bioreactor operations are mass conservation equations for the product and each by-product synthesized in the cell which can be excreted or secreted into the fermentation broth, considering their batchwise formations

$$r_p V = \frac{d(C_p V)}{dt} \quad (2.13)$$

$r_p$  is defined as the product formation rate and is shown in the following equation;

$$r_p = q_p C_x \quad (2.14)$$

where,  $q_p$  is the specific product formation rate. By substituting equation 2.14 into equation 2.13, and by rearranging  $q_p$  is formulated as:



$$q_p = \frac{1}{c_x} \left( \frac{dc_p}{dt} + \frac{Q(t)}{dt} C_p \right) \quad (2.15)$$

#### 2.6.4. Mathematical model for fed-batch bioreactor with continuous feed stream

The mathematical model of a fed-batch bioreactor with a continuous feed flow rate,  $Q(t)$ , can be derived (G. Çalık et al., 2016). For the cell, by combining equation 2.4 and equation 2.5:

$$\frac{d(C_x V)}{dt} - \mu C_x V = 0 \quad (2.16)$$

For each substrate transferred into fed-batch bioreactor by continuous feed stream, rearranging Eq-2.12 gives:

$$\frac{dC_s}{dt} + \frac{Q(t)}{V} C_s + q_s C_x = \frac{Q(t)}{V} C_s^o \quad (2.17)$$

For the product or each by-product, by rearranging equation 2.15:

$$\frac{dc_p}{dt} + \frac{Q(t)}{V} C_p - q_s C_x = 0 \quad (2.18)$$

If the cultivation time derivative of  $C_s$  is assumed to be zero, equation 2.10 becomes:

$$Q(t)C_s^o + r_s V = C_s \frac{dV}{dt} \quad (2.19)$$

Using the definitions of the yield coefficient  $Y_{x/s}$  and by substituting equation 2.11 into equation 2.19:

$$Q(t)C_s^o - \frac{r_x}{Y_{x/s}} V = C_s \frac{dV}{dt} \quad (2.20)$$

By substituting equation 2.5 into equation 2.4, after separation of the variables, integration from between the boundary conditions which are condition-1 ( $t = 0$ ) and condition-2 ( $t = t$ ):

$$C_x V = C_{x,0} V_0 e^{\mu t} \quad (2.21)$$

Therefore, by substituting equation 2.5 and equation 2.21 into equation 2.20,  $Q(t)$  is formulated as:

$$Q(t) = \frac{\mu V_0 C_{x,0}}{Y_{x/s}(C_s^0 - C_s)} \exp(\mu t) \quad (2.22)$$

Further, assuming  $C_s^0 \gg C_s$ , continuous feed stream flow rate is formulated as:

$$Q(t) = \frac{\mu V_0 C_{x,0}}{C_s^0 Y_{x/s}} \exp(\mu t) \quad (2.23)$$

where,  $\mu$  is the pre-determined specific growth rate,  $V_0$  is the initial fermentation volume,  $C_{x,0}$  is the initial cell concentration,  $C_s^0$  is the feed substrate concentration, and  $Y_{x/s}$  is the cell yield on the substrate glucose.

### 2.6.5. Overall yield coefficients

Product ( $Y_{P/S}$ ) or biomass ( $Y_{X/S}$ ) yields demonstrate the efficiency of the substrate or product formation conversion. Mathematically, yields are calculated with ratio change of amounts of different parameters in the same time interval. For the instantaneous parameters;

$$Y_{P/S} = \frac{dP}{dS} = \frac{d(C_p V)/dt}{d(C_s V)/dt} = \frac{r_p V}{(-r_s) V} = \frac{r_p}{(-r_s)} \quad (2.24)$$

$$Y_{P/X} = \frac{dP}{dX} = \frac{d(C_p V)/dt}{d(C_x V)/dt} = \frac{r_p V}{r_x V} = \frac{r_p}{r_x} \quad (2.25)$$

$$Y_{X/S} = \frac{dX}{dS} = \frac{d(C_x V)/dt}{d(C_p V)/dt} = \frac{r_x V}{(-r_s) V} = \frac{r_x}{(-r_s)} \quad (2.26)$$

For overall yield coefficients;

$$Y_{X/S} = -\frac{\Delta X}{\Delta S} \quad (2.27)$$

$$Y_{P/S} = -\frac{\Delta P}{\Delta S} \quad (2.28)$$

where X is biomass, S is substrate, P is product.

**Table 2. 3** Yield demonstration with unit and definition for a system

| Symbol    | Definition  | Unit                                |
|-----------|---|-------------------------------------|
| $Y_{X/S}$ | Mass of cells produced per unit mass of substrate consumed  | g cell g <sup>-1</sup> substrate    |
| $Y_{X/O}$ | Mass of cells produced per unit mass of oxygen consumed     | g cell g <sup>-1</sup> oxygen       |
| $Y_{S/O}$ | Mass of substrate consumed per unit mass of oxygen consumed | g substrate g <sup>-1</sup> oxygen  |
| $Y_{P/X}$ | Mass of product formed per unit mass of cells produced      | g product g <sup>-1</sup> cell      |
| $Y_{P/S}$ | Mass of product formed per unit mass of substrate consumed  | g product g <sup>-1</sup> substrate |

### 2.7. Protein separation and purification methods

Proteins consist of amino acid chains naturally occurring miscellaneous macromolecules, or biomolecules, in organisms, by this way serving a broad array of functions at every point of the life cycle. Some of these work on transportation and storage of other molecules, catalyzing of metabolic reactions and DNA replication. Classification of proteins according to their structural and functional properties are shown in Table 2.4 and Table 2.5.

**Table 2. 4** Categorization of proteins by structural characteristics (Scopes, 2001)

| Structural characteristic | Examples  | Comments   |
|---------------------------|---|--|
| <b>Monomeric</b>          | Lysozyme, growth hormone  | Usually extracellular; often have disulfide bonds              |
| <b>Oligomeric</b>         |   |  |
| <b>Identical subunits</b> | Glyceraldehyde-3-phosphate dehydrogenase, catalase, alcohol dehydrogenase, hexokinase | Mostly intracellular enzymes; rarely have disulfide bonds      |
| <b>Mixed subunits</b>     | Aspartate carbamoyltransferase, pertussis toxin                                       | Allosteric enzymes; different subunits have separate functions |
| <b>Membrane-bound</b>     |   |  |
| <b>Peripheral</b>         | Mitochondrial ATPase, alkaline phosphatase  | Readily solubilized by detergents                              |
| <b>Integral</b>           | Porins, cytochromes P450, insulin receptor  | Require lipid for stability                                    |
| <b>Conjugated</b>         | Glycoproteins, lipoproteins, nucleoproteins   | Many extracellular proteins contain carbohydrate               |

**Table 2. 5** Categorization of proteins by function (Scopes, 2001)

| <b>Function</b>           | <b>Examples</b>  |
|---------------------------|--|
| <b>Amino acid storage</b> | Seed proteins (e.g., gluten), milk proteins (e.g., casein)                       |
| <b>Structural</b>         |  |
| <b>Inert</b>              | Collagen, keratin  |
| <b>With activity</b>      | Actin, myosin, tubulin   |
| <b>Binding</b>            |  |
| <b>Soluble</b>            | Albumin, hemoglobin, hormones  |
| <b>Insoluble</b>          | Surface receptors (e.g., insulin receptor), antigens (e.g., viral coat proteins) |
| <b>With activity</b>      | Enzymes, membrane transporters (e.g., amino acid uptake systems, ion pumps)      |

More than 200 years have passed on the first protein purification attempt which was reported in 1789 by Fourcroy. It related to the isolation of a substance having similar properties like egg white. In 1840, the first crystals of hemoglobin were prepared by Felix Hoppe-Seyler (Eisenberg, 2002). In 1889, the first crystalline protein, ovalbumin, was obtained by Hofmeister (Scopes, 1995). In 1903, the botanist Mikhail Tswett used a calcium carbonate column to separate plant pigments. Thereafter, in 1906, the term chromatography was introduced by him. The timeline of protein purification history is given in Table 2.6. Nowadays many recombinant proteins are produced with the help of genetic engineering and different separation and purification systems are searched to provide pure recombinant proteins in research laboratories and downstream processes of industries. The main aim of downstream processes is a separation of desired proteins within the protection of the chemical integrity and the biological activity. Also, it should be entirely free from either contaminants or isoforms (Kalyanpur, 2002). Therefore, to separate and purify the target protein from other proteins and nonprotein components of the mixture, different separation methods are used depending on the properties of the target protein such as shape, charge, charge distribution, isoelectric point, size, density, hydrophobicity, metal binding and ligand-binding affinity (Labrou, 2014). Some chromatographic methods and membrane-based methods like nanofiltration (reverse osmosis) and ultrafiltration

are applied on various mediums because of the high selectivity, yield, and time-saving properties. Separation techniques are given with basis of separation and resolution in Table 2.7

**Table 2. 6** Timeline of protein purification (GE Healthcare, 2010)

| Study  | Year | Reference                                  |
|--|------|--|
| Precipitation  | 1789 | Fourcroy                                   |
| Crystalline ovalbumin  | 1889 | Hofmeister                                 |
| Chromatography   | 1903 | Tswett                                     |
| Affinity-ligand coupling chemistry for affinity chromatography | 1967 | (Axén, Porath, & Ernback, 1967)            |
| Affinity chromatography  | 1968 | (Cuatrecasas, Wilchek, & Anfinsen, 1968)   |
| Immobilized metal ion affinity chromatography                  | 1975 | (J Porath et al., 1975)                    |
| Histidine affinity tagging                                     | 1988 | (Smith et al., 1988; Hochuli et al., 1988) |

**Table 2. 7** Common separation methods by physicochemical basis (Labrou, 2014)

| Separation                           | Basis of separation               | Resolution |
|--------------------------------------|-----------------------------------|------------|
| <b>Precipitation</b>                 |                                   |            |
| <b>Ammonium sulfate</b>              | Solubility                        | Low        |
| <b>Organic solvents</b>              | Solubility                        | Low        |
| <b>Polyethyleneimine</b>             | Charge, size                      | Low        |
| <b>Polyethylene glycol</b>           | Solubility                        | Low        |
| <b>Isoelectric</b>                   | Solubility, pI                    | Low        |
| <b>Affinity precipitation</b>        | Molecular recognition, solubility | Low        |
| <b>Phase partitioning</b>            |                                   |            |
| <b>Aqueous two-phase partition</b>   | Solubility/hydrophobicity         | Low/medium |
| <b>Three phase partitioning</b>      | Solubility/hydrophobicity         | Low/medium |
| <b>Chromatography</b>                |                                   |            |
| <b>Ion exchange</b>                  | Charge, charge distribution       | High       |
| <b>Hydrophobic interaction</b>       | Hydrophobicity                    | High       |
| <b>Reverse-phase HPLC</b>            | Hydrophobicity, size              | High       |
| <b>Affinity chromatography</b>       | Molecular recognition             | High       |
| <b>Gel filtration/size exclusion</b> | Size, shape                       | High       |

### 2.7.1. Chromatographic Separation Methods

Chromatographic methods became one of the most popular separation techniques because of their higher yield and selectivity than the other separation methods. Therefore, different chromatographic techniques are mostly used in laboratories and industries which can be classified regarding the structural and chemical properties of proteins. In Table 2.8 shows the main chromatographic ways with their properties to separate proteins.

**Table 2. 8** Chromatographic techniques with their separation basis (GE Healthcare Life Sciences, 2016)

| <b>Property</b>                            | <b>Technique</b>  |
|--|---|
| <b>Biorecognition (ligand specificity)</b> | Affinity chromatography (AC)  |
| <b>Charge</b>                              | Ion exchange chromatography (IEX)   |
| <b>Size</b>                                | Size exclusion chromatography (SEC),<br>also called gel filtration (GF)             |
| <b>Hydrophobicity</b>                      | Hydrophobic interaction chromatography (HIC)<br>Reversed phase chromatography (RPC) |

#### 2.7.1.1. Affinity chromatography

Separation mechanism of affinity chromatography is based on a reversible reaction between a biomolecule and a ligand attached to a matrix. The method provides high selectivity, separation capacity and purity with the selection of suitable ligand-chelate combination on the target biomolecules or biomolecule groups. (GE Healthcare Life Sciences, 2016)

Separation of a biomolecule does not only depend on the tertiary structure of the protein or property of separation technique. Various parameters are also effective on separation like secretion location of the protein and protein solubility.

##### 2.7.1.1.1. Protein location in microorganism

Before the separation process, protein location should be determined. Extra separation steps can be required whether the protein location in a cytoplasmic

inclusion body or periplasmic space (Mitraki & King, 1989). If protein is soluble after lysis, native conditions are applied but unless protein is insoluble denaturing conditions are applied. For native conditions, sonication or homogenization can be applied to get inclusion body and the protein in the supernatant by disrupting cell. On the other hand, an extra step is required after lysis of cell or inclusion body for denaturing conditions. The step is especially necessary for proteins that insoluble in the supernatant. To get them from the pellet strong denaturants are used like urea to solubilized inclusion bodies and proteins (GE Healthcare, 2007). Protein activity cannot be protected under denaturing conditions; therefore, denaturant concentration should not be high.

#### **2.7.1.1.2. Affinity chromatography separation steps**

Solubilized protein with native or denaturing conditions becomes ready for the separation process. Affinity chromatography process consists of several steps which are;

- ❖ Equilibration
- ❖ Sample application and wash
- ❖ Elution
- ❖ Re-equilibration
- Equilibration

Equilibration is the first step of affinity chromatography. Equilibration is used to prepare the resin for separation. Different binding buffers contain different compounds in order to equilibrate the matrix of affinity chromatography according to the various pH values and imidazole amounts.

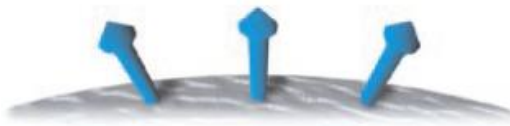


**Figure 2. 5** Affinity chromatography matrix (GE Healthcare Life Sciences, 2016)

➤ Sample Application and Wash

With regard to the protein secretion (intracellular or extracellular), nature or denature conditions are applied to the cell to get protein, especially for intracellular protein secretion. Then, the sample is applied to the matrix with optimized system conditions according to the target protein specifications such as temperature, pH, solvent medium. The target protein binds to the matrix specifically. After binding step, washing step is applied to separate the unbound target proteins with undesired biomolecules and other structures from the column.



**Figure 2. 6** Illustration of selective binding (GE Healthcare Life Sciences, 2016)

➤ Elution

After reversible binding of the target protein, it is regained and purified with an appropriate elution solvent without any breakdown at the tertiary structure of the protein to protect its activity. End of the elution step, protection of activity and capacity of the resin is an important parameter for affinity chromatography.



**Figure 2. 7** Elution of target protein (GE Healthcare Life Sciences, 2016)



➤ Re-equilibration

End of the separation and purification steps of the protein, the column is re-equilibrated for new utilization. However, after the each of applications, matrix performance can decrease so protein holding capacity, and purification ratio should be checked.



**Figure 2. 8** Re-equilibration of matrix (GE Healthcare Life Sciences, 2016)

**2.8. Surface adsorption phenomena**

For separation of desired proteins, some parameters are effective such as tag, spacer arm, and ligand. Before mention about detailed IMAC system and system components, adsorption isotherm and phenomena should be investigated to understand the binding system of protein on matrix.

Adsorption system is effectively used in separation and purification areas like protein separation (Burke et al., 1992; Norde & Anusiem, 1992; Y.-H. Yang, Wu, Suen, & Lin, 2011) and pollutant removing from wastewater and drinking water (Ho & McKay, 1999; Jian, Liu, Zhang, Liu, & Zhang, 2015; Mudhoo, Garg, & Wang, 2012). Also, modeling and experimental methods provide predictions and understanding of adsorption phenomena in these areas (X. Chen, 2015).

One of the most popular methods is the Langmuir isotherm (Langmuir, 1916) to describe the adsorption phenomena which is formulated;

$$q_e = \frac{Q_0 K_L C_e}{1 + K_L C_e} \quad (2.29)$$

According to the assumption of Langmuir isotherm;

- The surface is homogeneous.
- Monolayer coverage is possible for each site.
- There is no interaction between adsorbates.
- Each of sites is equivalent.

Linear forms of isotherms are widely used to find unknown parameters and linear forms are used to determine the most fitted model due to uncomplicated mathematical form (X. Chen, 2015).

**Table 2. 9** Linear forms of Langmuir isotherm

| <b>Isotherm Models</b> | <b>Linear Forms</b>  |
|------------------------|--|
| <b>Langmuir I</b>      | $\frac{C_e}{q_e} = \frac{1}{Q_0 K_L} + \frac{C_e}{Q_0}$                          |
| <b>Langmuir II</b>     | $\frac{1}{q_e} = \left[ \frac{1}{Q_0 K_L} \right] \frac{1}{C_e} + \frac{1}{Q_0}$ |
| <b>Langmuir III</b>    | $q_e = Q_0 - \left[ \frac{1}{K_L} \right] \frac{q_e}{C_e}$                       |
| <b>Langmuir IV</b>     | $\frac{q_e}{C_e} = K_L Q_0 + K_L q_e$  |

Another one is Freundlich isotherm which is formulated;

$$q_e = K_f C_e^{\frac{1}{n}} \quad (2.30)$$

This isotherm is used to determine the adsorption on the heterogeneous surface.

**Table 2. 10** Linear form of Freundlich isotherm

| <b>Isotherm Model</b> | <b>Linear Form</b>                           |
|-----------------------|--|
| <b>Freundlich</b>     | $\log q_e = \log K_f + \frac{1}{n} \log C_e$ |

Effects of different types of adsorbent were investigated for wastewater treatment, gas storage, and protein separation in the literature. For wastewater treatments, Fe(III)-coordinated amino-functionalized mesoporous silica adsorbents (X. Chen, 2015), biosorbents (Mudhoo et al., 2012), ZIF-8 (Jian, Liu, Zhang, et al., 2015); for gas storage, activated carbon (Matranga, Myers, & Glandt, 1992), metal-organic frameworks (Mason, Veenstra, & Long, 2014), ZIF-8 (Tanaka et al., 2015); for protein separation, hematite and silica (Norde & Anusiem, 1992), glass and polyester (Burke et al., 1992), metal ion-loaded hydroxyapatite (Y.-H. Yang et al., 2011), ZIF-8 (Zheng, Lin, Lin, Yang, & Zhang, 2015) were used as an adsorbent.

After mentioned about different adsorbents, usage of ZIF-8 should be detailed particularly as an adsorbent, especially aim of this study is considered. Zheng and friends stated that Fe<sub>3</sub>O<sub>4</sub>@ZIF-8 was used to separate model proteins which are histidine-rich. Higher adsorption was observed at histidine-rich protein, bovine hemoglobin (BHb) when compared with other proteins. For Langmuir model 6198 µg/g and for Freundlich model 3.011 µg/g adsorption was achieved with Fe<sub>3</sub>O<sub>4</sub>@ZIF-8 (Zheng et al., 2015). Also, in another research, ZIF-8 was used in a fixed bed column as an adsorbent to detract oxytetracycline (OTC) from aqueous media. The highest adsorption was reached 28.3 mg/g (dos Santos Ferreira da Silva et al., 2015).

### **2.9. Parameters controlling adsorption**

Protein adsorption cannot be understandable with isotherms only. It depends on the parameters controlling adsorption, individual and ensemble behaviors of proteins.

Temperature, ionic strength and pH are the main factors. The effects of the parameters can be listed;

➤ Temperature: An increment at temperature causes increasing at adsorption rate because proteins diffusivities speed up to the adsorbent surface (Nakanishi, Sakiyama, & Imamura, 2001).

➤ Ionic strength: Generally, an increase in the ionic strength reduces repulsive parts between proteins and as a result of this case adsorption increases. (Jones & O'Melia, 2000; Nakanishi et al., 2001).

➤ pH: At the equality of pH to isoelectric point (pI), all opposite charges become a balance; therefore molecule gets the neutral situation. In addition, at high pH which is higher than pI proteins become negatively charged. However, at low pH values which are lower than pI proteins become positively charged. When the pH value is increased, adsorption decreases because of the electrostatic effect. Also, reducing the pH value causing an increment at salt concentration. As a result of this increase, electrostatic repulsion will decrease for positively charged proteins. Therefore, adsorption will increase but, electrostatic repulsion will decrease between opposite charged protein and surface for this reason adsorption decreases (Jones & O'Melia, 2000).

### **2.9.1. Effects of protein properties on adsorption**

Proteins consist of 20 amino acids and proteins show variety with regard to the charge of these amino acids or side chains properties. With this diversity; structure, composition, and size of a protein present unique properties. For example, a protein can have neutral, positive and negative charges or hydrophobic surfaces, and based on these requirements; adsorption surface can be gained a functionality for these properties which will provide the most selective separation for the target protein (Andrade, Hlady, & Wei, 1992). Additionally, small proteins can diffuse easily and rapidly when they are compared with larger proteins showing another parameter for adsorption.

### **2.9.2. Effects of surface properties of adsorbent on adsorption**

Adsorption of a protein on the particle surface depends on temperature, ionic strength, and pH mentioned before. Moreover, proteins are in the tendency to bind to non-polar, high surface tension and charged surfaces (Rabe, Verdes, & Seeger, 2011). Non-polar surfaces cause destabilization, so it provides ease to conformational reorientations. As a result of reorientation, protein-protein and protein-surface interactions become more powerful (Anand, Sharma, Dutta, Kumar, & Belfort, 2010). When the focused on the charge of the surface, neutral surfaces refuse proteins; therefore adsorption occurs less level. On the other hand, adsorption of oppositely charged proteins is higher than same charged proteins for charged surfaces (Szeleifer, 1997).

### **2.9.3. Vroman effect**

Small size proteins faster diffuse than larger proteins at the beginning of adsorption mechanism but larger proteins bind stronger to the surface than smaller ones because of the larger contact area (Hirsh et al., 2013). Also, during adsorption, binding strength and interactions between proteins influence each other, and they can repel first adsorbed proteins and the adsorbed amount protein reaches a maximum point during adsorption (Rabe et al., 2011). This phenomenon is called as Vroman effect.

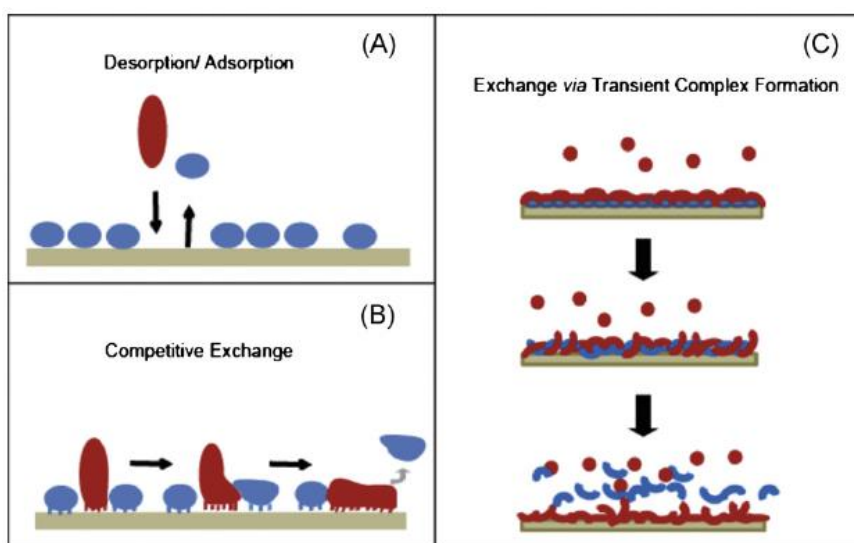


**Figure 2. 9** The illustration presents three different processes with respect to change at the surface during adsorption. (A) First adsorbed protein 1 (blue) desorbs in order to protein 2 (red) adsorption. (B) While protein 2 is attaching strongly, protein 1 desorbs. (C) Protein 2 anchors on the pre-adsorbed protein 1 and causes position change and desorption of protein 1 (Hirsh et al., 2013).

#### 2.9.4. Effect of IMAC components

IMAC system consists of several components which are ligand, chelate, support, tag, and spacer arm. Designing of the matrix (adsorbent) for IMAC system shows changes according to the target protein structure and properties. Mainly, designing of a resin is displayed in Figure 2.10. The spacer arm is bonded to support material with a covalent bond. Selected ligand and metal ion should be more effective on the target protein and purification conditions. To prevent any releasing of metal ions or other components on a support material, the binding type is more important so covalent bind provides a strong and permanent binding.

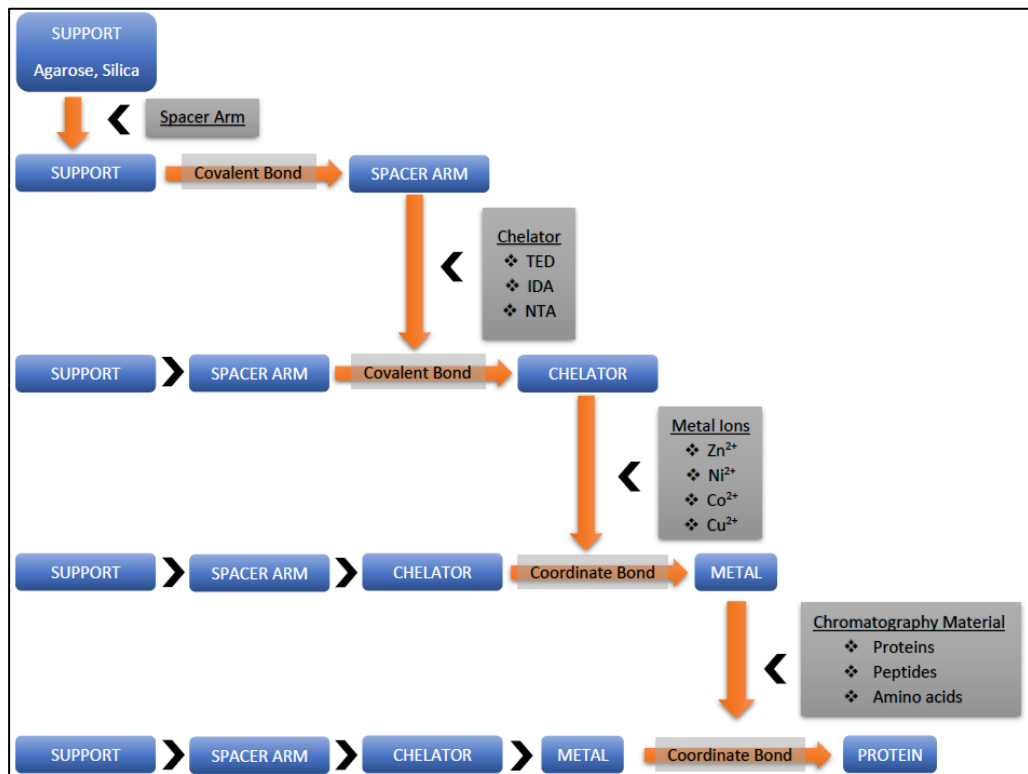


**Figure 2. 10** IMAC process steps from preparation of resin to adsorption of protein (Winzerling, Berna, & Porath, 1992)

#### 2.9.4.1. Influences of affinity tags on protein separation

Affinity tags become popular due to moderate elution conditions in separation and purification of the target protein from production medium. Furthermore, to define the best tag for process, some parameters should be considered which are;

- the least influence on biological activity,
- specific separation and purification of the target protein,
- feasible protein numbers which can be used with desired affinity tags,
- facilitation of purification procedure for selection of affinity tag (Terpe, 2003).

The most used of affinity tags are listed in Table 2.11 with their advantage and disadvantages.

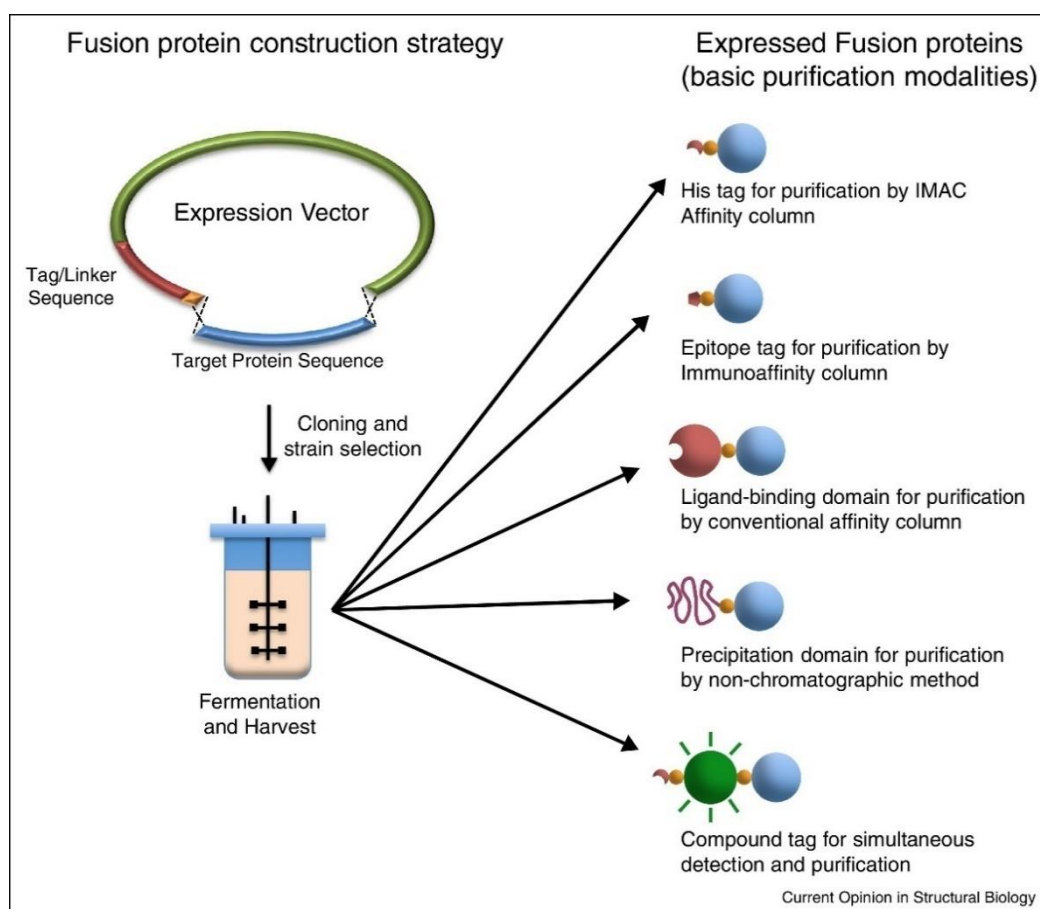
**Table 2. 11** The most used affinity tags and properties (Terpe, 2003; Waugh, 2005)

| Tag*     | Residues            | Size (kDa) | Advantages  | Disadvantages   |
|----------|---------------------|------------|---|---|
| GST      | 211                 | 26         | Cheap affinity resin<br>Moderate elution condition  | Metabolic burden is high<br>Ineffective on solubility                       |
| MBP      | 396                 | 40         | Cheap affinity resin<br>Moderate elution condition<br>Increment at solubility   | Metabolic burden is high  |
| FLAG     | 8                   | 1.01       | Metabolic burden is low<br>High specificity   | Expensive resin<br>Difficult elution condition                              |
| Poly-His | 2-10<br>(usually 6) | 0.84       | Metabolic burden is low<br>Cheap resin<br>Moderate elution condition<br>Available for both native and under native conditions | Higher specificity only for IMAC<br>Ineffective on solubility               |
| SBP      | 38                  | 4.03       | Metabolic burden is low<br>High specificity   | Expensive resin<br>Ineffective on solubility                                |
| CBP      | 51                  | 5.59       | Metabolic burden is low<br>High specificity<br>Moderate elution condition   | Expensive resin<br>Ineffective on solubility                                |
| S-tag    | 15                  | 1.75       | Metabolic burden is low<br>High specificity   | Expensive resin<br>Ineffective on solubility<br>Difficult elution condition |

\*GST, glutathione S-transferase; MBP, maltose binding protein; FLAG, FLAG-tag peptide; Poly-His, polyhistidine-tag; SBP, streptavidin-binding peptide; CBP, calmodulin-binding peptide

Also, tags can be categorized based on purification methods. For IMAC system, His<sub>n</sub>-tag; for immunoaffinity column, peptide/epitope tags like FLAG, c-Myc, GM-CSF; for conventional affinity column, folded domain tags like MBP, GST, Fluorapatite; for non-chromatographic methods, precipitation/aggregation tags like ELP, RTX, Fh8; for detection and purification, detection tags like eGFP, Heme and PYP can be used (Wood, 2014).

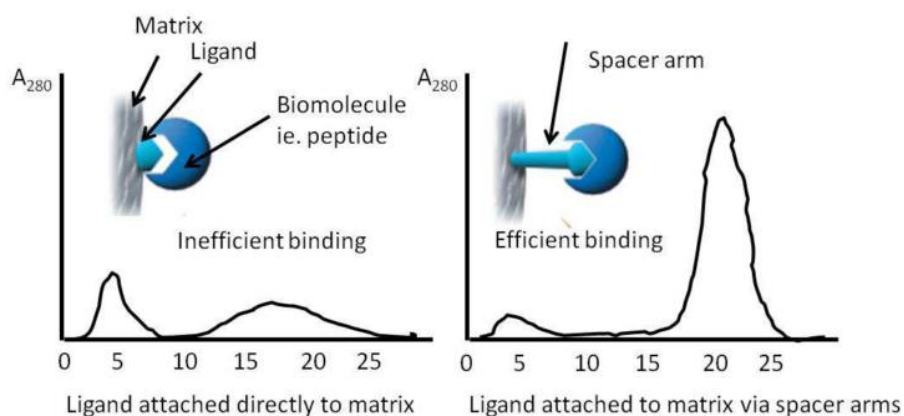




**Figure 2. 11** Mainly used purification systems with fundamental cloning (Wood, 2014)

#### 2.9.4.2. Influences of spacer arms on protein separation

The spacer arm which has not got enough length causes difficulty for target biomolecule to reach the spacer arm as a reason for steric hindrance. Therefore, too long or too short spacer arms cause low binding efficiency and non-specific binding for ligand and the target protein (Magdeldin & Moser, 2012). Commonly used hydrocarbon spacer arms bring about non-specific adsorption as a result of hydrophobic interactions between biomolecule and spacer arm. Using of hydrophilic arms can be more beneficial due to this reason (O'Carra, Barry, & Griffin, 1974).

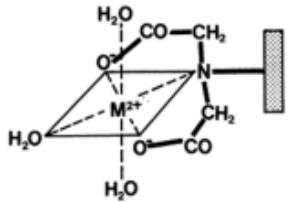
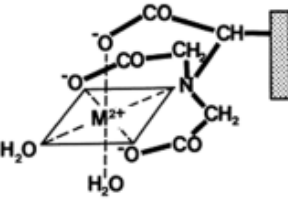
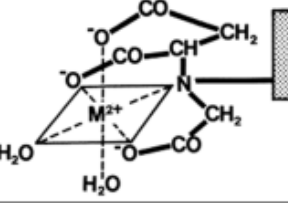
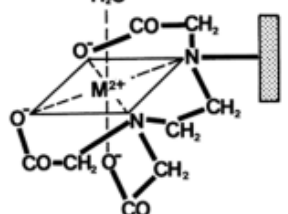


**Figure 2. 12** Chromatogram indicates spacer arm effect between matrix and biomolecule during ligation and elution phases (Magdeldin & Moser, 2012)

#### 2.9.4.3. Influences of chelate on protein separation

IMAC system is based on the relation of protein and the metal ion in consequence of coordination binding between electron donor part of the protein and immobilized metal ion on resin (Gaberc-Porekar & Menart, 2001). Metal ions can be categorized according to the soft and hard bases and acids system (Pearson, 1973) whereby one atom moves like a Lewis base and other one moves as a Lewis acid while two atoms binding. As stated in this theory, classification can be hard, borderline, and soft.  $Zn^{2+}$ ,  $Ni^{2+}$ ,  $Co^{2+}$ ,  $Cu^{2+}$  are borderline metal ions, and they prefer to bind to oxygen, sulfur and aromatic nitrogen (Gutiérrez, Martín del Valle, & Galán, 2007). These are electron pair acceptors, and ligands include electron-donor atoms such as N, S, and O to create a chelate compound. Various ligands have been used such as nitrilotriacetic acid (NTA) (Hochuli et al., 1988), tris-carboxy-methylated ethylenediamine (TED) (Jerker Porath & Olin, 1983), iminodiacetic acid (IDA) (Jerker Porath & Olin, 1983), carboxy-methylated aspartic acid (CM-Asp) (Wong, Albright, & Wang, 1991), tris(2-aminoethyl)amine (TREN) (Winzerling et al., 1992), etc. Based on number of the coordination binding, the ligand can be classified like bidentate, tridentate, etc.

**Table 2. 12** Structure of ligands (Gaberc-Porekar & Menart, 2001)

| Name  | Structure  | Type         |
|---|--|--------------|
| Iminodiacetic acid (IDA)                      |    | Tridentate   |
| Nitrilotriacetic acid (NTA)                   |    | Tetradentate |
| Carboxymethyl aspartate (CM-Asp)              |   | Tetradentate |
| Tris-carboxy-methylated ethylenediamine (TED) |  | Pentadentate |

Divalent cations indicate different specificity and affinity with various ligands. For example, affinities of metals are in the following order:  $\text{Cu}^{2+} > \text{Ni}^{2+} > \text{Zn}^{2+} > \text{Co}^{2+}$  for IDA (Gaberc-Porekar & Menart, 2001). However, when a comparative ordering is made for the specificity of ions, the comparative ordering becomes to vice versa of adsorption property of chelating ligand (Chaga, 2001). Immobilized  $\text{Cu}^{2+}$ ,  $\text{Ni}^{2+}$ ,  $\text{Zn}^{2+}$ ,  $\text{Co}^{2+}$  ions interact with amino acid residues such as thiol, imidazolyl, and indolyl functional groups on the protein. Besides, phosphate and carboxyl functional groups are in interaction with  $\text{Fe}^{3+}$ ,  $\text{Mg}^{2+}$  ions (Ueda, Gout, & Morganti, 2003).

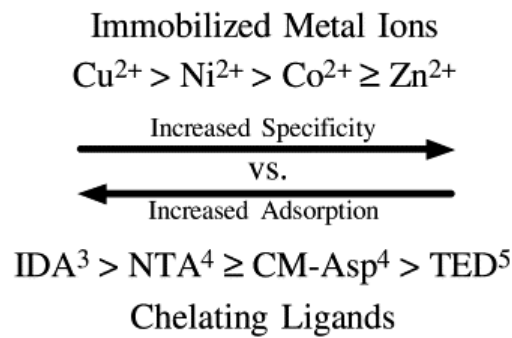


**Figure 2. 13** Comparison of adsorption and specificity (Chaga, 2001)

Number of coordination bond affects the binding strength of metal ion on the ligand. The leaching of metal ions from support becomes hard, the result of metal ions strongly binding to the matrix. On the other hand, free valence number of the metal ion decreases while more coordination bonds provide less leaching. As a result of this decreasing, adsorption capacity decreases during the adsorption step. Furthermore, as a consequence of less valence number, the strength of coordination bond between metal and protein increases. Thus, elution conditions become the harsh situation.

In addition, immobilization of ligand is a crucial parameter to hold binding sites open for binding to metal ions and the target protein (Magdeldin & Moser, 2012). Possible problems are shown in Figure 2.14 during the immobilization of the ligand.

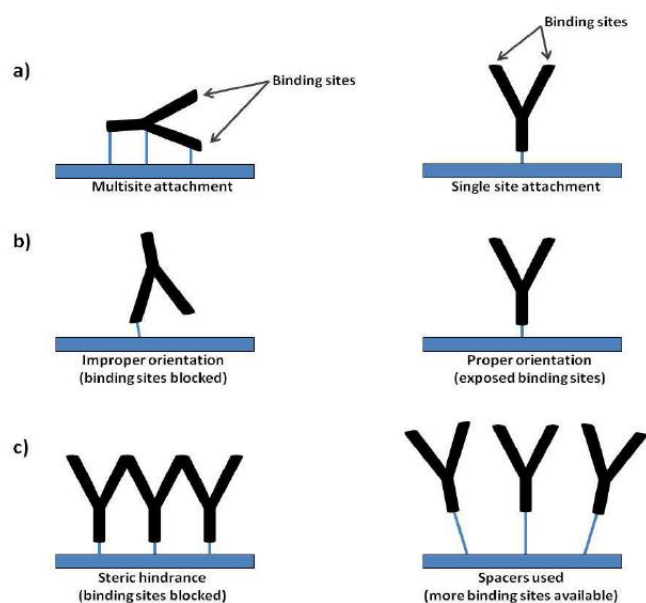


**Figure 2. 14** Possible binding problems of ligand a) multi-site attachment, b) improper orientation, and c) steric hindrance (Magdeldin & Moser, 2012)

#### 2.9.4.4. Influences of support for protein separation

Mainly, support materials or matrices are based on soft-gel matrices, such as agarose, beaded cellulose or cross-linked dextran yet, these are not suitable for chromatography system because they are compressible and restricted in order to low flow rate (Prasanna & Vijayalakshmi, 2010). To provide requirements for fast flow rate, and high efficiency, new matrices should be designed for chromatographic systems. One of the promising supports is porous silica having large pores and providing narrow pore size distribution in this area but non-specific adsorptions and low stability at basic conditions constitute a restriction for protein separation (Gutiérrez et al., 2007). That's why further modifications are required like hydrophilic coating to overcome negative properties of silica. The coating can increase the stability and capacity but pores structure can change, and all point should be coated to prevent any interaction between silica and the target protein. As an option and a new trend, magnetic porous composites can be used with silica or coating to separate protein, and during separation, the magnetic property

provides ease for separation of particles from the medium. If the features expected from a support are listed (Gutiérrez et al., 2007);

- ❖ Large surface area,
- ❖ Easy to derivatize,
- ❖ Small, uniform structure
- ❖ Hydrophilic structure,
- ❖ Chemically inert,
- ❖ Low non-specific adsorption,
- ❖ Stability at different chemical, thermal, physical and mechanic conditions,
- ❖ Allow reuse of columns,
- ❖ Allow the use of high flow rates.

## **2.10. IMAC**

Nowadays, usage of magnetic supports materials becomes a trend for separation of proteins by immobilized metal affinity chromatography. The popularity of this material as a result of exclusive properties such as simple control, rapid purification, automation simplicity and high throughput (Liao, Cheng, & Li, 2007). Various kind of magnetic materials is used with different coatings or supports. NTA/Co<sup>2+</sup>-linked silica/boron-coating was applied on magnetite nanoparticles to prevent iron leakage and non-specific interactions (Liao et al., 2007). IDA/Ni<sup>2+</sup> adsorbed, poly(4-vinylbenzylchloride) (PVBC) shell integrated and silica-coated Fe<sub>3</sub>O<sub>4</sub> magnetic nanoparticles were used for separation of bovine hemoglobin protein (BHb) (Cao et al., 2013). Also, IDA/Ni<sup>2+</sup> immobilized superparamagnetic Fe<sub>3</sub>O<sub>4</sub>@silica core-shell nanoparticles were used for 6xHis-tagged proteins (Mohapatra, Pal, Ghosh, & Pramanik, 2007). Ni<sup>2+</sup>-NTA immobilized, and poly(ethyleneglycol) (PEG) coated magnetic submicron particles (MSP) was used for 6xHis-ECAP (Y. Li et al., 2015).

Additionally, magnetic nanoparticles can be composed of various structures to present new ways and composites for protein separation and purification. For

example, magnetic nanoparticles encapsulated with NTA-phospholipids micelle used for protein immobilization and magnetic probes (Lim et al., 2006). At the same time, nano-magnetite impregnated mesocellular foam (MCF) composite with Cu ligand is another example and by the way, Cu and nano-magnetite added foam composite shows higher protein content and specific activity when the modified foam is compared with MCF and MCF-Cu (Woo, Kwon, & Lee, 2015).

Moreover, different metals or bimetallic supports can be used as an option for separation and purification of the protein. NTA/Ni<sup>2+</sup> modified FePt magnetic nanoparticles (C. Xu et al., 2004), NTA/Ni<sup>2+</sup>-gold (Hainfeld et al., 1999), NTA/Ni<sup>2+</sup>-Fe<sub>3</sub>O<sub>4</sub>/Au composite nanoparticles (Xie et al., 2010) were studied as a support material. Usage of gold is becoming more popular when compared with magnetic nanoparticles. Magnetic nanoparticles can easily aggregate, lose magnetism and stability of surface yet; gold presents chemical stability, biocompatibility; therefore, composite nanomaterials formation with a combination of gold and magnetic nanoparticles provides more opportunity to overcome the disadvantage of magnetic particles.

As an alternative to NTA, IDA and other derivatives, usage of Ni/NiO core/shell nanoparticles can provide a convenient method for separation without any ligand like NTA or IDA (Lee et al., 2006). Also, Fe<sub>3</sub>O<sub>4</sub>@Ni<sub>x</sub>SiO<sub>y</sub> microspheres were used as another material (Wu et al., 2014). Likewise Wu and coworkers study, a magnetic core was combined with a nickel-silica composite matrix to provide fast purification and to exclude coupling step (Frenzel et al., 2003). Furthermore, nickel-based magnetic mesoporous silica such as Ni<sup>2+</sup>-MMS and Ni-MMS also nickel doped silica-coated magnetic nanoparticles (Ni<sup>2+</sup>-MNPs) was used, and Ni<sup>2+</sup>-MMS adsorption efficiency is the highest, 100 ±1.93%, respectively (Lee et al., 2013).

In addition, hydrogels are also used as a support material to separate His-tagged proteins because of the porous structure, modification availability on composition

and features (Yu et al., 2005). Different groups worked on separation of protein with various hydrogels such as 2-Hydroxyethyl methacrylate (HEMA) hydrogel with Ni-NTA complex (Yu et al., 2005), Ni<sup>2+</sup>-poly(2-acetamidoacrylic acid) (PAAA) hydrogel (Ha et al., 2008, 2013). Ha and colleagues results give approximately adsorption of 6xHis-GFP was reached 81% with 59% recovery and almost 99% purity (Ha et al., 2008).

ZIF-8 is a new material in separation area. Therefore, more research is required to understand the interaction between ZIF-8 and protein. Magnetic ZIF-8 nanocomposites (Fe<sub>3</sub>O<sub>4</sub>@ZIF-8) give impressive results especially for the capacity (>6000 mg/g), capture time (10 min) and recyclability (4% loss for 10 cycles), when compared with other magnetic composite material in order to separate bovine hemoglobin (BHb) (Zheng et al., 2015). In another study, ZIF-8 was used for adsorption of oxytetracycline antibiotic in a fixed-bed column (dos Santos Ferreira da Silva et al., 2015). The highest adsorption capacity was attained 28.3 mg/g.

In this study, rhGH and recombinant granulocyte colony stimulating factor (rGCSF) proteins were used as model proteins. If focused on the separation and purification of the target model proteins in studies, it has been observed that agarose-based matrices have been used in the immobilized metal affinity chromatography system for many years. Maisano and friends worked on separation of human growth hormone with commercial Sepharose 6B resin including IDA-agarose combination and with this adsorbent different metal ions were used such as Cu<sup>2+</sup>, Ni<sup>2+</sup>, Co<sup>2+</sup>, Zn<sup>2+</sup>. Co<sup>2+</sup> and Zn<sup>2+</sup> metal ions do not cause any retention but, Cu<sup>2+</sup> ions loaded gels provides strong binding. However, decreasing of pH from 7 to 5 provides elution for Ni<sup>2+</sup> metal ions (Maisano, Testori, & Grandi, 1989). In another study, commercial Ni-NTA agarose column was used to separate recombinant His-hGH, and 90% of hGH can be recovered (Kim et al., 2013).

For GCSF, many types of separation systems were used step by step within a combination. For denatured protein, HPLC AKTA Purifier system, Superdex 75



PG size-exclusion chromatography (SEC) column and to observe correctness of protein folding Zn-IDA chelating Sepharose Fast Flow chromatographic medium was used but, for native protein, any interaction was not detected between IMAC column and G-CSF (Kraševc et al., 2014). Besides, HisTrap HP column was operated two times before and after the TEV protease digestion step. At the first purification, 54% yield was succeeded with 73.3% purity, and at the second step, while yield is decreasing to 36.7%, purity is increasing to 99% (Do et al., 2014).

Other than resins and target proteins, eluents are also a crucial factor for IMAC system. During many years, various materials and chelating agents have been used, and several eluents have also been tested like EDTA, L-histidine, imidazole (Gort & Maloy, 1998), 2-methylimidazole (Zheng et al., 2015) to get more protein at purification step. Especially, imidazole is the most popular eluent but, according to the ligand, chelate and protein properties, used concentrations changes in the literature such as 1 M (Wu et al., 2014), 200 mM (Mohapatra et al., 2007), 100, 250, 500 mM and 1 M (Xie et al., 2010), 10, 80, 500 mM (C. Xu et al., 2004), 0.2 g/ml (Cao et al., 2013) imidazole solutions.

Imidazole can be used alone as an eluent as well as it can be combined with different chemicals to improve the efficiency of purification. As an elution buffer, 1x PBS containing 150 mM NaCl, 200 mM imidazole, 0.1% Triton X- 100, 10% glycerol (Kim et al., 2013), 50 mM Tris-HCl pH=8, 0.5 M NaCl, 0.5 M imidazole (Levarski et al., 2014), 50 mM PB, at pH=8.0 containing 300 mM NaCl, 250 mM imidazole (Frenzel et al., 2003; Ha et al., 2008; Y.-H. Yang et al., 2011) with 0.05% Tween 20 (Liao et al., 2007), 20 mM Tris-HCl containing 0.4 M NaCl and 100 mM imidazole at pH=8.0 (Y. Li et al., 2015) were used.

## 2.11. Metal-organic frameworks (MOFs)

Omar Yaghi and colleagues made metal-organic framework definition for the first time (Yaghi, Li, & Li, 1995). MOFs consist of linking of inorganic and organic parts with a strong bond. The number of synthesized MOFs is more than 20,000 due to the flexibility of size, geometry, and functionality (Furukawa et al., 2013). Therefore, MOFs can be applied in various areas such as hydrogen and methane storage, selective gas adsorption, catalysis, sensor and drug storage and delivery (Kuppler et al., 2009).

### 2.11.1. Zeolitic imidazolate frameworks (ZIFs)

Zeolitic imidazolate frameworks are a special class of MOFs which have been investigated for years and up to now, over 150 ZIF structure was found with the combination of functional groups (Pimentel et al., 2014). The structure of ZIFs consists of imidazole linkers creating a bridge between metal ions (M-Im-M). The ZIFs structure is very similar to aluminosilicate zeolites (Si-O-Si), an angle consists approximately  $145^\circ$  between both of the metal ions and silicon (Bhattacharjee et al., 2014).

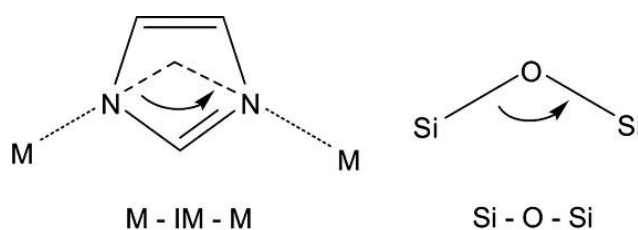


**Figure 2. 15** Bond angle between metal ions and silicones (K. S. Park et al., 2006)

For ZIF synthesis, various metal ions like Zn (II), Ni (II), Co (II), etc. used with different linkers are presented in Figure 2.16.

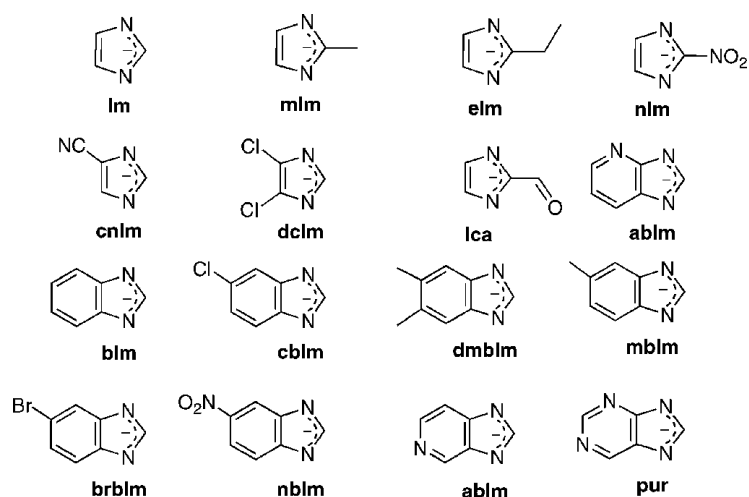


**Figure 2. 16** Imidazole ligands (Phan et al., 2010)

Topologies of ZIFs shows variety through linker-metal combinations (Phan et al., 2010). ZIFs structures can have different topology such as *sod*, *gis*, *dft*, *crb*, *cag*, *gme*, *moz*, *rho*, *bct*, *gar*, *ana*, *mer*, *poz*, *cha*, and *lta* (Banerjee et al., 2008). ZIF topologies can be divided into two main groups based on used linkers like mixed-linker ZIFs and single linker ZIFs. Also used metal ions, synthesis medium, external parameters (temperature, mixing, etc.) are effective on the topology of ZIF crystals (Pimentel et al., 2014). Furthermore, the structure of ZIF does not only exist from the tetrahedral form (Phan et al., 2010). For instance, ZIF-5 is an example to mixed-linker ZIFs. ZIF-5 includes In (III) and Zn (II) ions creating octahedral and tetrahedral structures based upon garnet (*gar*) construction, respectively (K. S. Park et al., 2006).

Changing structure and properties of ZIFs present a significant opportunity for investigation and enhancement of new areas. Especially, ZIFs demonstrate porosity, high surface areas, unimodal micropores, high crystallinity, robust chemical, mechanical and thermal stability. These extraordinary properties of ZIFs allow several applications such as gas storage, gas separation, catalyst, membranes, drug delivery, sensing and in electronic devices (Pan et al., 2011; Chen et al., 2014; Pimentel et al., 2014).

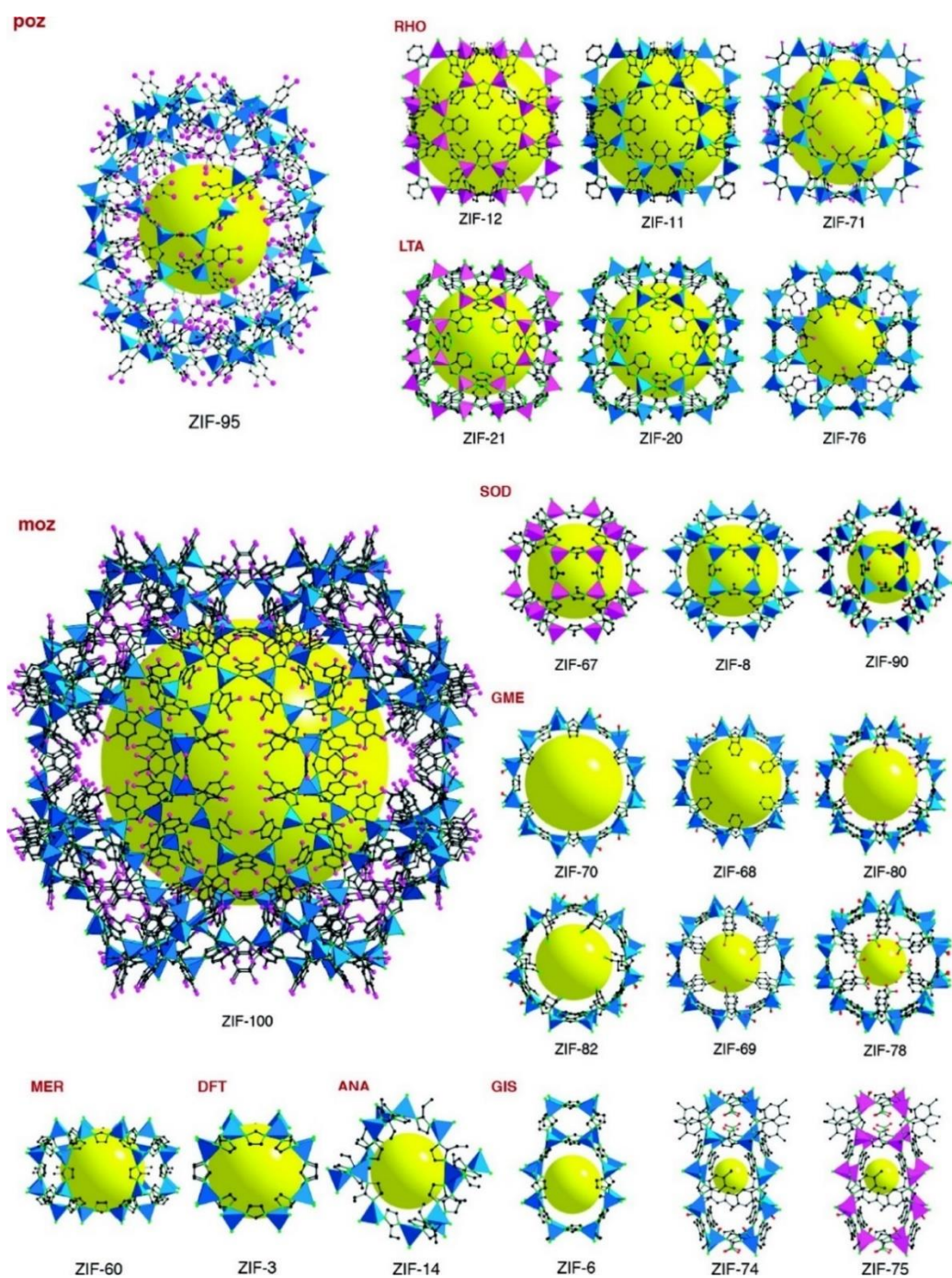


**Figure 2. 17** Crystal structures given and categorized based on topologies (three-letter symbol). ZnN<sub>4</sub> (blue) is the largest cage for all ZIFs, CoN<sub>4</sub> in pink polyhedral. Space in the cage is shown in yellow. H atoms are excluded to provide clear presentation (C, black; N, green; O, red; Cl, pink) (Phan et al., 2010).

### 2.11.1.1. Zeolitic imidazolate framework-8 (ZIF-8)

One of the most focused and studied ZIFs is ZIF-8 consisting of N atoms of imidazole bridging between two Zn metal ions (Venna, Jasinski, & Carreon, 2010). The only difference between of the ZIF-8 and ZIF-67 components is 2-methylimidazole anions bridge Co cations (Qian, Sun, & Qin, 2012). Both of ZIFs type at sodalite (SOD) structure and  $ZnN_4$  and  $CoN_4$  tetrahedral clusters that have 4-, 6-, 8-, and 12- membered rings give tunable nanosized pores (Venna et al., 2010). In addition, ZIFs can have a naturally hydrophobic if the imidazole linkers do not include hydrophilic parts, so ZIF-8 is an example to hydrophobic ZIFs (Zhang, et al., 2013; Ortiz et al., 2014). Zhang and friends stated that even though ZIF-8 has large inner surface area and pore volume, the outer surface of ZIF-8 is becoming more important while ZIF-8 crystals are getting a smaller size. In addition, according to their hypothesize, uncoordinated zinc metals with imidazole linkers occur defect sites showing higher adsorption energy (Zhang et al., 2013). Moreover, the external surface of ZIF-8 shows multifunctionality. Zn cations having low coordination number acting as a Lewis acid sites. Also, N<sup>-</sup> points of imidazole are Lewis and Brønsted bases. On the other hand, NH parts play a role as a Brønsted acid. In addition, ZnO exhibiting basic sites, hydroxyl groups and hydrogenocarbonates on zinc core probably may be slightly acidic and even they can show base features. (Chizallet & Bats, 2010).



**Figure 2. 18** Possible functionality of external surface structure of ZIF-8. Color of atoms are presented in; Zn (green), C (grey), N (blue), H (white), O (red) (Chizallet & Bats, 2010)

Depending on the topology, properties of ZIFs change. In the light of SOD structure of ZIF-8 giving excellent structural properties such as high thermal stability (over 400 °C), pore apertures diameter 3.4 Å, large pore diameter (11.6 Å), large surface area (>1900 m<sup>2</sup>/g) and cubic space group ( $\bar{I}4_3m$ ) with unit cell dimensions of 16.32 Å (H. L. Jiang et al., 2009; K. S. Park et al., 2006; Venna et al., 2010). Also, SOD topology shows mechanical stability up to 0.4 GPa (Bouëssel Du Bourg et al., 2014). ZIF-8 crystal morphology demonstrates the evolution from cube structure with 6 {100} facets to rhombic dodecahedra with 12 {110} facets with time up to get stable morphology (Yao, He, & Wang, 2015).

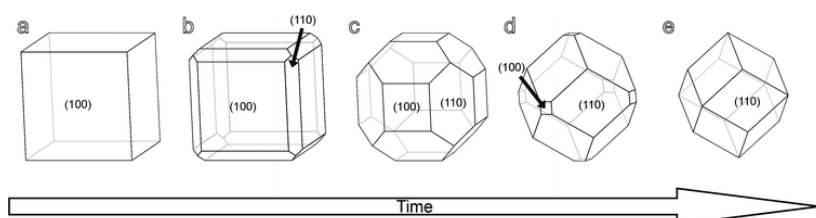


**Figure 2. 19** Structural evolution of crystal morphology with time a) cube, b) cube with truncated edges, c) and d) rhombic dodecahedron with truncated corners (truncated rhombic dodecahedron) and e) rhombic dodecahedron (Cravillon et al., 2012)

Kinetic of ZIF-8 crystals can be divided into three sections which are nucleation, growth and stationary phases. To get homogenous ZIF-8 crystal required time should be given to overcome metastable phases.

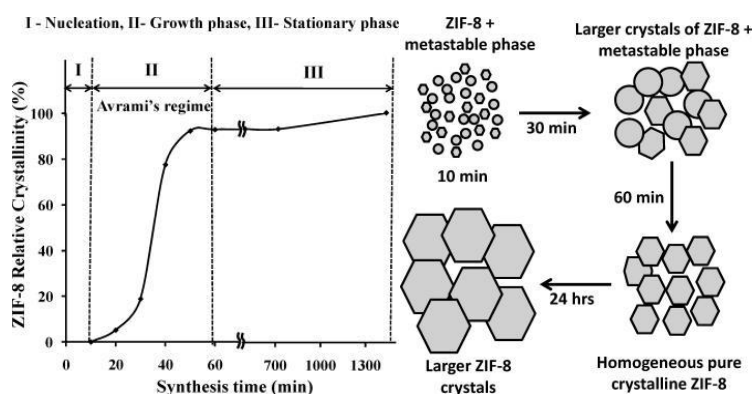


**Figure 2. 20** Formation of ZIF-8 crystals with time (Venna et al., 2010)

ZIF-8 crystal evolution with time consists of three stages;

- i) Fast nucleation occurs less than 10 minutes.
- ii) The growth phase occurs between 10 minutes and an hour.
- iii) The stationary phase occurs over an hour. Crystallization is constant at this step but ZIF-8 crystals become larger at Ostwald ripening. When the energetical situation of particles was considered, smaller particles were utilized for the growth of larger particles. Therefore, 1 hour is convenient for ZIF-8 synthesis to reach a fully developed situation of crystals (Schejn et al., 2014).

Size-controlling of ZIF crystals is succeeded with new methods like the application of extra bidentate ligands as a bridge or different kind of assistant monodentate ligands conjunction with side parts such as alkylamine, N-heterocycle, carboxylate, etc. Auxiliary monodentate ligands show a competitive behavior with multidentate ligands (Cravillon et al., 2011; Tsuruoka et al., 2009). Besides that, modulating/capping (monodentate) ligands are not just moving in a competition, also act as bases on bridging ligands deprotonation (Cravillon et al., 2011). To regulate crystal size and to get nano-sized crystals diverse modulating ligands were used on different ZIF or MOF structures such as sodium formate (Cravillon et al., 2012), 1-methylimidazole (Cravillon et al., 2011; Enomoto, Ueno, Hosono, Hagiwara, & Fujihara, 2017; J. Shi, Wang, Zhang, Tang, & Jiang, 2016; Yanai, Sindoro, Yan, & Granick, 2013), n-butylamine (Cravillon et al., 2011) for ZIF-8 crystals, polyvinylsulfonic acid (sodium salt) for MOF-5 (Hermes et al., 2007), 1-methylimidazole for ZIF-71 (Schweinefuß et al., 2014).

Capping agents/ligands promotes modification of ZIF structures and contributes the usage of ZIFs in new application areas. For instance, 1-methylimidazole provides an opportunity for attachment of fluorescence dyes and other functionalities with the help of surface ligand exchange. (Kondo, Furukawa, Hirai, & Kitagawa, 2010; Yanai & Granick, 2012; Yanai et al., 2013). Thus, new

properties can be gained to ZIF crystals in order to use in separation and purification of proteins and water treatment.

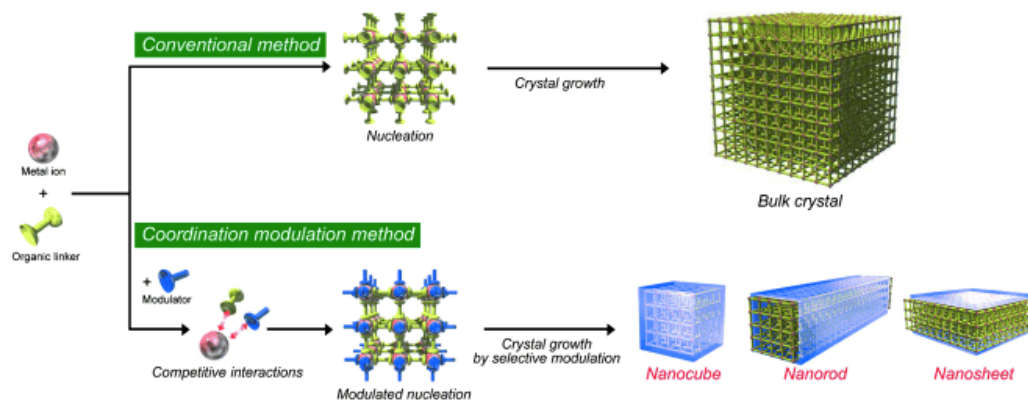


**Figure 2. 21** Conventional synthesis and synthesis with modulating ligand (Tsuruoka et al., 2009).

Additionally, usage of different internal and external conditions like temperature, the ratio of compositions, mixing speed, time are promising factors for size controlling of ZIF crystals. An increment at the Hmim/Zn molar ratio causes higher monodispersity as well as decrease the average particle size. Also, additional Hmim provides chiseled crystal structure. Increasing at the molar ratio of Hmim/Zn causes pH increase, and as a result of this situation, electrostatic repulsion occurs between negatively charged nuclei and particles affected by increasing of ligand deprotonation, at the same time. So, crystals growth becomes slower after nucleation because of inhibition of coagulation between the nuclei and crystals. Crystallization is hereby promoted by reduction of pH (Tanaka, Kida, Okita, Ito, & Miyake, 2012).

When the pH value is increased at nucleation step of crystal formation, deprotonation becomes faster and resulted in fast nucleation. Due to the higher nucleation growth can halt because of the decrement at the supersaturation dramatically. So, the creation of nanocrystals can be produced in the absence of capping agent, too (Guo et al., 2012).



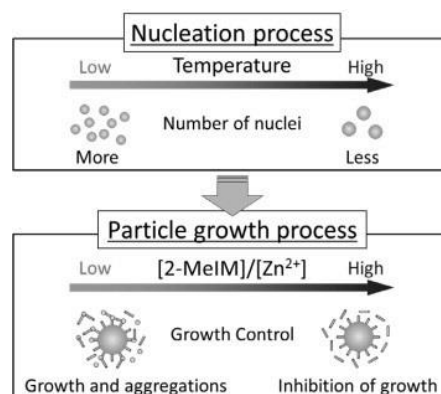


**Figure 2. 22** Composition and temperature effect on nucleation step of ZIF-8 synthesis (2-methylimidazole is shown in 2-MeIM abbreviation) (Yamamoto et al., 2013)

Yamamoto and coworkers (Yamamoto et al., 2013) were stated that mixing of the components caused a reduction in particle size while flow rates of components were increasing at laminar state ( $Re < 2000$ ). Interestingly, any kind of relationship was not observed between the size and shape of the crystal and flow rate while the flow rate was more than  $Re > 2000$  situation (transition state) because of the well-mixing (Yamamoto et al., 2013). Temperature is effective on nucleation step because the solubility of components is related to temperature. Lower temperatures cause less solubility so; nucleation becomes possible due to the high-level supersaturation and concluded with the formation of smaller size crystals (Yamamoto et al., 2013).

#### 2.11.1.2. ZIF-8 synthesis

Various ways can be used for the synthesis of ZIFs but mainly solvothermal/hydrothermal synthesis is used because of the low synthesis temperature, low time consuming, and high textural properties (Bhattacharjee et al., 2014; K. S. Park et al., 2006). Apart from the solvothermal/hydrothermal method, microwave, mechanochemical, microfluidic, electrochemical, dry-gel conversion, sonochemical and solvent-free oxide/hydroxide-based methods present an option for the synthesis of ZIFs (Bhattacharjee et al., 2014).

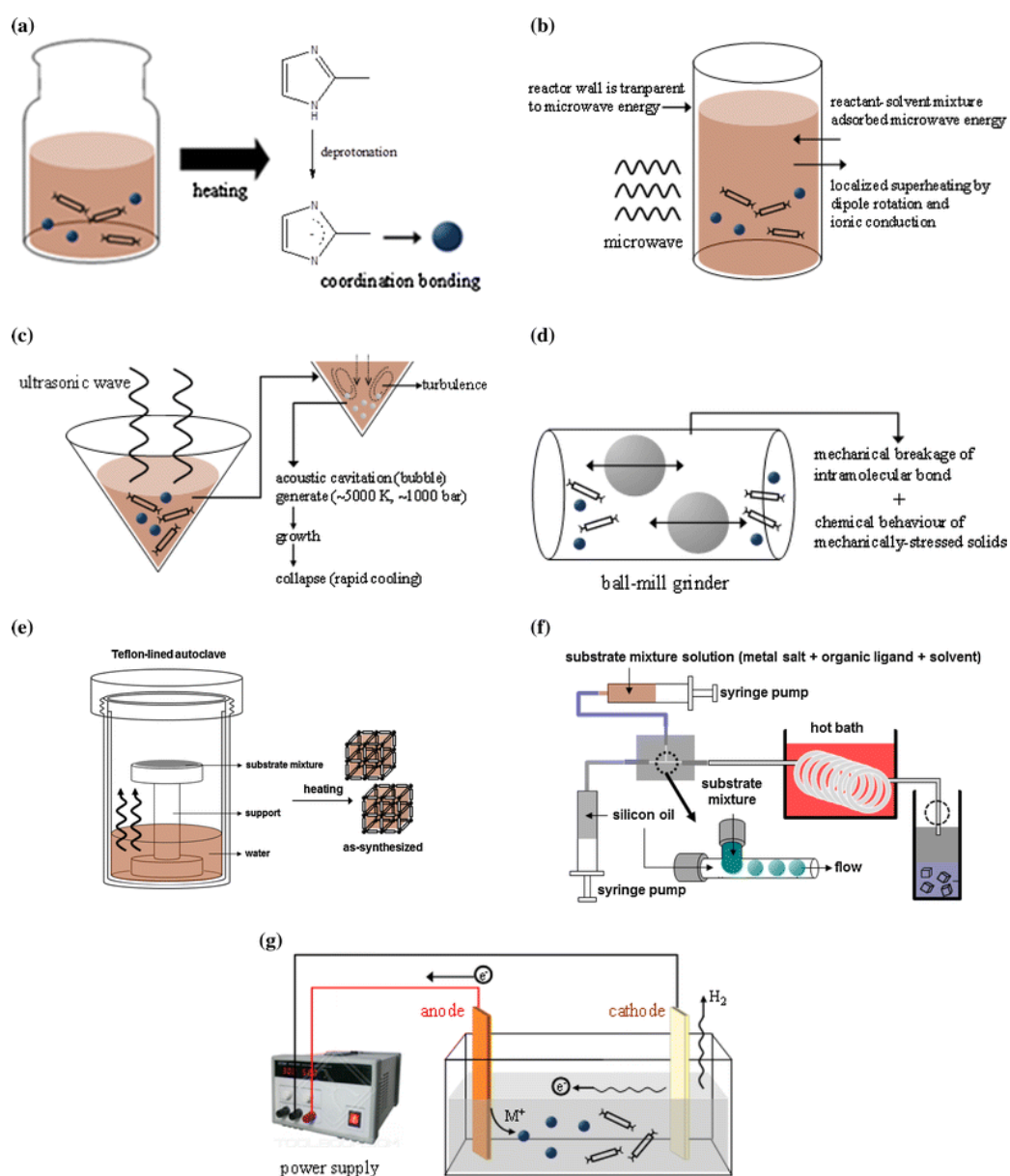


**Figure 2.23** Synthesis methods; a solvothermal, b microwave, c sonochemical, d mechanochemical, e dry-gel conversion, f microfluidic, and g electrochemical method (Bhattacharjee et al., 2014)

In literature, several types of research were done with different components, synthesis methods and conditions at various application areas. In Table 2.13, productions of ZIF-8 were listed with variables.

**Table 2. 13** Studies of ZIF-8 synthesis (Bhattacharjee et al., 2014)

| Synthesis Method                 | Synthesis Conditions |            | Textural Properties |                                      | Comments | References  |
|----------------------------------|----------------------|------------|---------------------|--------------------------------------|----------|---|
|                                  | Solvent              | Temp. (°C) | Time                | S <sub>BET</sub> (m <sup>2</sup> /g) |          |   |
|                                  | DMF                  | 120        | 24 h                | 1644                                 | -        | Ni <sub>60</sub> Rh <sub>34</sub> @ZIF-8, catalyst for hydrogen generation (Xia et al., 2014) |
|                                  | DMF                  | 140        | 24 h                | 1947                                 | 0.663    | Synthesis of ZIF-8 Gas sorption (K. S. Park et al., 2006)                                     |
|                                  | DMF                  | 140        | 24 h                | 1632                                 | -        | Catalyst for Friedel-Crafts Acylation (Nguyen, Le, and Phan, 2012)                            |
|                                  | DMF                  | 140        | 24 h                | -                                    | -        | Calcined ZIF-8 as electrode for supercapacitor applications (Gao et al., 2014)                |
| <b>Solvothermal/Hydrothermal</b> | DMF                  | 140        | 24 h                | 279                                  | 0.9      | Synthesis of micro/nano ZIF-8@MCF (Sue et al., 2014)  |
|                                  | H <sub>2</sub> O     | RT         | 30 min              | 935                                  | 0.64     | Mixed-matrix membrane preparation ethanol/water separation (Pan et al., 2011)                 |
|                                  | H <sub>2</sub> O     | RT         | 5 min               | 1079                                 | 0.31     | Synthesis of ZIF-8 nanocrystals in aqueous system (Jian et al., 2015)                         |
|                                  | H <sub>2</sub> O     | RT         | 5 min               | 1063.5                               | 0.57     | Removal of arsenic from aqueous solutions (Zhao et al., 2015)                                 |
|                                  | H <sub>2</sub> O     | RT         | 5 h                 | 1065                                 | 0.31     | Removal of heavy metal ions from aqueous solutions (Jian et al., 2015)                        |
|                                  | H <sub>2</sub> O     | RT         | 24 h                | 1126                                 | 0.57     | Water-based ZIF-8 synthesis (Jian et al., 2015)   |

**Table 2. 13** Studies of ZIF-8 synthesis (*cont'd*)

| Synthesis Method                 | Synthesis Conditions                          |            | Textural Properties |                                      | Comments   | References  |
|----------------------------------|---|------------|---------------------|--------------------------------------|------------|---|
|                                  | Solvent                                       | Temp. (°C) | Time                | S <sub>BET</sub> (m <sup>2</sup> /g) |            |   |
|                                  | MeOH  | RT         | 1 h                 | 1710 ±60                             | 0.58 ±0.03 | Sonication-induced Ostwald ripening of ZIF-8 nanoparticles<br>(Thompson et al., 2012)   |
|                                  | ZIF-8/polymer composite membranes             |            |                     |                                      |            |   |
|                                  | Separation of CO <sub>2</sub> /N <sub>2</sub> |            |                     |                                      |            |   |
|                                  | MeOH  | RT         | 8 h                 | -                                    | -          | Catalyst for styrene carbonate synthesis (Zhu et al., 2013)                             |
|                                  | MeOH  | RT         | 24 h                | 1264                                 | 0.51       | Adsorption of CO <sub>2</sub> , CH <sub>4</sub> , N <sub>2</sub> (Nune et al., 2010)    |
|                                  | MeOH  | 70         | 15 min              | 1652.9                               | 0.77       | HPLC separation (Fu, Yang, & Yan, 2013)   |
|                                  | MeOH  | 90         | 6 h                 | 1839                                 | 0.74       | Synthesis of ZIF-8/carbon nanotube composites (Yang et al., 2014)                       |
|                                  | MeOH  | 120        | 5 h                 | 1256.1                               | 0.6        | Removal of Congo red from aqueous solution (Jiang et al., 2016)                         |
| <b>Solvothermal/Hydrothermal</b> | MeOH  | 150        | 5 h                 | 1072                                 | 0.53       | ZIF-8 membranes for CO <sub>2</sub> /CH <sub>4</sub> separation (Venna & Carreon, 2010) |
|                                  |   |            | 20 min              | 180                                  |            |   |
|                                  |   |            | 30 min              | 193                                  |            |   |
|                                  |   |            | 40 min              | 489                                  |            |   |
|                                  | MeOH  | 150        | 50 min              | 613                                  | -          | Structural evolution of ZIF-8 (Venna et al., 2010)                                      |
|                                  |   |            | 1h                  | 744                                  |            |   |
|                                  |   |            | 12 h                | 814                                  |            |   |
|                                  |   |            | 24 h                | 798                                  |            |   |

**Table 2. 13** Studies of ZIF-8 synthesis (*cont'd*)

| Synthesis Method          | Synthesis Conditions                 |                | Textural Properties |                                      | Comments  | References   |
|---------------------------|--------------------------------------|----------------|---------------------|--------------------------------------|-----------|--|
|                           | Solvent                              | Temp. (°C)     | Time                | S <sub>BET</sub> (m <sup>2</sup> /g) |           |  |
| <b>Microwave</b>          | DMF                                  | 140            | 3 h                 | 646                                  | 0.23      | Comparison of conventional and microwave synthesis (J. H. Park, Park, & Jung, 2009)      |
|                           | MeOH                                 | 100            | 4 h                 | 1496                                 | 0.77      | ZIF-8 membrane preparation (Bux et al., 2009)  |
|                           | Ionic liquid [bmin]BF <sub>4</sub>   | 140            | 1 h                 | 471                                  | 0.34      | Comparison of conventional and microwave synthesis (L. Yang & Lu, 2012)                  |
| <b>Mechanochemical</b>    | H <sub>2</sub> O                     | 120            | 30 min              | 1075                                 | 0.49      | Synthesis study (Bao et al., 2013)   |
|                           | Ethanol                              | RT/40 Hz       | 30 min              | 1390                                 | -         | Substituting Zn with Ni (Li, et al., 2014)   |
| <b>Sonochemical</b>       | Ethanol                              | RT/40 Hz       | 30 min              | -                                    | -         | Introduction of poloxometallates on ZIFs<br>Methylene blue adsorption (Li, et al., 2014) |
|                           | DMF                                  | 45-60<br>110 W | 4-9 h               | -                                    | -         | Comparison of conventional and sonochemical synthesis (Seoane et al., 2012)              |
| <b>Dry-gel conversion</b> | DMF                                  | 60%            | 2 h                 | 1174                                 | 0.5       | Knoevenagel reaction (Cho et al., 2013)  |
|                           | H <sub>2</sub> O (liquid phase)      | 120            | 24 h                | 1470                                 | 0.69      | ZIF-8 as additives to liquid lubricants (Shi et al., 2011)                               |
| <b>Electrochemical</b>    | DMF, H <sub>2</sub> O, MeOH, Ethanol | RT             | 10 min              | 1262-1695                            | 0.56-0.66 | Influence of the solvent, temperature and density (Martinez Joaristi et al., 2012)       |

**Table 2. 13** Studies of ZIF-8 synthesis (*cont'd*)

| Synthesis Method             | Synthesis Conditions  |            |       | Textural Properties                  |  |   | References              |
|------------------------------|-----------------------|------------|-------|--------------------------------------|--|---|-------------------------|
|                              | Solvent               | Temp. (°C) | Time  | S <sub>BET</sub> (m <sup>2</sup> /g) | V <sub>porc</sub> (cm <sup>3</sup> /g) | Comments  |                         |
| <b>Oxide/hydroxide-based</b> | Solvent/additive-free | 180        | 12 h  | 1450                                 | 0.56                                   | Synthesis and CO <sub>2</sub> adsorption  | (Lin et al., 2011)      |
| <b>solvent-free</b>          | Solvent free          | 100-160    | -     | 1961                                 | -                                      | Synthesis study   | (Lanchas et al., 2012)  |
| <b>Microfluidic</b>          | MeOH                  | 50         | 5 min | -                                    | -                                      | Synthesis of Fe <sub>3</sub> O <sub>4</sub> @ZIF-8 magnetic core-shell microspheres<br>Knoevenagel reaction | (Faustini et al., 2013) |
|                              | H <sub>2</sub> O      | RT         | 1 h   | -                                    | -                                      | N <sub>2</sub> gas adsorption   | (Yamamoto et al., 2013) |

Besides the synthesis methods, zinc source and solvent effects are also important for each production process of ZIF-8. Not only are DMF and methanol more expensive and toxic organic solvents, but it is also challenging to remove DMF, especially from crystal pores. For the purpose of overcome these problems, new green solvents should be used, like water. In spite of the fact that, water is cheap and non-toxic, it requires an extra amount of Hmim for ZIF-8 synthesis (He et al., 2014; Jian, Liu, Liu, et al., 2015).

Several studies have worked on zinc sources;  $\text{ZnBr}_2$ ,  $\text{Zn(OAc)}_2$ ,  $\text{ZnSO}_4$ ,  $\text{ZnI}_2$ ,  $\text{ZnCl}_2$ , and  $\text{Zn(NO}_3)_2$  to understand effects on synthesis.  $\text{Zn(OAc)}_2$  and  $\text{ZnSO}_4$  was found useful salt sources to get well-shaped ZIF-8 crystals with the less Hmim amount and larger particle size (Jian, Liu, Liu, et al., 2015).





## CHAPTER 3

### MATERIALS AND METHODS

#### 3.1. Chemicals

All chemicals were analytical grade products attained from Merck Ltd., Sigma Ltd., and TCI Ltd.

#### 3.2. Microorganism and Plasmid

For rhGH production, recombinant *P. pastoris* single copy strain pGAPZ $\alpha$ A::hGH was used (Massahi and Çalık, 2016). The constructed recombinant microorganisms were stored in microbank in -80 °C.

#### 3.3. Growth Media

All growth media were sterilized at 121 °C for 20 minutes and antibiotics were added at the below 50 °C.

##### 3.3.1. Solid Media

Stored recombinant *P. pastoris* strains in the microbank were inoculated on yeast extract-peptone-dextrose (YPD) agar containing antibiotic, Zeocin, which was stored at 4 °C.

**Table 3. 1** Solid YPD medium composition

| <b>Compound</b>      | <b>Concentration g/L</b> |
|----------------------|--------------------------|
| <b>Yeast Extract</b> | 10                       |
| <b>Peptone</b>       | 20                       |
| <b>Agar</b>          | 20                       |
| <b>Dextrose</b>      | 20                       |
| <b>Zeocin*</b>       | 0.25 ml                  |

\*Added after sterilization and cooling

### 3.3.2. Pre-cultivation Media

Harvested grown recombinant *P. pastoris* strain on YPD agar was transferred into the precultivation media, buffered glycerol complex medium (BMGY). The composition of the BMGY is given in Table 3.2. After sterilization step, biotin and chloramphenicol were added to the precultivation media.

**Table 3. 2** BMGY composition

| <b>Compound</b>                                   | <b>Concentration g/L</b> |
|---|--------------------------|
| <b>Yeast Extract</b>                              | 10                       |
| <b>Peptone</b>                                    | 20                       |
| <b>Potassium Phosphate Buffer (pH=6.0)</b>        | 0.1 M                    |
| <b>Yeast Nitrogen Base (YNB) (w/o aminoacids)</b> | 13.4                     |
| <b>Ammonium Sulphate</b>                          | 10                       |
| <b>Glycerol</b>                                   | 10                       |
| <b>After Sterilization</b>                        |                          |
| <b>Biotin</b>                                     | $4 \times 10^{-5}$       |
| <b>Chloramphenicol</b>                            | 1 ml                     |

### 3.3.3. Carbon Source Starvation Media (Synchronization)

Yeast extract and peptone were used as a carbon source starvation media. Chloramphenicol was added after sterilization.

**Table 3. 3** Composition of carbon source starvation medium

| <b>Compound</b>         | <b>Concentration g/L</b> |
|-------------------------|--------------------------|
| <b>Yeast Extract</b>    | 10                       |
| <b>Peptone</b>          | 20                       |
| <b>Chloramphenicol*</b> | 1 ml                     |

\*Added after sterilization and cooling

### 3.3.4. Production media

After carbon source starvation, grown *P. pastoris* pGAPZ $\alpha$ A::hGH strain (Massahi and Çalık, 2016) was harvested by centrifugation and inoculated into the production medium. Basal salt medium (BSM) was used for pilot scale fed-batch bioreactor experiments. PTM1 was used after sterilization by 0.2  $\mu$ m syringe filter. 10% v/v diluted antifoam was sterilized in an autoclave and then used.

**Table 3. 4** Composition of production medium, BSM

| <b>Compound</b>                         | <b>Concentration g/L</b> |
|---|--------------------------|
| <b>85% H<sub>3</sub>PO<sub>4</sub></b>  | 26.7 ml                  |
| <b>CaSO<sub>4</sub>.2H<sub>2</sub>O</b> | 1.17                     |
| <b>MgSO<sub>4</sub>.7H<sub>2</sub>O</b> | 14.9                     |
| <b>KOH</b>                              | 4.13                     |
| <b>K<sub>2</sub>SO<sub>4</sub></b>      | 18.2                     |
| <b>Glycerol</b>                         | 40                       |
| <b>After Sterilization</b>              |                          |
| <b>Chloramphenicol</b>                  | 1 ml                     |
| <b>PTM1</b>                             | 4.35 ml                  |
| <b>Antifoam*</b>                        | 1 ml                     |

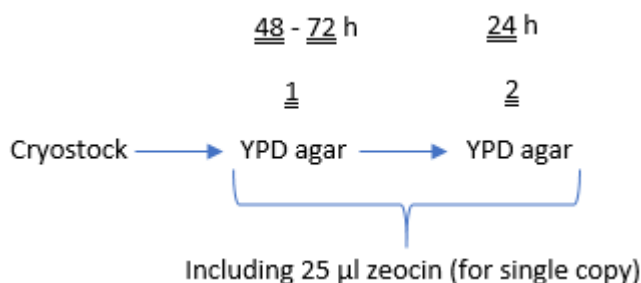
\*Sterilized before adding

**Table 3. 5** Composition of trace salt solution, PTM1

| Compound  | Concentration g/L |
|---|-------------------|
| CuSO <sub>4</sub> .5H <sub>2</sub> O                | 6                 |
| NaI   | 0.08              |
| MnSO <sub>4</sub> .H <sub>2</sub> O                 | 3                 |
| Na <sub>2</sub> MoO <sub>4</sub> .2H <sub>2</sub> O | 0.2               |
| H <sub>3</sub> BO <sub>3</sub>                      | 0.02              |
| ZnCl <sub>2</sub>                                   | 20                |
| FeSO <sub>4</sub> .7H <sub>2</sub> O                | 65                |
| CoCl <sub>2</sub>                                   | 0.5               |
| H <sub>2</sub> SO <sub>4</sub>                      | 5                 |
| Biotin  | 0.2               |

### 3.4. Recombinant human growth hormone production

Initially, *P. pastoris* strains in microbank were inoculated on a YPD agar. The agar waited at 30 °C for 48-72 hours in an incubator. Then, grown microorganisms harvested and again they were inoculated at 30 °C for 24 hours on another agar.



End of the 24<sup>th</sup> hours of the second YPD agar, microorganisms were transferred into the pre-cultivation medium in the 250-ml shake-flask bioreactors (baffled erlenmeyer flasks). The working volume of the pre-cultivation medium was 50 ml. To get same optical density, cultivation of microorganisms from agar to pre-cultivation medium, the harvested amount should be equal. The flasks were placed into a shaker which was set to 30 °C and 175-225 rpm for inoculation. The pre-cultivation proceeded 15-18 hours to reach OD<sub>600</sub>=16. After, the medium was

centrifuged at 2000 rcf and 10 °C to separate microorganisms. Centrifugation was repeated two times; the first centrifugation was for 2 minutes, the second one was for 3 minutes. The collected pellets were dissolved in the 50-ml carbon source starvation medium and transferred again into the 250-ml shake-flask bioreactors (baffled erlenmeyer flasks). For the synchronization step, shaker was set to 200 rpm and 30 °C for 6 hours. End of the carbon source starvation, optical densities were analyzed from MilliporeSigma Spectroquant Pharo 300 Spectrophotometer. at 600 nm to calculate the volume of medium containing the required amount of microorganism to provide  $OD_{600}=2$  ( $1 \times 10^8$  cells/ml) for working volume (WV), 1.9 L, in the pilot scale bioreactor.

$$V_{WV} * 2 OD_{600} = V * \text{Read } OD_{600} * \text{Dilution Factor} \quad (3.1)$$

According to the calculated volume, V, the carbon source starvation medium was weighed in falcon tubes and centrifuged at 2000 rcf and 10 °C for the firstly 2 minutes, the secondly 3 minutes. The centrifuged pellets were solved in the 50-ml sterilized UP water and transported into the BSM medium with a peristaltic pump in the pilot scale bioreactor. The overview of the bioreactor was given in Figure 3.1.

Before the transportation of the BSM and the microorganisms into the bioreactor, preliminary of the bioreactor should be done. After the pH calibration, sterilization and O<sub>2</sub> calibration the reactor became ready for fermentation step. The bioreactor later filled with sterilized 1.8 L BSM medium with peristaltic pump and agitation rate (N) was adjusted to 600 rpm for batch mode. The pH of BSM medium was adjusted to  $5.5 \pm 0.1$  with ammonia solution 28-30%. Also, the temperature and the dissolved oxygen concentration (C<sub>DO</sub>) were set to 30 °C and 20%. When the all adjustments were finished and the sterilization mode of the bioreactor was changed to fermentation mode, the microorganisms are solved in 50 ml sterilized UP water and transported in the bioreactor. After the pH adjustment and the adding of the microorganism, the working volume reached to 1.9 L. To prevent foam during the

process, sterilized 10% v/v antifoam solution was used. The batch mode took 18-19 hours approximately.

When the cell concentration,  $C_x$ , was reached to 21-24 g/L, the fed-batch mode was started. For calculation of the exponential feeding profile of the glucose solution at the fed-batch mode, dynamic flow rate ( $Q_s$ ) was calculated for the pre-determined specific growth rate;

$$Q_s = \frac{\mu_0 * C_{X_0} * V_0}{Y_{X/S} * (C_s^0 - C_s)} \exp(\mu_0 * t) \quad (3.2)$$

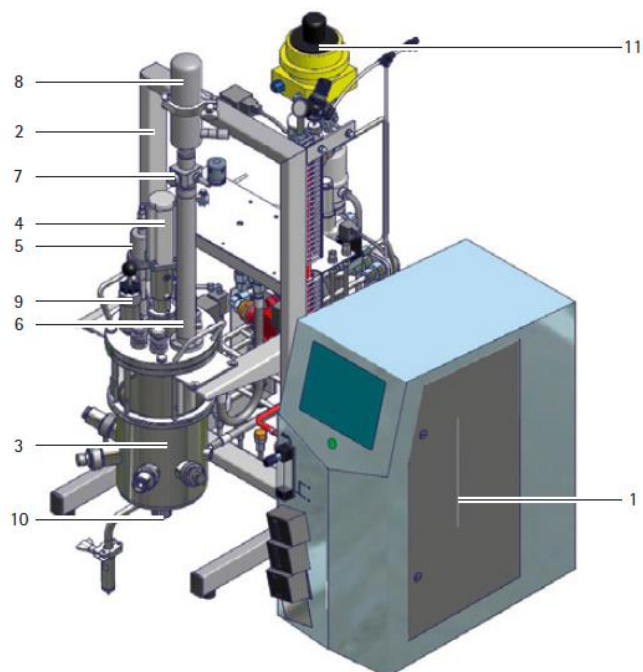
where  $Q_s$  (L/h) is the volumetric flow rate of the feed,  $C_{X_0}$  (g/L) is the initial cell concentration at fed-batch mode,  $\mu_0$  ( $h^{-1}$ ) is the pre-determined specific growth rate,  $V_0$  (L) is the initial working volume of the fed-batch mode,  $Y_{X/S}$  ( $g\ g^{-1}$ ) is the cell yield on the substrate,  $C_s^0$  (g/L) is the feed substrate concentration at the beginning, and  $C_s$  is the substrate concentration at any time in the bioreactor.  $C_s$  was accepted zero during the fed-batch mode. In the fed-batch mode,  $V_0 = 1.9$  L,  $C_{X_0} = 21.5$  g/L,  $\mu_0 = 0.1\ h^{-1}$ ,  $C_s^0 = 500$  g/L,  $Y_{X/S} = 0.47\ g\ g^{-1}$ . For the calculation of  $C_x$ , the equation is;

$$C_x = \text{Read OD}_{600} * \text{Dilution Factor} * 0.24 \quad (3.3)$$

0.24 is the calibration constant for MilliporeSigma Spectroquant Pharo 300 Spectrophotometer.

Before the fed-batch, time profile was entered to the control mechanism of the bioreactor and then, 12 ml/L PTM1 solution was added into the 500 g/L sterilized glucose anhydrous solution and it was connected to bioreactor with a peristaltic pump. According to the time profile, glucose was given automatically into the bioreactor. The PTM1 solution is light sensitive so the glucose solution including PTM1 should be protected from the light. The DO, temperature, pH, base-, antifoam-, addition and substrate volume were recorded at every 30 minutes. Also,

every 3 hours, the sample was taken from the system and OD<sub>600</sub> was read. 2 production medium, 2 pellet, 5 supernatant and 3 filtrate samples were stored in 80 °C for future experiments.



| Pos. | Description                                 |
|------|---|
| 1    | Control unit with pumps and aeration module |
| 2    | Frame                                       |
| 3    | Culture vessel                              |
| 4    | Drive motor                                 |
| 5    | Supply air filter                           |
| 6    | Exhaust cooler                              |
| 7    | High foam adapter (optional)                |
| 8    | Exhaust air filter                          |
| 9    | Culture vessel safety valve                 |
| 10   | Floor drain valve                           |
| 11   | Pressure control valve (optional)           |

**Figure 3. 1** BIostat Cplus bioreactor overview

### 3.4.1. Organic acid analysis

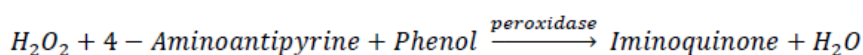
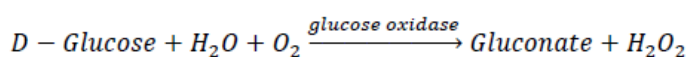
Waters, Alliance 2695 model High-Performance Liquid Chromatography (HPLC) was used to analyze organic acid concentrations in the medium. Dilutions were made by injection volume for calibration curves given in Appendix C.

**Table 3. 6** Organic acid measurement parameters for HPLC system (Ileri & Çalik, 2006)

| Column                       | Capital Optimal ODS, 5µm   |
|------------------------------|--|
| Column dimensions            | 4.6x250 mm   |
| System                       | Reversed phase chromatography  |
| Mobile phase                 | 3.12% NaH <sub>2</sub> PO <sub>4</sub> (w/v) and %0.62x10 <sup>-3</sup> (v/v) H <sub>3</sub> PO <sub>4</sub> |
| Mobile phase flow rate       | 0.8 mL/min   |
| Column temperature           | 30°C   |
| Detector type and wavelength | Waters 2487 Dual absorbance detector, 210 nm   |
| Detector temperature         | 30°C   |
| Injection volume             | 5 µL   |
| Analysis period              | 15 min   |
| Space time                   | 5 min  |

### 3.4.2. Glucose analysis

Unconsumed glucose concentration in the production medium was measured with Biyozim-Biasis Glucose Analysis Kit and 505 nm was used to detect glucose in the medium. The detection principle of the glucose analysis kit is that D-glucose is catalyzed with glucose oxidase and hydrogen peroxide and gluconate were produced as a result of this reaction. Thereafter, as a result of the reaction of hydrogen peroxide with 4-aminoantipyrine and phenol, iminoquinone and water are produced at the presence of peroxidase used as a catalyzer. In a conclusion, a red color is obtained which is parallel to the glucose concentration and the iminoquinone concentration.

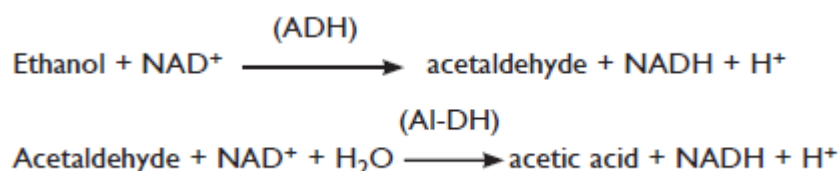




### 3.4.3. Ethanol analysis

Ethanol accumulation in the production medium was measured with Megazyme Ethanol Kit. The principle of the kit is that to measure ethanol amount in the production medium two enzyme reactions are requiring and the first one is that;

Nicotinamide-adenine dinucleotide ( $\text{NAD}^+$ ) is used to oxidize the ethanol to acetaldehyde under the presence of alcohol dehydrogenase (ADH). The second one is oxidation of acetaldehyde which is produced from the first reaction. The second reaction is applied at the presence of the aldehyde dehydrogenase (Al-DH) and  $\text{NAD}^+$ . Acetic acid is produced as a result of oxidation of acetaldehyde. Also,  $\text{NADH}$  and  $\text{H}^+$  occur at the end of the reaction. The amount of  $\text{NADH}$  is stoichiometric with twice the ethanol amount.  $\text{NADH}$  is analyzed at 340 nm.



### 3.4.4. Homogenization and preparation of rGCSF medium

As rGCSF is produced as an intracellular protein (Ersoy, 2017) and cell disruptor (Constant Systems Ltd. Z plus series) was used at 2 kbar to disrupt the cell wall. The reactor medium was passed from the disruptor three times. Thereafter, the medium was prepared to separation and purification step. To clean debris and to solubilize the inclusion bodies, urea solution was used (Ersoy, 2017). Initially, 40 ml 2.5 M urea was added on to the 10-ml medium and during 15 minutes the mixture was shaken in ice. Then, the falcon tube was centrifuged at 10,000 rcf and 25 °C for 10 minutes and the supernatant was separated. This step was repeated once more. As the last step for the preparation of the medium, 7.5 M urea solution was added on to the pellet and shaken in ice for 6 hours. Centrifuge step was repeated at same conditions and the final supernatant was stored for later steps (Ersoy, 2017).

### 3.5. ZIF-8 Synthesis

#### 3.5.1. Procedure of ZIF-8 synthesis

An empty beaker was weighed. Then, 2.4 gr zinc nitrate hexahydrate ( $\text{Zn}(\text{NO}_3)_2 \cdot 6\text{H}_2\text{O}$ , 98%) was weighed and added into the 90.4 gr methanol (MeOH, 98%) which was mixed in the beaker. In another beaker, 90.4 gr methanol (MeOH, 98%) and 5.28 gr 2-methylimidazole (Hmim, 99%) were mixed in the beaker. At room temperature, to provide homogeneity, both of the beakers were stirred at 700 rpm on different magnetic stirrers. When both of the mixtures became homogeneity, the  $\text{Zn}(\text{NO}_3)_2 \cdot 6\text{H}_2\text{O}$  mixture was added into the mixture of Hmim. The final solution was mixed at 700 rpm for 1 hour (Venna et al., 2010). The molar composition of the mixture is  $\text{Zn}^{+2}:7.9$  Hmim:695.1 MeOH. At the end of the 1 hour, the mixture was centrifuged in 50 ml falcon tubes at 6000 rpm for 5 min. At the end of the centrifuge, the liquid phase was separated in each tube and put into the weight known beaker to weigh liquid phase. After all of the mixtures were centrifuged, tubes were washed with MeOH gently and then placed into the centrifuge again. For washing, the centrifuge was set to 6000 rpm for 20 min. This step was repeated two times. At the end of the washing, the liquid part was transferred into another weight known beaker, and the waste MeOH was weighed to calculate the excess amount of Zn and Hmim. Finally, after the washing, the solid part was dried at 80 °C overnight.

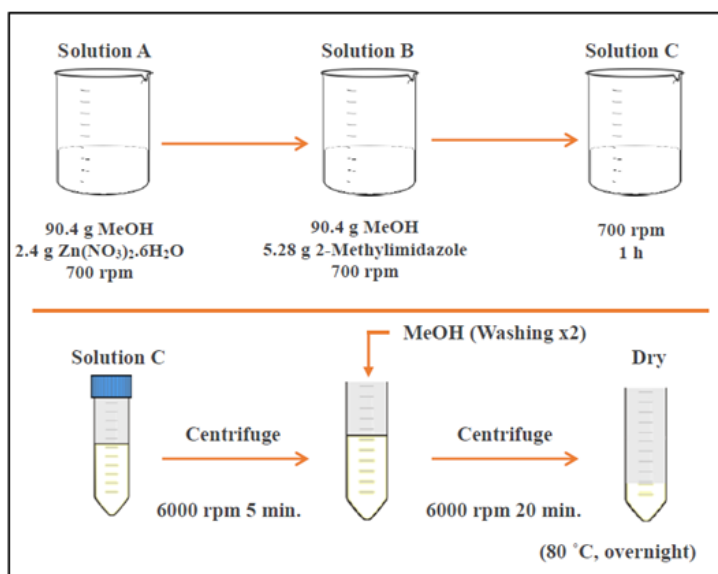


**Figure 3. 2** Procedure of ZIF-8 synthesis

### 3.5.2. Procedure of bimetallic ZIF-8 synthesis (Ni/ZIF-8)

Zn(NO<sub>3</sub>)<sub>2</sub>·6H<sub>2</sub>O (1.0 mmol) and Ni(NO<sub>3</sub>)<sub>2</sub>·6H<sub>2</sub>O (1.0 mmol) were weighed and added into the 30 ml methanol (MeOH, 98%) which was mixed in the beaker. 30 ml methanol (MeOH, 98%) and Hmim (15.8 mmol) were mixed in another beaker. At room temperature, to provide homogeneity, both of the beakers were stirred at 700 rpm on different magnetic stirrers. When both of the mixtures became homogeneity, the mixture of Zn(NO<sub>3</sub>)<sub>2</sub>·6H<sub>2</sub>O and Ni(NO<sub>3</sub>)<sub>2</sub>·6H<sub>2</sub>O was added into the mixture of Hmim. The final solution was mixed at 700 rpm for 24 hours (R. Li, Ren, Ma, et al., 2014). At the end of the 24 hours, the mixture was centrifuged in 50 ml falcon tubes at 6000 rpm for 10 min. At the end of the centrifuge, the liquid phase was separated in each tube and put into the weight known beaker to weigh liquid phase. After all of the mixtures were centrifuged, tubes were washed with MeOH gently and then placed into the centrifuge again. For washing, the centrifuge was set to 6000 rpm for 20 min. This step was repeated three times. At the end of the washing, the liquid part was transferred into another weight known beaker, and the waste MeOH was weighed to calculate the excess amount of Zn and Hmim. Finally, after the washing, the solid part was dried at 80 °C overnight.

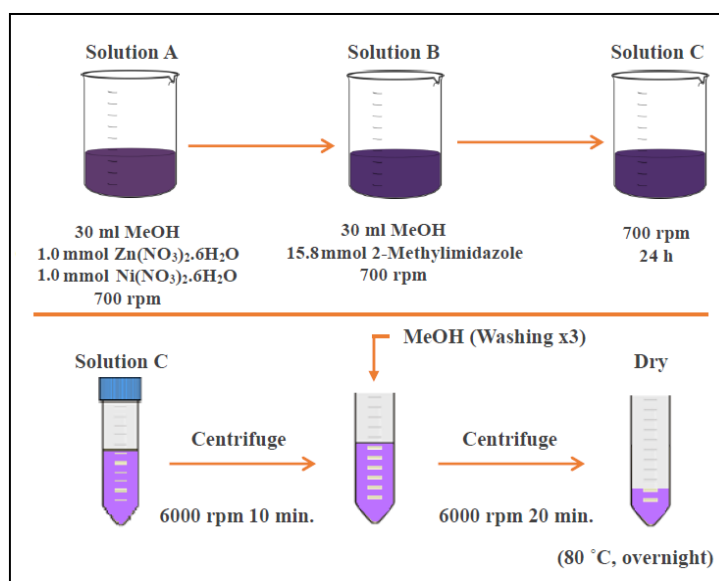


**Figure 3. 3** Procedure of Ni/ZIF-8 synthesis

### 3.5.3. Nickel impregnation on ZIF-8 (Ni-ZIF-8)

0.29 g  $\text{Ni}(\text{NO}_3)_2 \cdot 6\text{H}_2\text{O}$  was weighed in a 100-ml beaker (1 mmol) and 50 ml UP water was added to it. The mixture was mixed at room temperature and 700 rpm up to get a homogeneous solution. Another 100-ml beaker was prepared and 1 g ZIF-8 was weighed in the beaker and 50 ml UP water was added to it. The ZIF-8 suspension was prepared at same conditions like  $\text{Ni}(\text{NO}_3)_2 \cdot 6\text{H}_2\text{O}$  solution. Then,  $\text{Ni}(\text{NO}_3)_2 \cdot 6\text{H}_2\text{O}$  solution was added into ZIF-8 suspension. The final mixture was mixed at 700 rpm and room temperature during 12 hours. End of the 12 hours mixture was centrifuged at 6000 rpm for 20 minutes. Collected Ni-ZIF-8 particles were washed with water two times and centrifuged again at 6000 rpm and 20 minutes. Finally, the Ni-ZIF-8 particles were dried at 80 °C during the overnight.

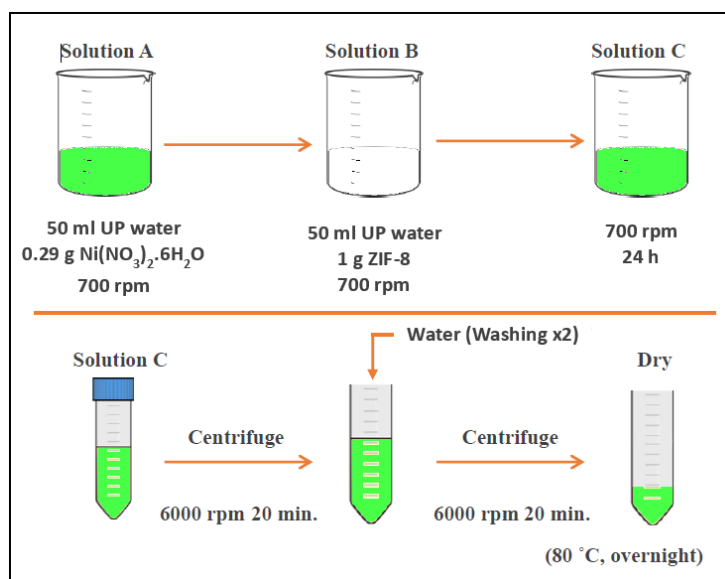


**Figure 3. 4** Nickel impregnation on ZIF-8 (Ni-ZIF-8)

#### 3.5.4. Synthesis of ZIF-8 with modulating ligand 1-methylimidazole

For the production of ZIF-8 with modulating ligand 1-methylimidazole (1-MI-ZIF-8), 2.4 g of zinc nitrate hexahydrate was dissolved in 90.4 g methanol. Another solution was prepared with 2.64 g of 2-methylimidazole, 2.64 g of 1-methylimidazole, and 90.4 g of MeOH. End of the 3 hours mixing at 700 rpm, the mixture was centrifuged at 6000 rpm for 10 minutes. Finally, the 1-MI-ZIF-8 particles were dried at 80 °C during the overnight.

#### 3.5.5. Surface modifications

For future works, surface modifications were also worked on ZIF-8 and 1-MI-ZIF-8 crystals. The study of Yanai and Granick was applied for surface ligand exchange method (Yanai & Granick, 2012). The obtained 1-MI-ZIF-8 particles dispersed in methanol (0.1 wt%, calculated based on the dried particle weight). 0.75 ml of 1 mM methanol solution of the histamine dihydrochloride was added to 13 ml of the particle dispersion. The mixture was incubated at 700 rpm and room temperature

for 24 hours. The incubated particles were washed with methanol three times then dried at 80 °C for overnight.

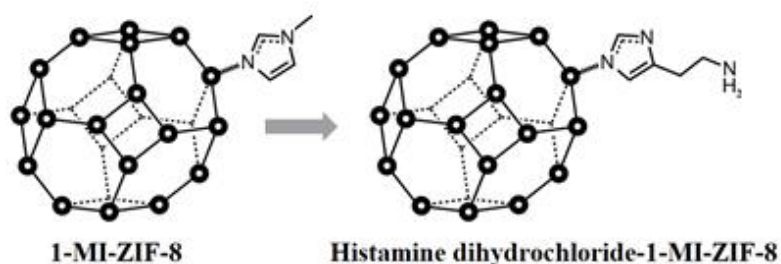


**Figure 3. 5** Mechanism of the surface ligand exchange on 1-MI-ZIF-8

For surface modification of ZIF-8, method of Tsai and colleagues was modified and used (Tsai, Niemantsverdriet, & Langner, 2018). 0.3 g ZIF-8 was sonicated in 25 ml methanol and then excess NaOH was added, approximately 1 g, to hold over pH 8.0. Thereafter, 0.6 g histamine dihydrochloride was dissolved in 25 ml methanol and added on the ZIF-8. The mixture was mixed at 60 °C and 600 rpm for 168 h under reflux. End of the process, the mixture was centrifuged at 10,000 rpm at room temperature. The particles were washed with methanol three times and dried at 80 °C for overnight.

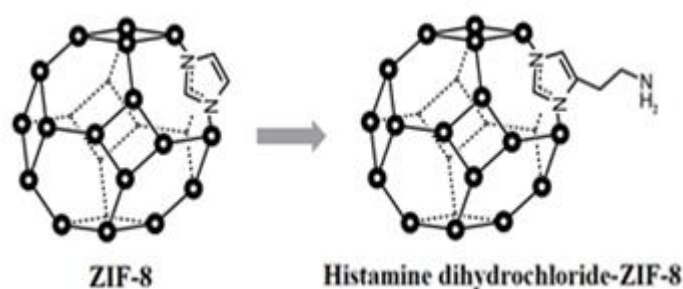


**Figure 3. 6** Mechanism of the surface ligand exchange on ZIF-8

### **3.6. Characterization of ZIF-8**

Shimadzu IRPrestige-21 FTIR-ATR was used in order to define organic compounds of synthesized powders. Phase identification of the crystal particles was made by Philips model PW1840 (1729) X-ray diffractometer using Ni-filtered Cu-K $\alpha$  radiation at a scan rate of 0.1 °/sec. Data were taken from 5 to 40 degrees. The XRD analyze was made at 30 kV voltage and 24 mA currents. For TGA analyze, Shimadzu DTG-60H was used to determine the thermal behavior of the synthesized ZIF-8 crystals. The analysis was made at air and nitrogen conditions and heated with 10 °C/min rate up to 600 °C. For determination of crystal morphology and size, particles were viewed by QUANTA 400F field emission scanning electron microscope (SEM) having a resolution of 1.2 nm. Also, Tristar II 3020 was used for BET analysis.

### **3.7. Incubation, separation and purification procedure for rhGH and rGCSF**

0.1 g dried synthesized resin was used for separation and purification. 1 ml rhGH reactor medium supernatant or rGCSF homogenized reactor medium was added to the adsorbent. The medium incubated with adsorbent in a shaker at 35 °C and 50 rpm for 2 hours. When the incubation finished afterward, the tube was centrifuged at 4000 rpm and room temperature for 10 minutes. For removing of the unbonded proteins, 1 ml washing solvents was used in washing step. Then, the supernatant was centrifuged and discharged at same conditions. This step was applied three times. Thereafter, 1 ml eluent was added on to the ZIF-8 particles and incubated at 35 °C and 50 rpm for 30 minutes. After the centrifugation, pellet, and supernatant were saved for later steps.

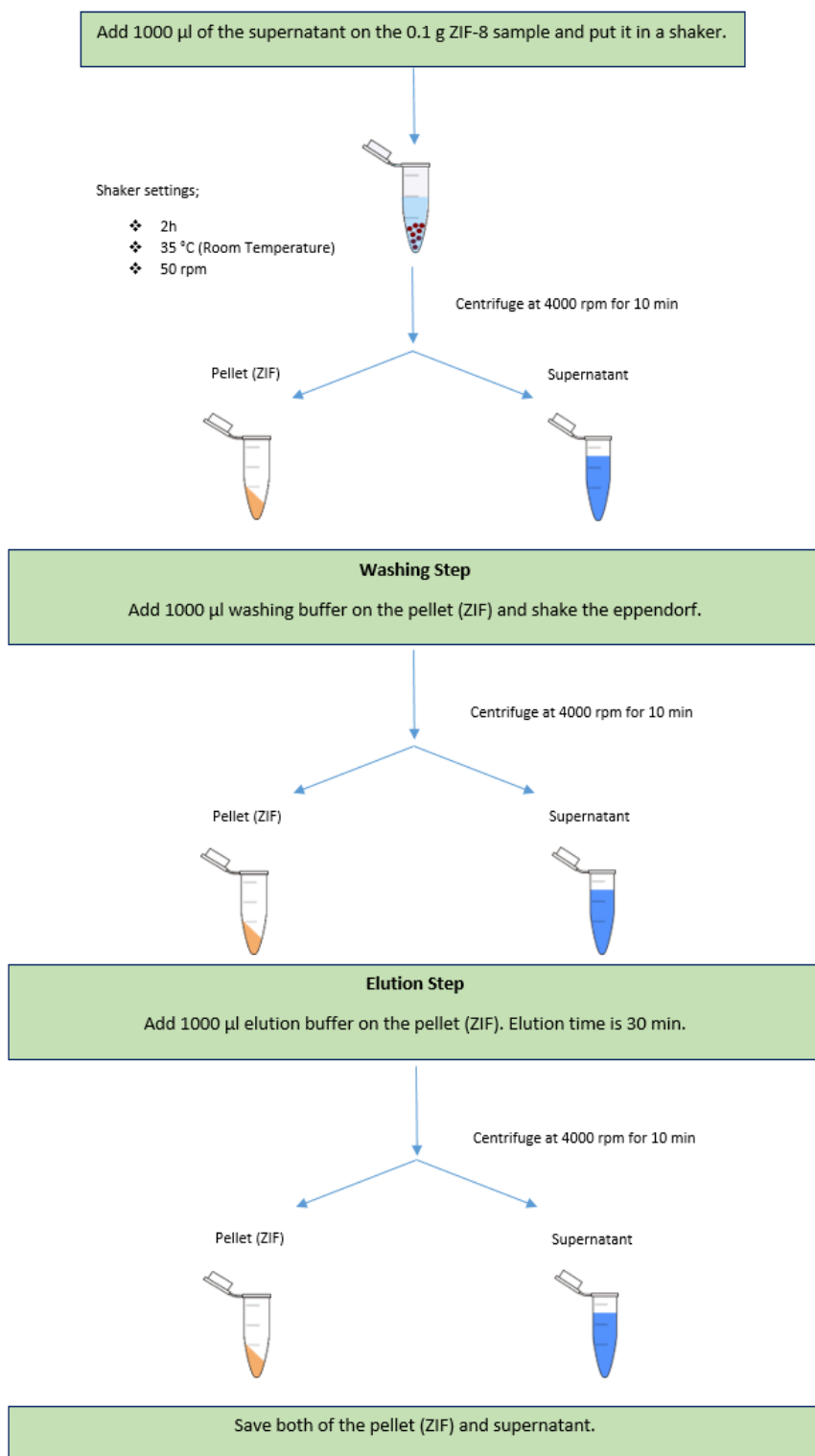


**Figure 3. 7** Separation and purification process



### **3.8. Bradford Analyse**

For total protein calculation, Bradford reagent was purchased from Sigma Aldrich. Initially, a standard curve was prepared with bovine serum albumin (BSA) as a model protein given in Appendix B. The curve was used to calculate the concentration of total protein. 1.5 ml Bradford reagent, at room temperature, was taken into 2 ml UV-spectrometer cuvette. 0.05 ml sample was added to it and inverted gently. For the reading of optical density, UP water was used as a blank. End of the 5 minutes, optical density values were read at 595 nm.

### **3.9. Sodium dodecyl sulfate polyacrylamide gel electrophoresis (SDS-PAGE)**

SDS method was applied, as Laemmli described (Laemmli, 1970). 15  $\mu$ l mixture was loaded into the wells. The mixture consists of 13  $\mu$ l sample or standard, 5  $\mu$ l x4 loading buffer (LB) and 2  $\mu$ l 1 M Dithiothreitol (DTT) for rhGH. DTT was used for disruption of disulfide bonds of protein. For rGCSF, 15  $\mu$ l sample or standard and 5  $\mu$ l x3 LB was used. As a marker, PageRuler prestained protein ladder (Appendix A) was used to determine protein molecular weight and position in the gel. BIO-RAD Mini-PROTEAN tetra vertical electrophoresis cell was used at a constant voltage, 200 V, for running of proteins in the gel. Recipes of used LB and running buffers are given in Appendix A.

#### **3.9.1. Gel Preparation**

BIO-RAD TGX Stain-Free FastCast acrylamide solutions kit was used to prepare the gel. 1.0 mm glass plates were used. According to the procedure of kit, solutions were prepared and adding the each of the component solutions are inverted gently. Gels became ready to use in 45 minutes.

### 3.9.2. Silver Staining

Especially fixing, pretreatment, silver and developing solutions must be fresh. All of the solutions must be prepared with ultrapure (UP) water. Developing step was applied for 90 seconds especially for rGCSF protein. For rhGH, extra time can be required in developing step.

- ❖ 1 h **Fixing** (100 ml Methanol, 24 ml Acetic Acid, 100 µl Formaldehyde, 76 UP Water)
- ❖ 3x20 min. **Washing** (100 ml Ethanol, 100 ml UP Water)
- ❖ 3x20 sec. **Rinse** (100 ml UP Water)
- ❖ 1 min. **Pretreatment** (0.05 g Sodium Thiosulfate Pentahydrate, 100 ml UP Water)
- ❖ 3x20 sec. **Rinse** (100 ml UP Water)
- ❖ 20 min. **Impregnate**(0.2 g Silver Nitrate, 100 ml UP Water, 75 µl Formaldehyde)
- ❖ 2x20 sec. **Rinse** (100 ml UP Water)
- ❖ 1.30 min. **Developing** (2.25 g Potassium Carbonate, 100 ml UP Water, 2 ml Pretreatment Solution, 75 µl Formaldehyde)
- ❖ **Stop** (50 ml Methanol, 12 ml Acetic Acid, 38 ml UP Water)

### 3.9.3. Coomassie Blue Staining

Fixing solution must be fresh. Coomassie R250 staining solution and destain solutions 1 and 2 can be stored at 20 °C for several months.

- ❖ 1 h **Fixing** (4 ml formaldehyde, 150 ml ethanol, 13.61 g sodium acetate trihydrate and UP water up to 500 ml). Use it immediately.
- ❖ 1 h **Coomassie R250 Staining** (0.25 g Coomassie R250, 75 ml methanol, 12.5 ml acetic acid and UP water up to 250 ml).

- ❖ **Destain Solution 1** (300 ml methanol, 50 ml acetic acid and UP water up to 1 L). Wash with destain solution 1 up to reach clear gel background.
- ❖ **Destain Solution 2** (50 ml methanol, 70 ml acetic acid and UP water up to 1 L). Use destain solution to store gel.



## CHAPTER 4

### RESULTS AND DISCUSSION

The aim of the present research was to examine the effects of the oxygen transfer conditions on the rhGH production by *P. pastoris* under control of GAP promoter. In addition, separation and purification of the produced rhGH using synthesized and modified ZIF-8. Besides rhGH, rGCSF was used as a second model protein to compare the separation and purification results with rhGH.

Three different oxygen transfer conditions were investigated which are  $C_{DO} = 1\%$ ,  $5\%$ , and  $15\%$ . The oxygen transfer conditions were chosen according to low to moderate oxygen transfer conditions.

Secondly, ZIF-8 production and separation processes were optimized. ZIF-8 modifications were applied on ZIF-8 to enhance its selective adsorption and desorption properties. Diverse optimizations were conducted on the synthesis and surface modification of ZIF-8. Finally, separation and purification procedures were tested, to get pure protein from the production medium.

#### 4.1. Parameters of bioreactor conditions

Three types of strategy were designed to determine the effect of oxygen transfer condition on rhGH production. For all oxygen transfer conditions, the process parameters which are temperature (T), pH, agitation (N), dissolved oxygen concentration ( $C_{DO}$ ) were set to  $T = 30\text{ }^{\circ}\text{C}$ ,  $\text{pH} = 5.5$ , 600 rpm,  $C_{DO} = 20\%$  in batch mode, respectively. Then, the all parameters were held at same conditions except  $C_{DO}$  in fed-batch mode. Only the  $C_{DO}$  parameter was changed to analyze the response of microorganism in low to moderate oxygen transfer conditions. System parameters such as agitation, pH, and temperature were given in Table 4.1 for all

conditions. Also, gas flow (air) was set as an initial variable in cascade system to keep  $C_{DO}$  at the desired level, secondly oxygen enrichment was applied.

**Table 4. 1** System parameters for each experiment

| <b>Batch Mode</b>         |         |     |                  |              |
|---------------------------|---------|-----|------------------|--------------|
|                           | N (rpm) | pH  | Temperature (°C) | $C_{DO}$ (%) |
| <b>Bioreactor 1 (BR1)</b> | 600     | 5.5 | 30               | 20           |
| <b>Bioreactor 2 (BR2)</b> | 600     | 5.5 | 30               | 20           |
| <b>Bioreactor 3 (BR3)</b> | 600     | 5.5 | 30               | 20           |
| <b>Fed-Batch Mode*</b>    |         |     |                  |              |
|                           | N (rpm) | pH  | Temperature (°C) | $C_{DO}$ (%) |
| <b>Bioreactor 1 (BR1)</b> | 700     | 5.5 | 30               | 1            |
| <b>Bioreactor 2 (BR2)</b> | 700     | 5.5 | 30               | 5            |
| <b>Bioreactor 3 (BR3)</b> | 700     | 5.5 | 30               | 15           |

\*  $C_x = 21.5$  g/L at  $t = 0$  h for all bioreactor experiments

#### **4.2. Effect of oxygen transfer conditions on cell generation and rhGH production**

Variations in cell concentrations with oxygen concentration and cultivation time are presented in Figure 4.1. Under all the applied three strategies  $C_x$  increases with the cultivation time. The highest  $C_x$  was obtained at  $C_{DO} = 15\%$  at  $t = 30$  h, as 177.3 g/L. Same cell concentration loci were observed for  $C_{DO} = 5\%$  and  $C_{DO} = 15\%$  until  $t = 15$  h. The process of  $C_{DO} = 15\%$  condition was stopped because of the technical reason which is that the oxygen gas tube used for enrichment was over. After  $t = 15$  h, a significant increase was observed in the cell growth of  $C_{DO} = 15\%$  condition. The highest  $C_x$  was succeeded as  $C_x = 104.7$  g/L at  $t = 21$  h at  $C_{DO} = 5\%$ . After  $t = 21$  h, a decrease was observed at  $C_x$  of  $C_{DO} = 5\%$  condition. The highest  $C_x$  of  $C_{DO} = 1\%$  was obtained as 52.0 g/L at  $t = 9$  h. The  $C_x$  decreased after  $t = 9$  h at  $C_{DO} = 1\%$ .

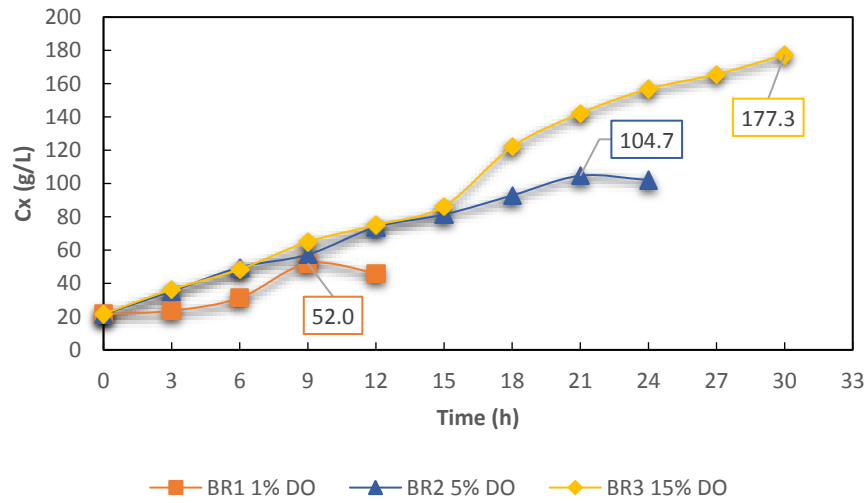


**Figure 4. 1** Variations in cell generation with the oxygen transfer condition and cultivation time

When all oxygen transfer conditions were compared with each other, the highest cell concentration, 177.3 g/L, is the 1.7-fold of the highest  $C_x$  value of the  $C_{DO} = 5\%$  and 3.4-fold of the highest  $C_x$  value of the  $C_{DO} = 1\%$ . These results obviously show that under low oxygen condition,  $C_{DO} = 1\%$ , high cell concentration cannot be achieved. Oxygen is an important parameter for eukaryotic cells (Adelantado et al., 2017). Oxygen is consumed in respiration to produce ATP and increase cell growth (Kuriyama & Kobayashi, 1993). Effects of oxygen were considered low oxygen condition,  $C_{DO} = 1\%$ , may cause energy depletion to provide adequate biomass. On the other hand, high cell densities were obtained for  $C_{DO} = 5\%$  and  $C_{DO} = 15\%$ . So,  $C_{DO} = 5\%$  condition is a limit to reach high cell density. However,  $C_{DO} = 15\%$  condition was considered higher cell concentration was succeeded with an increase of the  $C_{DO}$ . Effect of  $C_{DO} = 20\%$  was not investigated as Güneş and Çalık (2016) stated that  $C_{DO} = 15\%$  is better for the recombinant protein production than that of  $C_{DO} = 20\%$  (Güneş & Çalık, 2016).

As a result of these, oxygen limitation is the main reason for lower  $C_x$  of  $C_{DO} = 1\%$  and  $C_{DO} = 5\%$  conditions with respect to  $C_{DO} = 15\%$ . The relevance of oxygen is

clearly supported by the current findings. However, the produced protein concentration should be obtained to determine the oxygen transfer condition for high production yield per cell.

The variations in rhGH concentration with the oxygen transfer condition and cultivation time were presented in Figure 4.2. When the produced recombinant protein concentration,  $C_{rhGH}$ , was considered, the highest  $C_{rhGH}$  was obtained as 40.5 mg/L at  $t = 24$  h at  $C_{DO} = 15\%$ . In  $C_{DO} = 5\%$  condition,  $C_{rhGH}$  was close to that of  $C_{DO} = 15\%$  at  $t = 18$  h. However, a dramatic increase was observed after  $t = 18$  h at  $C_{DO} = 15\%$ . The highest  $C_{rhGH}$  was obtained at  $C_{DO} = 5\%$  at  $t = 24$  h, as 19.9 mg/L. The  $C_{DO} = 5\%$  condition was stopped at  $t = 24$  h because  $C_x$  decrease was observed. Further, as  $C_{DO} = 5\%$  condition increase in  $C_x$  was higher than  $C_{DO} = 1\%$ , higher rhGH production was obtained. However, the highest  $C_{rhGH}$  in  $C_{DO} = 5\%$  condition, was close to that of  $C_{DO} = 1\%$ . The highest  $C_{rhGH}$  was succeeded as 15.4 mg/L at  $t = 12$  h at  $C_{DO} = 1\%$ . The reason for the process stopping same as  $C_{DO} = 5\%$  condition.

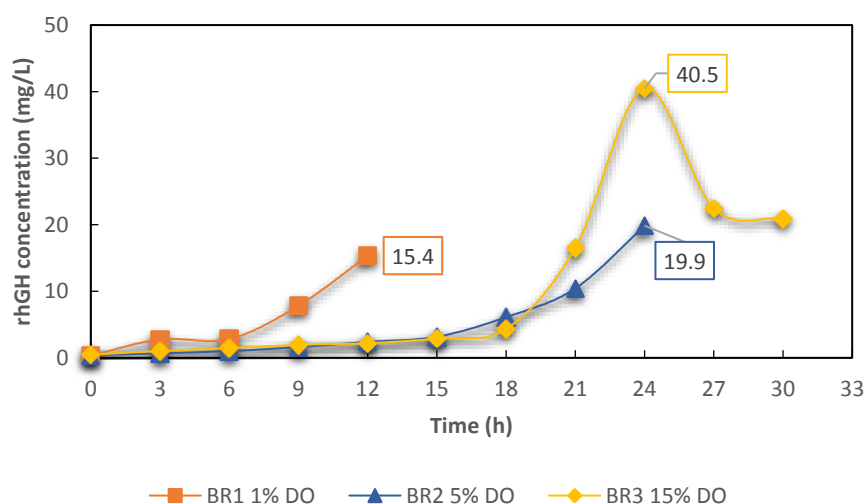


**Figure 4. 2** Variations in rhGH concentration with the oxygen transfer condition and cultivation time



The highest rhGH concentration was obtained at  $C_{DO} = 15\%$  which is 2.64 and 2.04-fold higher than  $C_{DO} = 1\%$  and  $C_{DO} = 5\%$ , respectively. rhGH production is related to  $C_x$ . A parallel increase is expected at rhGH production with  $C_x$  under  $P_{GAP}$ , constitutive promoter. So,  $C_x$  should be held at a higher level as much as possible. However, in  $C_{DO} = 15\%$  condition, while  $C_x$  is maintaining its increase after the 24<sup>th</sup> hour, produced rhGH amount per liter is decreasing dramatically. The reason for the decrement at the rhGH concentration should be related to the protease production. The protease production is the undesired situation that results in degradation of the rhGH.

In addition, when cultivation time and  $C_{rhGH}$  performance of  $C_{DO} = 1\%$  and  $C_{DO} = 5\%$  were considered, the highest  $C_{rhGH}$  obtained in  $C_{DO} = 5\%$  condition was close to that of  $C_{DO} = 1\%$  in less cultivation time. These close production performances of  $C_{DO} = 1\%$  and  $C_{DO} = 5\%$  can be related to oxygen utilization by the cell. Also, this difference can be interpreted like that low oxygen condition occurs a limitation for cell growth. Especially, this assessment is becoming prominent when effects of oxygen are considered on metabolic fluxes, pathway and cell formation reactions. In addition, related to the low oxygen condition, glucose accumulation and low growth were observed. As a result of growth limitation, the lowest growth was reached at  $C_{DO} = 1\%$  showing that utilization of oxygen shifted to the rhGH production. However, low cell growth is a disadvantage in spite of the advantage of low oxygen consumption. The relation between the  $C_x$  and rhGH shows the importance of  $C_x$  to reach high protein production.

Moreover, substrate consumption and byproduct production should be analyzed because oxygen is effective on both of the metabolic fluxes and pathways. Byproduct and substrate concentrations in the medium can be toxic at the high levels. In this study, glucose was used as a substrate and unconsumed glucose concentration was obtained. An increase was observed at the remained glucose concentration in the medium with the rise of  $C_{DO}$ . The glucose concentrations were

given in Figure 4.3 for all oxygen transfer conditions. The highest glucose concentration,  $C_G$ , was obtained as 0.10 g/L at  $t = 24$  h for  $C_{DO} = 15\%$  condition. Until  $t = 9$  h, accumulation of  $C_G$  was not observed for  $C_{DO} = 5\%$  and  $C_{DO} = 15\%$ . The highest  $C_G$  was obtained as 0.06 g/L and 0.03 g/L for  $C_{DO} = 5\%$  and  $C_{DO} = 1\%$ , respectively. Contrary to  $C_G$  of  $C_{DO} = 5\%$  and  $C_{DO} = 15\%$ , accumulation was observed throughout the process. However, the accumulated  $C_G$  values are very low for all oxygen transfer conditions. In addition, any decrease was not observed related to  $C_x$ , and therefore, it can be said that it was consumed almost totally.

Additionally, ethanol was produced as a byproduct of fermentative growth showing growth shifted from respiratory mode to fermentation. *P. pastoris* is an anaerobic microorganism and the shifting to the fermentation mode resulting in the promotion of the byproduct production in this growth mode. The ethanol production was analyzed just for  $C_{DO} = 15\%$  because the highest  $C_x$  and rhGH production were reached in the  $C_{DO} = 15\%$  condition. Variations in ethanol concentration with the cultivation time at  $C_{DO} = 15\%$  were given in Figure 4.4. The highest ethanol concentration was obtained at 18 h as 9.8 g/L. Until  $t = 15$  h, ethanol accumulation was not observed.

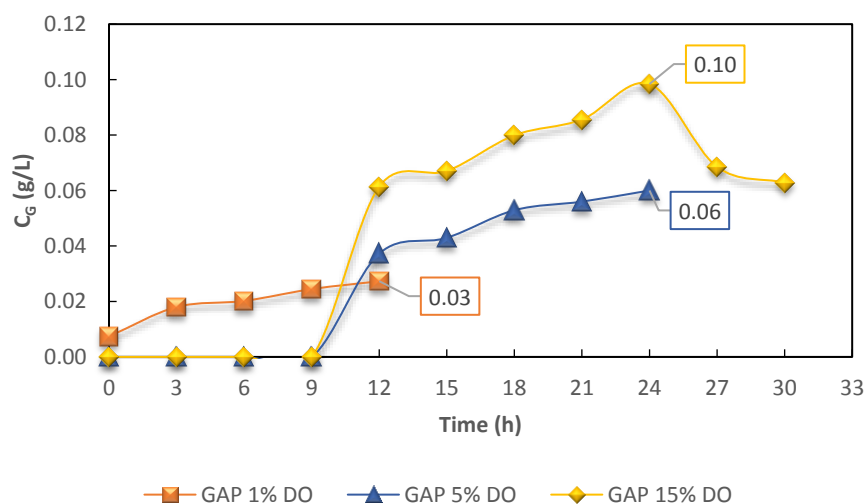


**Figure 4. 3** Variations in glucose concentration with the oxygen transfer condition and cultivation time

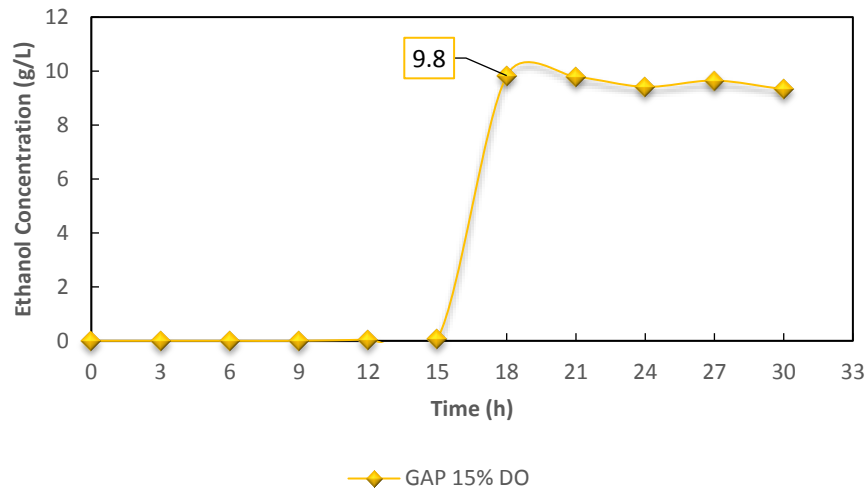


**Figure 4. 4** Variations in ethanol concentration with the cultivation time at  $C_{DO} = 15\%$

When the total substrate fed into the bioreactor at three oxygen transfer conditions were compared, same feeding, 924.1 g, was applied at  $C_{DO} = 5\%$  and  $C_{DO} = 15\%$  conditions where the highest  $C_{thGH}$  was obtained. On the other hand, the highest  $C_{thGH}$  was obtained at  $t = 12$  h for  $C_{DO} = 1\%$  condition; thus, the total substrate fed into the bioreactor was measured as 220.6 g at  $C_{DO} = 1\%$  condition which is less than  $C_{DO} = 5\%$  and  $C_{DO} = 15\%$  conditions. Comparison of the  $C_{DO} = 1\%$  and  $C_{DO} = 5\%$  conditions shows that close values of  $C_{thGH}$  were attained while the total substrate fed for  $C_{DO} = 5\%$  was approximately four times higher than the total substrate fed for  $C_{DO} = 1\%$  condition. Thus,  $C_{DO} = 1\%$  condition is more preferable than  $C_{DO} = 5\%$ .

**Table 4. 2** Total substrate fed into the bioreactor related to the highest rhGH concentration

| Oxygen Transfer Condition, at | t h | The highest $C_{rhGH}$ mg/L | Total substrate fed into the bioreactor g |
|-------------------------------|-----|-----------------------------|---|
| $C_{DO} = 1\%$                | 12  | 15.4                        | 220.6                                     |
| $C_{DO} = 5\%$                | 24  | 19.9                        | 924.1                                     |
| $C_{DO} = 15\%$               | 24  | 40.5                        | 924.1                                     |

#### 4.3. Effect oxygen transfer condition on the yield coefficients and the specific rates

The specific growth rate,  $\mu$ , yield coefficient of mass of cell produced per unit mass of substrate consumed,  $Y_{X/S}$ , yield coefficient of mass of product produced per unit mass of substrate consumed,  $Y_{P/S}$ , yield coefficient of mass of product produced per unit mass of cell produced,  $Y_{P/X}$ , the specific substrate consumption rate,  $q_s$ , and the specific product production rate,  $q_p$ , were given in Table 4.3. For all oxygen transfer conditions, the pre-determined specific growth rate,  $\mu_0 = 0.1 \text{ h}^{-1}$ , was used.

For  $C_{DO} = 1\%$  when the  $C_X$  and rhGH production data were checked, after  $t = 6 \text{ h}$  a dramatically increasing was observed for both of them. This increase can be related to  $\mu$  value because  $\mu$  reached the highest value,  $0.167 \text{ h}^{-1}$ , at the  $t = 6 \text{ h}$  of the process. The highest  $Y_{X/S}$  was calculated,  $0.91 \text{ g g}^{-1}$ , at  $t = 9 \text{ h}$  then decreasing was observed because of the decrement of the  $C_X$ . Also, the specific substrate consumption rate decreased with  $C_X$  increasing up to  $t = 9 \text{ h}$ , as expected.

For  $C_{DO} = 5\%$ , the highest  $\mu$  value,  $0.145 \text{ h}^{-1}$ , was calculated and after that gradually decreasing was observed with increasing  $C_X$ . The highest  $Y_{P/S}$  and  $Y_{P/X}$  were calculated,  $0.16 \text{ mg g}^{-1}$  and  $0.96 \text{ mg g}^{-1}$  at the  $t = 24 \text{ h}$ , respectively.  $Y_{X/S}$  showed decreasing through the process. In addition, substrate consumption rate shows increment with time. The same locus was observed when  $Y_{X/S}$  value changing of  $C_{DO} = 15\%$  was compared with  $C_{DO} = 5\%$  condition. Also, higher  $\mu$  value,  $0.135 \text{ h}^{-1}$ , was calculated at  $t = 3 \text{ h}$  of  $C_{DO} = 15\%$  condition like  $C_{DO} = 5\%$ . After  $t = 24$

h,  $Y_{P/X}$  value decreased but substrate consumption rate increased while product formation rate was decreasing. As mentioned before, the protease activity can cause this situation or we can mention about a shifting from recombinant protein production to cell growth.

**Table 4. 3** Variations in the fermentation characteristics with the cultivation time and oxygen transfer conditions in fed-batch bioreactor experiments

| Oxygen transfer condition, at | t, h           | $\mu$ , h <sup>-1</sup> | $Y_{X/S}$ , g g <sup>-1</sup> | $Y_{P/S}$ , mg g <sup>-1</sup> | $Y_{P/X}$ , mg g <sup>-1</sup> | $q_s$ , g g <sup>-1</sup> h <sup>-1</sup> | $q_P$ , mg g <sup>-1</sup> h <sup>-1</sup> |
|-------------------------------|----------------|-------------------------|-------------------------------|--------------------------------|--------------------------------|---|--|
| <b>C<sub>DO</sub> = 1%</b>    | 3              | 0.081                   | 0.18                          | 0.14                           | 0.9                            | 0.246                                     | 0.019                                      |
|                               | 6              | 0.167                   | 0.45                          | 0.01                           | 0.02                           | 0.24                                      | 0.0282                                     |
|                               | 9              | 0.066                   | 0.91                          | 0.21                           | 0.23                           | 0.185                                     | 0.0431                                     |
|                               | $t_{max} = 12$ | -                       | -                             | 0.26                           | -                              | 0.226                                     | 0.0618                                     |
| <b>C<sub>DO</sub> = 5%</b>    | 3              | 0.145                   | 0.97                          | 0.02                           | 0.02                           | 0.164                                     | 0.0031                                     |
|                               | 6              | 0.089                   | 0.82                          | 0.02                           | 0.02                           | 0.151                                     | 0.0034                                     |
|                               | 9              | 0.09                    | 0.41                          | 0.03                           | 0.06                           | 0.168                                     | 0.0046                                     |
|                               | 12             | 0.079                   | 0.65                          | 0.03                           | 0.04                           | 0.165                                     | 0.0043                                     |
|                               | 15             | 0.069                   | 0.34                          | 0.02                           | 0.07                           | 0.187                                     | 0.0088                                     |
|                               | 18             | 0.079                   | 0.4                           | 0.07                           | 0.17                           | 0.2                                       | 0.0155                                     |
|                               | 21             | 0.059                   | 0.39                          | 0.09                           | 0.22                           | 0.212                                     | 0.0263                                     |
|                               | $t_{max} = 24$ | 0.036                   | 0.17                          | 0.16                           | 0.96                           | 0.217                                     | 0.0394                                     |
| <b>C<sub>DO</sub> = 15%</b>   | 3              | 0.135                   | 1.03                          | 0.04                           | 0.04                           | 0.159                                     | 0.0049                                     |
|                               | 6              | 0.114                   | 0.71                          | 0.02                           | 0.03                           | 0.155                                     | 0.0037                                     |
|                               | 9              | 0.087                   | 0.77                          | 0.02                           | 0.03                           | 0.148                                     | 0.0025                                     |
|                               | 12             | 0.072                   | 0.45                          | 0.01                           | 0.03                           | 0.162                                     | 0.0028                                     |
|                               | 15             | 0.121                   | 0.44                          | 0.02                           | 0.05                           | 0.176                                     | 0.0051                                     |
|                               | 18             | 0.113                   | 0.93                          | 0.04                           | 0.04                           | 0.152                                     | 0.0199                                     |
|                               | 21             | 0.085                   | 0.6                           | 0.22                           | 0.37                           | 0.156                                     | 0.0475                                     |
|                               | $t_{max} = 24$ | 0.077                   | 0.51                          | 0.39                           | 0.78                           | 0.166                                     | 0.0197                                     |
|                               | 27             | 0.08                    | 0.43                          | 0.16                           | 0.36                           | 0.18                                      | 0.0096                                     |
|                               | 30             | 0.079                   | 0.47                          | 0.03                           | 0.06                           | 0.16                                      | 0.0036                                     |

As a result, if all oxygen transfer conditions were compared with each other,  $\mu$  value showed a decrement. The reason for this situation can be explained by increasing energy demand, lacking trace elements, and oxygen transfer limitation which are results of  $C_x$  increasing.

**Table 4. 4** Overall yield coefficient of oxygen transfer conditions

| <b>Oxygen Transfer Condition, at</b> | <b>Overall <math>Y_{X/S}</math>,<br/><math>g\ g^{-1}</math></b> | <b>Overall <math>Y_{P/S}</math>,<br/><math>mg\ g^{-1}</math></b> | <b>Overall <math>Y_{P/X}</math>,<br/><math>mg\ g^{-1}</math></b> |
|--------------------------------------|---|--|--|
| <b><math>C_{DO} = 1\%</math></b>     | 0.33  | 0.18   | 0.55   |
| <b><math>C_{DO} = 5\%</math></b>     | 0.39  | 0.09   | 0.22   |
| <b><math>C_{DO} = 15\%</math></b>    | 0.54  | 0.07   | 0.12   |

Overall yield coefficients were given in Table 4.4. The highest overall  $Y_{X/S}$ , 0.54  $g\ g^{-1}$ , was obtained at  $C_{DO} = 15\%$ . The overall  $Y_{X/S}$  of  $C_{DO} = 1\%$  and  $5\%$  were determined as 0.33 and 0.39  $g\ g^{-1}$ , respectively. Thus,  $C_{DO} = 1\%$  is preferable than  $C_{DO} = 5\%$  condition because of the higher specific product formation rate, process time and cost of the process. When the overall  $Y_{P/S}$  values of all oxygen transfer conditions were compared, the overall yield coefficient decreased with increasing of  $C_{DO}$  because substrate consumption increases with  $C_X$  increment resulted from the  $C_{DO}$ . In addition, overall  $Y_{P/X}$  values were compared  $C_{DO} = 1\%$  gives the best value, 0.55  $mg\ g^{-1}$ . However,  $C_{DO} = 1\%$  condition has the lower protein production than other conditions so, it should be repeated approximately 3-fold to reach the protein production of  $C_{DO} = 15\%$  condition which has the highest protein production when the ratio of produced protein was considered. This finding shows the significance of the relationship between  $C_X$  and  $C_{thGH}$ .

#### **4.4. Effect of oxygen transfer condition on organic acid concentrations**

Organic acid analyses provide a better idea, to understand the effect of oxygen on the metabolic fluxes and response of microorganism under different oxygen concentrations. Variations of organic acids concentrations with time for  $C_{DO} = 15\%$  are given in Figure 4.5. The numerical data and calibration curves of organic acids are given in Appendix B. Through the fermentation process, pyruvic acid concentration in the medium had been obtained at very low levels. Besides, other organic acids, especially, oxalic, acetic and malic acids show accumulation at  $t =$

24 h. The highest rhGH production was succeeded at  $t = 24$  h so, organic acid concentrations were investigated until  $t = 24$  h.

At  $t = 24$  h, oxalic acid is slightly increasing. In order to understand the direction of the pathway citric acid level becomes important parameter because oxaloacetate which is in the mitochondria can be transported to the cytosol. Hence, the oxaloacetate in the cytosol can be included the phenol-pyruvate that represses the formation of pyruvate. Pyruvate consumption is divided into two ways. The one is the production of byproducts which are ethanol and acetic acid. Both of the byproducts are fermentation products and which can be toxic in the high cell concentration (G. P. L. Cereghino et al., 2002). After  $t = 18$  h, ethanol production increase was observed and acetic acid accumulation was obtained at  $t = 24$  h.

The other one is acetyl-CoA which is produced as a result of oxidation of pyruvate and joined to the TCA cycle from citrate formation. Citric acid accumulation was not detected so that citric acid was consumed totally in TCA cycle. Also, an accumulation was not obtained for succinic acid so that consumption rates from succinate to fumarate or  $\alpha$ -ketoglutarate are equals to the formation of succinate from the  $\alpha$ -ketoglutarate.

In TCA cycle, the reactions between the oxaloacetate-malate and malate-fumarate are reversible. On the other hand, the reaction from succinate to fumarate is irreversible. The reactions related to the formation and the consumption of the fumaric acid are in balance because any accumulation is not observed for fumaric acid. However, when the malic acid was considered, a significant increase was obtained which shows that formation rate of malic acid is higher than the consumption rate. This point can be a bottleneck for the TCA cycle. Low concentrations of the fumaric and oxalic acids support the idea that related to the bottleneck. The reason for the bottleneck can be based on the lower consumption rates than formation rates which are from fumaric and oxalic acids. However, when the accumulated organic acid concentrations were considered, the accumulated

organic acid concentrations are low so, it can be stated that TCA cycle worked efficiently. On the other hand, acetic acid accumulation at  $t = 24$  h and ethanol accumulation at  $t = 18$  h show the respiratory mode shifted slightly to fermentation mode.

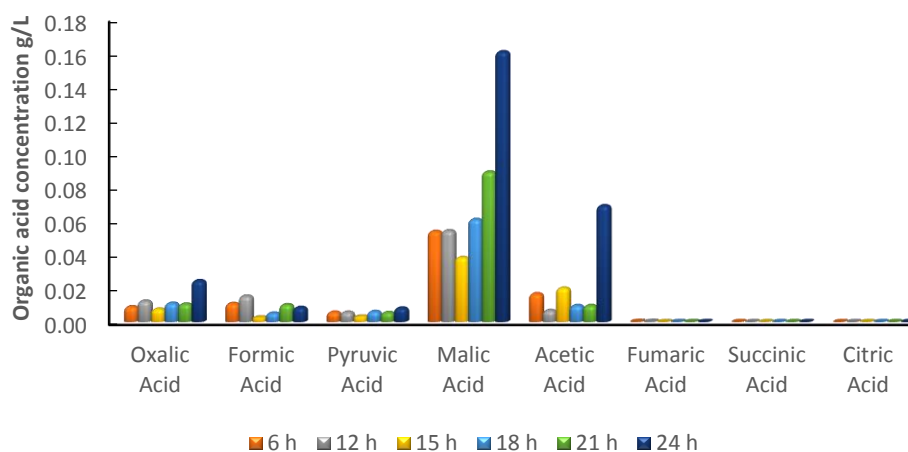


**Figure 4. 5** Variations of organic acid concentrations with cultivation time for  $C_{DO} = 15\%$

#### 4.5. Characterization of ZIF-8 synthesis

To control the crystallinity of the synthesized ZIF-8 particles, XRD pattern was used to compare with the reference data. All peaks matched with simulated pattern of ZIF-8 peaks (K. S. Park et al., 2006) as presented in Figure 4.6. The dominant peak of ZIF-8 crystals, (011), and other can be clearly seen in XRD patterns.



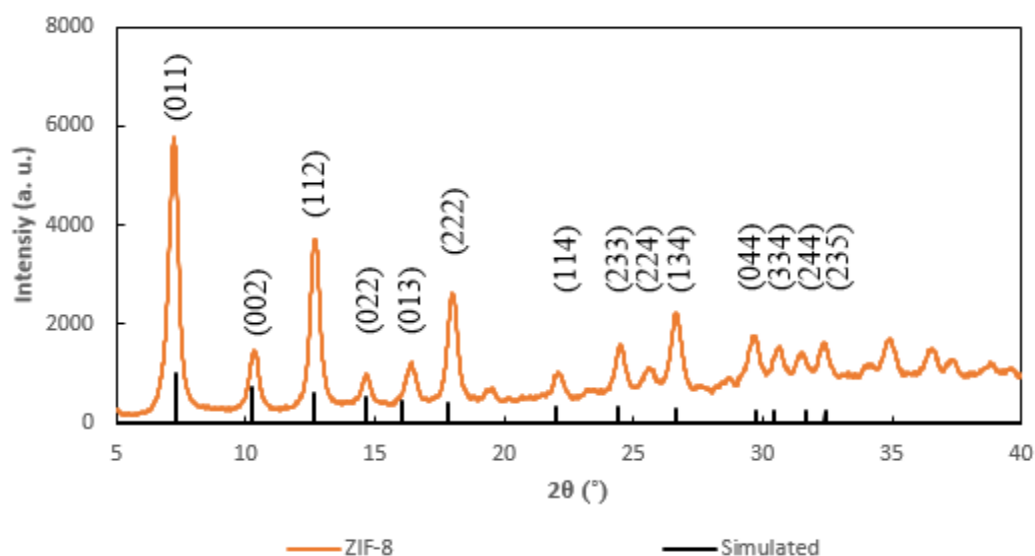


**Figure 4. 6** XRD pattern of ZIF-8

Moreover, FTIR analysis was done to define bands and compare with the literature. The band at the  $3135\text{ cm}^{-1}$  is related to N-H stretching of 2-methylimidazole and  $2931\text{ cm}^{-1}$  is attributed to an aliphatic C-H stretch of the imidazole. Another band at  $1585\text{ cm}^{-1}$  is attributed to C=N stretch mode. The bands between the  $1350$  and  $1500\text{ cm}^{-1}$  are assigned as stretching of the ring. The peaks between the  $900$  and  $1350\text{ cm}^{-1}$  interval associated with in-plane bending of the ring and the others which are below the  $800\text{ cm}^{-1}$  are attributed to out-of-plane bending. As expected, FTIR spectrum is matching with the literature.

SEM micrographs of ZIF-8 crystals were given in Appendix F. Well dispersed and uniform ZIF-8 crystals were observed and crystal sizes were obtained approximately 50-60 nm.

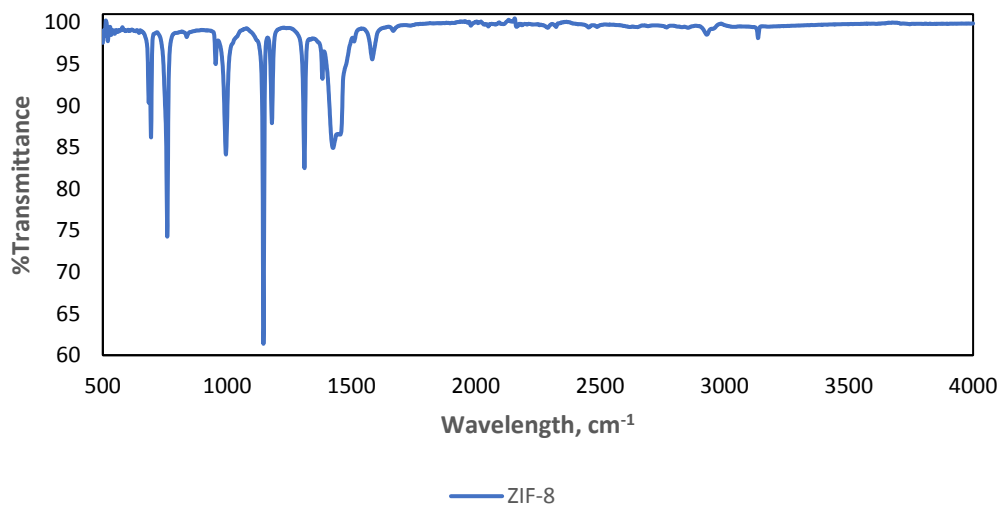


**Figure 4. 7** FTIR spectrum of ZIF-8

Thermogravimetric analysis (TGA) was applied on ZIF-8 in the air medium. Approximately, 35% weight loss was observed and the decomposition temperature was measured 445 °C. At the beginning of the heat treatment, removal of guest molecules like methanol was observed. When the temperature exceeded 400 °C, ZnO occurs. The result of TGA thermogram supports the information about temperature stability of the ZIF-8 in the literature.

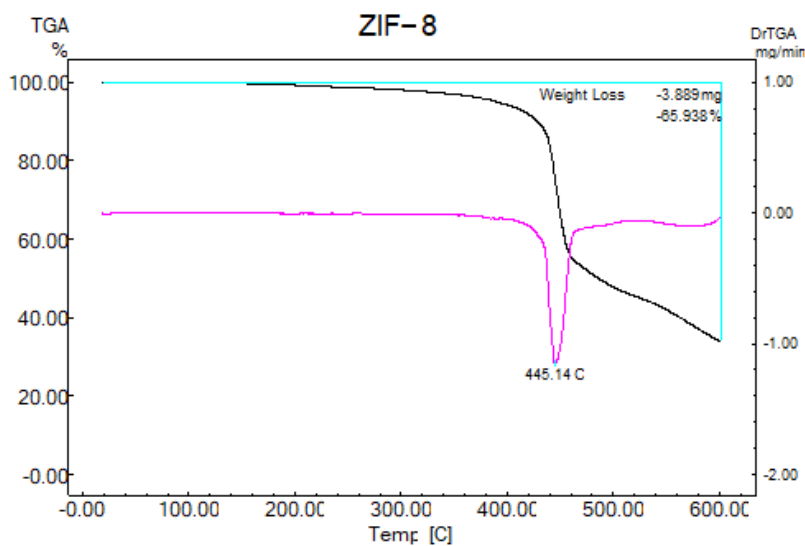


**Figure 4. 8** TGA thermogram of ZIF-8

#### 4.5.1. Effect of Hmim/Zn<sup>2+</sup> ratio on ZIF-8

ZIF-8 samples were synthesized at room temperature with different molar ratios of Hmim and Zn<sup>2+</sup>. For ZIF-8 synthesis, Zn<sup>2+</sup>:7.9Hmim:695.1 MeOH (2.4 g Zn(NO<sub>3</sub>)<sub>2</sub>.6H<sub>2</sub>O:5.28 g Hmim:181 g MeOH) molar ratios were used as based components for synthesis (Venna et al., 2010).

**Table 4. 5** Experimental components of synthesis

| Experimental Code | Zn(NO <sub>3</sub> ) <sub>2</sub> .6H <sub>2</sub> O (g) | Hmim (g) | MeOH (g) |
|-------------------|--|----------|----------|
| ZIF-8-1           | 2.4  | 5.28     | 181      |
| ZIF-8-2           | 2.4  | 2.64     | 181      |
| ZIF-8-3           | 1.2  | 5.28     | 181      |
| ZIF-8-4           | 1.0  | 5.28     | 181      |
| ZIF-8-5           | 0.6  | 5.28     | 181      |

Effect of MeOH was not investigated in this study because similar experiments were done by Demir and coworkers (Keser Demir, Topuz, Yilmaz, & Kalipcilar, 2014) on the same production conditions. According to the results of their study, low MeOH/Zn<sup>2+</sup> ratio causes dense mixture showing Hmim and Zn<sup>2+</sup> concentrations are higher in synthesis medium. As a consequence of the low MeOH/Zn<sup>2+</sup> ratio, nucleation decreases and promoting the larger crystal formation.

In this study, ZIF-8 crystals were synthesized at different Hmim/Zn<sup>2+</sup> ratios. XRD patterns of ZIF-8 crystals were given in Figure 4.9. Also, experimental components were given in Table 4.5. The most interesting aspect of this graph is that when XRD patterns of each experiment were compared with simulated pattern (K. S. Park et al., 2006), all peaks of the ZIF-8 samples match with simulated peaks. The difference at the ratio of Hmim/Zn<sup>2+</sup> may reduce the crystal size but the morphology of ZIF-8 crystals was well-preserved as presented in Figure 4.9 like reported by Pan and friends (Pan et al., 2011; Tanaka et al., 2012).

On the other hand, the zinc-based yield percentages of syntheses are presented in Figure 4.10 for various Hmim/ $Zn^{2+}$  ratios. The yield decreased dramatically with the decreasing of the Hmim at ZIF-8-2 sample. Also, regarding the Hmim/ $Zn^{2+}$  ratios, crystallinity decreases with higher Hmim/ $Zn^{2+}$  ratio. These are rather significant outcomes to understand the effect of Hmim on the formation of ZIF-8.

The maximum yield was obtained at ZIF-8-4 sample, as  $50\pm 0.5\%$ . The theoretical maximum product amount calculations were given in Appendix D. According to the calculation for ZIF-8-1, ZIF-8-2, ZIF-8-3, ZIF-8-4, and ZIF-8-5 syntheses, the maximum reachable product amounts are 1.84 g, 1.84 g, 0.92 g, 0.77 g, 0.47 g, respectively. When the maximum theoretical product amount and experimental yields were considered, ZIF-8-4 and ZIF-8-5 samples provide less amount of product. That's why, to get a higher amount of product, ZIF-8-1, and ZIF-8-3 samples are better than others but, ZIF-8-3 provides 1.2-fold higher yield than ZIF-8-1 sample. Nevertheless, ZIF-8-1 supplies 2-fold higher production possibility than ZIF-8-3. Also, when the experimental produced ZIF-8 amounts were considered, 0.692 g, 0.487 g, 0.412 g, 0.384 g, and 0.225 g productions were obtained for ZIF-8-1, ZIF-8-2, ZIF-8-3, ZIF-8-4, and ZIF-8-5, respectively. For the ZIF-8 production, minimum utilization of MeOH is desired in the synthesis because of the toxic properties of methanol. So, ZIF-8-1 sample production was chosen for higher production with minimum methanol utilization in this study. In addition, BET surface area,  $1259\text{ m}^2/\text{g}$  was obtained for the ZIF-8-1 production. The ZIF-8-1 production presents high surface area providing high protein adsorption on the resin surface.

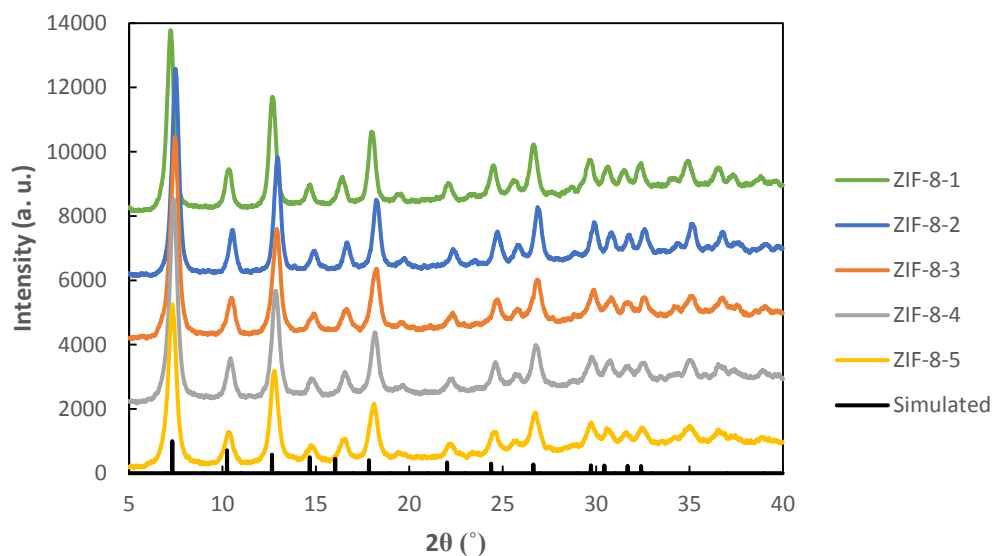


**Figure 4. 9** XRD patterns of various Hmim/Zn<sup>2+</sup> experiments of ZIF-8

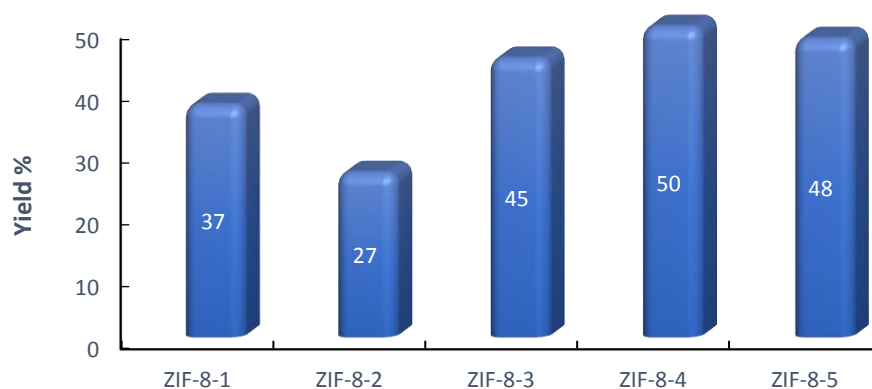


**Figure 4. 10** Yield percentage of various Hmim/Zn<sup>2+</sup> experiments of ZIF-8

#### 4.5.2. Effect of NaOH on ZIF-8 production

NaOH was used to overcome low yield problem. In presence of NaOH, ZIF-8 shows high stability and also if ZIF-8 crystals are synthesized in a basic medium, ZIF-8 crystal formation is promoted because of the deprotonation effect of NaOH.

Approximately 1 g NaOH was added at the different time interval to the different ZIF-8 syntheses. XRD patterns were compared in Figure 4.11. What is interesting

about the data in this table is that when the NaOH added productions were compared with standard ZIF-8 synthesis, the addition of the NaOH to the production medium at the beginning of the synthesis causes low crystallinity. However, the addition of the NaOH to the batch medium after 30 minutes indicates similar crystallinity with standard ZIF-8 production. One interesting finding for these patterns is that addition of the NaOH after  $t = 30$  min of the synthesis promotes the growth of ZIF-8 crystals which reached to required nucleation level.

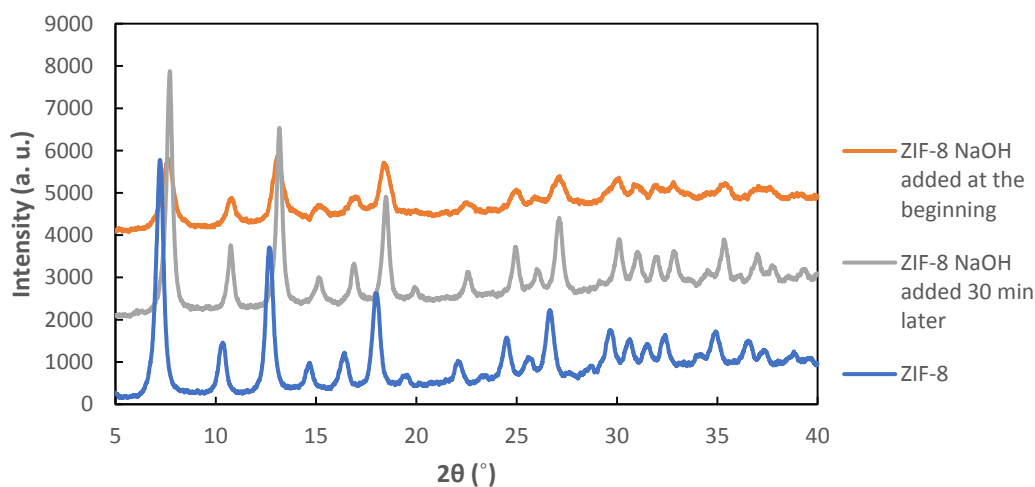


**Figure 4. 11** XRD patterns of NaOH added experiments into the ZIF-8 synthesis

Furthermore, NaOH addition into the production medium is definitely increasing the production yield. Especially, 2.64-fold higher production yield percentage was succeeded for NaOH was added 30 minutes later to ZIF-8 synthesis. The maximum production, 1.82 g, as well as high crystallinity were reached as a result of the addition of NaOH after 30 minutes into the medium as presented in Figure 4.11 and Figure 4.12.

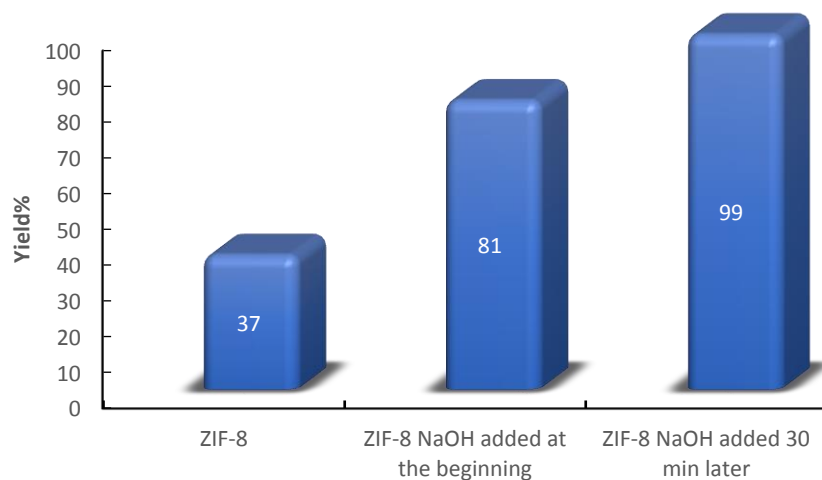


**Figure 4. 12** Effect of NaOH addition on yield percentage of ZIF-8

SEM micrographs were taken for 30 min. later NaOH added ZIF-8 are given in Appendix F. Homogeneous distribution was observed yet, crystal size increased to approximately 100 nm. As a result, NaOH is promoting the crystal growth.

#### **4.5.3. Effect of modifications on ZIF-8**

ZIF-8 crystals were modified to design selective particles on separation and purification of His-tagged proteins. The first step is the adding of the 1-methylimidazole (1-MI) as a terminating ligand into the ZIF-8 synthesis. The usage reason for 1-MI was to stop the crystal growth and create an imidazole ring outside of the crystal surface for further modifications.

When the 1-MI was added into the synthesis medium, zinc ions bind with nitrogen part which is at the non-methyl bonded side of the 1-MI. Then, new zinc cannot bind to the 1-MI because the other nitrogen part has a bond with a methyl group. Hence, 1-MI indicates the termination property on the ZIF-8 crystal formation. As a result of slower growth, larger crystals are obtained rather than unmodified ZIF-8 crystals. The most striking result to emerge from the XRD patterns is that higher crystallinity was observed at modified ZIF-8 with 1-methylimidazole (1-MI-ZIF-

8). The XRD patterns of the modified and unmodified ZIF-8 particles were presented in Figure 4.13.

On the other hand, production yield decreases with the addition of 1-MI into the synthesis medium because of the terminating property of 1-MI on ZIF-8 framework structure as mentioned before. Synthesis time was optimized to find the most effective 1-MI-ZIF-8 production. The comparison of the three syntheses at the different production time reveals that any increase in yield was not observed with increasing synthesis time after 3 hours. As a result of these data, 3 hours was found more favor than the others and so, it was defined as a production time. The yield of ZIF-8 decreased to  $9\pm 0.5\%$  after the modification. The differences in the yield of 1-MI-ZIF-8 and ZIF-8 productions are presented in Figure 4.14 and XRD patterns were given in Figure 4.15 to compare crystal structures.

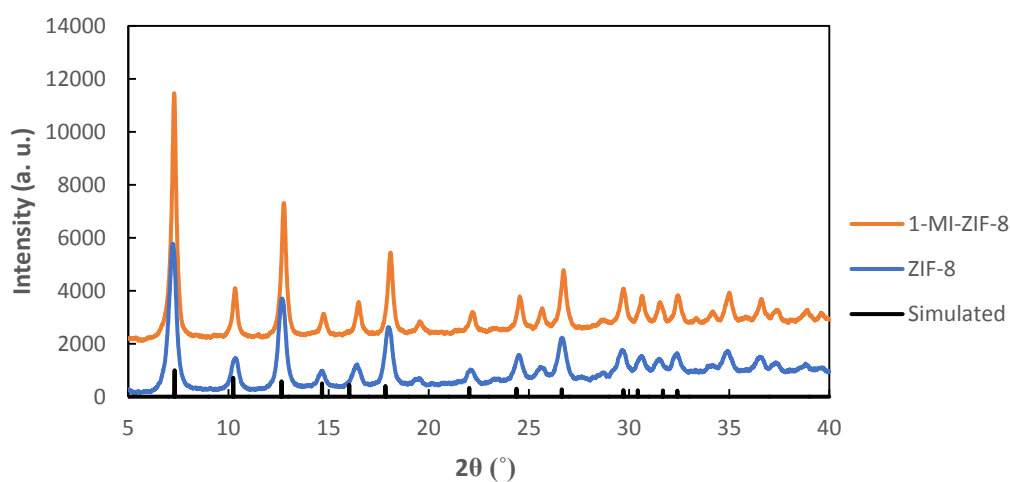


**Figure 4. 13** XRD pattern of 1-MI-ZIF-8 modification



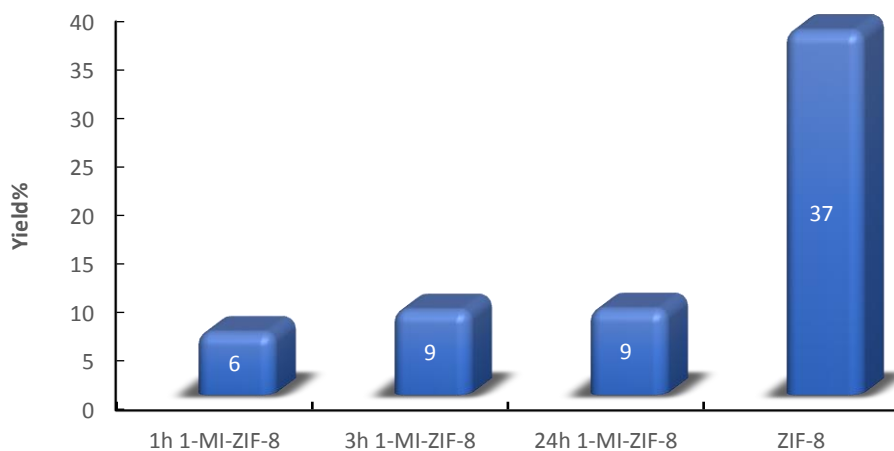


**Figure 4. 14** Yield percentage change of 1-MI-ZIF-8 with time

As it can be seen from the Figure 4.15, there are not any differences in XRD patterns. The particle structure is not affected by synthesis time and the desired crystal structure was obtained for each of the production.

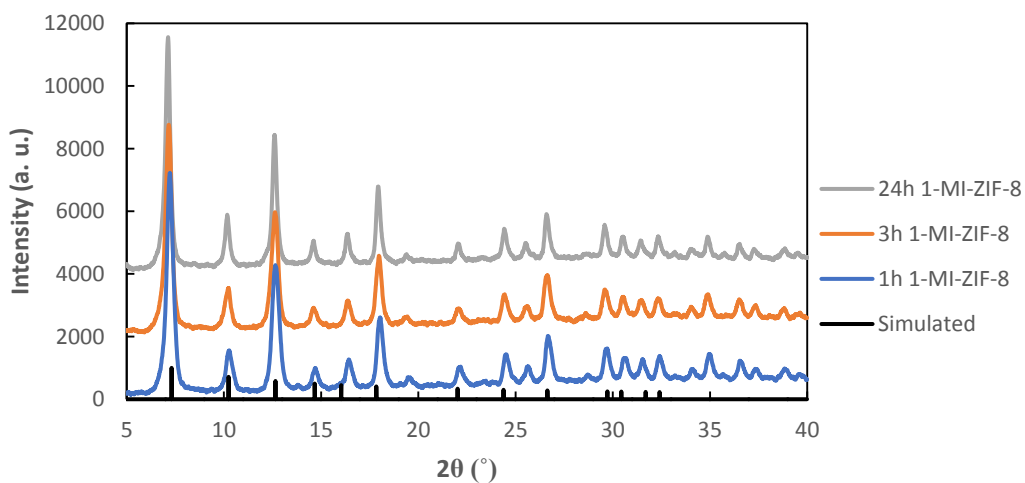


**Figure 4. 15** Variation of crystal structure of 1-MI-ZIF-8 with time

#### 4.5.3.1. Effect of Hmim/1-MI ratio

The Hmim/1-MI ratio was changed, to understand the effects of 1-MI in detailed for 1-MI-ZIF-8 synthesis. While the ratio alteration was applied on the synthesis, the total imidazole source amount was held constant at 5.28 g.

**Table 4. 6** Experimental design of Hmim/1-MI experiments

| Experimental Code | Zn(NO <sub>3</sub> ) <sub>2</sub> ·6H <sub>2</sub> O (g) | Hmim (g) | 1-MI (g) | MeOH (g) |
|-------------------|--|----------|----------|----------|
| ZIF-8-1           | 2.4  | 5.28     | -        | 181      |
| 1-MI-ZIF-8-1      | 2.4  | 2.64     | 2.64     | 181      |
| 1-MI-ZIF-8-2      | 2.4  | 3.52     | 1.76     | 181      |
| 1-MI-ZIF-8-3      | 2.4  | 4.224    | 1.056    | 181      |

XRD patterns are given in Figure 4.16. The crystallinity of 1-MI-ZIF-8 particles was increased by adding of 1-MI for all samples. The highest crystallinity was seen at 1-MI-ZIF-8-1 but the crystallinity is approximately similar with 1-MI-ZIF-2. However, the crystallinity of 1-MI-ZIF-3 is lower than others because it has the lowest 1-MI amount. In addition, an increase was observed in the production yield, while added 1-MI amount was decreasing because of the terminating property of 1-MI on ZIF-8 crystals growth. To provide higher crystallinity, 1-MI-ZIF-8-1 was chosen as a production system.

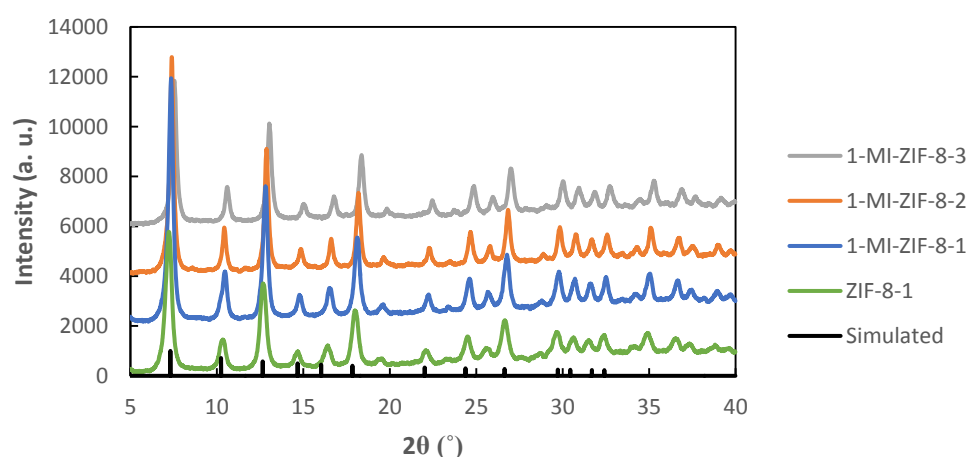


**Figure 4. 16** XRD patterns of various Hmim/1-MI experiments of 1-MI-ZIF-8

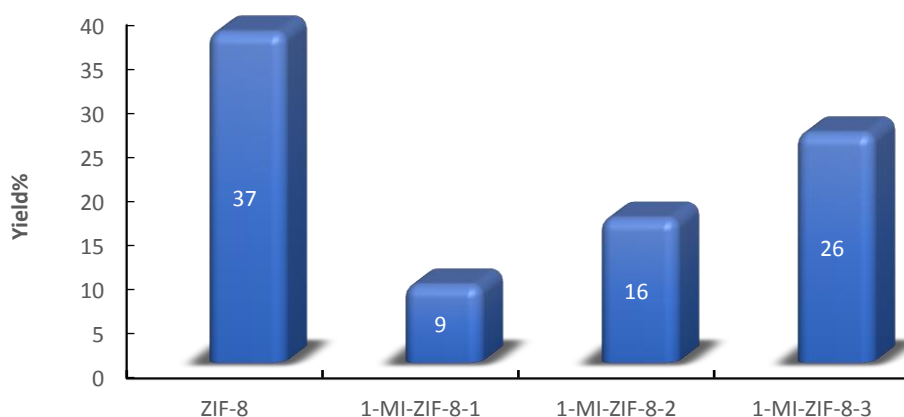


**Figure 4. 17** Yield percentage of various Hmim/1-MI experiments of 1-MI-ZIF-8

Unfortunately, the 1-MI-ZIF-8 yield is very low, so to increase the yield NaOH was used. The same procedure of ZIF-8 was applied for the addition of NaOH into the synthesis of 1-MI-ZIF-8. XRD patterns and yields were given in Figure 4.18 and Figure 4.19, respectively.

Same results were observed in XRD patterns of 1-MI-ZIF-8 productions. NaOH addition at the beginning causes low crystallinity because of the low nucleation but if NaOH was added after 1 hour, crystallinity is better than the addition of NaOH at the beginning. However, NaOH addition causes lower crystallinity than standard 1-MI-ZIF-8. To overcome low crystallinity, addition time of NaOH can be increased yet, XRD pattern of ZIF-8 and 1 hour later NaOH added 1-MI-ZIF-8 pattern are similar each other.

Additionally, NaOH promotes the formation of 1-MI-ZIF-8 crystals. The maximum yield,  $64 \pm 0.5$  %, was reached with the addition of NaOH at the beginning of the 1-MI-ZIF-8 synthesis. However, when XRD patterns were considered, crystallinity decreased with the addition of NaOH at the beginning of the synthesis. Therefore, 1 hour later NaOH added synthesis is better than the other despite the lower yield,  $41 \pm 0.5$  %.

SEM micrographs showed the non-homogeneous distribution for crystal size changing from 200 nm to 1.0  $\mu\text{m}$  and crystals are well-shaped. However, when the NaOH added to 1-MI-ZIF-8 synthesis after 1-hour, higher crystal size, approximately 400 nm, were observed with smaller structures. The images were given in Appendix F for both conditions.

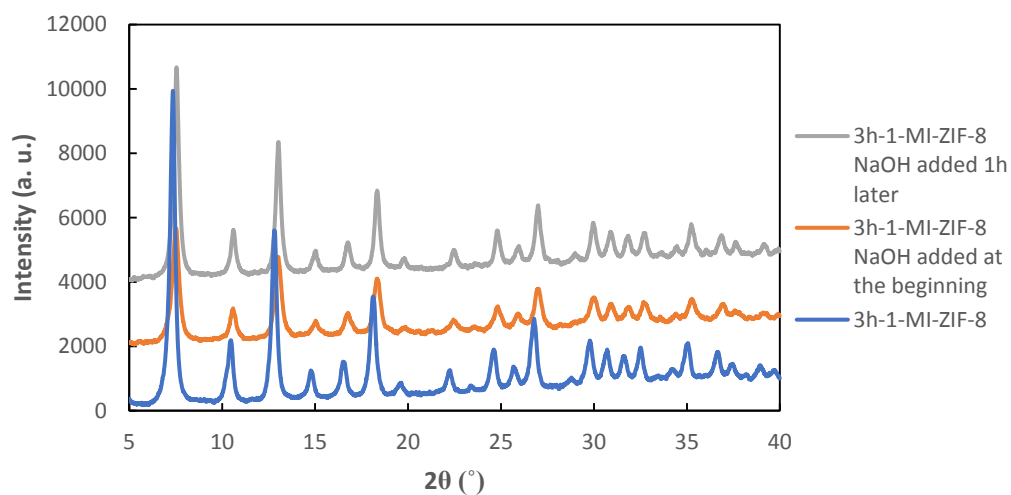


**Figure 4. 18** XRD patterns of NaOH added experiments into the 1-MI-ZIF-8 synthesis

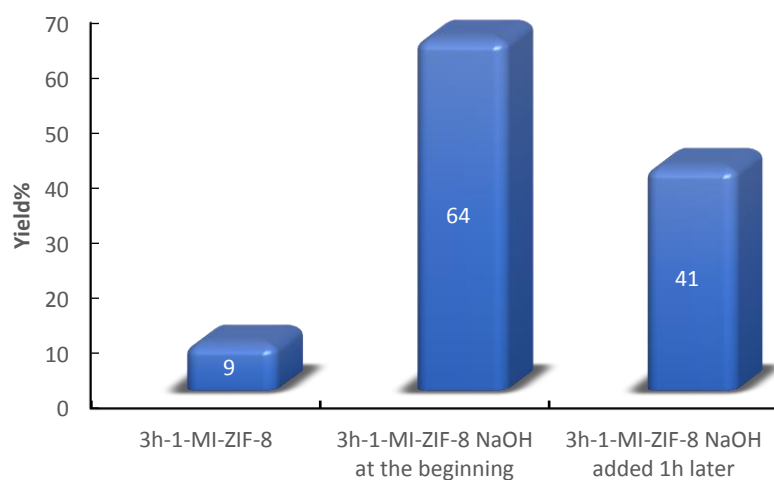


**Figure 4. 19** Yield of 1-MI-ZIF-8 syntheses with addition time of NaOH

#### **4.6. Separation and Purification Experiments**

Usage of ZIF-8 as an adsorbent for separation and purification of recombinant proteins is a new application, therefore, required adsorption, washing or elution conditions should be determined. When all of the parameters were considered, initially temperature effect was investigated to find the optimum value for experiments. The effect of temperature was just applied on elution step because adsorption capacity of ZIF-8 was observed between 90%- 100%, so elution step was identified as a key point for determination of optimum temperature.

Then, different chemicals were tested with different molarity to find the best eluent for the ZIF-8 crystals. In the light of the literature, NaOH, NaCl, imidazole, glycerol, Triton X-100 and others were applied. With the results of the experiments, the suitable eluent was detected and different parameters were used like pI point and time in order to improve the purification performance.

##### **4.6.1. Separation and purification performance of ZIF-8 on rhGH**

Initially, adsorption, washing, and elution steps were tested on ZIF-8 crystals in order to see the performance of ZIF-8. All solutions were used in each phase of the separation and purification were prepared according to the literature. In washing step, 0.4 M NaCl and 0.03 M imidazole was used to get unbound target proteins and undesired proteins. Then, 1.5 M imidazole elution was used. When the 0.1 g ZIF-8 crystals were incubated with 1 ml rhGH production medium, the remained medium was saved and then washing and elution steps were applied.

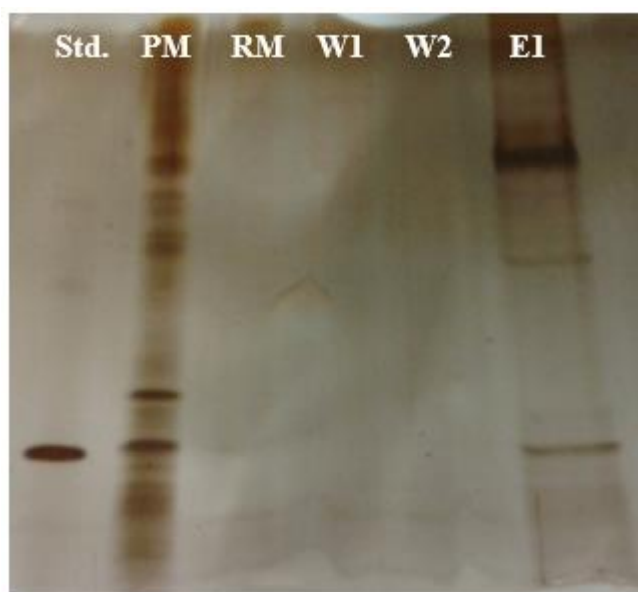


**Figure 4. 20** rhGH separation by ZIF-8 (Std, standard; PM, production medium; RM, remained medium after adsorption; W, wash; E, elution).

It is quite surprising that any protein cannot be observed in the medium after the adsorption step because all proteins in the production medium are held by ZIF-8. The adsorption performance of ZIF-8 is good but the adsorption is not selective. Any unbounded protein could not be observed during washing phase. Furthermore, the low and promiscuous separation was performed through elution process.

To overcome the non-selective adsorption or elution, the separation and purification steps or ZIF-8 crystal can be optimized and redesigned to get better results. Bimetallic production systems for ZIF-8 synthesis, impregnation of a second metal on ZIF-8, adding terminating ligand into the ZIF-8 production system for further modification, and surface ligand exchange reactions can be applied to modify ZIF-8 crystals. In addition, temperature, time, different solutions with different concentration can be applied for separation and purification step.

#### 4.6.2. Modification of ZIF-8 with nickel metal

Different types of impregnation and synthesis methods were used to observe the effect of nickel with impregnation or bimetallic (Ni-Zn) effect on ZIF-8. When nickel was impregnated on ZIF-8 with different sources, nickel amount was held constant. Bimetallic ZIF-8 synthesis procedure is same with ZIF-8 synthesis. After impregnation of nickel on ZIF-8 crystals, the color of particles changed from white to light green. On the other hand, when the nickel source was added into the synthesis medium, particle colors turn into violet, but synthesis of ZIF-8 with a different nickel source,  $\text{NiCl}_2 \cdot 6\text{H}_2\text{O}$ , was resulted in unsuccessful ZIF-8 synthesis. Yellow flakes occurred and the color changed into black when the product was dried at  $80\text{ }^\circ\text{C}$ . Any specific peak could not be taken from XRD pattern (data not shown), so it was not used as a nickel source for synthesis method. Ni/ZIF-8-5 was synthesized according to the Li and friends study (R. Li, Ren, Ma, et al., 2014). SEM micrographs and XRD pattern of Ni/ZIF-8-5 were given in Appendix F. Interestingly, smaller crystal size, 30-35 nm, was obtained than ZIF-8 when the nickel was added to the synthesis medium.

**Table 4. 7** Composition of Nickel impregnation on ZIF-8 and synthesis of bimetallic ZIF-8

| Code                | $\text{Zn}(\text{NO}_3)_2 \cdot 6\text{H}_2\text{O}$ | ZIF-8 | Hmim      | Water | MeOH  | $\text{NiCl}_2 \cdot 6\text{H}_2\text{O}$ | $\text{Ni}(\text{NO}_3)_2 \cdot 6\text{H}_2\text{O}$ |
|---------------------|--|-------|-----------|-------|-------|---|--|
| <b>Impregnation</b> |  |       |           |       |       |   |  |
| Ni-ZIF-8-1          | -  | 0.5 g | -         | 25 ml | -     | 0.4 mmol                                  | -  |
| Ni-ZIF-8-2          | -  | 0.5 g | -         | 25 ml | -     | -   | 0.6 mmol   |
| <b>Synthesis</b>    |  |       |           |       |       |   |  |
| Ni/ZIF-8-3          | 0.5 mmol   | -     | 60 mmol   | -     | 50 ml | -   | 0.5 mmol   |
| Ni/ZIF-8-4          | 1.0 mmol   | -     | 15.8 mmol | -     | 30 ml | -   | 1.0 mmol   |
| Ni/ZIF-8-5          | 1.0 mmol   | -     | 15.8 mmol | -     | 60 ml | -   | 1.0 mmol   |

### 4.6.3. Comparison of Ni/ZIF-8 and Ni impregnated ZIF-8 resins for separation and purification of rhGH

Nickel is one of the most used metal ions for the separation and purification of 6xHis-tagged recombinant proteins. Therefore, nickel was used as a second metal ion and added to synthesis medium.

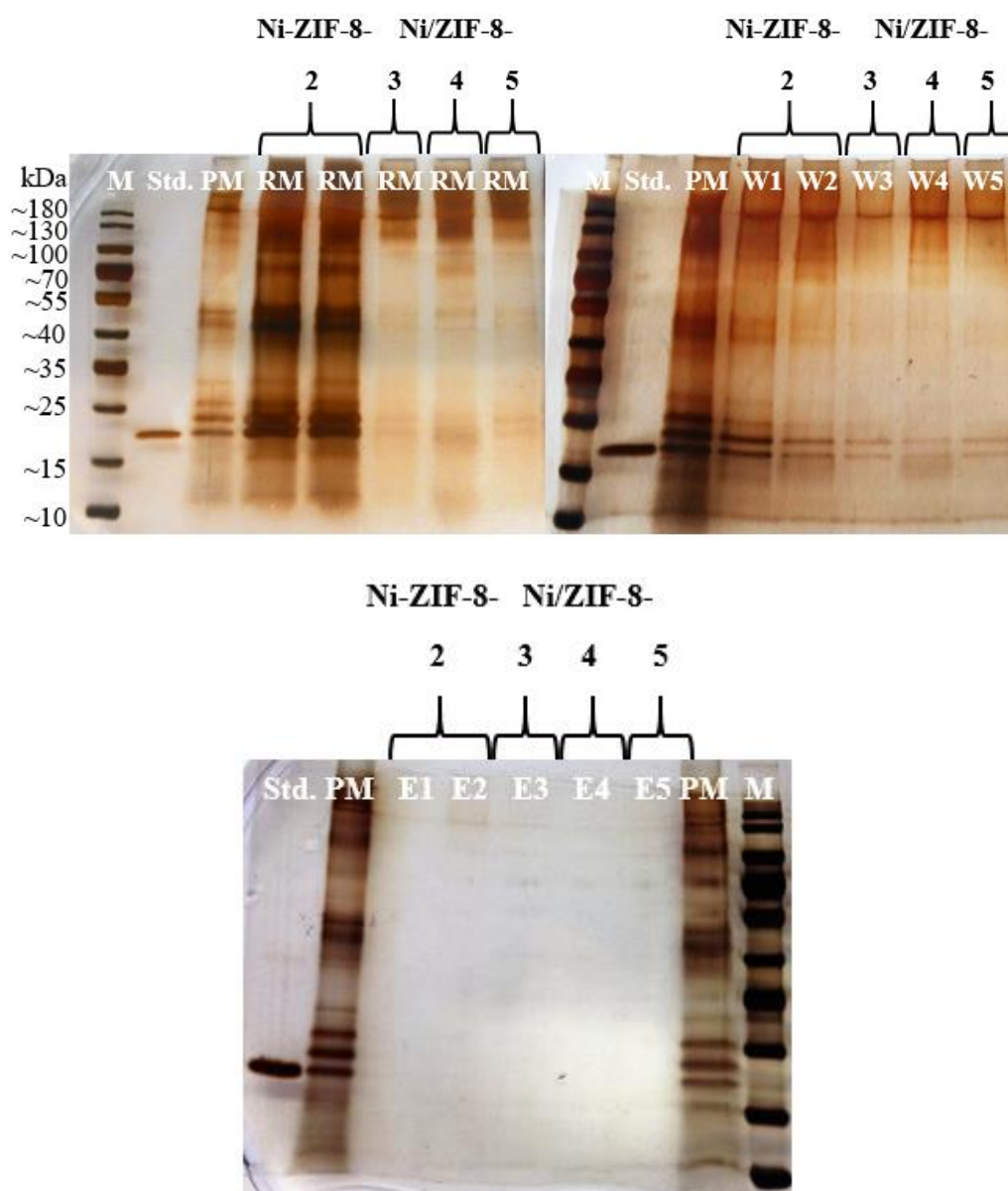


**Figure 4. 21** Comparison of Ni-ZIF-8 and Ni/ZIF-8 crystals



When the remained medium after adsorption were compared with each other, Ni impregnated ZIF-8 structures were not effective than Ni/ZIF-8 (bimetallic) synthesized products, definitely. Also, similar outcomes were observed at washing steps. However, any positive result could not be reached for all of the production methods.

As a result of these experiments, adsorption performance of nickel impregnated ZIF-8 is not more effective than others. The reason for this result related to the competitive effect of zinc and nickel metals which can be explained coordination number of  $Zn^{2+}$  and  $Ni^{2+}$  ions. The coordination number of these ions is 4 and make tetrahedral structures. Hence, the competitive interaction occurs between metal ions because of the similar tetrahedral complexes (Nielsen, 1984).

#### 4.6.4. Comparison of ZIF-8 and bimetallic Ni/ZIF-8 particles

ZIF-8 and Ni/ZIF-8-5 crystals were compared with each other to understand the effect of nickel on the performance of ZIF-8 crystals. As can be seen from the SDS-PAGE image shown in Figure 4.22, adsorption performance of the ZIF-8 is better than Ni/ZIF-8-5. However, none of them presented a positive elution as expected.

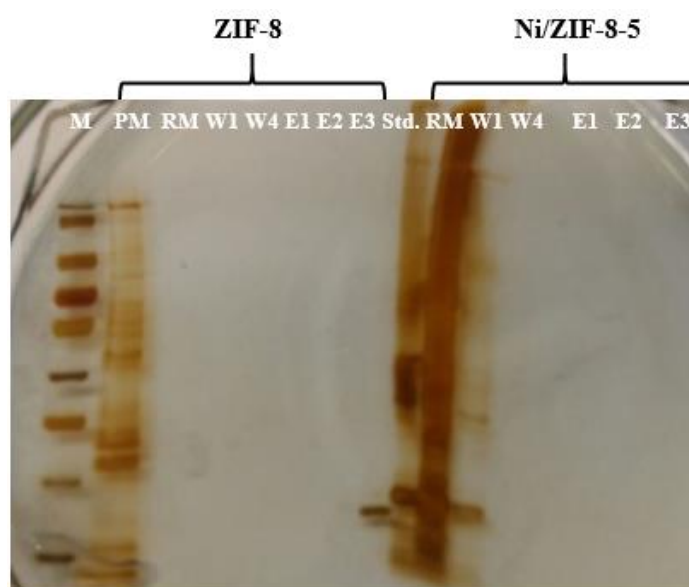


**Figure 4. 22** Comparison of ZIF-8 and Ni/ZIF-8

#### 4.6.5. Temperature effects on elution step

Three experiments were prepared to observe the effect of temperature on the elution step. For temperature experiments, 25 °C, 35 °C, and 40 °C were chosen. Over 40 °C was not tested regarding maximum body temperature of a human. Also, below the 40 °C temperature, protein can protect its stability.

When the elution columns were compared with each other, eluted protein amount is the highest at 35 °C. The elution was applied on 35 °C, E2, is 4.2-fold higher than E1 and 3.3-fold higher than E3 elution. So, 35 °C was chosen for separation and purification experiments.

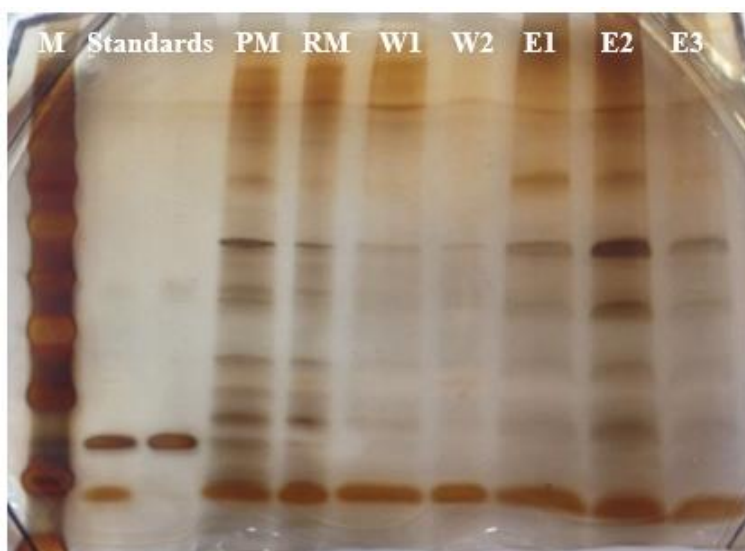


**Figure 4. 23** Effect of temperature on elution (M, marker; hGH standard with lysozyme and hGH standard; PM, production medium x10 diluted; RM, supernatant after adsorption; W, wash; E1, elution at 25 °C; E2, elution at 35 °C; elution at 40 °C).

#### 4.6.6. Determination of the suitable washing and elution composition for ZIF-8 adsorbent

In the literature, NaCl was used to get rid of hydrophobic interactions between the protein-protein or protein-resin. In addition, low amount of imidazole was used in

washing step to get unbounded biomolecules on the adsorbent surface after that for elution step, imidazole was used at higher molarity than washing step. Initially, 0.4 M NaCl and 0.03 M imidazole was used in washing step then, different eluent concentrations were tried at 0.5 M, 1 M, 1.5 M imidazole solutions for elution step.

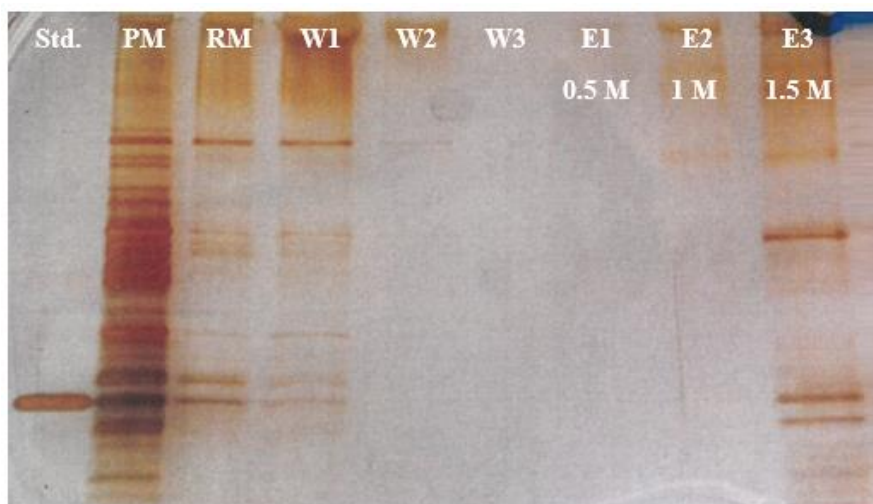


**Figure 4. 24** Eluent concentration effect on elution step

rhGH protein elution was provided with higher imidazole concentration but eluate is including other proteins in the production medium. 1.5 M imidazole is the best than the 0.5 M and 1 M imidazole solutions, definitely. However, the Ni/ZIF-8 crystals showed physical change with an increment of imidazole concentration. The color of Ni/ZIF-8 crystals changed into white from violet at the elution step. In order to understand the reason for the change SEM micrographs were taken for each step of separation and purification process.



**Figure 4. 25** Color change of Ni/ZIF-8 structure at elution step

In order to observe the effect of washing and elution steps on Ni/ZIF-8 crystals, SEM micrographs were taken to understand the effect of imidazole on the resin. In Figure 4.26, SEM micrographs were given EDX results. The Ni/ZIF-8 crystals are homogeneous and the average size was calculated 30 nm. After the washing step, 0.4 M NaCl and 0.03 M imidazole, the crystals are still homogeneous but they are making clusters. The average particle size was obtained as approximately 35 nm which is higher than the initial size and when the EDX results were investigated, sodium and chloride elements were observed as expected. However, SEM micrographs showed that the influence of the elution step on the crystals can be seen easily. The particle size was increased from nano size to micro size. The mean of this result is that crystals are continuing to grow so crystal size is increasing and color of crystals is changing with growth. Therefore, using the imidazole is not suitable for ZIF-8. Maybe, in order to get rid of unbounded proteins, low imidazole concentration can be used.

As rhGH is an extracellular product, production medium contains other proteins. On the other hand, for rGCSF, after cell disruption a cleaning procedure was applied and undesired structures were cleaned as much as possible. In addition, when rhGH and rGCSF proteins were compared, rGCSF provided faster and easier detection at SDS-PAGE analysis due to its characteristic properties. Therefore, to overcome undesired problems an intracellular protein, rGCSF was considered. rGCSF protein provides simplicity for further investigations on separation and purification, due to pre-cleaning steps and ease of SDS-PAGE analysis.

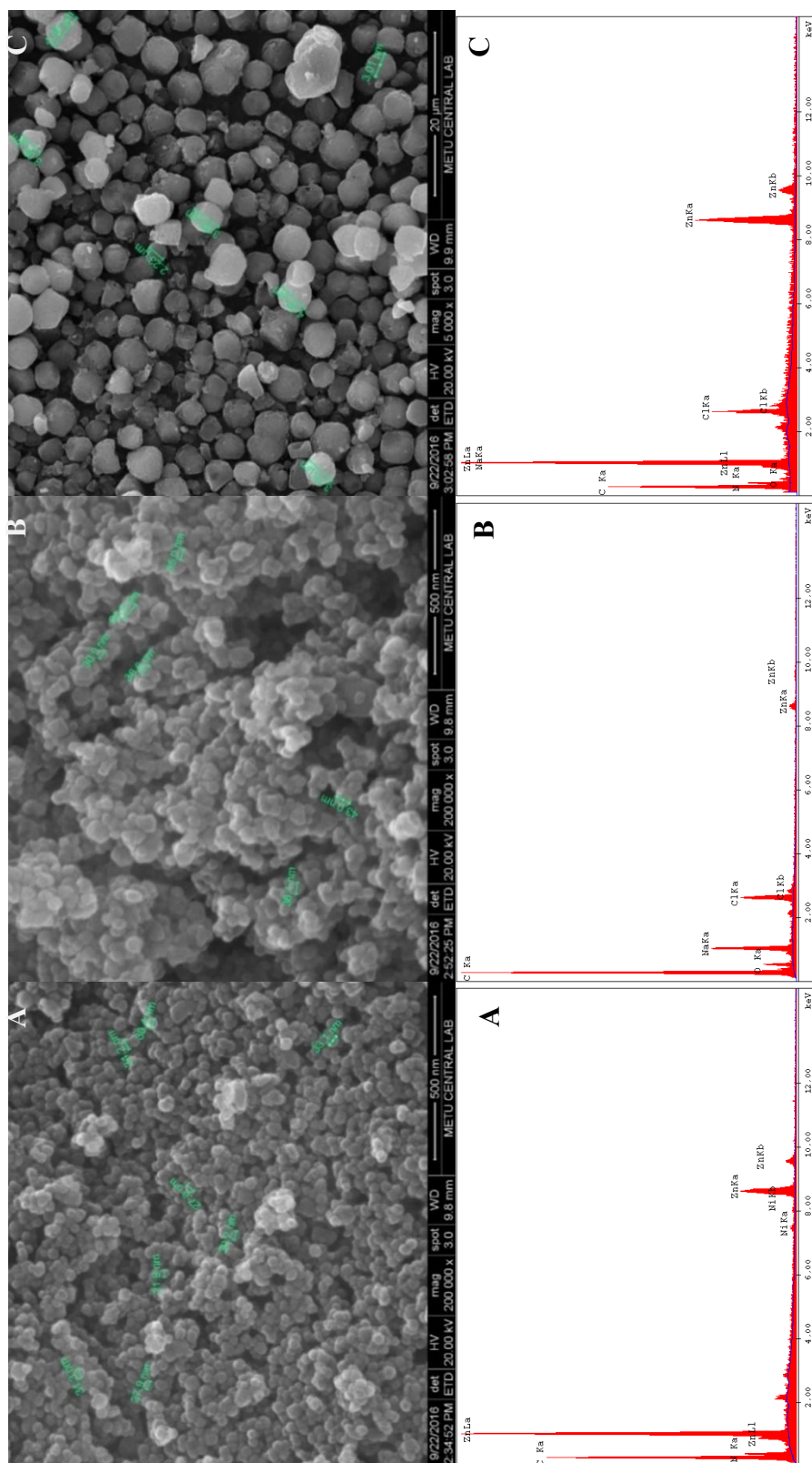


**Figure 4. 26** SEM micrographs of Ni/ZIF-8 crystals during separation and purification process (A, Ni/ZIF-8 crystals; B, after washing; C, after elution)

#### 4.6.7. Time optimization for rGCSF

rGCSF is a new protein in the laboratory so, required time was determined. In Figure 4. 27, 0-1, 1-2, and 2-3 minutes were tested and according to the SDS-PAGE gels, the result of 0-1 minute between is not trustable because developing step of the SDS-PAGE method is not enough to see all of proteins in the medium. Between 1-2 and 2-3 minutes results, developing step which is at 1-2 minutes is more acceptable because the color and width of bands become darker and large at 2-3 minutes. These cause wrong readings at concentration of protein bands so 1-2 minutes was selected favor time interval.

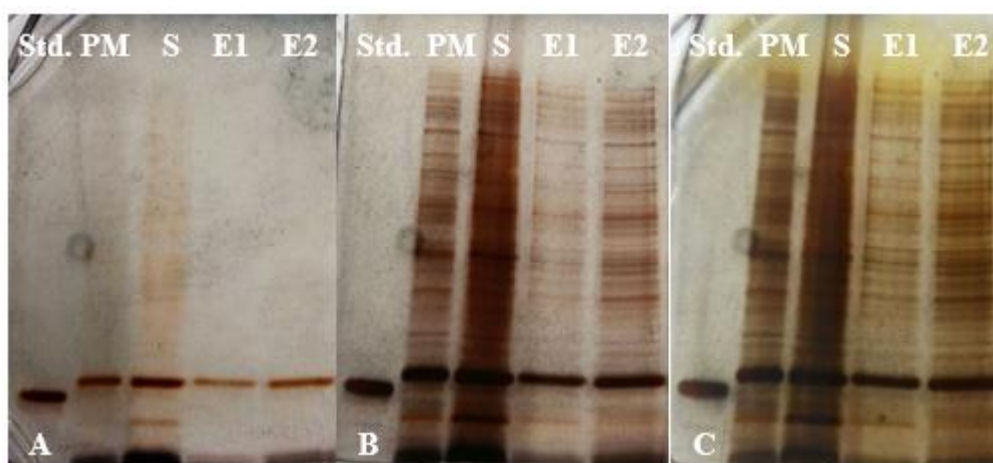


**Figure 4. 27** Time optimization of rGCSF for SDS-PAGE (A, 0-1 minute; B, 1-2 minutes; C, 2-3 minutes)

Production (reactor) medium is 20 times diluted in Figure 4.27. Concentrations of the target protein were calculated from readings of photograph B. 98% of rGCSF protein, 0.4 mg, was adsorbed but only 11% of reactor medium was eluted and the separation and purification were not selective.

#### 4.6.8. Comparison of Ni-ZIF-8 and Ni impregnated ZIF-8 resin for separation and purification of recombinant rGCSF

Similar experiments were applied, to understand the manner of ZIF-8 and Ni/ZIF-8 for rGCSF adsorption, separation and purification. When the remained protein amount in the production medium was compared with each other, ZIF-8 adsorption performance was found better in Figure 4.28. However, when the elution performances were compared with each other, unfortunately, elution steps are unsuccessful for both of them.

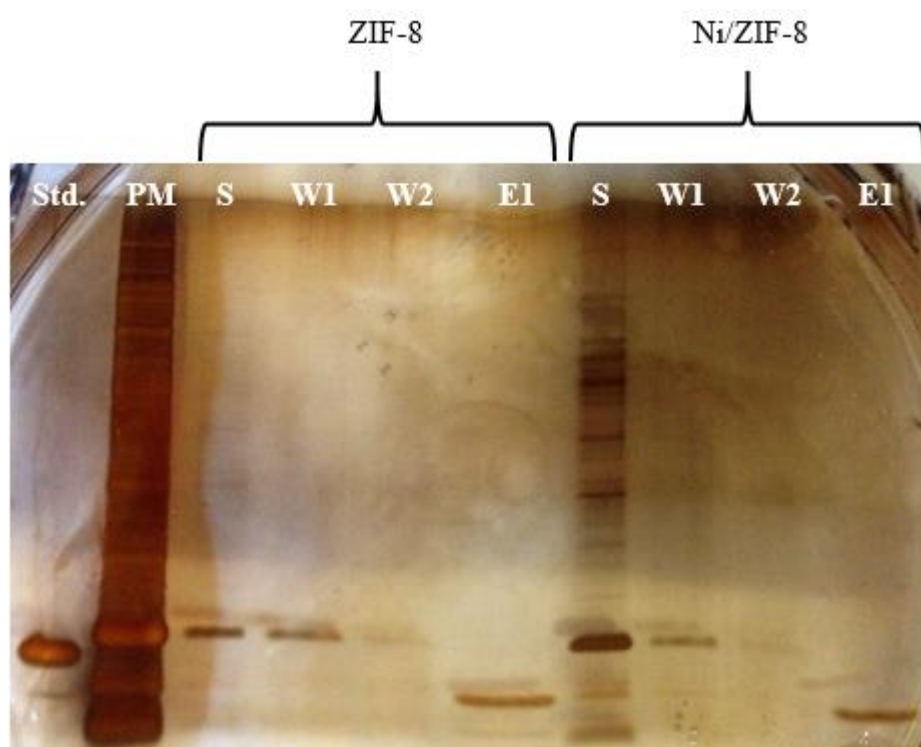


**Figure 4. 28** Comparison of ZIF-8 and Ni/ZIF-8 separation and purification performance

The adsorption performance of ZIF-8 is more than 2-fold of Ni/ZIF-8 adsorption. In the light of this result, further experiments were made with ZIF-8 crystals because usage of nickel is not providing any positive effect on purification.

#### 4.6.9. Adsorption equilibrium of rGCSF on ZIF-8

Adsorption equilibrium was calculated to determine the adsorption capacity of ZIF-8 crystals. In experiment, 0.2, 0.15, 0.1, 0.075, 0.05, 0.03, 0.02, and 0.01 g ZIF-8 were used for adsorption equilibrium calculation in Figure 4. 29.

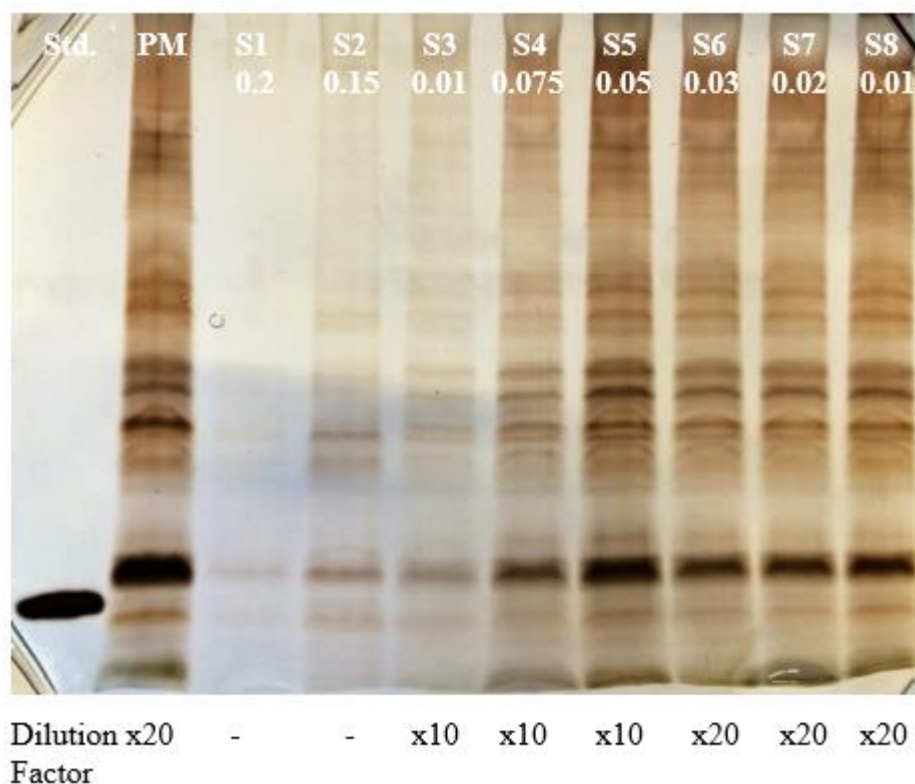


**Figure 4. 29** Adsorption performance of various amount of ZIF-8

Adsorbed recombinant rGCSF concentrations for each experiment were read from the SDS-PAGE analyze. From the graph below, adsorbed 6xHis-rGCSF amounts were indicated for different ZIF-8 amounts. In these experiments, production medium including 0.27 mg/ml 6xHis-rGCSF was used. When the SDS-PAGE results were investigated, 99% and 97% adsorptions were succeeded for 2 g and 1 g ZIF-8, respectively. The used ZIF-8 amounts and adsorption performances were considered, 0.1 g ZIF-8 was determined as an experimental amount. Used formulas for calculations were given in Appendix G.



Regarding the used ZIF-8 amount, changes at the adsorbed rGCSF amount were indicated in Figure 4.30, also  $q_e$  and  $C_e$  values were calculated and graphed in Figure 4.31 for adsorption equilibrium calculations.

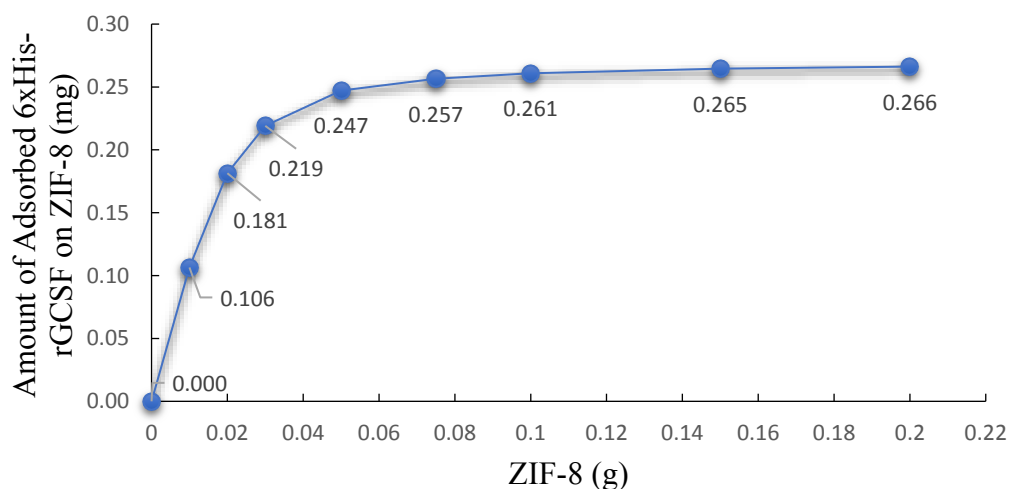


**Figure 4. 30** Adsorbed rGCSF amount versus ZIF-8 amount

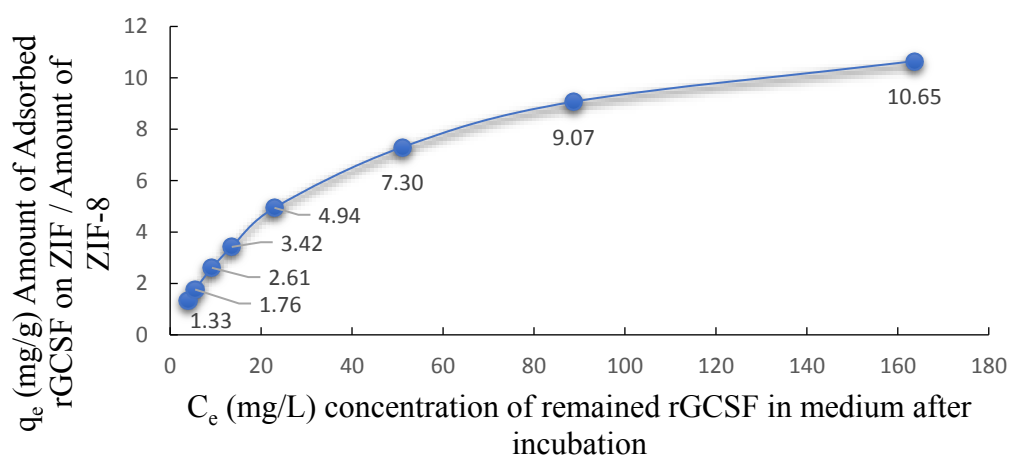


**Figure 4. 31**  $q_e$  (mg/g) versus  $C_e$  (mg/L)

Langmuir and Freundlich isotherms were shown in Figure 4. 32 and Figure 4. 33. To determine which isotherm is fitting to adsorption values of ZIF-8, regression factor was found and the one having closer value to 1 was selected as a more

appropriate isotherm. When isotherms were compared, Langmuir isotherm is better than Freundlich isotherm. This result shows that surface adsorption is possible and diffusion of the protein into pores is not effective on adsorption. Ineffectiveness of diffusion into the pores can be related to diffusion paths are being less with decreasing particle size.

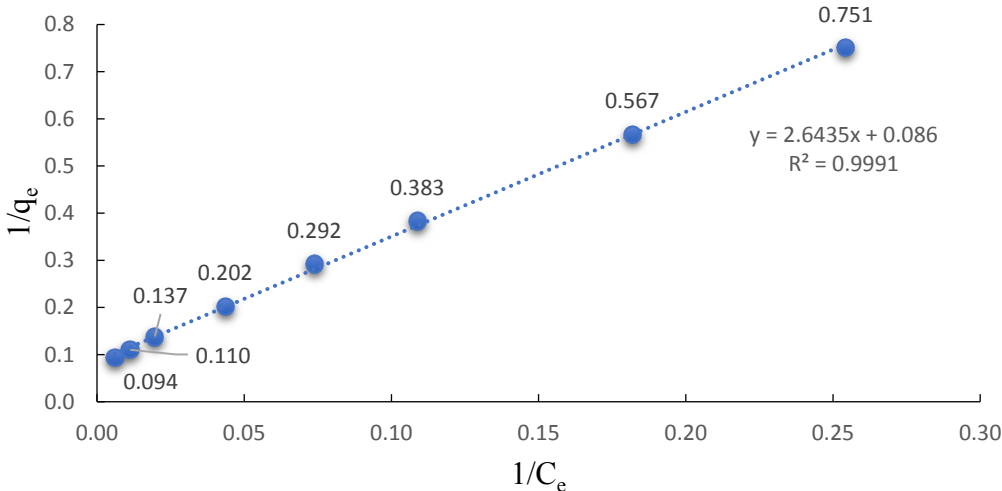


**Figure 4. 32** Langmuir isotherm of rGCSF

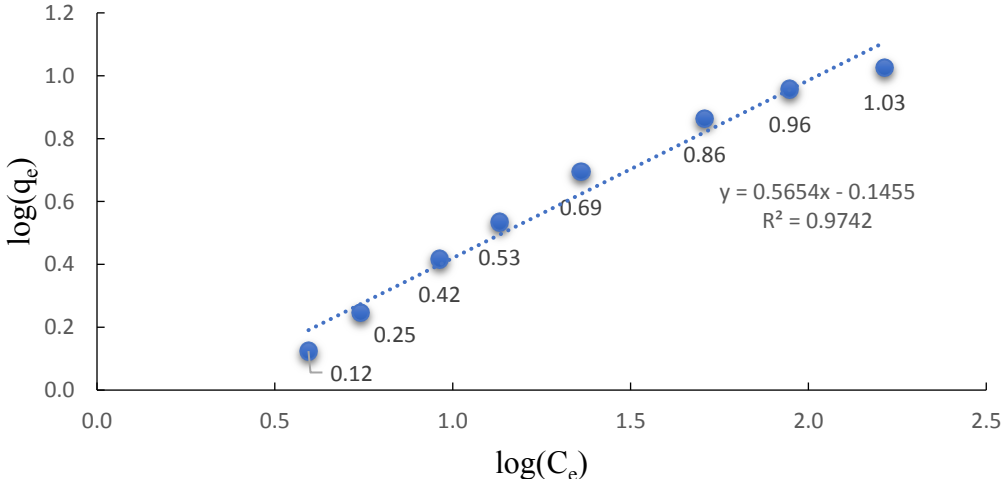


**Figure 4. 33** Freundlich isotherm of rGCSF

The maximum monolayer coverage capacity (mg/g),  $Q_0$ , Langmuir isotherm constant (L/mg),  $K_L$ , Freundlich isotherm constant (mg/g),  $K_f$ , and adsorption intensity,  $n$ , were calculated which are 11.6 mg/g, 0.0325 L/mg, 0.72 mg/g, and 1.77, respectively.

#### 4.6.10. Investigation of pH effect on adsorption and elution steps

2D electrophoresis experiment was applied to find pI point of rGCSF. In order to determine the molecular weight Spectra™ Multicolor Broad Range Protein Ladder was used.

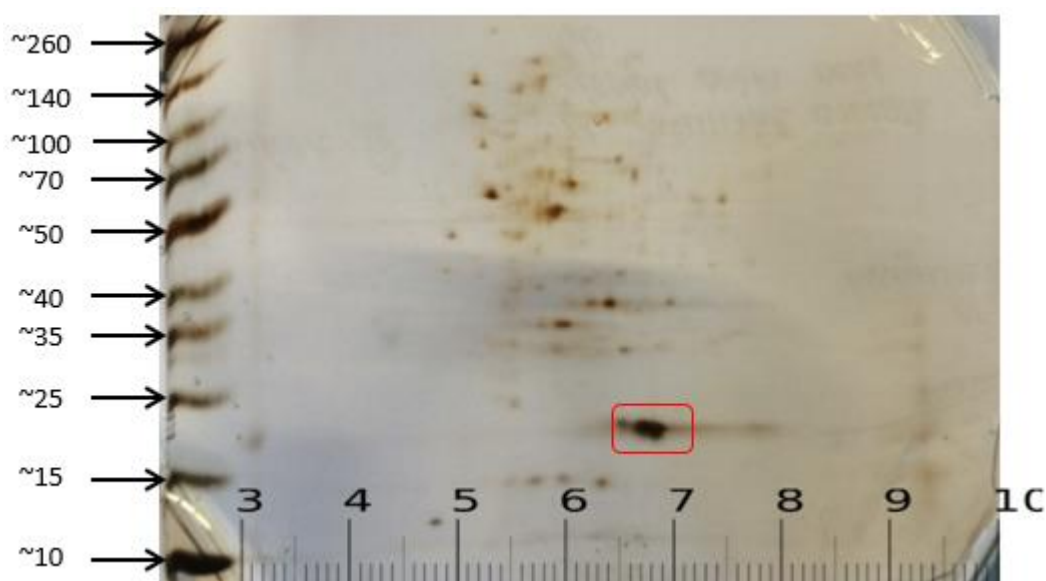


**Figure 4. 34** 2D Electrophoresis of rGCSF

Isoelectric point, pI, indicating the pH where the net protein charge is zero. In nature, proteins include ionizable parts at their amino acid sequence or amino acid. Also, the amino or carboxyl termini can be added into the ionizable chains. Proteins can be categorized regarding basic or acidic groups on the side chains. The basic group consists of arginine, histidine, and lysine and the acidic group includes asparagine and glutamine. Generally, if the pH of the solution is higher than pI, protein has net negative charge and if the pH of the solution is lower than pI, protein has net positive charge. The reason for this change can be explained like that

increasing at the pH of the solution causes deprotonation, so carboxylic groups turn into carboxylate anions and ammonium groups turn into amino groups.

As a result of 2D electrophoresis, in Figure 4.34, the pI point was found approximately 6.7-6.8 which is close to neutral value. To understand the comprehensive effect of pH, various pH conditions were tested on production medium, washing and elution steps in order to see pH effects on each step of separation and purification. The given images below show the effect of pH on adsorption of proteins on ZIF-8. The results obtained from the SDS-PAGE analyze, Figure 4.35, were set out that at low pH value, 5, adsorption of proteins is higher than others. While pH value of production medium is being increased, adsorption performance is decreasing gradually. Hence, pH of the medium, 5.5, was not changed and adsorption was held maximum level. On the other hand, any selective binding could not be observed both of the pH = 5 and the others.

When the elution steps were investigated, any selective elution could not be succeeded with pH changing. The most striking result to emerge from the data is that pH = 6 and 7 is the most effective value for elution step except for pH = 5 adsorption. Interestingly, pH = 5 and 8 are negatively influencing the elution of proteins. In addition, the reason for proteins could not be eluted can be that pH = 5 can cause strong adsorption of the proteins on ZIF-8.

As a result, the main reason for this experiment is considered, generally using of pH difference is one of the key parameters in the separation of the target protein. Unfortunately, pH effect on adsorption and elution is not selective when the behavior of the target protein and the others were compared. On the other hand, low pH was found better for adsorption and the most elution was succeeded at pH = 6 and 7. In the light of these findings, experiments were tried to design.

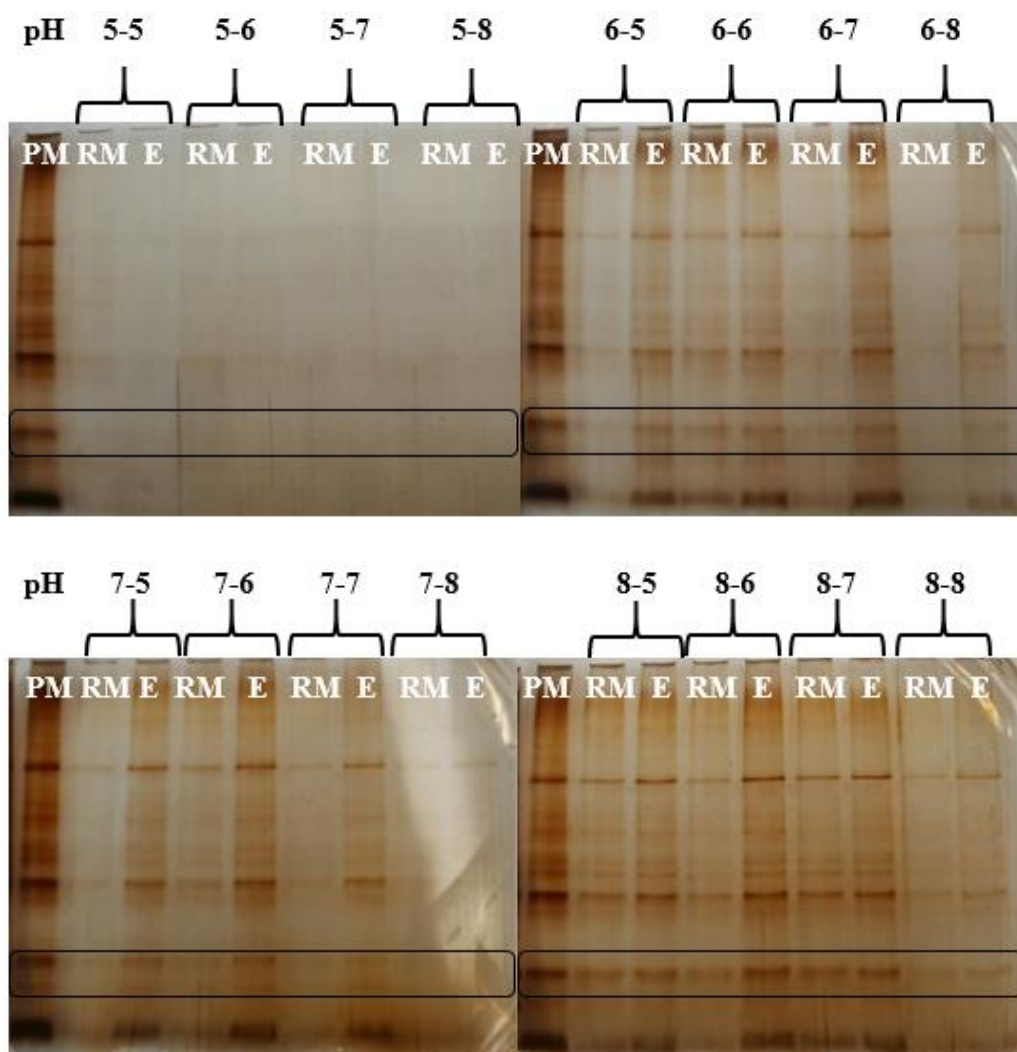


**Figure 4. 35** Effect of production medium pH on adsorption

The first pH value is for production medium, the second value represents the elution pH.

#### 4.6.11. Performance of different solvents for elution step

Up to now, as an eluent imidazole and NaCl was used so different solvents were tried to observe the performances of them at elution step. Used solvents which were selected for elution step were decided according to the literature studies. While different eluents were tested, the pH values of each solvent were recorded to perceive the effect of pH at elution step.

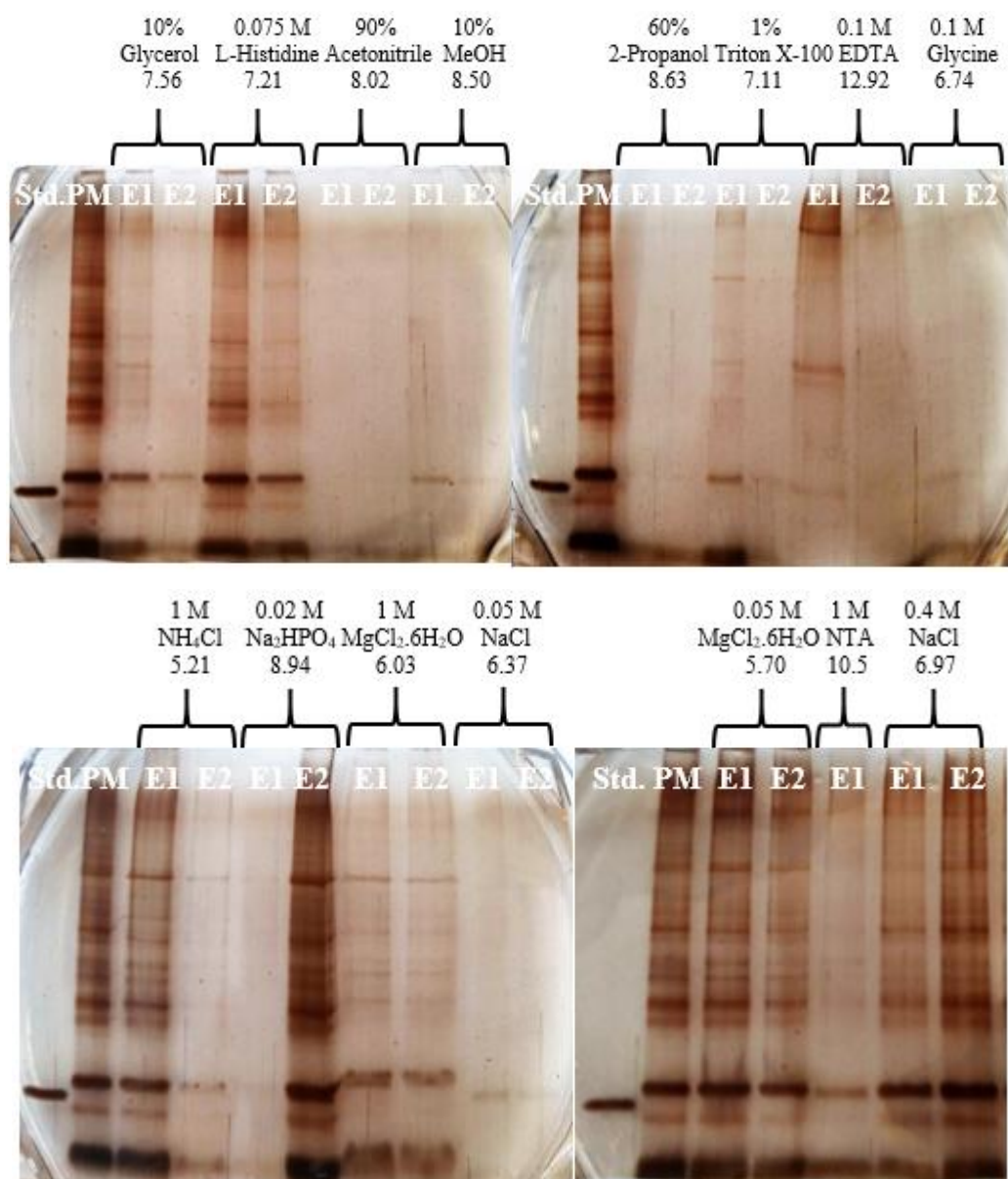


**Figure 4. 36** Elution step with different eluents

For each column in the SDS-PAGE, total protein concentration, the concentration of rGCSF, yield, and ratios of components were calculated. The calculations and results were given in Appendix E. When the eluents are compared with each other, especially, glycerol, L-histidine,  $\text{MgCl}_2 \cdot 6\text{H}_2\text{O}$ , NTA,  $\text{Na}_2\text{HPO}_4$ , and NaCl are found as promising solvents. Another important finding is that when the 0.05 M

and 0.4 M NaCl eluents were compared, eluted protein amount is increasing unselectively with NaCl concentration. The meaning of this finding shows that ionic interactions between surface and proteins are strong. Also, yield percentages of salts which are  $\text{NH}_4\text{Cl}$ ,  $\text{MgCl}_2 \cdot 6\text{H}_2\text{O}$ , and NaCl were compared with other chemicals, significant high yields were observed. This finding is supporting the previous comment about NaCl. Unfortunately, the ratio of separated protein to total protein amount and undesired protein amount is low. Besides that, the yield for all eluents is very low when the dilution factor, x20, of production medium is considered. On the other hand, to check the repeatability of experiments and to be sure about the performance of eluents, the promising eluents were tested again on ZIF-8.

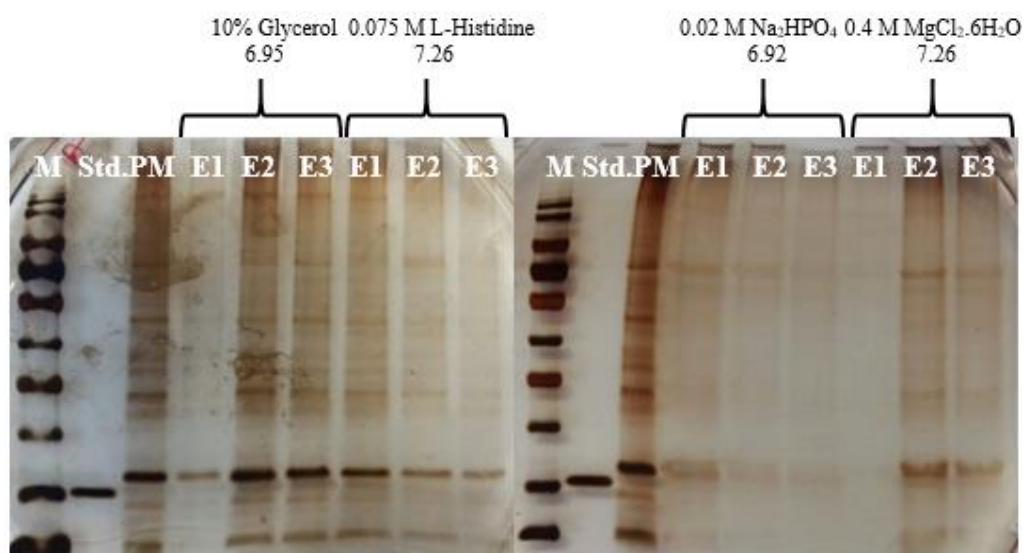


**Figure 4. 37** Elution steps of promising eluents

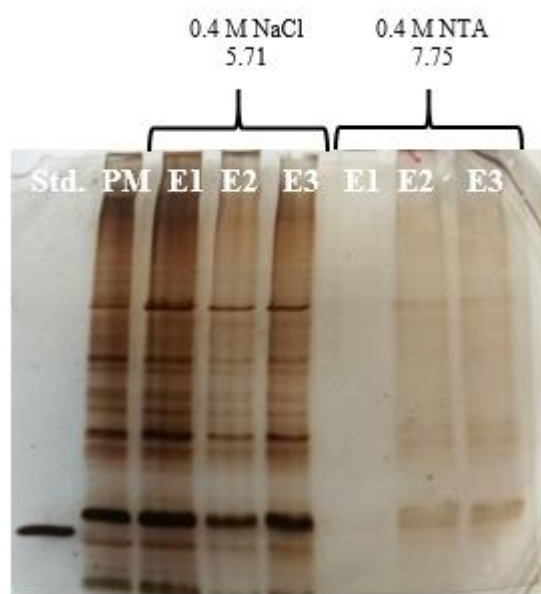


**Figure 4.37** Elution steps of promising eluents (*cont'd*)

Production medium was diluted with a factor of 20 for SDS-PAGE analysis. Selectivity ( $S_1$ ) is defined as the ratio of rGCSF concentration to undesired protein concentration ( $S_1$ ) and selectivity 2 ( $S_2$ ) is defined as the ratio of rGCSF concentration to total protein concentration ( $S_2$ ) in the elution. Yield percentage is defined as the ratio of separated rGCSF concentration to total rGCSF concentration in the production medium.

When  $S_1$ ,  $S_2$ , and yield percentages were considered, elution with NaCl provided 15% yield but  $S_1$  and  $S_2$  were 5.0 and 1.8, respectively. On the other hand, when elution was conducted with glycerol and L-histidine, 10% and 4% yields were obtained, respectively. In spite of the lower yield performance, glycerol and L-histidine provided higher  $S_1$  which are 9.9 and 8.9, respectively. In addition,  $S_2$  values were 2.3 and 2.2 with glycerol and L-histidine, respectively.  $S_1$ ,  $S_2$ , and yield percentage values of NTA,  $\text{Na}_2\text{HPO}_4$ , and  $\text{MgCl}_2 \cdot 6\text{H}_2\text{O}$  were lower than those of glycerol and L-histidine. In the light of these results, glycerol and L-histidine were used in different pH and different concentration combinations. To get detailed information, pH values were kept constant and different elution time intervals were



applied on the combination of glycerol and L-histidine were tested to find the best condition for these promising solvents in elution step. In Figure 4.38, SDS-PAGE results are given. For all conditions, there is no significant difference in elution steps with respect to elution time.

Moreover, comparison of 10% glycerol and 75 mM L-histidine demonstrates the remarkable performance superiority of 10% glycerol for all time intervals. On the other hand, combination of two eluents and effects of concentration were investigated. Concentrations were increased 50% of initial values. The increment from 10% to 15% glycerol did not present positive results. However, when the 75 mM L-histidine concentration was increased to 112.5 mM, elution performance decreased for all time intervals, so glycerol was chosen as an eluent. The higher performance of glycerol can be related to that glycerol causes stabilization of the protein and it prevents hydrophobic interactions between the resin and the protein. It creates an amphiphilic interface between the polar solvent and hydrophobic solvent, also reacts with adjacent hydrophobic parts (Vagenende, Yap, & Trout, 2009).

Also, combination of these two eluents was tested and the performance of combination is better than L-histidine performance as expected but the elution performance is worse than glucose. This expected result shows that existing of L-histidine is repressing the glycerol performance.

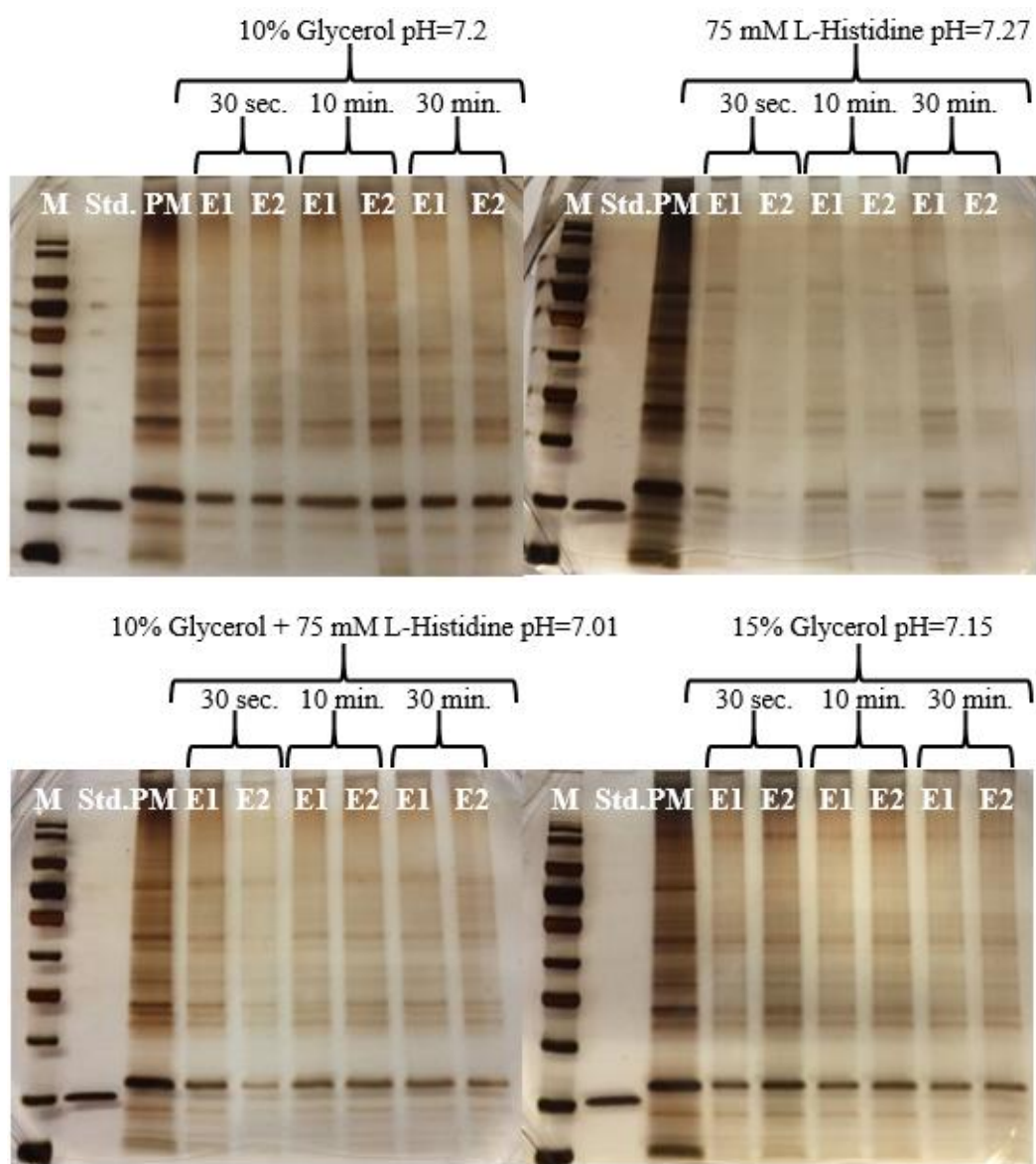


**Figure 4. 38** Variation in elution performance with elution time

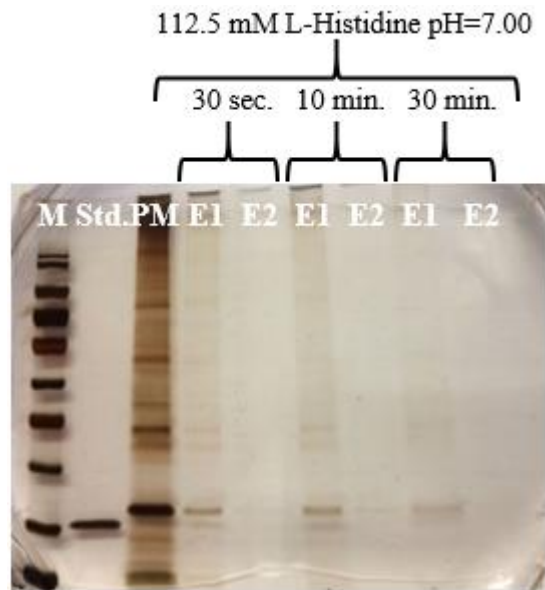


**Figure 4.38** Variation in elution performance with elution time (*cont'd*)

Selectivity of separation can increase with application of more elution steps so, after adsorption, eight times elution step was applied yet, any differences were not observed for yield or selectivity of the target protein.

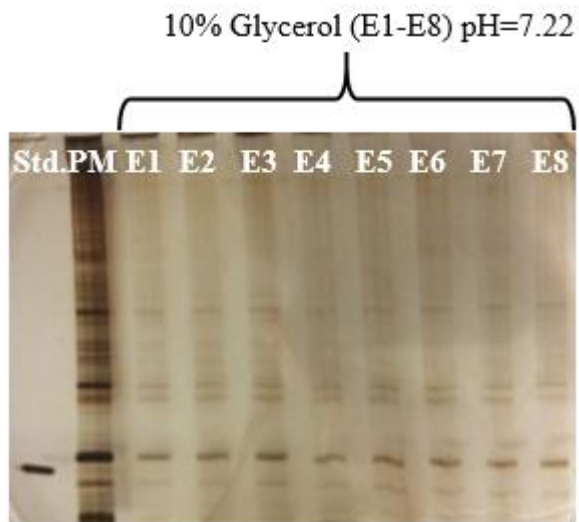


**Figure 4. 39** Variation in eluate with increasing elution number

#### 4.6.12. Surface ligand exchange of ZIF-8 for further modifications

Surface ligand exchange reactions are an exchange reaction and occur on the surface of particles. Thus particle structure can be protected but the topology of crystals can change with high exchange amount (Tsai et al., 2018). In this study, application reason for the surface ligand exchange reaction, SLER, on the ZIF-8 is that when the non-selective behavior of ZIF-8 was considered in separation and purification process, creating a ligand at the surface of the ZIF-8 crystal provides a side chain for further modifications.

At the beginning, to create  $\text{NH}_2$  groups at the surface, histamine dihydrochloride was used. Histamine dihydrochloride molecules exchange with 1-methylimidazole due to similarity of imidazole rings but after modification experiments,  $\text{NH}_2$  group could not be observed in FTIR results (data not shown) so SLER was applied.

When the SLER was applied to ZIF-8, the white color of the ZIF-8 crystals changed to light brown color. FTIR, SEM and XRD analyses were performed to observe changes. XRD patterns show that ZIF-8 crystal structure can be protected. All peaks are matching with ZIF-8 crystals. To be sure about crystal structure, SEM micrographs were given in Appendix F. Homogeneous distribution and approximately 60 nm crystal size were observed like ZIF-8.

Furthermore, FTIR analysis was shown in Appendix H. FTIR results of  $\text{NH}_2$ -ZIF-8 (SLER) and ZIF-8 were compared, to understand whether the modification is applied to ZIF-8 successfully or not. When the FTIR results were investigated in detailed, between  $665\text{-}910\text{ cm}^{-1}$  N-H wags were observed. C-N stretching of aliphatic amines was detected  $1020\text{-}1250\text{ cm}^{-1}$  interval and N-H stretching of primary amines was identified between  $3150\text{-}3400\text{ cm}^{-1}$ .

In addition, TGA result was given in Figure 4.40. The decomposition temperature was measured at same point. The weight loss was measured close to ZIF-8 weight

loss. In the light of these findings, it can be said that the modification of ZIF-8 crystals by SLER was done successfully.

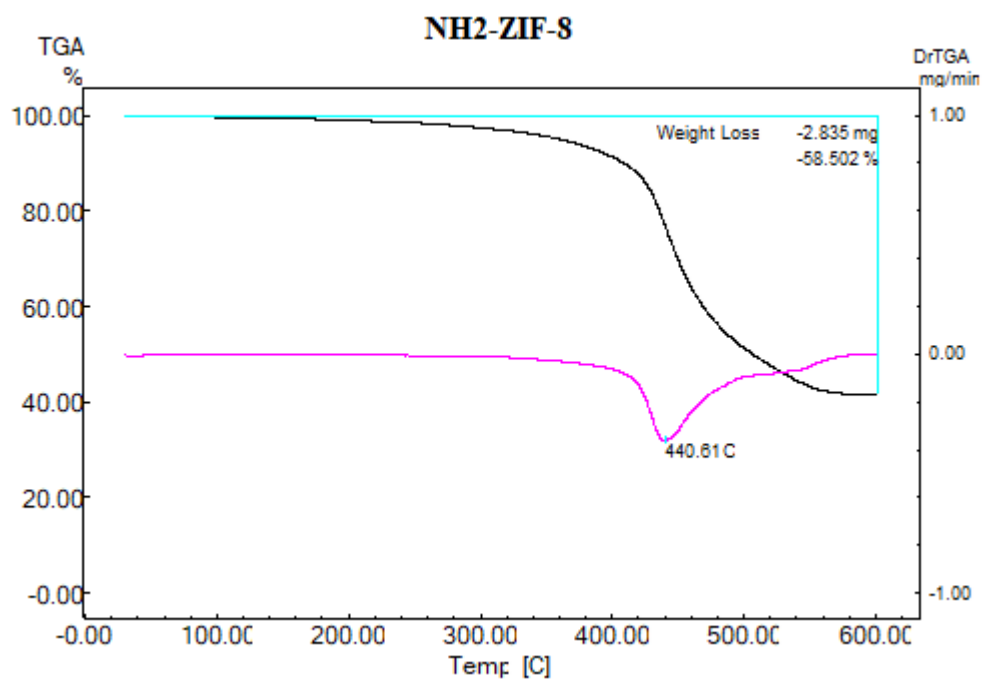


**Figure 4. 40** TGA thermogram of NH<sub>2</sub>-ZIF-8 (SLER)

Moreover, separation and purification by NH<sub>2</sub>-ZIF-8 was tried. Low adsorption performance was observed also any protein could not be separated at both of the washing and elution steps (data not shown).

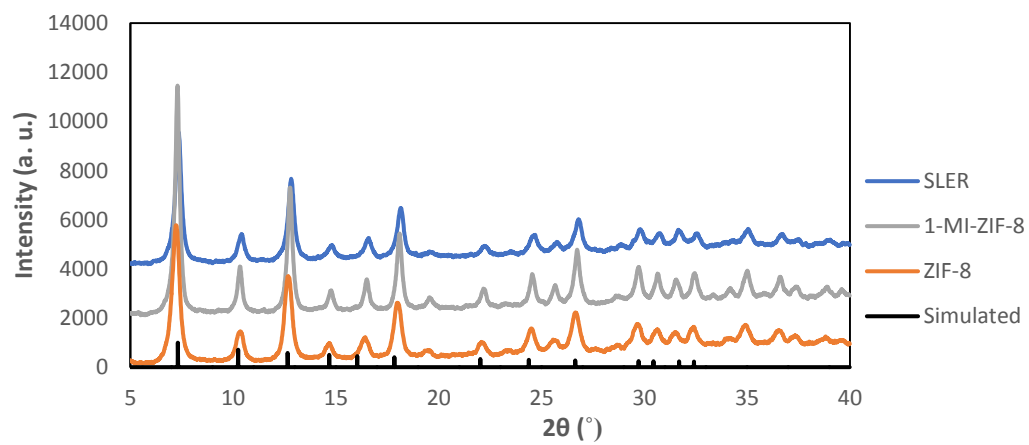


**Figure 4. 41** XRD pattern of SLER

## CHAPTER 5

### CONCLUSIONS

In this study, effects of the oxygen transfer conditions were studied at three oxygen transfer conditions at constant dissolved oxygen concentrations ( $C_{DO}$ ) of  $C_{DO} = 1\%$ ,  $5\%$ , and  $15\%$  by *Pichia pastoris* under  $P_{GAP}$ . The highest cell and rhGH concentrations were obtained at  $C_{DO} = 15\%$ , respectively as,  $177.3 \text{ g/L}$  and  $40.5 \text{ mg/L}$ . While cell concentration was 1.7- and 3.4- fold higher than those of  $C_{DO} = 5\%$  and  $C_{DO} = 1\%$ ,  $C_{rhGH}$  was 2.04- and 2.64-fold higher those of  $C_{DO} = 5\%$  and  $C_{DO} = 1\%$ . When the cultivation time and amount of substrate used were considered,  $C_{DO} = 1\%$  is much preferable than  $C_{DO} = 5\%$ . Considering  $C_X$ , an increment was observed at  $C_{DO} = 5\%$  and  $C_{DO} = 15\%$ , which proves that under limited oxygen transfer condition,  $C_{DO} = 1\%$ , *P. pastoris* cannot grow successfully. Unlike  $C_{DO} = 5\%$  and  $C_{DO} = 15\%$ , at  $C_{DO} = 1\%$  rhGH was produced starting from the beginning of the process. At  $C_{DO} = 5\%$  and  $C_{DO} = 15\%$  rhGH was produced after  $t = 15 \text{ h}$ .

To understand process dynamics and to interpret the effect of  $C_{DO}$  correctly, glucose accumulation, ethanol production, organic acid production, yield coefficients, and the specific rates were calculated. Glucose accumulation was obtained after the  $t = 12 \text{ h}$  of the process for  $C_{DO} = 5\%$  and  $C_{DO} = 15\%$  conditions. However, glucose accumulation was detected starting from  $t = 0 \text{ h}$  at  $C_{DO} = 1\%$  condition because of the effect of oxygen limitation on the substrate consumption. In fed-batch operation, glucose accumulation is not desired. Further, by-products are ethanol and acetic acid should be prevented by designing bioreactor operation conditions. Ethanol accumulated at  $C_{DO} = 15\%$  condition after  $t = 15 \text{ h}$ . The ethanol

accumulation showed the shift of the metabolism from respiratory mode to fermentation mode which is undesired. To get detailed information about the effect of oxygen on the intracellular reaction network, TCA cycle organic acids were analyzed.

Throughout the process, any accumulation was not detected for fumaric, succinic and citric acids. For oxalic acid, negligible accumulation was observed as 0.025 g/L at  $t = 24$  h. Similar accumulation loci were observed for formic and pyruvic acids and approximately 0.008 g/L accumulation was detected for both of them. For malic acid, an accumulation was observed from  $t = 6$  h to  $t = 24$  h of the process. Dramatically increase was observed at malic acid when the highest  $C_{rhGH}$  was obtained at  $t = 24$  h. 0.16 g/L malic acid accumulation was detected at  $t = 24$  h for  $C_{DO} = 15\%$  condition. When organic acids in TCA cycle were considered, a bottleneck can be at malic acid consumption. There should be an unbalance between formation and consumption rates of malic acid. For acetic acid, a sharp accumulation was attained as 0.07 g/L at  $t = 24$  h. The acetic acid accumulation at  $t = 24$  h and ethanol accumulation at  $t = 18$  h show the respiratory mode shifted slightly to fermentation mode. When the accumulated organic acid concentrations were considered, the accumulation levels are low so, it can be said that TCA cycle worked efficiently.

Furthermore, yield coefficients and production or consumption rates were calculated.  $\mu$  values decreased during the process which can be related to substrate accumulation, oxygen transfer limitation, lacking trace elements. When the overall yields were calculated, the highest  $Y_{X/S}$ , 0.54 g g<sup>-1</sup>, was obtained at  $C_{DO} = 15\%$  where the highest  $C_X$ , 177.3 g/L, was obtained. For overall  $Y_{P/S}$ , a decrease was observed with increasing oxygen concentration because medium oxygen concentration meets the needs of the cell growth and substrate consumption.

For  $C_{DO} = 1\%$  condition, the total substrate fed into the bioreactor was measured as 220.6 g when the highest  $C_{rhGH}$  was obtained as 15.4 mg/L at  $t = 12$  h. Unlike



$C_{DO} = 1\%$ , at  $C_{DO} = 5\%$  and  $C_{DO} = 15\%$  conditions the total substrate fed into the bioreactor was measured as 924.1 g when the highest  $C_{rhGH}$  was obtained as 19.9 mg/L and 40.5 mg/L, respectively at  $t = 24$  h.  $C_{DO} = 1\%$  and  $C_{DO} = 5\%$  conditions were compared,  $C_{DO} = 1\%$  provides higher  $C_{rhGH}$  with less the total substrate fed into the bioreactor; thus  $C_{DO} = 1\%$  is more preferable than  $C_{DO} = 5\%$  condition.

Also, when the cultivation time was considered, used substrate amount decreased so, the highest overall  $Y_{P/S}$  was succeeded, as  $0.18 \text{ mg g}^{-1}$  at  $C_{DO} = 1\%$  condition. In addition, the overall  $Y_{P/X}$  showed that the highest yield,  $0.55 \text{ mg g}^{-1}$  was observed at  $C_{DO} = 1\%$  condition but produced protein concentration was obtained as 15.4 mg/L. The recombinant protein production performance is worse than  $C_{DO} = 5\%$  and  $C_{DO} = 15\%$  conditions. In the light of these findings, limited oxygen concentration promotes protein production than  $C_X$  but to reach same production performance of  $C_{DO} = 15\%$  condition,  $C_{DO} = 1\%$  condition process should be repeated approximately 3 times. So,  $C_{DO} = 15\%$  performance presents better results, though it has the lowest overall  $Y_{P/X}$ ,  $0.12 \text{ mg g}^{-1}$ . When the relationship between the  $C_X$  and produced protein concentration is considered, the highest protein production, 40.5 mg/L, at  $C_{DO} = 15\%$  condition is becoming more sensible. In the second part of this study, separation and purification of the produced rhGH by ZIF-8 was focused. rGCSF was used as a second model protein. Different synthesis methods were applied. ZIF-8 in different forms, bimetallic ZIF-8 with nickel, nickel impregnation, and different component ratios were synthesized. ZIF-8 is a promising adsorbent for proteins. The maximum monolayer coverage capacity was calculated  $11.6 \text{ mg g}^{-1}$ .  $\text{pH} = 5$  was found better for protein adsorption on ZIF-8. Therefore, production medium was used without changing pH of the medium. Also,  $T = 35 \text{ }^\circ\text{C}$  was found better for elution step.

Glycerol and L-histidine showed a promising performance for elution step. NaCl provided 15% yield but  $S_1$  ( $S_1 = \text{rGCSF concentration} / \text{undesired protein concentration}$ ) and  $S_2$  ( $S_2 = \text{rGCSF concentration} / \text{total protein concentration}$ )

were calculated as 5.0 and 1.8, respectively. On the other hand, for glycerol and L-histidine, 10% and 4% yields were obtained, respectively. In spite of the lower yield performance, glycerol and L-histidine provided higher  $S_1$  which are 9.9 and 8.9, respectively. In addition, for  $S_2$ , 2.3 and 2.2 selectivities were calculated for glycerol and L-histidine, respectively.  $S_1$ ,  $S_2$ , and yield percentage values of NTA,  $\text{Na}_2\text{HPO}_4$ , and  $\text{MgCl}_2 \cdot 6\text{H}_2\text{O}$  were calculated lower than the glycerol and L-histidine.

Moreover, for separation and purification of the target protein, optimizations and modifications were applied on the ZIF-8.  $37 \pm 0.5\%$  yield was obtained for the synthesis of ZIF-8 by the solvothermal/hydrothermal method. To increase the yield of ZIF-8, NaOH was used and when XRD results were considered, 30 minutes later NaOH addition to the synthesis medium was found better with  $99 \pm 0.5\%$  yield increment.

The nickel impregnated ZIF-8 and bimetallic Ni/ZIF-8 were presented worse performance than ZIF-8 at adsorption step. Therefore, a terminating ligand addition and SLER modifications were applied to ZIF-8. When 1-methylimidazole was used as a terminating ligand, the yield decreased to  $9 \pm 0.5\%$ . 3 hours synthesizing was found better because any significant increase was not observed in the yield of the 1-MI-ZIF-8 after 3 hours. NaOH was added to synthesis medium to increase the yield of 1-MI-ZIF-8 and  $41 \pm 0.5\%$  yield was obtained. Crystal size increased to 200 nm-1.0  $\mu\text{m}$  with 1-MI addition and non-homogeneous particle size distribution was observed.

In addition, another modification method, SLER was applied to ZIF-8. Histamine dihydrochloride was used as an  $\text{NH}_2$  source. Any change was not observed at the crystal structure of ZIF-8 with the addition of  $\text{NH}_2$ . Same thermal stability,  $> T = 400\text{ }^\circ\text{C}$ , was observed. Also, crystal size was protected at 50-60 nm like ZIF-8. From FTIR results, between  $665\text{-}910\text{ cm}^{-1}$  N-H wags,  $1020\text{-}1250\text{ cm}^{-1}$  C-N

stretching of aliphatic amines, and 3150-3400  $\text{cm}^{-1}$  N-H stretching of primary amines were observed.

As a future work, further steps of modifications will be continued and a chelate, IDA, will be created on the ZIF-8 surface to make selective ZIF-8 crystals for the IMAC process.



## REFERENCES

- Adelantado, N., Tarazona, P., Grillitsch, K., García-Ortega, X., Monforte, S., Valero, F., ... Ferrer, P. (2017). The effect of hypoxia on the lipidome of recombinant *Pichia pastoris*. *Microbial Cell Factories*, *16*(1), 86. <http://doi.org/10.1186/s12934-017-0699-4>
- Anand, G., Sharma, S., Dutta, A. K., Kumar, S. K., & Belfort, G. (2010). Conformational Transitions of Adsorbed Proteins on Surfaces of Varying Polarity. *Langmuir*, *26*(13), 10803–10811. <http://doi.org/10.1021/la1006132>
- Anasontzis, G. E., Penã, M. S., Spadiut, O., Brumer, H., & Olsson, L. (2014). Effects of temperature and glycerol and methanol-feeding profiles on the production of recombinant galactose oxidase in *Pichia pastoris*. *Biotechnology Progress*, *30*(3), 728–735. <http://doi.org/10.1002/btpr.1878>
- Andrade, J. D., Hlady, V., & Wei, A. P. (1992). Adsorption of complex proteins at interfaces. *Pure & Appl. Chem*, *64*(11), 1777–1781. Retrieved from <http://citeseerx.ist.psu.edu/viewdoc/download?doi=10.1.1.548.1093&rep=rep1&type=pdf>
- Apte- Deshpande, A., Rewanwar, S., Kotwal, P., Raiker, V. A., & Padmanabhan, S. (2009). Efficient expression and secretion of recombinant human growth hormone in the methylotrophic yeast *Pichia pastoris* : potential applications for other proteins. *Biotechnology and Applied Biochemistry*, *54*(4), 197–205. <http://doi.org/10.1042/BA20090179>
- Arnau, J., Lauritzen, C., Petersen, G. E., & Pedersen, J. (2006). Current strategies for the use of affinity tags and tag removal for the purification of recombinant proteins. *Protein Expression and Purification*, *48*(1), 1–13. <http://doi.org/10.1016/j.pep.2005.12.002>
- Axén, R., Porath, J., & Ernback, S. (1967). Chemical Coupling of Peptides and Proteins To Polysaccharides By Means of Cyanogen Halides. *Nature*,

- 214(5059), 1302–1304. <http://doi.org/10.1038/2141302a0>
- Ayyar, V. (2011). History of growth hormone therapy. *Indian Journal of Endocrinology and Metabolism*, 15(7), 162. <http://doi.org/10.4103/2230-8210.84852>
- Banerjee, R., Phan, A., Wang, B., Knobler, C., Furukawa, H., O’Keeffe, M., & Yaghi, O. M. (2008). High-Throughput Synthesis of Zeolitic Imidazolate Frameworks and Application to CO<sub>2</sub> Capture. *Science*, 319(5865), 939–943. <http://doi.org/10.1126/science.1152516>
- Bao, Q., Lou, Y., Xing, T., & Chen, J. (2013). Rapid synthesis of zeolitic imidazolate framework-8 (ZIF-8) in aqueous solution via microwave irradiation. *Inorganic Chemistry Communications*, 37, 170–173. <http://doi.org/10.1016/j.inoche.2013.09.061>
- Baumann, K., Maurer, M., Dragosits, M., Cos, O., Ferrer, P., & Mattanovich, D. (2008). Hypoxic fed-batch cultivation of *Pichia pastoris* increases specific and volumetric productivity of recombinant proteins. *Biotechnology and Bioengineering*, 100(1), 177–183. <http://doi.org/10.1002/bit.21763>
- Bhattacharjee, S., Jang, M. S., Kwon, H. J., & Ahn, W. S. (2014). Zeolitic Imidazolate Frameworks: Synthesis, Functionalization, and Catalytic/Adsorption Applications. *Catalysis Surveys from Asia*. <http://doi.org/10.1007/s10563-014-9169-8>
- Bouëssel Du Bourg, L., Ortiz, A. U., Boutin, A., & Coudert, F.-X. (2014). Thermal and Mechanical Stability of Zeolitic Imidazolate Frameworks Polymorphs. *APL Materials*, 2(Md), 124110. <http://doi.org/10.1063/1.4904818>
- Brems, D. N., Brown, P. L., & Becker, G. W. (1990). Equilibrium denaturation of human growth hormone and its cysteine-modified forms. *Journal of Biological Chemistry*, 265(10), 5504–5511. Retrieved from <http://www.jbc.org/content/265/10/5504.full.pdf>
- Burke, C. J., Steadman, B. L., Volkin, D. B., Tsai, P.-K., Bruner, M. W., & Middaugh, C. R. (1992). The adsorption of proteins to pharmaceutical

- container surfaces. *International Journal of Pharmaceutics*, 86(1), 89–93. [http://doi.org/10.1016/0378-5173\(92\)90034-Y](http://doi.org/10.1016/0378-5173(92)90034-Y)
- Bux, H., Liang, F., Li, Y., Cravillon, J., Wiebcke, M., & Caro, J. (2009). Zeolitic imidazolate framework membrane with molecular sieving properties by microwave-assisted solvothermal synthesis. *Journal of the American Chemical Society*, 131(44), 16000–16001. <http://doi.org/10.1021/ja907359t>
- Byrne, B. (2015). Pichia pastoris as an expression host for membrane protein structural biology. *Current Opinion in Structural Biology*. <http://doi.org/10.1016/j.sbi.2015.01.005>
- Çalık, P., Ata, Ö., Güneş, H., Massahi, A., Boy, E., Keskin, A., ... Özdamar, T. H. (2015). Recombinant protein production in Pichia pastoris under glyceraldehyde-3-phosphate dehydrogenase promoter: From carbon source metabolism to bioreactor operation parameters. *Biochemical Engineering Journal*, 95, 20–36. <http://doi.org/10.1016/j.bej.2014.12.003>
- Çalık, G., Kocabaş, P., Afşar, H., Çalık, P., & Özdamar, T. H. (2016). Parametric continuous feed stream design to fine-tune fed-batch bioreactor performance: recombinant human growth hormone production in Bacillus subtilis. *Journal of Chemical Technology & Biotechnology*, 91(11), 2740–2750. <http://doi.org/10.1002/jctb.4864>
- Çalık, P., Bayraktar, E., İnankur, B., Soyaslan, E. Ş., Şahin, M., Taşpınar, H., ... Özdamar, T. H. (2010). Influence of pH on recombinant human growth hormone production by Pichia pastoris. *Journal of Chemical Technology & Biotechnology*, 85(12), 1628–1635. <http://doi.org/10.1002/jctb.2474>
- Çalık, P., Bozkurt, B., Zerze, G. H., İnankur, B., Bayraktar, E., Boy, E., ... Özdamar, T. H. (2013). Effect of co-substrate sorbitol different feeding strategies on human growth hormone production by recombinant Pichia pastoris. *Journal of Chemical Technology & Biotechnology*, 88(9), 1631–1640. <http://doi.org/10.1002/jctb.4011>

- Cao, J., Zhang, X., He, X., Chen, L., & Zhang, Y. (2013). Facile synthesis of a Ni(ii)-immobilized core–shell magnetic nanocomposite as an efficient affinity adsorbent for the depletion of abundant proteins from bovine blood. *Journal of Materials Chemistry B*, *1*(30), 3625. <http://doi.org/10.1039/c3tb20573h>
- Carnicer, M., Baumann, K., Topf, I., Sanchez-Ferrando, F., Mattanovich, D., Ferrer, P., & Albiol, J. (2009). Macromolecular and elemental composition analysis and extracellular metabolite balances of *Pichia pastoris* growing at different oxygen levels. *Microbial Cell Factories*, *8*(1), 65. <http://doi.org/10.1186/1475-2859-8-65>
- Çelik, E., & Çalık, P. (2012). Production of recombinant proteins by yeast cells. *Biotechnology Advances*, *30*(5), 1108–1118. <http://doi.org/10.1016/J.BIOTECHADV.2011.09.011>
- Cereghino, G. P. L., Cereghino, J. L., Ilgen, C., & Cregg, J. M. (2002). Production of recombinant proteins in fermenter cultures of the yeast *Pichia pastoris*. *Current Opinion in Biotechnology*, *13*(4), 329–332. [http://doi.org/10.1016/S0958-1669\(02\)00330-0](http://doi.org/10.1016/S0958-1669(02)00330-0)
- Cereghino, J. L., & Cregg, J. M. (2000). Heterologous protein expression in the methylotrophic yeast *Pichia pastoris*. *FEMS Microbiology Reviews*, *24*(1), 45–66. <http://doi.org/10.1111/j.1574-6976.2000.tb00532.x>
- Chaga, G. S. (2001). Twenty-five years of immobilized metal ion affinity chromatography: past, present and future. *Journal of Biochemical and Biophysical Methods*, *49*(1–3), 313–334. <http://doi.org/S0165022X01002068> [pii]
- Chawla, R. K., Parks, J. S., & Rudman, D. (1983). Structural variants of human growth hormone: biochemical, genetic, and clinical aspects. *Annual Review of Medicine*, *34*(1), 519–47. <http://doi.org/10.1146/annurev.me.34.020183.002511>
- Chen, B., Yang, Z., Zhu, Y., & Xia, Y. (2014). Zeolitic imidazolate framework materials: recent progress in synthesis and applications. *J. Mater. Chem. A*,



- 2(40), 16811–16831. <http://doi.org/10.1039/C4TA02984D>
- Chen, X. (2015). Modeling of Experimental Adsorption Isotherm Data. *Information*, 6(1), 14–22. <http://doi.org/10.3390/info6010014>
- Chizallet, C., & Bats, N. (2010). External surface of zeolite imidazolate frameworks viewed ab initio: Multifunctionality at the organic-inorganic interface. *Journal of Physical Chemistry Letters*, 1(1), 349–353. <http://doi.org/10.1021/jz900192x>
- Cho, H. Y., Kim, J., Kim, S. N., & Ahn, W. S. (2013). High yield 1-L scale synthesis of ZIF-8 via a sonochemical route. *Microporous and Mesoporous Materials*, pp. 180–184. <http://doi.org/10.1016/j.micromeso.2012.11.012>
- Cogan, J. D., & John A. Phillips, I. I. I. (2014). Inherited Defects in Growth Hormone Synthesis and Action. In A. L. Beaudet, B. Vogelstein, K. W. Kinzler, S. E. Antonarakis, A. Ballabio, K. M. Gibson, & G. Mitchell (Eds.), *The Online Metabolic and Molecular Bases of Inherited Disease*. New York, NY: The McGraw-Hill Companies, Inc. Retrieved from [ommbid.mhmedical.com/content.aspx?aid=1102900534](http://ommbid.mhmedical.com/content.aspx?aid=1102900534)
- Cos, O., Ramón, R., Montesinos, J. L., & Valero, F. (2006). Operational strategies, monitoring and control of heterologous protein production in the methylotrophic yeast *Pichia pastoris* under different promoters: a review. *Microbial Cell Factories*, 5(1), 17. <http://doi.org/10.1186/1475-2859-5-17>
- Cravillon, J., Münzer, S., Lohmeier, S. J., Feldhoff, A., Huber, K., & Wiebcke, M. (2009). Rapid room-temperature synthesis and characterization of nanocrystals of a prototypical zeolitic imidazolate framework. *Chemistry of Materials*, 21(8), 1410–1412. <http://doi.org/10.1021/cm900166h>
- Cravillon, J., Nayuk, R., Springer, S., Feldhoff, A., Huber, K., & Wiebcke, M. (2011). Controlling zeolitic imidazolate framework nano- and microcrystal formation: Insight into crystal growth by time-resolved in situ static light scattering. *Chemistry of Materials*, 23(8), 2130–2141. <http://doi.org/10.1021/cm103571y>

- Cravillon, J., Schröder, C. A., Bux, H., Rothkirch, A., Caro, J., & Wiebecke, M. (2012). Formate modulated solvothermal synthesis of ZIF-8 investigated using time-resolved in situ X-ray diffraction and scanning electron microscopy. *CrystEngComm*, *14*(2), 492–498. <http://doi.org/10.1039/C1CE06002C>
- Cregg, J. M., Vedvick, T. S., & Raschke, W. C. (1993). Recent Advances in the Expression of Foreign Genes in *Pichia pastoris*. *Bio/Technology*, *11*(8), 905–910. <http://doi.org/10.1038/nbt0893-905>
- Cuatrecasas, P., Wilchek, M., & Anfinsen, C. B. (1968). Selective enzyme purification by affinity chromatography. *Proceedings of the National Academy of Sciences*, *61*(2), 636–643. <http://doi.org/10.1073/pnas.61.2.636>
- de Lima, P. B. A., Mulder, K. C. L., Melo, N. T. M., Carvalho, L. S., Menino, G. S., Mulinari, E., ... Parachin, N. S. (2016). Novel homologous lactate transporter improves L-lactic acid production from glycerol in recombinant strains of *Pichia pastoris*. *Microbial Cell Factories*, *15*(1), 158. <http://doi.org/10.1186/s12934-016-0557-9>
- Do, B. H., Ryu, H.-B., Hoang, P., Koo, B.-K., & Choe, H. (2014). Soluble prokaryotic overexpression and purification of bioactive human granulocyte colony-stimulating factor by maltose binding protein and protein disulfide isomerase. *PloS One*, *9*(3), e89906. <http://doi.org/10.1371/journal.pone.0089906>
- dos Santos Ferreira da Silva, J., López Malo, D., Anceski Bataglioni, G., Nogueira Eberlin, M., Machado Ronconi, C., Alves Júnior, S., & de Sá, G. F. (2015). Adsorption in a Fixed-Bed Column and Stability of the Antibiotic Oxytetracycline Supported on Zn(II)-[2-Methylimidazolate] Frameworks in Aqueous Media. *PLOS ONE*, *10*(6), e0128436. <http://doi.org/10.1371/journal.pone.0128436>

- Dragosits, M., Stadlmann, J., Albiol, J., Baumann, K., Maurer, M., Gasser, B., ... Mattanovich, D. (2009). The effect of temperature on the proteome of recombinant *Pichia pastoris*. *Journal of Proteome Research*, 8(3), 1380–1392. <http://doi.org/10.1021/pr8007623>
- Ecamilla, L., Viader, M., Barrera, A., & Guerrero, M. (2000). Biosynthesis and secretion of recombinant human growth hormone in *Pichia pastoris*. *Biotechnology Letters*, 22, 109–114. Retrieved from <http://download.springer.com/static/pdf/360/art%253A10.1023%252FA%253A1005675920451.pdf?originUrl=http%3A%2F%2Flink.springer.com%2Farticle%2F10.1023%2FA%3A1005675920451&token2=exp=1497650943~acl=%2Fstatic%2Fpdf%2F360%2Fart%25253A10.1023%25252FA%25253A1005>
- Eisenberg, H. (2002). Macromolecular marvels. *Nature*, 415(6869), 261–262. <http://doi.org/10.1038/415261a>
- Enomoto, T., Ueno, S., Hosono, E., Hagiwara, M., & Fujihara, S. (2017). Size-controlled synthesis of ZIF-8 particles and their pyrolytic conversion into ZnO aggregates as photoanode materials of dye-sensitized solar cells. *CrystEngComm*, 19(21), 2823–2962. <http://doi.org/10.1039/C7CE00415J>
- Ersoy, O. (2017). Granulocyte-colony stimulating factor analog production by recombinant *Escherichia coli*, (Master Thesis), Middle East Technical University, 2017.
- Faustini, M., Kim, J., Jeong, G. Y., Kim, J. Y., Moon, H. R., Ahn, W. S., & Kim, D. P. (2013). Microfluidic approach toward continuous and ultrafast synthesis of metal-organic framework crystals and hetero structures in confined microdroplets. *Journal of the American Chemical Society*, 135(39), 14619–14626. <http://doi.org/10.1021/ja4039642>
- Frenzel, A., Bergemann, C., Köhl, G., & Reinard, T. (2003). Novel purification system for 6xHis-tagged proteins by magnetic affinity separation. *Journal of Chromatography B: Analytical Technologies in the Biomedical and Life*

- Sciences*, 793(2), 325–329. [http://doi.org/10.1016/S1570-0232\(03\)00332-5](http://doi.org/10.1016/S1570-0232(03)00332-5)
- Fu, Y. Y., Yang, C. X., & Yan, X. P. (2013). Fabrication of ZIF-8@SiO<sub>2</sub> core-shell microspheres as the stationary phase for high-performance liquid chromatography. *Chemistry - A European Journal*, 19(40), 13484–13491. <http://doi.org/10.1002/chem.201301461>
- Furukawa, H., Cordova, K. E., O’Keeffe, M., & Yaghi, O. M. (2013). The chemistry and applications of metal-organic frameworks. *Science (New York, N.Y.)*, 341(6149), 1230444. <http://doi.org/10.1126/science.1230444>
- Gaberc-Porekar, V., & Menart, V. (2001, October 30). Perspectives of immobilized-metal affinity chromatography. *Journal of Biochemical and Biophysical Methods*. [http://doi.org/10.1016/S0165-022X\(01\)00207-X](http://doi.org/10.1016/S0165-022X(01)00207-X)
- Gao, Y., Wu, J., Zhang, W., Tan, Y., Gao, J., Zhao, J., & Tang, B. (2014). The calcined zeolitic imidazolate framework-8 (ZIF-8) under different conditions as electrode for supercapacitor applications. *Journal of Solid State Electrochemistry*, 18(11), 3203–3207. <http://doi.org/10.1007/s10008-014-2578-9>
- Garcia-Ochoa, F., & Gomez, E. (2009). Bioreactor scale-up and oxygen transfer rate in microbial processes: An overview. *Biotechnology Advances*. <http://doi.org/10.1016/j.biotechadv.2008.10.006>
- Garcia-Ochoa, F., Gomez, E., Santos, V. E., & Merchuk, J. C. (2010). Oxygen uptake rate in microbial processes: An overview. *Biochemical Engineering Journal*. <http://doi.org/10.1016/j.bej.2010.01.011>
- Garcia-Ortega, X., Valero, F., & Montesinos-Seguí, J. L. (2017). Physiological state as transferable operating criterion to improve recombinant protein production in *Pichia pastoris* through oxygen limitation. *Journal of Chemical Technology & Biotechnology*, 92(10), 2573–2582. <http://doi.org/10.1002/jctb.5272>

- Garland, J. M., Quesenberry, P. J., & Hilton, D. J. (1997). *Colony-stimulating factors : molecular and cellular biology*. M. Dekker. Retrieved from <https://www.crcpress.com/Colony-Stimulating-Factors-Molecular--Cellular-Biology-Second-Edition/John-M-Garland/p/book/9780824794927>
- GE Healthcare. (2007). Purifying Challenging Proteins. *General Electric Company*, 28-9095-31, 1-107. <http://doi.org/10.1002/anie.200802483>
- GE Healthcare. (2010). Strategies for Protein Purification Handbook, 167.
- GE Healthcare Life Sciences. (2016). Affinity Chromatography Vol. 3: Specific Groups of Biomolecules, 3, 153.
- Gmeiner, C., Saadati, A., Maresch, D., Krasteva, S., Frank, M., Altmann, F., ... Spadiut, O. (2015). Development of a fed-batch process for a recombinant *Pichia pastoris*  $\Delta$ och1 strain expressing a plant peroxidase. *Microbial Cell Factories*, 14(1), 1. <http://doi.org/10.1186/s12934-014-0183-3>
- Gort, S., & Maloy, S. (1998). Purification of a hexahistidine-tagged protein using L-histidine as the eluent. *Technical Tips Online*, 3(1), 54-55. [http://doi.org/10.1016/S1366-2120\(08\)70098-9](http://doi.org/10.1016/S1366-2120(08)70098-9)
- Güneş, H., & Çalık, P. (2016). Oxygen transfer as a tool for fine-tuning recombinant protein production by *Pichia pastoris* under glyceraldehyde-3-phosphate dehydrogenase promoter. *Bioprocess and Biosystems Engineering*, 39(7), 1-12. <http://doi.org/10.1007/s00449-016-1584-y>
- Guo, H., Zhu, Y., Wang, S., Su, S., Zhou, L., & Zhang, H. (2012). Combining coordination modulation with acid-base adjustment for the control over size of metal-organic frameworks. *Chemistry of Materials*, 24(3), 444-450. <http://doi.org/10.1021/cm202593h>
- Gutiérrez, R., Martín del Valle, E. M., & Galán, M. A. (2007). Immobilized Metal- Ion Affinity Chromatography: Status and Trends. *Separation & Purification Reviews*, 36(1), 71-111. <http://doi.org/10.1080/15422110601166007>

- Ha, E. J., Kim, K. K., Park, H. S., Lee, S. G., Lee, J. O., Seong Soo, A. A., & Paik, H. J. (2013). One-step immobilization and purification of his-tagged enzyme using poly(2-acetamidoacrylic acid) hydrogel. *Macromolecular Research*, *21*(1), 5–9. <http://doi.org/10.1007/s13233-013-1007-8>
- Ha, E. J., Kim, Y. J., An, S. S. A., Kim, Y. R., Lee, J. O., Lee, S. G., & Paik, H. jong. (2008). Purification of His-tagged proteins using Ni<sup>2+</sup>-poly(2-acetamidoacrylic acid) hydrogel. *Journal of Chromatography B: Analytical Technologies in the Biomedical and Life Sciences*, *876*(1), 8–12. <http://doi.org/10.1016/j.jchromb.2008.10.020>
- Hainfeld, J. F., Liu, W., Halsey, C. M. R., Freimuth, P., & Powell, R. D. (1999). Ni-NTA-Gold Clusters Target His-Tagged Proteins. *Journal of Structural Biology*, *127*(2), 185–198. <http://doi.org/10.1006/jsbi.1999.4149>
- He, M., Yao, J., Liu, Q., Wang, K., Chen, F., & Wang, H. (2014). Facile synthesis of zeolitic imidazolate framework-8 from a concentrated aqueous solution. *Microporous and Mesoporous Materials*, *184*, 55–60. <http://doi.org/10.1016/j.micromeso.2013.10.003>
- Hermes, S., Witte, T., Hikov, T., Zacher, D., Bahnmüller, S., Langstein, G., ... Fischer, R. A. (2007). Trapping metal-organic framework nanocrystals: An in-situ time-resolved light scattering study on the crystal growth of MOF-5 in solution. *Journal of the American Chemical Society*, *129*(17), 5324–5325. <http://doi.org/10.1021/ja068835i>
- Hirsh, S. L., McKenzie, D. R., Nosworthy, N. J., Denman, J. A., Sezerman, O. U., & Bilek, M. M. M. (2013). The Vroman effect: Competitive protein exchange with dynamic multilayer protein aggregates. *Colloids and Surfaces B: Biointerfaces*, *103*, 395–404. <http://doi.org/10.1016/j.colsurfb.2012.10.039>
- Hitzeman, R. A., Hagie, F. E., Levine, H. L., Goeddel, D. V., Ammerer, G., & Hall, B. D. (1981). Expression of a human gene for interferon in yeast. *Nature*, *293*(5835), 717–722. <http://doi.org/10.1038/293717a0>

- Ho, Y. ., & McKay, G. (1999). Pseudo-second order model for sorption processes. *Process Biochemistry*, 34(5), 451–465. [http://doi.org/10.1016/S0032-9592\(98\)00112-5](http://doi.org/10.1016/S0032-9592(98)00112-5)
- Hochuli, E., Bannwarth, W., Döbeli, H., Gentz, R., & Stüber, D. (1988). Genetic Approach to Facilitate Purification of Recombinant Proteins with a Novel Metal Chelate Adsorbent. *Bio/Technology*, 6(11), 1321–1325. <http://doi.org/10.1038/nbt1188-1321>
- Hong, F., Meinander, N. Q., & Jönsson, L. J. (2002). Fermentation strategies for improved heterologous expression of laccase in *Pichia pastoris*. *Biotechnology and Bioengineering*, 79(4), 438–449. <http://doi.org/10.1002/bit.10297>
- Hu, X. Q., Chu, J., Zhang, Z., Zhang, S. L., Zhuang, Y. P., Wang, Y. H., ... Yuan, Z. Y. (2008). Effects of different glycerol feeding strategies on S-adenosyl-l-methionine biosynthesis by PGAP-driven *Pichia pastoris* overexpressing methionine adenosyltransferase. *Journal of Biotechnology*, 137(1–4), 44–49. <http://doi.org/10.1016/j.jbiotec.2008.04.009>
- Ileri, N., & Çalık, P. (2006). Effects of pH strategy on endo- and exo-metabolome profiles and sodium potassium hydrogen ports of  $\beta$ -lactamase-producing *Bacillus licheniformis*. *Biotechnology Progress*, 22(2), 411–419. <http://doi.org/10.1021/bp050373+>
- Invitrogen. (2002). *Pichia Expression Kit. A Manual of Methods for Expression of Recombinant Proteins in Pichia pastoris*. Retrieved from [www.invitrogen.com](http://www.invitrogen.com)
- Jahic, M., Gustavsson, M., Jansen, A. K., Martinelle, M., & Enfors, S. O. (2003). Analysis and control of proteolysis of a fusion protein in *Pichia pastoris* fed-batch processes. *Journal of Biotechnology*, 102(1), 45–53. [http://doi.org/10.1016/S0168-1656\(03\)00003-8](http://doi.org/10.1016/S0168-1656(03)00003-8)
- Jian, M., Liu, B., Liu, R., Qu, J., Wang, H., & Zhang, X. (2015). Water-based

- synthesis of zeolitic imidazolate framework-8 with high morphology level at room temperature. *RSC Adv.*, 5(60), 48433–48441. <http://doi.org/10.1039/C5RA04033G>
- Jian, M., Liu, B., Zhang, G., Liu, R., & Zhang, X. (2015). Adsorptive removal of arsenic from aqueous solution by zeolitic imidazolate framework-8 (ZIF-8) nanoparticles. *Colloids and Surfaces A: Physicochemical and Engineering Aspects*, 465, 67–76. <http://doi.org/10.1016/j.colsurfa.2014.10.023>
- Jiang, C., Fu, B., Cai, H., & Cai, T. (2016). Efficient adsorptive removal of Congo red from aqueous solution by synthesized zeolitic imidazolate framework-8. *Chemical Speciation and Bioavailability*, 28(1), 199–208. <http://doi.org/10.1080/09542299.2016.1224983>
- Jiang, H. L., Liu, B., Akita, T., Haruta, M., Sakurai, H., & Xu, Q. (2009). Au@ZIF-8: CO oxidation over gold nanoparticles deposited to metal-organic framework. *Journal of the American Chemical Society*, 131(32), 11302–11303. <http://doi.org/10.1021/ja9047653>
- Jones, K. L., & O'Melia, C. R. (2000). Protein and humic acid adsorption onto hydrophilic membrane surfaces: effects of pH and ionic strength. *Journal of Membrane Science*, 165(1), 31–46. [http://doi.org/10.1016/S0376-7388\(99\)00218-5](http://doi.org/10.1016/S0376-7388(99)00218-5)
- Kalyanpur, M. (2002). Downstream Processing in the Biotechnology Industry. *Molecular Biotechnology*, 22(1), 087–098. <http://doi.org/10.1385/MB:22:1:087>
- Keser Demir, N., Topuz, B., Yilmaz, L., & Kalipcilar, H. (2014). Synthesis of ZIF-8 from recycled mother liquors. *Microporous and Mesoporous Materials*, 198, 291–300. <http://doi.org/10.1016/j.micromeso.2014.07.052>
- Khlebnikov, A., Risa, Ø., Skaug, T., Trent, A., Keasling, J. D., & Carrier, T. A. (2000). Regulatable Arabinose-Inducible Gene Expression System with Consistent Control in All Cells of a Culture Regulatable Arabinose-Inducible Gene Expression System with Consistent Control in All Cells of a Culture.



- Journal of Bacteriology*, 182(24), 7029–7034.  
<http://doi.org/10.1128/JB.182.24.7029-7034.2000>. Updated
- Kim, M.-J., Park, H. S., Seo, K. H., Yang, H.-J., Kim, S.-K., & Choi, J.-H. (2013). Complete Solubilization and Purification of Recombinant Human Growth Hormone Produced in *Escherichia coli*. *PLoS ONE*, 8(2), e56168.  
<http://doi.org/10.1371/journal.pone.0056168>
- Kondo, M., Furukawa, S., Hirai, K., & Kitagawa, S. (2010). Coordinatively immobilized monolayers on porous coordination polymer crystals. *Angewandte Chemie - International Edition*, 49(31), 5327–5330.  
<http://doi.org/10.1002/anie.201001063>
- Kraševc, N., Milunović, T., Lasnik, M. A., Lukančič, I., Komel, R., & Porekar, V. G. (2014). Human granulocyte colony stimulating factor (G-CSF) produced in the filamentous fungus *Aspergillus niger*. *Acta Chimica Slovenica*, 61(4), 709–17. Retrieved from <https://journals.matheo.si/index.php/ACSi/article/viewFile/318/295>
- Kuppler, R. J., Timmons, D. J., Fang, Q.-R., Li, J.-R., Makal, T. A., Young, M. D., ... Zhou, H.-C. (2009). Potential applications of metal-organic frameworks. *Coordination Chemistry Reviews*, 253(23–24), 3042–3066.  
<http://doi.org/10.1016/j.ccr.2009.05.019>
- Kuriyama, H., & Kobayashi, H. (1993). Effects of oxygen supply on yeast growth and metabolism in continuous fermentation. *Journal of Fermentation and Bioengineering*, 75(5), 364–367. [http://doi.org/10.1016/0922-338X\(93\)90135-U](http://doi.org/10.1016/0922-338X(93)90135-U)
- Labrou, N. E. (2014). Protein purification: An overview. *Methods in Molecular Biology*, 1129, 3–10. [http://doi.org/10.1007/978-1-62703-977-2\\_1](http://doi.org/10.1007/978-1-62703-977-2_1)
- Laemmli, U. K. (1970). Cleavage of structural proteins during the assembly of the head of bacteriophage T4. *Nature*, 227(5259), 680–5.  
<http://doi.org/10.1038/227680a0>
- Lanchas, M., Vallejo-Sánchez, D., Beobide, G., Castillo, O., Aguayo, A. T., Luque,

- A., & Román, P. (2012). A direct reaction approach for the synthesis of zeolitic imidazolate frameworks: template and temperature mediated control on network topology and crystal size. *Chemical Communications*, 48(79), 9930. <http://doi.org/10.1039/c2cc34787c>
- Langmuir, I. (1916). THE CONSTITUTION AND FUNDAMENTAL PROPERTIES OF SOLIDS AND LIQUIDS. PART I. SOLIDS. *Journal of the American Chemical Society*, 38(11), 2221–2295. <http://doi.org/10.1021/ja02268a002>
- Lee, I. S., Lee, N., Park, J., Kim, B. H., Yi, Y. W., Kim, T., ... Hyeon, T. (2006). Ni/NiO core/shell nanoparticles for selective binding and magnetic separation of histidine-tagged proteins. *Journal of the American Chemical Society*, 128(33), 10658–10659. <http://doi.org/10.1021/ja063177n>
- Lee, J., Lee, S. Y., Park, S. H., Lee, H. S., Lee, J. H., Jeong, B.-Y., ... Chang, J. H. (2013). High throughput detection and selective enrichment of histidine-tagged enzymes with Ni-doped magnetic mesoporous silica. *J. Mater. Chem. B*, 1(5), 610–616. <http://doi.org/10.1039/C2TB00232A>
- Lee, J. Y., Kang, S. K., Li, H. S., Choi, C. Y., Park, T. E., Bok, J. D., ... Choi, Y. J. (2015). Production of Recombinant Human Growth Hormone Conjugated with a Transcytotic Peptide in *Pichia pastoris* for Effective Oral Protein Delivery. *Molecular Biotechnology*, 57(5), 430–438. <http://doi.org/10.1007/s12033-014-9835-0>
- Levarski, Z., Šoltýsová, A., Krahulec, J., Stuchlík, S., & Turňa, J. (2014). High-level expression and purification of recombinant human growth hormone produced in soluble form in *Escherichia coli*. *Protein Expression and Purification*, 100, 40–47. <http://doi.org/10.1016/j.pep.2014.05.003>
- Li, C. H., & Evans, H. M. (1944). The Isolation of pituitary growth hormone. *Science (New York, N.Y.)*, 99(2566), 183–4. <http://doi.org/10.1126/science.99.2566.183>
- Li, C. H., & Papkoff, H. (1956). Preparation and properties of growth hormone

- from human and monkey pituitary glands. *Science*, 124(3235), 1293–1294.  
<http://doi.org/10.1126/science.124.3235.1293>
- Li, R., Ren, X., Ma, H., Feng, X., Lin, Z., Li, X., ... Wang, B. (2014). Nickel-substituted zeolitic imidazolate frameworks for time-resolved alcohol sensing and photocatalysis under visible light. *Journal of Materials Chemistry A*, 2(16), 5724. <http://doi.org/10.1039/c3ta15058e>
- Li, R., Ren, X., Zhao, J., Feng, X., Jiang, X., Fan, X., ... Wang, B. (2014). Polyoxometallates trapped in a zeolitic imidazolate framework leading to high uptake and selectivity of bioactive molecules. *J. Mater. Chem. A*, 2(7), 2168–2173. <http://doi.org/10.1039/C3TA14267A>
- Li, Y., Long, G., Yang, X., Hu, X., Feng, Y., Tan, D., ... Liao, F. (2015). Approximated maximum adsorption of His-tagged enzyme/mutants on Ni<sup>2+</sup>-NTA for comparison of specific activities. *International Journal of Biological Macromolecules*, 74, 211–217. <http://doi.org/10.1016/j.ijbiomac.2014.12.009>
- Li, Z., Xiong, F., Lin, Q., D'Anjou, M., Daugulis, A. J., Yang, D. S. C., & Hew, C. L. (2001). Low-Temperature Increases the Yield of Biologically Active Herring Antifreeze Protein in *Pichia pastoris*. *Protein Expression and Purification*, 21(3), 438–445. <http://doi.org/10.1006/prev.2001.1395>
- Liao, Y., Cheng, Y., & Li, Q. (2007). Preparation of nitrilotriacetic acid/Co<sup>2+</sup>-linked, silica/boron-coated magnetite nanoparticles for purification of 6 × histidine-tagged proteins. *Journal of Chromatography A*, 1143(1–2), 65–71. <http://doi.org/10.1016/j.chroma.2006.12.063>
- Lim, Y. T., Lee, K. Y., Lee, K., & Chung, B. H. (2006). Immobilization of histidine-tagged proteins by magnetic nanoparticles encapsulated with nitrilotriacetic acid (NTA)-phospholipids micelle. *Biochemical and Biophysical Research Communications*, 344(3), 926–930. <http://doi.org/10.1016/j.bbrc.2006.03.209>
- Lin, J.-B., Lin, R.-B., Cheng, X.-N., Zhang, J.-P., & Chen, X.-M. (2011). Solvent/additive-free synthesis of porous/zeolitic metal azolate frameworks

- from metal oxide/hydroxide. *Chemical Communications*, 47(32), 9185.  
<http://doi.org/10.1039/c1cc12763b>
- Lübbert, A., & Bay Jorgensen, S. (2001, February 13). Bioreactor performance: A more scientific approach for practice. *Journal of Biotechnology*. Elsevier.  
[http://doi.org/10.1016/S0168-1656\(00\)00366-7](http://doi.org/10.1016/S0168-1656(00)00366-7)
- Macauley-Patrick, S., Fazenda, M. L., McNeil, B., & Harvey, L. M. (2005). Heterologous protein production using the *Pichia pastoris* expression system. *Yeast*, 22(4), 249–270. <http://doi.org/10.1002/yea.1208>
- Magdeldin, S., & Moser, A. (2012). Affinity Chromatography: Principles and Applications. In *Affinity Chromatography*. InTech.  
<http://doi.org/10.5772/39087>
- Maisano, F., Testori, S. A., & Grandi, G. (1989). Immobilized metal-ion affinity chromatography of human growth hormone. *Journal of Chromatography*, 472(2), 422–7. [http://doi.org/10.1016/S0021-9673\(00\)94144-X](http://doi.org/10.1016/S0021-9673(00)94144-X)
- Martinez Joaristi, A., Juan-Alcañiz, J., Serra-Crespo, P., Kapteijn, F., & Gascon, J. (2012). Electrochemical Synthesis of Some Archetypical Zn<sup>2+</sup>, Cu<sup>2+</sup>, and Al<sup>3+</sup> Metal Organic Frameworks. *Crystal Growth & Design*, 12(7), 3489–3498. <http://doi.org/10.1021/cg300552w>
- Mason, J. A., Veenstra, M., & Long, J. R. (2014). Evaluating metal–organic frameworks for natural gas storage. *Chem. Sci.*, 5(1), 32–51.  
<http://doi.org/10.1039/C3SC52633J>
- Massahi, A., & Çalık, P. (2016). Endogenous signal peptides in recombinant protein production by *Pichia pastoris*: From in-silico analysis to fermentation. *Journal of Theoretical Biology*, 408, 22–33.  
<http://doi.org/10.1016/J.JTBI.2016.07.039>
- Matranga, K. R., Myers, A. L., & Glandt, E. D. (1992). Storage of natural gas by adsorption on activated carbon. *Chemical Engineering Science*, 47(7), 1569–1579. [http://doi.org/10.1016/0009-2509\(92\)85005-V](http://doi.org/10.1016/0009-2509(92)85005-V)
- Mitraki, A., & King, J. (1989, July 1). Protein Folding Intermediates and Inclusion

- Body Formation. *Bio/Technology*. Nature Publishing Group.  
<http://doi.org/10.1038/nbt0789-690>
- Mohapatra, S., Pal, D., Ghosh, S. K., & Pramanik, P. (2007). Design of Superparamagnetic Iron Oxide Nanoparticle for Purification of Recombinant Proteins. *Journal of Nanoscience and Nanotechnology*, 7(9), 3193–3199.  
<http://doi.org/10.1166/jnn.2007.869>
- Mudhoo, A., Garg, V. K., & Wang, S. (2012). Removal of heavy metals by biosorption. *Environmental Chemistry Letters*, 10(2), 109–117.  
<http://doi.org/10.1007/s10311-011-0342-2>
- Müller, J. M., Bruhn, S., Flaschel, E., Friehs, K., & Risse, J. M. (2016). GAP promoter-based fed-batch production of highly bioactive core streptavidin by *Pichia pastoris*. *Biotechnology Progress*, 32(4), 855–864.  
<http://doi.org/10.1002/btpr.2283>
- Nagata, S., Tsuchiya, M., Asano, S., Kaziro, Y., Yamazaki, T., Yamamoto, O., ... Et Al. (1986). Molecular cloning and expression of cDNA for human granulocyte colony-stimulating factor. *Nature*, 319(6052), 415–418.  
<http://doi.org/10.1038/319415a0>
- Nakanishi, K., Sakiyama, T., & Imamura, K. (2001). On the adsorption of proteins on solid surfaces, a common but very complicated phenomenon. *Journal of Bioscience and Bioengineering*, 91(3), 233–244.  
[http://doi.org/10.1016/S1389-1723\(01\)80127-4](http://doi.org/10.1016/S1389-1723(01)80127-4)
- NGUYEN, L. T. L., LE, K. K. A., & PHAN, N. T. S. (2012). A Zeolite Imidazolate Framework ZIF-8 Catalyst for Friedel-Crafts Acylation. *Chinese Journal of Catalysis*, 33(4–6), 688–696. [http://doi.org/10.1016/S1872-2067\(11\)60368-9](http://doi.org/10.1016/S1872-2067(11)60368-9)
- Nielsen, F. H. (1984). Nickel. In *Biochemistry of the Essential Ultratrace Elements* (pp. 293–308). Boston, MA: Springer US. [http://doi.org/10.1007/978-1-4684-4775-0\\_12](http://doi.org/10.1007/978-1-4684-4775-0_12)
- Norde, W., & Anusiem, A. C. I. (1992). Adsorption, desorption and re-adsorption of proteins on solid surfaces. *Colloids and Surfaces*, 66(1), 73–80.

- [http://doi.org/10.1016/0166-6622\(92\)80122-I](http://doi.org/10.1016/0166-6622(92)80122-I)
- Norman, A. W., & Litwack, G. (1997). Anterior Pituitary Hormones. In *Hormones 2<sup>a</sup> Edition* (pp. 133–168). <http://doi.org/10.1016/B978-0-12-521441-4.50006-7>
- Nune, S. K., Thallapally, P. K., Dohnalkova, A., Wang, C., Liu, J., & Exarhos, G. J. (2010). Synthesis and properties of nano zeolitic imidazolate frameworks. *Chemical Communications*, *46*(27), 4878. <http://doi.org/10.1039/c002088e>
- O'Carra, P., Barry, S., & Griffin, T. (1974). Spacer arms in affinity chromatography: Use of hydrophilic arms to control or eliminate nonbiospecific adsorption effects. *FEBS Letters*, *43*(2), 169–175. [http://doi.org/10.1016/0014-5793\(74\)80993-2](http://doi.org/10.1016/0014-5793(74)80993-2)
- Ortiz, A. U., Freitas, A. P., Boutin, A., Fuchs, A. H., & Coudert, F.-X. (2014). What makes zeolitic imidazolate frameworks hydrophobic or hydrophilic? The impact of geometry and functionalization on water adsorption. *Phys. Chem. Chem. Phys.*, *16*(21), 9940–9949. <http://doi.org/10.1039/C3CP54292K>
- Pan, Y., Liu, Y., Zeng, G., Zhao, L., & Lai, Z. (2011). Rapid synthesis of zeolitic imidazolate framework-8 (ZIF-8) nanocrystals in an aqueous system. *Chemical Communications*, *47*(7), 2071. <http://doi.org/10.1039/c0cc05002d>
- Park, J. H., Park, S. H., & Jung, S. H. (2009). Microwave-syntheses of zeolitic imidazolate framework material, ZIF-8. *Journal of the Korean Chemical Society*, *53*(5), 553–559. <http://doi.org/10.5012/jkcs.2009.53.5.553>
- Park, K. S., Ni, Z., Cote, A. P., Choi, J. Y., Huang, R., Uribe-Romo, F. J., ... Yaghi, O. M. (2006). Exceptional chemical and thermal stability of zeolitic imidazolate frameworks. *Proceedings of the National Academy of Sciences*, *103*(27), 10186–10191. <http://doi.org/10.1073/pnas.0602439103>
- Pearson, R. G. (1973). Benchmark Papers in Inorganic Chemistry: Hard and Soft Acids and bases. *Stroudsburg: Dowden, Hutchinson & Ross*, 480 pp.
- Phan, A., Doonan, C. J., Uribe-Romo, F. J., Knobler, C. B., Okeeffe, M., & Yaghi,

- O. M. (2010). Synthesis, structure, and carbon dioxide capture properties of zeolitic imidazolate frameworks. *Accounts of Chemical Research*, 43(1), 58–67. <http://doi.org/10.1021/ar900116g>
- Pimentel, B. R., Parulkar, A., Zhou, E., Brunelli, N. A., & Lively, R. P. (2014). Zeolitic Imidazolate Frameworks: Next-Generation Materials for Energy-Efficient Gas Separations. *ChemSusChem*, 7(12), 3202–3240. <http://doi.org/10.1002/cssc.201402647>
- Ponte, X., Montesinos-Segui, J. L., & Valero, F. (2016). Bioprocess efficiency in *Rhizopus oryzae* lipase production by *Pichia pastoris* under the control of PAOX1 is oxygen tension dependent. *Process Biochemistry*, 51(12), 1954–1963. <http://doi.org/10.1016/j.procbio.2016.08.030>
- Porath, J., Carlsson, J., Olsson, I., & Belfrage, G. (1975). Metal chelate affinity chromatography, a new approach to protein fractionation. *Nature*, 258(5536), 598–9. <http://doi.org/10.1038/258598a0>
- Porath, J., & Olin, B. (1983). Immobilized metal affinity adsorption and immobilized metal affinity chromatography of biomaterials. Serum protein affinities for gel-immobilized iron and nickel ions. *Biochemistry*, 22(7), 1621–1630. <http://doi.org/10.1021/bi00276a015>
- Prasanna, R. R., & Vijayalakshmi, M. A. (2010). Immobilized metal-ion affinity systems for recovery and structure–function studies of proteins at molecular, supramolecular, and cellular levels. *Pure and Applied Chemistry*, 82(1), 39–55. <http://doi.org/10.1351/PAC-CON-09-01-18>
- Qian, J., Sun, F., & Qin, L. (2012). Hydrothermal synthesis of zeolitic imidazolate framework-67 (ZIF-67) nanocrystals. *Materials Letters*, 82, 220–223. <http://doi.org/10.1016/j.matlet.2012.05.077>
- Qin, X., Qian, J., Yao, G., Zhuang, Y., Zhang, S., & Chu, J. (2011). GAP promoter library for fine-tuning of gene expression in *Pichia pastoris*. *Applied and Environmental Microbiology*, 77(11), 3600–3608. <http://doi.org/10.1128/AEM.02843-10>

- Rabe, M., Verdes, D., & Seeger, S. (2011). Understanding protein adsorption phenomena at solid surfaces. *Advances in Colloid and Interface Science*, *162*(1–2), 87–106. <http://doi.org/10.1016/j.cis.2010.12.007>
- Romanos, M. A., Scorer, C. A., & Clare, J. J. (1992). Foreign gene expression in yeast: a review. *Yeast*, *8*(6), 423–488. <http://doi.org/10.1002/yea.320080602>
- Sallerfors, B., & Olofsson, T. (1992). Granulocyte-macrophage colony-stimulating factor (GM-CSF) and granulocyte colony-stimulating factor (G-CSF) secretion by adherent monocytes measured by quantitative immunoassays. *European Journal of Haematology*, *49*(4), 199–207. <http://doi.org/10.1111/j.1600-0609.1992.tb00047.x>
- Schejn, A., Balan, L., Falk, V., Aranda, L., Medjahdi, G., & Schneider, R. (2014). Controlling ZIF-8 nano- and microcrystal formation and reactivity through zinc salt variations. *CrystEngComm*, *16*(21), 4493. <http://doi.org/10.1039/c3ce42485e>
- Schweinefuß, M. E., Springer, S., Baburin, I. A., Hikov, T., Huber, K., Leoni, S., & Wiebcke, M. (2014). Zeolitic imidazolate framework-71 nanocrystals and a novel SOD-type polymorph: solution mediated phase transformations, phase selection via coordination modulation and a density functional theory derived energy landscape. *Dalton Transactions*, *43*(9), 3528. <http://doi.org/10.1039/c3dt52992d>
- Scopes, R. K. (1995). Overview of Protein Purification and Characterization. In *Current Protocols in Protein Science* (p. 1.1.1-1.1.6). Hoboken, NJ, USA: John Wiley & Sons, Inc. <http://doi.org/10.1002/0471140864.ps0101s00>
- Scopes, R. K. (2001). Strategies for protein purification. *Current Protocols in Protein Science*, *Chapter 1*(1995), Unit 1.2. <http://doi.org/10.1002/0471140864.ps0102s00>
- Seoane, B., Zamaro, J. M., Tellez, C., & Coronas, J. (2012). Sonocrystallization of zeolitic imidazolate frameworks (ZIF-7, ZIF-8, ZIF-11 and ZIF-20).



- CrystEngComm*, 14(9), 3103. <http://doi.org/10.1039/c2ce06382d>
- Shi, J., Wang, X., Zhang, S., Tang, L., & Jiang, Z. (2016). Enzyme-conjugated ZIF-8 particles as efficient and stable Pickering interfacial biocatalysts for biphasic biocatalysis. *J. Mater. Chem. B*, 4(15), 2654–2661. <http://doi.org/10.1039/C6TB00104A>
- Shi, Q., Chen, Z., Song, Z., Li, J., & Dong, J. (2011). Synthesis of ZIF-8 and ZIF-67 by steam-assisted conversion and an investigation of their tribological behaviors. *Angewandte Chemie - International Edition*, 50(3), 672–675. <http://doi.org/10.1002/anie.201004937>
- Shi, X., Karkut, T., Chamankhah, M., Alting-Mees, M., Hemmingsen, S. M., & Hegedus, D. (2003). Optimal conditions for the expression of a single-chain antibody (scFv) gene in *Pichia pastoris*. *Protein Expression and Purification*, 28(2), 321–330. [http://doi.org/10.1016/S1046-5928\(02\)00706-4](http://doi.org/10.1016/S1046-5928(02)00706-4)
- Smith, M. C., Furman, T. C., Ingolia, T. D., & Pidgeon, C. (1988). Chelating peptide immobilized metal ion affinity chromatography. A new concept in affinity chromatography for recombinant proteins. *J. Biol. Chem.*, 263(15), 7211–7215. Retrieved from <http://www.jbc.org/content/263/15/7211.full.pdf>
- Souza, L., Boone, T., Gabilove, J., Lai, P., Zsebo, K., Murdock, D., ... Et, A. (1986). Recombinant human granulocyte colony-stimulating factor: effects on normal and leukemic myeloid cells. *Science*, 232(4746), 61–65. <http://doi.org/10.1126/science.2420009>
- Sreekrishna, K., Brankamp, R. G., Kropp, K. E., Blankenship, D. T., Tsay, J. T., Smith, P. L., ... Birkenberger, L. A. (1997). Strategies for optimal synthesis and secretion of heterologous proteins in the methylotrophic yeast *Pichia pastoris*. In *Gene* (Vol. 190, pp. 55–62). [http://doi.org/10.1016/S0378-1119\(96\)00672-5](http://doi.org/10.1016/S0378-1119(96)00672-5)
- Sreekrishna, K., & Kropp, K. E. (1996). *Pichia pastoris*. In *Nonconventional Yeasts in Biotechnology* (Vol. 398, pp. 203–253). Berlin, Heidelberg: Springer Berlin Heidelberg. [http://doi.org/10.1007/978-3-642-79856-6\\_6](http://doi.org/10.1007/978-3-642-79856-6_6)

- Sue, Y. C., Wu, J. W., Chung, S. E., Kang, C. H., Tung, K. L., Wu, K. C. W., & Shieh, F. K. (2014). Synthesis of hierarchical micro/mesoporous structures via solid-aqueous interface growth: Zeolitic imidazolate framework-8 on siliceous mesocellular foams for enhanced pervaporation of water/ethanol mixtures. *ACS Applied Materials and Interfaces*, *6*(7), 5192–5198. <http://doi.org/10.1021/am5004188>
- Szleifer, I. (1997). Polymers and proteins: interactions at interfaces. *Current Opinion in Solid State and Materials Science*, *2*(3), 337–344. [http://doi.org/10.1016/S1359-0286\(97\)80125-8](http://doi.org/10.1016/S1359-0286(97)80125-8)
- Tanaka, S., Fujita, K., Miyake, Y., Miyamoto, M., Hasegawa, Y., Makino, T., ... Denayer, J. F. M. (2015). Adsorption and Diffusion Phenomena in Crystal Size Engineered ZIF-8 MOF. *The Journal of Physical Chemistry C*, *119*(51), 28430–28439. <http://doi.org/10.1021/acs.jpcc.5b09520>
- Tanaka, S., Kida, K., Okita, M., Ito, Y., & Miyake, Y. (2012). Size-controlled Synthesis of Zeolitic Imidazolate Framework-8 (ZIF-8) Crystals in an Aqueous System at Room Temperature. *Chemistry Letters*, *41*(10), 1337–1339. <http://doi.org/10.1246/cl.2012.1337>
- TANNER, J. M. (1972). Human Growth Hormone. *Nature*, *237*(5356), 433–439. <http://doi.org/10.1038/237433a0>
- Terpe, K. (2003). Overview of tag protein fusions: from molecular and biochemical fundamentals to commercial systems. *Applied Microbiology and Biotechnology*, *60*(5), 523–533. <http://doi.org/10.1007/s00253-002-1158-6>
- Thompson, J. A., Chapman, K. W., Koros, W. J., Jones, C. W., & Nair, S. (2012). Sonication-induced Ostwald ripening of ZIF-8 nanoparticles and formation of ZIF-8/polymer composite membranes. *Microporous and Mesoporous Materials*, *158*, 292–299. <http://doi.org/10.1016/j.micromeso.2012.03.052>
- Toksöz, A., Yenice, I., Üzgün, M., & Öner, F. (2011, July 6). A novel process for preparing G-CSF (granulocyte colony stimulating factor). Google Patents.

Retrieved from <https://www.google.com/patents/EP2341061A1?cl=tr>

- Tsai, C.-W., Niemantsverdriet, J. W., & Langner, E. H. G. (2018). Enhanced CO<sub>2</sub> adsorption in nano-ZIF-8 modified by solvent assisted ligand exchange. *Microporous and Mesoporous Materials*, 262, 98–105. <http://doi.org/10.1016/J.MICROMESO.2017.11.024>
- Tsuruoka, T., Furukawa, S., Takashima, Y., Yoshida, K., Isoda, S., & Kitagawa, S. (2009). Nanoporous nanorods fabricated by coordination modulation and oriented attachment growth. *Angewandte Chemie - International Edition*, 48(26), 4739–4743. <http://doi.org/10.1002/anie.200901177>
- Ueda, E. K. M., Gout, P. W., & Morganti, L. (2003). Current and prospective applications of metal ion-protein binding. *Journal of Chromatography. A*, 988(1), 1–23. [http://doi.org/10.1016/S0021-9673\(02\)02057-5](http://doi.org/10.1016/S0021-9673(02)02057-5)
- Vagenende, V., Yap, M. G. S., & Trout, B. L. (2009). Mechanisms of protein stabilization and prevention of protein aggregation by glycerol. *Biochemistry*, 48(46), 11084–11096. <http://doi.org/10.1021/bi900649t>
- Venna, S. R., & Carreon, M. A. (2010). Highly permeable zeolite imidazolate framework-8 membranes for CO<sub>2</sub>/CH<sub>4</sub> separation. *Journal of the American Chemical Society*, 132(1), 76–78. <http://doi.org/10.1021/ja909263x>
- Venna, S. R., Jasinski, J. B., & Carreon, M. A. (2010). Structural evolution of zeolitic imidazolate framework-8. *Journal of the American Chemical Society*, 132(51), 18030–18033. <http://doi.org/10.1021/ja109268m>
- Walsh, G. (2007). *Pharmaceutical Biotechnology: Concepts and Applications*. (Intergovernmental Panel on Climate Change, Ed.), *Pharmaceutical Biotechnology*. Cambridge: Cambridge University Press. Retrieved from [http://site.iugaza.edu.ps/tbashiti/files/2013/02/2.Pharmaceutical\\_Biotechnology\\_ConceptsApplications-Gary\\_Walsh.pdf](http://site.iugaza.edu.ps/tbashiti/files/2013/02/2.Pharmaceutical_Biotechnology_ConceptsApplications-Gary_Walsh.pdf)
- Waterham, H. R., Digan, M. E., Koutz, P. J., Lair, S. V., & Cregg, J. M. (1997). Isolation of the *Pichia pastoris* glyceraldehyde-3-phosphate dehydrogenase gene and regulation and use of its promoter. *Gene*, 186(1), 37–44.

[http://doi.org/10.1016/S0378-1119\(96\)00675-0](http://doi.org/10.1016/S0378-1119(96)00675-0)

- Winzerling, J. J., Berna, P., & Porath, J. (1992). How to use immobilized metal ion affinity chromatography. *Methods*, 4(1), 4–13. [http://doi.org/10.1016/1046-2023\(92\)90052-A](http://doi.org/10.1016/1046-2023(92)90052-A)
- Wong, J. W., Albright, R. L., & Wang, N.-H. L. (1991). Immobilized Metal Ion Affinity Chromatography (IMAC) Chemistry and Bioseparation Applications. *Separation and Purification Methods*, 20(1), 49–106. <http://doi.org/10.1080/03602549108021408>
- Woo, E. J., Kwon, H. S., & Lee, C. H. (2015). Preparation of nano-magnetite impregnated mesocellular foam composite with a Cu ligand for His-tagged enzyme immobilization. *Chemical Engineering Journal*, 274, 1–8. <http://doi.org/10.1016/j.cej.2015.03.123>
- Wood, D. W. (2014). New trends and affinity tag designs for recombinant protein purification. *Current Opinion in Structural Biology*. <http://doi.org/10.1016/j.sbi.2014.04.006>
- Wu, Y., Chang, G., Zhao, Y., & Zhang, Y. (2014). Hierarchical Fe<sub>3</sub>O<sub>4</sub>@Ni<sub>3</sub>SiO<sub>4</sub> microspheres for affinity separation of His-tagged proteins. *Journal of Nanoparticle Research*, 16(4), 2358. <http://doi.org/10.1007/s11051-014-2358-6>
- Xia, B., Cao, N., Dai, H., Su, J., Wu, X., Luo, W., & Cheng, G. (2014). Bimetallic nickel-rhodium nanoparticles supported on zif-8 as highly efficient catalysts for hydrogen generation from hydrazine in alkaline solution. *ChemCatChem*, 6(9), 2549–2552. <http://doi.org/10.1002/cctc.201402353>
- Xie, H. Y., Zhen, R., Wang, B., Feng, Y. J., Chen, P., & Hao, J. (2010). Fe<sub>3</sub>O<sub>4</sub>/au core/shell nanoparticles modified with Ni<sup>2+</sup>-nitrilotriacetic acid specific to histidine-tagged proteins. *Journal of Physical Chemistry C*, 114(11), 4825–4830. <http://doi.org/10.1021/jp910753f>
- Xu, C., Xu, K., Gu, H., Zhong, X., Guo, Z., Zheng, R., ... Xu, B. (2004). Nitrilotriacetic Acid-Modified Magnetic Nanoparticles as a General Agent to

- Bind Histidine-Tagged Proteins. *Journal of the American Chemical Society*, 126(11), 3392–3393. <http://doi.org/10.1021/ja031776d>
- Xu, S., Höglund, M., Håkansson, L., & Venge, P. (2000). Granulocyte colony-stimulating factor (G-CSF) induces the production of cytokines in vivo. *British Journal of Haematology*, 108(4), 848–853. <http://doi.org/10.1046/j.1365-2141.2000.01943.x>
- Yaghi, O. M., Li, G., & Li, H. (1995). Selective binding and removal of guests in a microporous metal–organic framework. *Nature*, 378(6558), 703–706. <http://doi.org/10.1038/378703a0>
- Yamamoto, D., Maki, T., Watanabe, S., Tanaka, H., Miyahara, M. T., & Mae, K. (2013). Synthesis and adsorption properties of ZIF-8 nanoparticles using a micromixer. *Chemical Engineering Journal*, 227, 145–150. <http://doi.org/10.1016/j.cej.2012.08.065>
- Yanai, N., & Granick, S. (2012). Directional self-assembly of a colloidal metal-organic framework. *Angewandte Chemie - International Edition*, 51(23), 5638–5641. <http://doi.org/10.1002/anie.201109132>
- Yanai, N., Sindoro, M., Yan, J., & Granick, S. (2013). Electric field-induced assembly of monodisperse polyhedral metal-organic framework crystals. *Journal of the American Chemical Society*, 135(1), 34–37. <http://doi.org/10.1021/ja309361d>
- Yang, L., & Lu, H. (2012). Microwave-assisted ionothermal synthesis and characterization of zeolitic imidazolate framework-8. *Chinese Journal of Chemistry*, 30(5), 1040–1044. <http://doi.org/10.1002/cjoc.201100595>
- Yang, Y.-H., Wu, T.-T., Suen, S.-Y., & Lin, S.-C. (2011). Equilibrium adsorption of poly(His)-tagged proteins on immobilized metal affinity chromatographic adsorbents. *Biochemical Engineering Journal*, 54(1), 1–9. <http://doi.org/10.1016/j.bej.2010.12.005>
- Yang, Y., Ge, L., Rudolph, V., & Zhu, Z. (2014). In situ synthesis of zeolitic imidazolate frameworks/carbon nanotube composites with enhanced CO<sub>2</sub>

- adsorption. *Dalton Transactions*, 43(19), 7028.  
<http://doi.org/10.1039/c3dt53191k>
- Yao, J., He, M., & Wang, H. (2015). Strategies for controlling crystal structure and reducing usage of organic ligand and solvents in the synthesis of zeolitic imidazolate frameworks. *CrystEngComm*, 17(27), 4970–4976.  
<http://doi.org/10.1039/C5CE00663E>
- Yardrung Suwannarat, Saeseaw, S., Chanasutthiprapa, N., & Tongta, A. (2013). Comparison between constant methanol feed and on-line monitoring feed control for recombinant human growth hormone production by *Pichia pastoris* KM71. *African Journal of ...*, 12(11), 1267–1274.  
<http://doi.org/10.5897/AJB12.1329>
- Yu, T., Wang, Q., Johnson, D. S., Wang, M. D., & Ober, C. K. (2005). Functional hydrogel surfaces: Binding kinesin-based molecular motor proteins to selected patterned sites. *Advanced Functional Materials*, 15(8), 1303–1309.  
<http://doi.org/10.1002/adfm.200400117>
- Zhang, A. L., Luo, J. X., Zhang, T. Y., Pan, Y. W., Tan, Y. H., Fu, C. Y., & Tu, F. Z. (2009). Recent advances on the GAP promoter derived expression system of *Pichia pastoris*. *Molecular Biology Reports*, 36(6), 1611–1619.  
<http://doi.org/10.1007/s11033-008-9359-4>
- Zhang, K., Lively, R. P., Dose, M. E., Brown, A. J., Zhang, C., Chung, J., ... Chance, R. R. (2013). Alcohol and water adsorption in zeolitic imidazolate frameworks. *Chemical Communications*, 49(31), 3245.  
<http://doi.org/10.1039/c3cc39116g>
- Zhang, K., Lively, R. P., Zhang, C., Koros, W. J., & Chance, R. R. (2013). Investigating the intrinsic ethanol/water separation capability of ZIF-8: An adsorption and diffusion study. *Journal of Physical Chemistry C*, 117(14), 7214–7225. <http://doi.org/10.1021/jp401548b>
- Zhao, Y., Pan, Y., Liu, W., & Zhang, L. (2015). Removal of Heavy Metal Ions from Aqueous Solutions by Adsorption onto ZIF-8 Nanocrystals. *Chemistry*

*Letters*, 44(6), 758–760. <http://doi.org/10.1246/cl.150137>

Zheng, J., Lin, Z., Lin, G., Yang, H., & Zhang, L. (2015). Preparation of magnetic metal–organic framework nanocomposites for highly specific separation of histidine-rich proteins. *J. Mater. Chem. B*, 3(10), 2185–2191. <http://doi.org/10.1039/C4TB02007C>

Zhu, M., Srinivas, D., Bhogeswararao, S., Ratnasamy, P., & Carreon, M. A. (2013). Catalytic activity of ZIF-8 in the synthesis of styrene carbonate from CO<sub>2</sub> and styrene oxide. *Catalysis Communications*, 32, 36–40. <http://doi.org/10.1016/j.catcom.2012.12.003>





## A. SDS-PAGE BUFFER SOLUTIONS AND REQUIRED COMPONENT INFORMATION

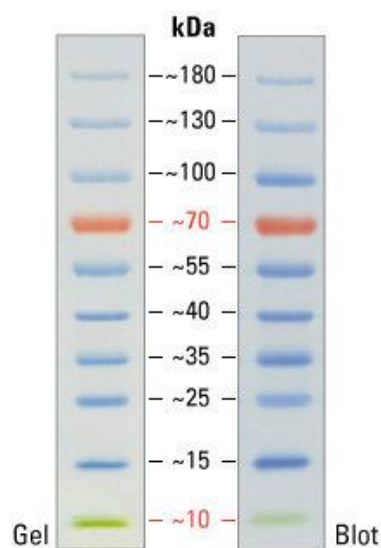


**Figure A. 1** Band profile of the PageRuler Prestained Protein Ladder for SDS-PAGE

**4X Loading Buffer (LB):** 200 mM Tris-HCl, pH 6.8; 40% glycerol; 6% SDS; 0.013% Bromophenol blue; 10% 2-mercaptoethanol. Distributed into microcentrifuge tubes and stored at -20°C.

**5X Running Buffer:** Dissolve 15 g Tris Base, 72 g glycine, 5 g SDS, in 1 L distilled water. Store at 2-8°C and diluted 5 times with dH<sub>2</sub>O before use. Use it up to 3 times.

**10% (w/v) Ammonium persulphate (APS):** Add 0.1 g APS to 1 mL dH<sub>2</sub>O, freshly prepared. It can be used up to a week.



## B. CALIBRATION CURVES AND NUMERICAL DATA OF ORGANIC ACIDS FOR HPLC

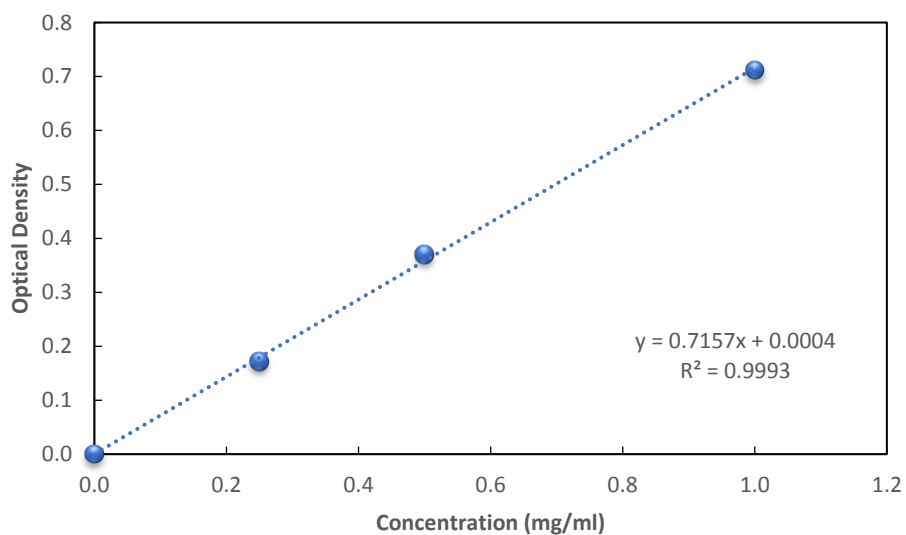


**Figure B. 1** Bovine serum albumin (BSA) standard curve

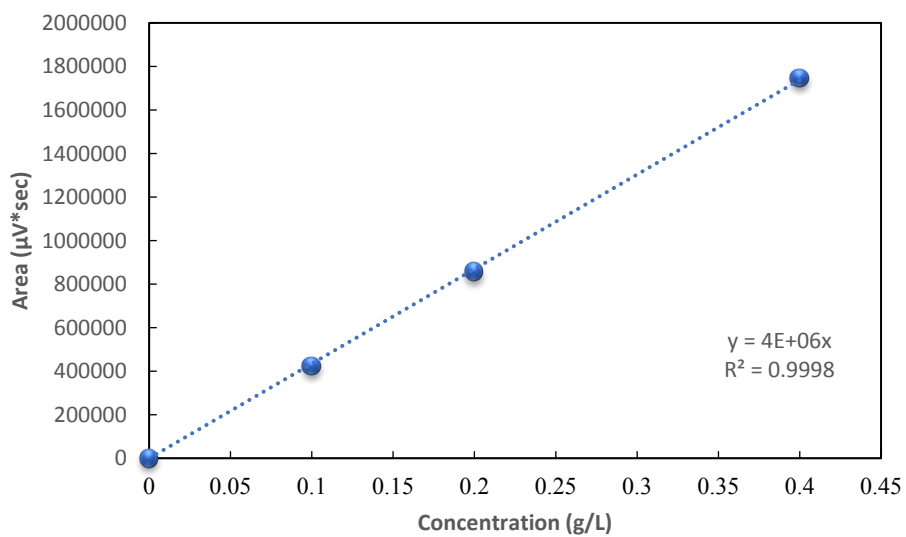


**Figure B. 2** Calibration curve of oxalic acid

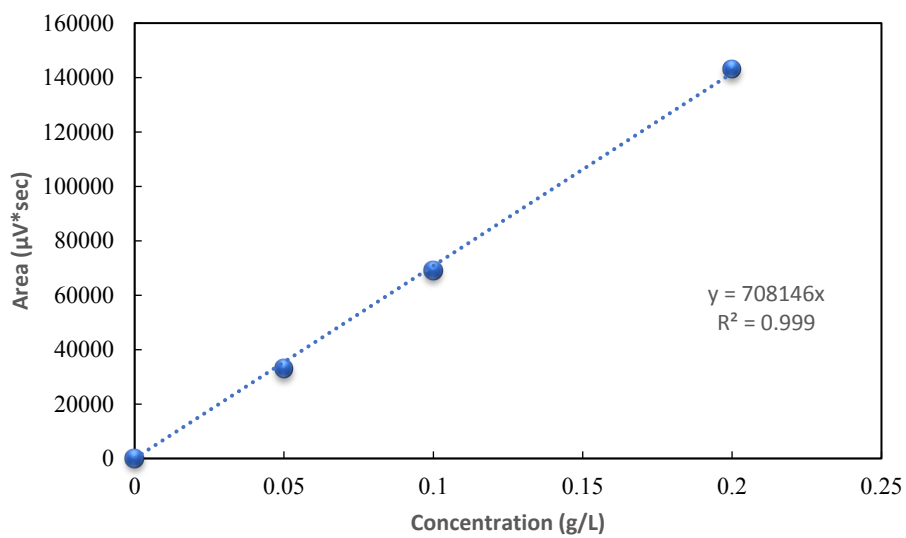


**Figure B. 3** Calibration curve of formic acid

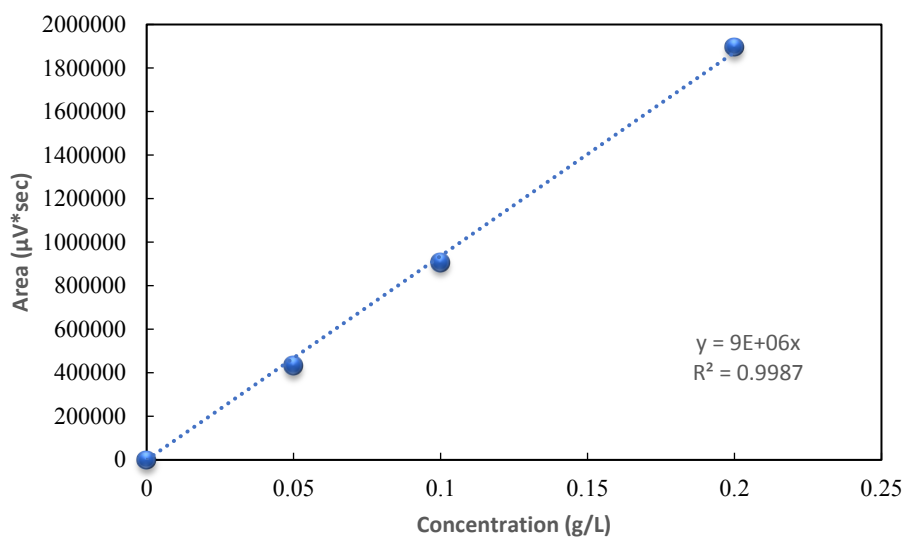


**Figure B. 4** Calibration curve of pyruvic acid

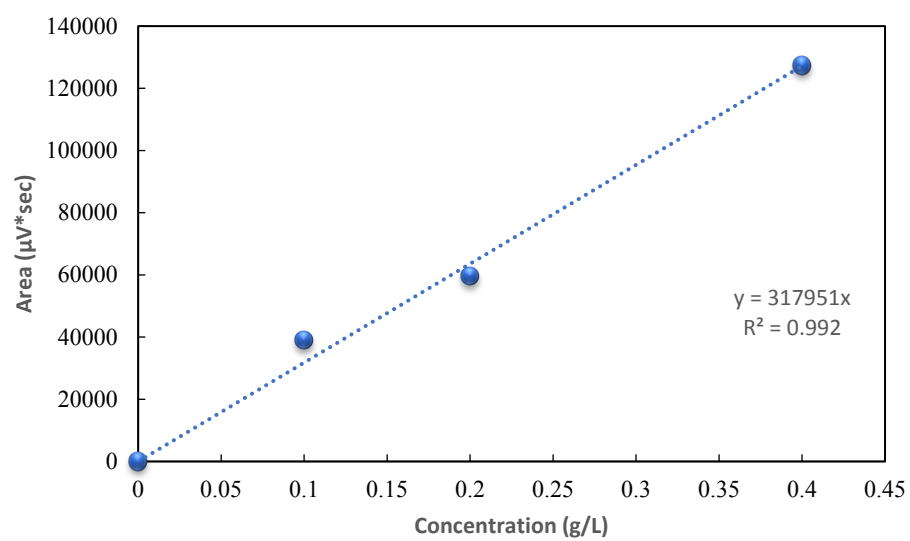


**Figure B. 5** Calibration curve of malic acid

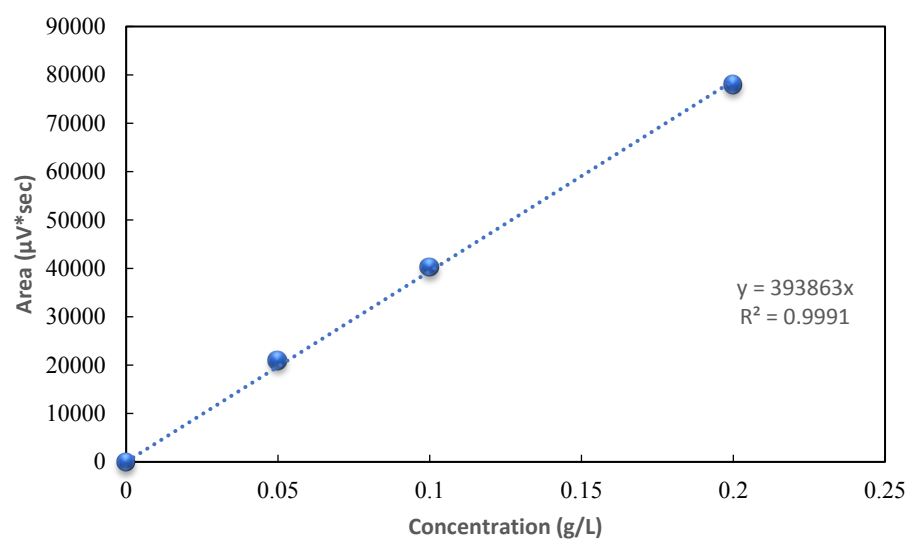


**Figure B. 6** Calibration curve of acetic acid

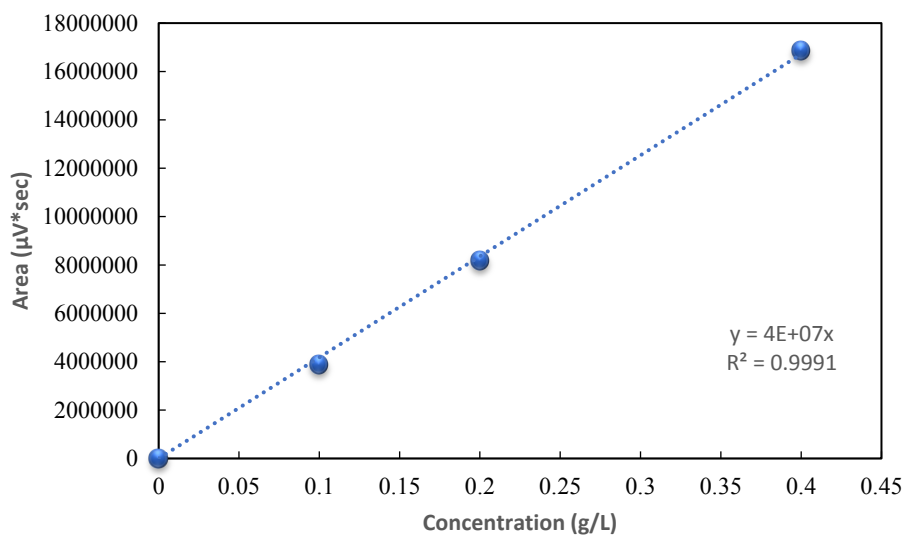


**Figure B. 7** Calibration curve of fumaric acid

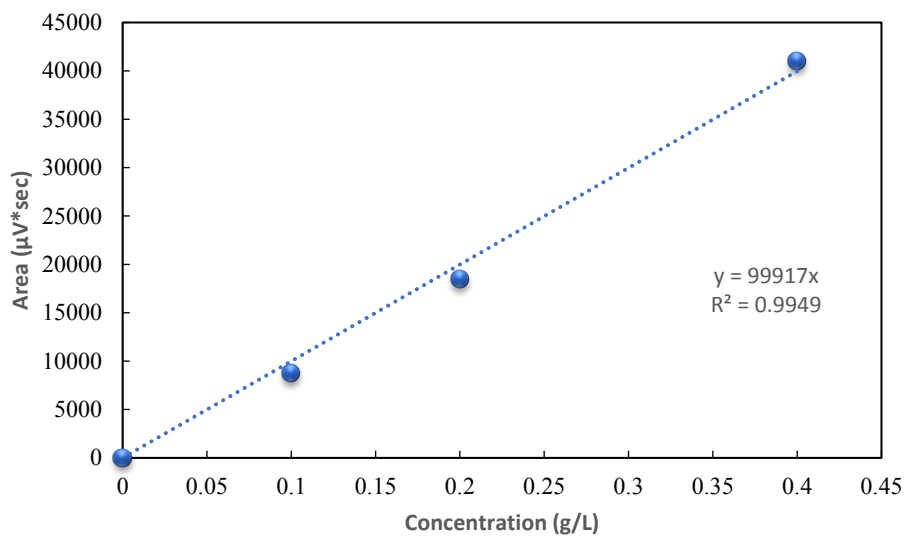


**Figure B. 8** Calibration curve of succinic acid

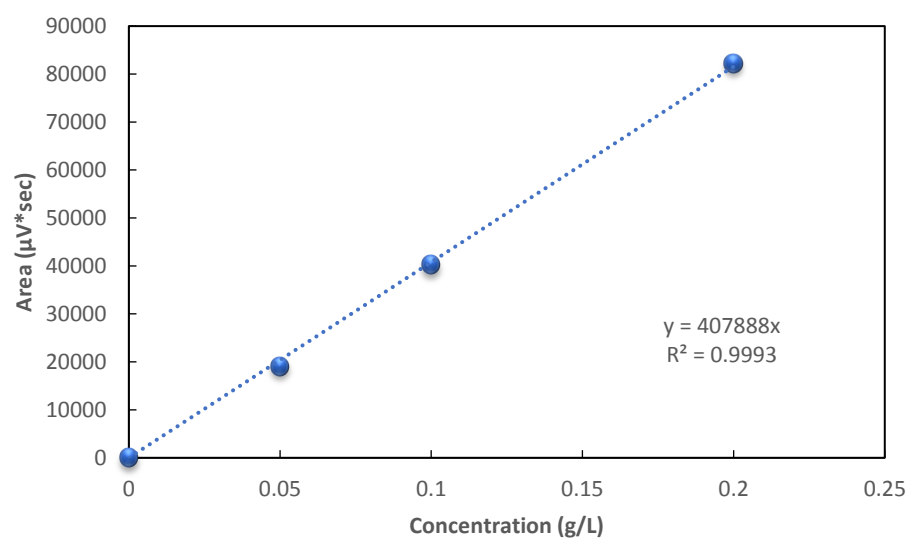


**Figure B. 9** Calibration curve of citric acid

**Table B. 1** HPLC values of organic acids

| Time (h) | Concentration (g/L) |             |              |            |             |              |               |             |
|----------|---------------------|-------------|--------------|------------|-------------|--------------|---------------|-------------|
|          | Oxalic Acid         | Formic Acid | Pyruvic Acid | Malic Acid | Acetic Acid | Fumaric Acid | Succinic Acid | Citric Acid |
| 6        | 0.009140            | 0.011057    | 0.005913     | 0.053986   | 0.016846    | 0.000225     | 0             | 0           |
| 12       | 0.012474            | 0.015435    | 0.005853     | 0.054332   | 0.006881    | 0.000227     | 0             | 0           |
| 15       | 0.007759            | 0.002867    | 0.003468     | 0.038465   | 0.020235    | 0            | 0             | 0           |
| 18       | 0.011209            | 0.005296    | 0.006284     | 0.061079   | 0.009851    | 0.000021     | 0             | 0           |
| 21       | 0.010724            | 0.010351    | 0.005675     | 0.089385   | 0.009813    | 0.000038     | 0             | 0           |
| 24       | 0.024611            | 0.008685    | 0.008348     | 0.160575   | 0.069237    | 0            | 0             | 0           |
| 27       | 0.027399            | 0.009250    | 0.015606     | 0.187891   | 0.027256    | 0.000138     | 0             | 0           |
| 30       | 0.026925            | 0.010005    | 0.150008     | 0.462430   | 0.086985    | 0            | 0             | 0           |





### C. NUMERICAL DATA OF ZIF-8 FOR ADSORPTION EQUILIBRIUM

**Table C. 1** Values of  $q_e$  and  $C_e$  data for each amount of ZIF-8

| <b>Amount of ZIF-8 (g)</b> | <b><math>q_e</math> (mg/g) Amount of Adsorbed rGCSF on ZIF / Amount of ZIF-8</b> | <b><math>C_e</math> (mg/ml) Concentration of Remained rGCSF in Medium After Incubation</b> |
|----------------------------|--|--|
| <b>0.2</b>                 | 1.33   | 3.93   |
| <b>0.15</b>                | 1.76   | 5.50   |
| <b>0.1</b>                 | 2.61   | 9.19   |
| <b>0.075</b>               | 3.42   | 13.55  |
| <b>0.05</b>                | 4.94   | 22.94  |
| <b>0.03</b>                | 7.30   | 51.05  |
| <b>0.02</b>                | 9.07   | 88.70  |
| <b>0.01</b>                | 10.65  | 163.64   |

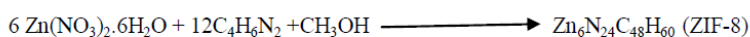
**Table C. 2**  $\log(q_e)$  versus  $\log(C_e)$

| <b>Amount of ZIF (g)</b> | <b><math>\log(q_e)</math></b> | <b><math>\log(C_e)</math></b> |
|--------------------------|-------------------------------|-------------------------------|
| <b>0.2</b>               | 0.12                          | 0.59                          |
| <b>0.15</b>              | 0.25                          | 0.74                          |
| <b>0.1</b>               | 0.42                          | 0.96                          |
| <b>0.075</b>             | 0.53                          | 1.13                          |
| <b>0.05</b>              | 0.69                          | 1.36                          |
| <b>0.03</b>              | 0.86                          | 1.71                          |
| <b>0.02</b>              | 0.96                          | 1.95                          |
| <b>0.01</b>              | 1.03                          | 2.21                          |



## D. ZINC-BASED YIELD CALCULATION OF ZIF-8

ZIF-8 Synthesis Reaction:



|  |  |
|--|--|
| 375.72 g batch solution consists of:                       |  |
| 180.8 g MeOH   | 180.8 g MeOH                             |
| +  | +  |
| 4.8 g $\text{Zn}(\text{NO}_3)_2 \cdot 6\text{H}_2\text{O}$ | 10.56 g $\text{C}_4\text{H}_6\text{N}_2$ |

### Molecular Weights of the Materials

- $\text{Zn}(\text{NO}_3)_2 \cdot 6\text{H}_2\text{O}$ : 297.49 g/mole
- $\text{C}_4\text{H}_6\text{N}_2$ : 82.11 g/mole
- $\text{CH}_3\text{OH}$ : 32.11 g/mole
- $\text{Zn}_6\text{N}_{24}\text{C}_{48}\text{H}_{60}$ : 1365.51 g/mole

Consumed Amount  $\text{Zn}^{+2}$

$$= \left( \frac{\text{Obtained amount of ZIF-8}}{1365.51 \frac{\text{g}}{\text{mol}} \text{ ZIF-8}} \right) * \left( \frac{6 \text{ mol Zn}^{+2}}{1 \text{ mol ZIF-8}} \right) * \left( \frac{297.49 \text{ g}}{1 \text{ mol Zn}^{+2}} \right)$$

$$\text{Remained Amount Zn}^{+2} = \text{Initial Amount Zn}^{+2} - \text{Consumed Amount Zn}^{+2}$$

Consumed Amount Hmim

$$= \left( \frac{\text{Obtained amount of ZIF-8}}{1365.51 \frac{\text{g}}{\text{mol}}} \right) * \left( \frac{12 \text{ mol Hmim}}{1 \text{ mol ZIF-8}} \right) * \left( \frac{82.11 \text{ g}}{1 \text{ mol Hmim}} \right)$$

$$\text{Remained Amount Hmim} = \text{Initial Amount Hmim} - \text{Consumed Amount Hmim}$$

Remained Amount MeOH

$$= \text{Initial Amount MeOH} - \text{Obtained Amount ZIF8} - \text{Remained Amount Zn}^{+2} - \text{Remained Amount Hmim}$$

$$\text{Max. ZIF-8} = \left( \frac{\text{Initial Amount Zn}^{+2}}{297.49 \frac{\text{g}}{\text{mol}}} \right) * \left( \frac{1 \text{ mol ZIF-8}}{6 \text{ mol Zn}^{+2}} \right) * \left( \frac{1365.51 \frac{\text{g}}{\text{mol}}}{1 \text{ mol ZIF-8}} \right)$$

$$\% \text{Yield} = \frac{\text{Obtained Amount of ZIF-8}}{\text{Maximum Amount of ZIF-8}} * 100$$



## E. SELECTIVITY AND YIELD CALCULATIONS OF VARIOUS ELUENTS WITH RESULTS

Regarding SDS-PAGE results,  $S_1$ ,  $S_2$ , and yield % values were calculated.

$C_{rGCSF_0}$ : rGCSF concentration in production medium

$C_{rGCSF_i}$ : Separated rGCSF concentration with respect to eluent

$C_{TP}$ : Total protein concentration

Formulas are given below;

$$S_1 = \frac{C_{rGCSF_i}}{C_{TP} - C_{rGCSF_i}}$$

$$S_2 = \frac{C_{rGCSF_i}}{C_{TP}}$$

$$Yield\% = \frac{C_{rGCSF_i} * 100}{C_{rGCSF_0}}$$

All parameters were calculated regarding elution step.

**Table E. 1** SDS-PAGE results of different eluents

| <b>Chemical Name</b>            | <b>C<sub>TP</sub> (mg/L)</b> | <b>C<sub>rGCSF</sub> (mg/L)</b> | <b>S<sub>1</sub></b> | <b>S<sub>2</sub></b> | <b>Yield%</b> |
|---------------------------------|------------------------------|---------------------------------|----------------------|----------------------|---------------|
| <b>Production Medium</b>        | 244.43                       | 131.74                          | 1.17                 | 0.54                 | 100.00        |
| <b>Glycerol (10%) E1</b>        | 2.55                         | 2.09                            | 4.51                 | 0.82                 | 1.59          |
| <b>Glycerol (10%) E2</b>        | 0.44                         | 0.44                            | -                    | 1.00                 | 0.33          |
| <b>L-Histidine (0.075 M) E1</b> | 10.05                        | 6.41                            | 1.77                 | 0.64                 | 4.87          |
| <b>L-Histidine (0.075 M) E2</b> | 3.70                         | 2.77                            | 2.99                 | 0.75                 | 2.11          |
| <b>Acetonitrile (90%) E1</b>    | -                            | -                               | -                    | -                    | -             |
| <b>Acetonitrile (90%) E2</b>    | -                            | -                               | -                    | -                    | -             |
| <b>MeOH (10%) E1</b>            | 0.50                         | 0.50                            | -                    | 1.00                 | 0.38          |
| <b>MeOH (10%) E2</b>            | 0.07                         | 0.07                            | -                    | 1.00                 | 0.05          |
| <b>Chemical Name</b>            | <b>C<sub>TP</sub> (mg/L)</b> | <b>C<sub>rGCSF</sub> (mg/L)</b> | <b>S<sub>1</sub></b> | <b>S<sub>2</sub></b> | <b>Yield%</b> |
| <b>Production Medium</b>        | 359.60                       | 222.58                          | 1.62                 | 0.62                 | 100.00        |
| <b>2-Propanol (60%) E1</b>      | -                            | -                               | -                    | -                    | -             |
| <b>2-Propanol (60%) E2</b>      | -                            | -                               | -                    | -                    | -             |
| <b>Triton X-100 (1%) E1</b>     | 1.93                         | 1.15                            | 1.48                 | 0.60                 | 0.52          |
| <b>Triton X-100 (1%) E2</b>     | 0.13                         | 0.13                            | -                    | 1.00                 | 0.06          |
| <b>EDTA (0.1 M) E1</b>          | 2.17                         | 0.20                            | 0.10                 | 0.09                 | 0.09          |
| <b>EDTA (0.1 M) E2</b>          | 0.71                         | 0.00                            | 0.00                 | 0.00                 | 0.00          |
| <b>Glycine (0.1 M) E1</b>       | 0.29                         | 0.29                            | -                    | 1.00                 | 0.13          |
| <b>Glycine (0.1 M) E2</b>       | -                            | -                               | -                    | -                    | -             |

**Table E. 1** SDS-PAGE results of different eluents (*cont'd*)

| <b>Chemical Name</b>                                | <b>C<sub>TP</sub> (mg/L)</b> | <b>C<sub>rGCSF</sub> (mg/L)</b> | <b>S<sub>1</sub></b> | <b>S<sub>2</sub></b> | <b>Yield%</b> |
|---|------------------------------|---------------------------------|----------------------|----------------------|---------------|
| <b>Production Medium</b>                            | 320.81                       | 185.42                          | 1.37                 | 0.58                 | 100.00        |
| <b>NH<sub>4</sub>Cl (1 M) E1</b>                    | 12.24                        | 7.82                            | 1.77                 | 0.64                 | 4.22          |
| <b>NH<sub>4</sub>Cl (1 M) E2</b>                    | 0.99                         | 0.77                            | 3.39                 | 0.77                 | 0.41          |
| <b>Na<sub>2</sub>HPO<sub>4</sub> (0.02 M) E1</b>    | 0.11                         | 0.08                            | 2.86                 | 0.74                 | 0.04          |
| <b>Na<sub>2</sub>HPO<sub>4</sub> (0.02 M) E2</b>    | 24.03                        | 13.14                           | 1.21                 | 0.55                 | 7.09          |
| <b>MgCl<sub>2</sub>.6H<sub>2</sub>O (1 M) E1</b>    | 5.79                         | 4.17                            | 2.56                 | 0.72                 | 2.25          |
| <b>MgCl<sub>2</sub>.6H<sub>2</sub>O (1 M) E2</b>    | 5.42                         | 4.13                            | 3.19                 | 0.76                 | 2.23          |
| <b>NaCl (0.05 M) E1</b>                             | 0.36                         | 0.36                            | -                    | 1.00                 | 0.20          |
| <b>NaCl (0.05 M) E2</b>                             | 0.10                         | 0.10                            | -                    | 1.00                 | 0.05          |
| <b>Chemical Name</b>                                | <b>C<sub>TP</sub> (mg/L)</b> | <b>C<sub>rGCSF</sub> (mg/L)</b> | <b>S<sub>1</sub></b> | <b>S<sub>2</sub></b> | <b>Yield%</b> |
| <b>Production Medium</b>                            | 327.29                       | 209.27                          | 1.77                 | 0.64                 | 100.00        |
| <b>MgCl<sub>2</sub>.6H<sub>2</sub>O (0.05 M) E1</b> | 14.51                        | 7.95                            | 1.21                 | 0.55                 | 3.80          |
| <b>MgCl<sub>2</sub>.6H<sub>2</sub>O (0.05 M) E2</b> | 10.50                        | 6.63                            | 1.72                 | 0.63                 | 3.17          |
| <b>NTA (1 M) E2</b>                                 | 0.86                         | 0.86                            | -                    | 1.00                 | 0.41          |
| <b>NaCl (0.4 M) E1</b>                              | 13.60                        | 10.46                           | 3.32                 | 0.77                 | 5.00          |
| <b>NaCl (0.4 M) E2</b>                              | 28.47                        | 18.45                           | 1.84                 | 0.65                 | 8.82          |

**Table E. 2** SDS-PAGE results of promising eluents

| <b>Chemical Name</b>                               | <b>C<sub>TP</sub> (mg/L)</b> | <b>C<sub>rGCSF</sub> (mg/L)</b> | <b>S<sub>1</sub></b> | <b>S<sub>2</sub></b> | <b>Yield%</b> |
|--|------------------------------|---------------------------------|----------------------|----------------------|---------------|
| <b>Production Medium</b>                           | 308.53                       | 184.24                          | 1.48                 | 0.60                 | 100.00        |
| <b>Glycerol (10%) E1</b>                           | 1.93                         | 1.57                            | 4.27                 | 0.81                 | 0.85          |
| <b>Glycerol (10%) E2</b>                           | 12.57                        | 9.43                            | 3.01                 | 0.75                 | 5.12          |
| <b>Glycerol (10%) E3</b>                           | 9.64                         | 6.97                            | 2.60                 | 0.72                 | 3.78          |
| <b>L-Histidine (0.075 M) E1</b>                    | 6.11                         | 4.63                            | 3.12                 | 0.76                 | 2.51          |
| <b>L-Histidine (0.075 M) E2</b>                    | 2.59                         | 1.80                            | 2.27                 | 0.69                 | 0.98          |
| <b>L-Histidine (0.075 M) E3</b>                    | 1.13                         | 0.88                            | 3.55                 | 0.78                 | 0.48          |
| <b>Chemical Name</b>                               | <b>C<sub>TP</sub> (mg/L)</b> | <b>C<sub>rGCSF</sub> (mg/L)</b> | <b>S<sub>1</sub></b> | <b>S<sub>2</sub></b> | <b>Yield%</b> |
| <b>Production Medium</b>                           | 273.13                       | 155.78                          | 1.33                 | 0.57                 | 100.00        |
| <b>Na<sub>2</sub>HPO<sub>4</sub> (0.02 M) E1</b>   | 2.07                         | 1.19                            | 1.36                 | 0.58                 | 0.76          |
| <b>Na<sub>2</sub>HPO<sub>4</sub> (0.02 M) E2</b>   | 0.46                         | 0.20                            | 0.79                 | 0.44                 | 0.13          |
| <b>Na<sub>2</sub>HPO<sub>4</sub> (0.02 M) E3</b>   | 0.12                         | 0.05                            | 0.71                 | 0.42                 | 0.03          |
| <b>MgCl<sub>2</sub>.6H<sub>2</sub>O (0.4 M) E1</b> | -                            | -                               | -                    | -                    | -             |
| <b>MgCl<sub>2</sub>.6H<sub>2</sub>O (0.4 M) E2</b> | 3.03                         | 2.37                            | 3.62                 | 0.78                 | 1.52          |
| <b>MgCl<sub>2</sub>.6H<sub>2</sub>O (0.4 M) E3</b> | 1.20                         | 0.94                            | 3.59                 | 0.78                 | 0.60          |
| <b>Chemical Name</b>                               | <b>C<sub>TP</sub> (mg/L)</b> | <b>C<sub>rGCSF</sub> (mg/L)</b> | <b>S<sub>1</sub></b> | <b>S<sub>2</sub></b> | <b>Yield%</b> |
| <b>Production Medium</b>                           | 376.20                       | 220.70                          | 1.42                 | 0.59                 | 100.00        |
| <b>NaCl (0.4 M) E1</b>                             | 25.23                        | 12.93                           | 1.05                 | 0.51                 | 5.86          |
| <b>NaCl (0.4 M) E2</b>                             | 11.70                        | 8.07                            | 2.23                 | 0.69                 | 3.66          |
| <b>NaCl (0.4 M) E3</b>                             | 17.89                        | 11.25                           | 1.70                 | 0.63                 | 5.10          |
| <b>NTA (0.4 M) E1</b>                              | -                            | -                               | -                    | -                    | -             |
| <b>NTA (0.4 M) E2</b>                              | 1.45                         | 1.01                            | 2.31                 | 0.70                 | 0.46          |
| <b>NTA (0.4 M) E3</b>                              | 1.83                         | 1.52                            | 4.93                 | 0.83                 | 0.69          |



**Table E. 3** SDS-PAGE results of glycerol and L-histidine with respect to elution time and concentration

| Chemical Name                                      | C <sub>TP</sub><br>(mg/L) | C <sub>rGCSF</sub><br>(mg/L) | S <sub>1</sub> | S <sub>2</sub> | Yield<br>% |
|--|---------------------------|------------------------------|----------------|----------------|------------|
| <b>Production Medium</b>                           | 419.21                    | 268.14                       | 1.77           | 0.64           | 100.00     |
| <b>10% Glycerol 30 sec. E1</b>                     | 4.71                      | 3.33                         | 2.42           | 0.71           | 1.24       |
| <b>10% Glycerol 30 sec. E2</b>                     | 4.09                      | 2.97                         | 2.67           | 0.73           | 1.11       |
| <b>10% Glycerol 10 min. E1</b>                     | 7.61                      | 5.85                         | 3.32           | 0.77           | 2.18       |
| <b>10% Glycerol 10 min. E2</b>                     | 9.54                      | 6.98                         | 2.72           | 0.73           | 2.60       |
| <b>10% Glycerol 30 min. E1</b>                     | 6.49                      | 5.13                         | 3.77           | 0.79           | 1.91       |
| <b>10% Glycerol 30 min. E2</b>                     | 7.66                      | 5.78                         | 3.07           | 0.75           | 2.16       |
| Chemical Name                                      | C <sub>TP</sub><br>(mg/L) | C <sub>rGCSF</sub><br>(mg/L) | S <sub>1</sub> | S <sub>2</sub> | Yield<br>% |
| <b>Production Medium</b>                           | 396.00                    | 197.31                       | 0.99           | 0.50           | 100.00     |
| <b>75 mM L-Histidine 30 sec. E1</b>                | 2.21                      | 1.02                         | 0.87           | 0.46           | 0.52       |
| <b>75 mM L-Histidine 30 sec. E2</b>                | 0.30                      | 0.09                         | 0.45           | 0.31           | 0.05       |
| <b>75 mM L-Histidine 10 min. E1</b>                | 1.55                      | 0.75                         | 0.93           | 0.48           | 0.38       |
| <b>75 mM L-Histidine 10 min. E2</b>                | 0.43                      | 0.15                         | 0.52           | 0.34           | 0.08       |
| <b>75 mM L-Histidine 30 min. E1</b>                | 2.63                      | 1.26                         | 0.93           | 0.48           | 0.64       |
| <b>75 mM L-Histidine 30 min. E2</b>                | 0.68                      | 0.30                         | 0.78           | 0.44           | 0.15       |
| Chemical Name                                      | C <sub>TP</sub><br>(mg/L) | C <sub>rGCSF</sub><br>(mg/L) | S <sub>1</sub> | S <sub>2</sub> | Yield<br>% |
| <b>Production Medium</b>                           | 386.70                    | 242.76                       | 1.69           | 0.63           | 100.00     |
| <b>10% Glycerol + 75 mM L-Histidine 30 sec. E1</b> | 4.61                      | 2.59                         | 1.29           | 0.56           | 1.07       |
| <b>10% Glycerol + 75 mM L-Histidine 30 sec. E2</b> | 1.16                      | 0.55                         | 0.91           | 0.48           | 0.23       |
| <b>10% Glycerol + 75 mM L-Histidine 10 min. E1</b> | 3.26                      | 2.11                         | 1.83           | 0.65           | 0.87       |
| <b>10% Glycerol + 75 mM L-Histidine 10 min. E2</b> | 3.83                      | 2.43                         | 1.74           | 0.63           | 1.00       |
| <b>10% Glycerol + 75 mM L-Histidine 30 min. E1</b> | 3.39                      | 2.04                         | 1.51           | 0.60           | 0.84       |
| <b>10% Glycerol + 75 mM L-Histidine 30 min. E2</b> | 2.64                      | 1.49                         | 1.29           | 0.56           | 0.61       |

**Table E. 3** SDS-PAGE results of glycerol and L-histidine with respect to elution time and concentration (*cont'd*)

| Chemical Name                     | C <sub>TP</sub> (mg/L) | C <sub>rGCSF</sub> (mg/L) | S <sub>1</sub> | S <sub>2</sub> | Yield% |
|-----------------------------------|------------------------|---------------------------|----------------|----------------|--------|
| <b>Production Medium</b>          | 470.33                 | 221.17                    | 0.89           | 0.47           | 100.00 |
| <b>15% Glycerol 30 sec. E1</b>    | 4.43                   | 2.63                      | 1.47           | 0.59           | 1.19   |
| <b>15% Glycerol 30 sec. E2</b>    | 9.69                   | 6.06                      | 1.67           | 0.63           | 2.74   |
| <b>15% Glycerol 10 min. E1</b>    | 4.39                   | 2.57                      | 1.41           | 0.59           | 1.16   |
| <b>15% Glycerol 10 min. E2</b>    | 6.46                   | 3.91                      | 1.54           | 0.61           | 1.77   |
| <b>15% Glycerol 30 min. E2</b>    | 3.92                   | 2.29                      | 1.40           | 0.58           | 1.03   |
| <b>15% Glycerol 30 min. E1</b>    | 4.43                   | 2.45                      | 1.24           | 0.55           | 1.11   |
| Chemical Name                     | C <sub>TP</sub> (mg/L) | C <sub>rGCSF</sub> (mg/L) | S <sub>1</sub> | S <sub>2</sub> | Yield% |
| <b>Production Medium</b>          | 396.01                 | 253.58                    | 1.78           | 0.64           | 100.00 |
| <b>50% L-Histidine 30 sec. E1</b> | 1.03                   | 0.79                      | 3.31           | 0.77           | 0.31   |
| <b>50% L-Histidine 30 sec. E2</b> | 0.02                   | 0.02                      | -              | 1.00           | 0.01   |
| <b>50% L-Histidine 10 min. E1</b> | 1.01                   | 0.81                      | 4.02           | 0.80           | 0.32   |
| <b>50% L-Histidine 10 min. E2</b> | 0.08                   | 0.08                      | -              | 1.00           | 0.03   |
| <b>50% L-Histidine 30 min. E1</b> | 0.28                   | 0.23                      | 4.48           | 0.82           | 0.09   |
| <b>50% L-Histidine 30 min. E2</b> | -                      | -                         | -              | -              | -      |

**Table E. 4** SDS-PAGE results for increasing elution number

| Chemical Name            | C <sub>TP</sub> (mg/L) | C <sub>rGCSF</sub> (mg/L) | S <sub>1</sub> | S <sub>2</sub> | Yield% |
|--------------------------|------------------------|---------------------------|----------------|----------------|--------|
| <b>Production Medium</b> | 676.31                 | 315.30                    | 0.87           | 0.47           | 100.00 |
| <b>10% Glycerol E1</b>   | 3.03                   | 1.68                      | 1.24           | 0.55           | 0.53   |
| <b>10% Glycerol E2</b>   | 3.52                   | 1.73                      | 0.97           | 0.49           | 0.55   |
| <b>10% Glycerol E3</b>   | 4.10                   | 2.29                      | 1.26           | 0.56           | 0.73   |
| <b>10% Glycerol E4</b>   | 2.35                   | 1.21                      | 1.06           | 0.52           | 0.38   |
| <b>10% Glycerol E5</b>   | 3.46                   | 1.90                      | 1.22           | 0.55           | 0.60   |
| <b>10% Glycerol E6</b>   | 3.74                   | 1.89                      | 1.02           | 0.51           | 0.60   |
| <b>10% Glycerol E7</b>   | 2.93                   | 1.59                      | 1.19           | 0.54           | 0.50   |
| <b>10% Glycerol E8</b>   | 2.71                   | 1.75                      | 1.83           | 0.65           | 0.56   |

## F. SEM MICROGRAPHS OF ZIF-8 SYNTHESSES AND MODIFICATIONS

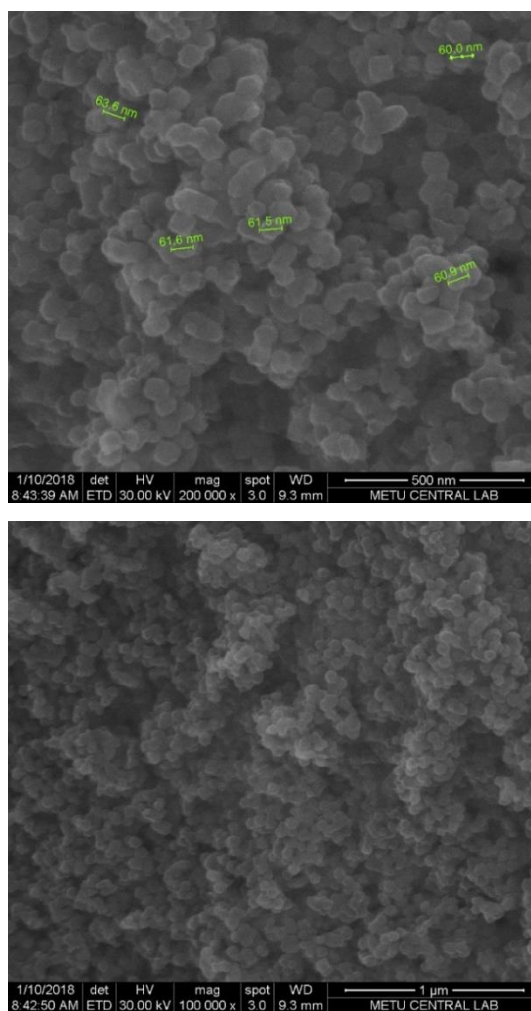


**Figure F. 1** SEM micrographs for NH<sub>2</sub>-ZIF-8

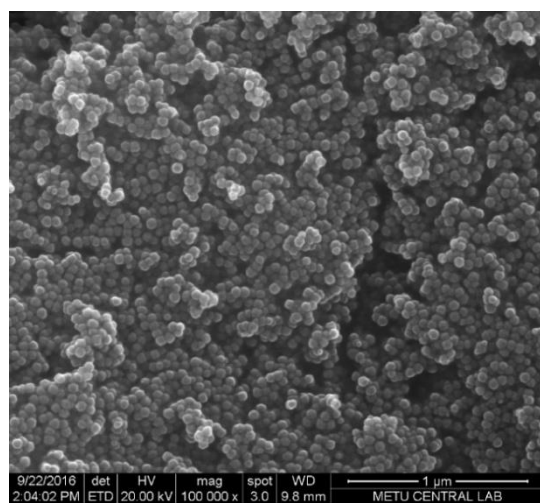
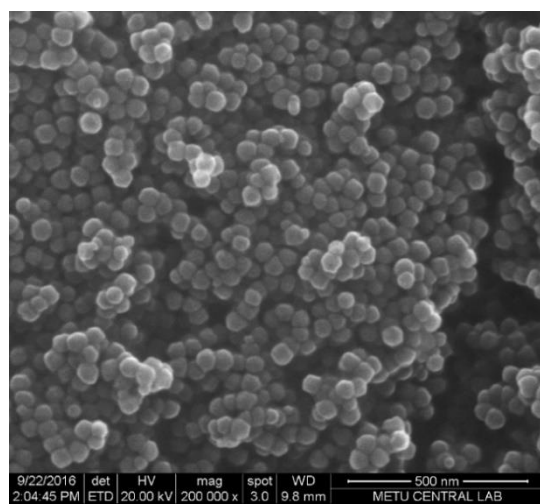
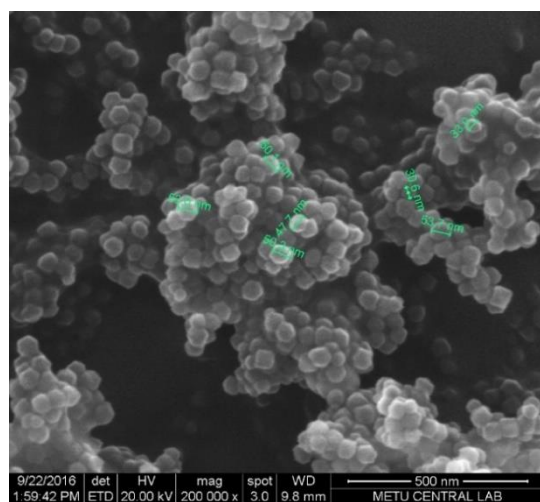


**Figure F. 2** SEM micrographs of ZIF-8

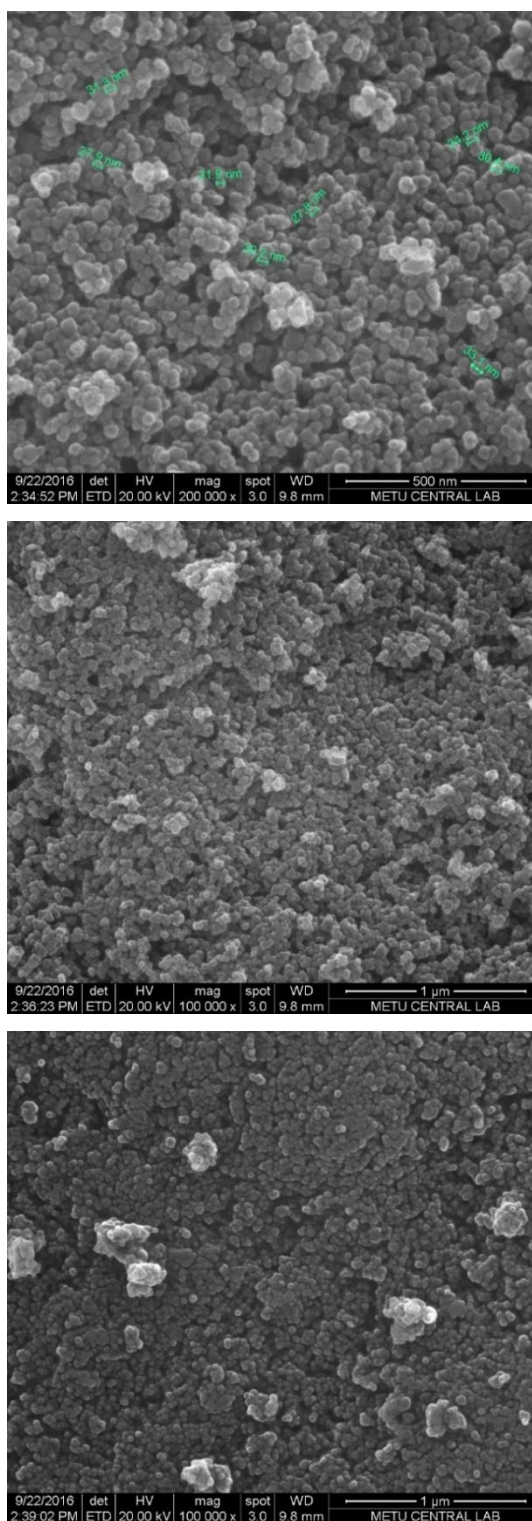


**Figure F. 3** SEM micrographs of Ni/ZIF-8-5

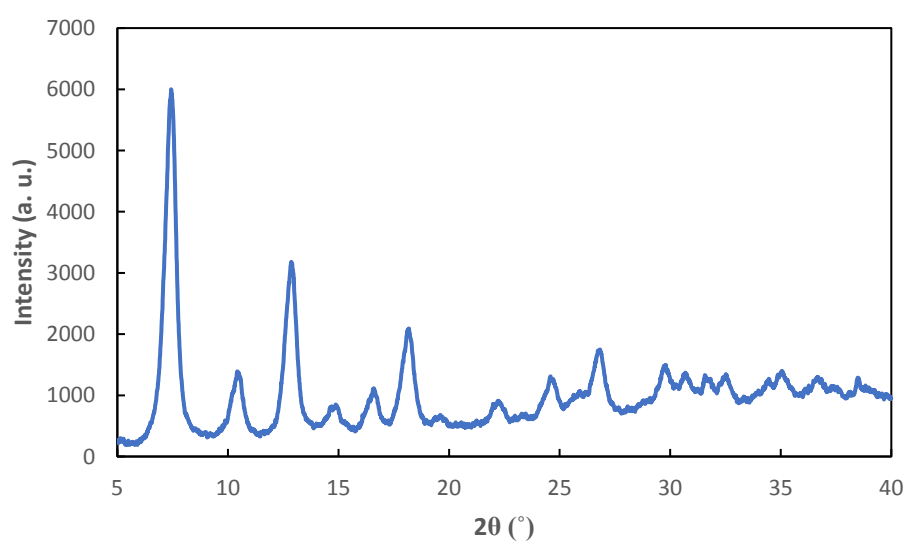


**Figure F. 4** XRD pattern of Ni/ZIF-8-5

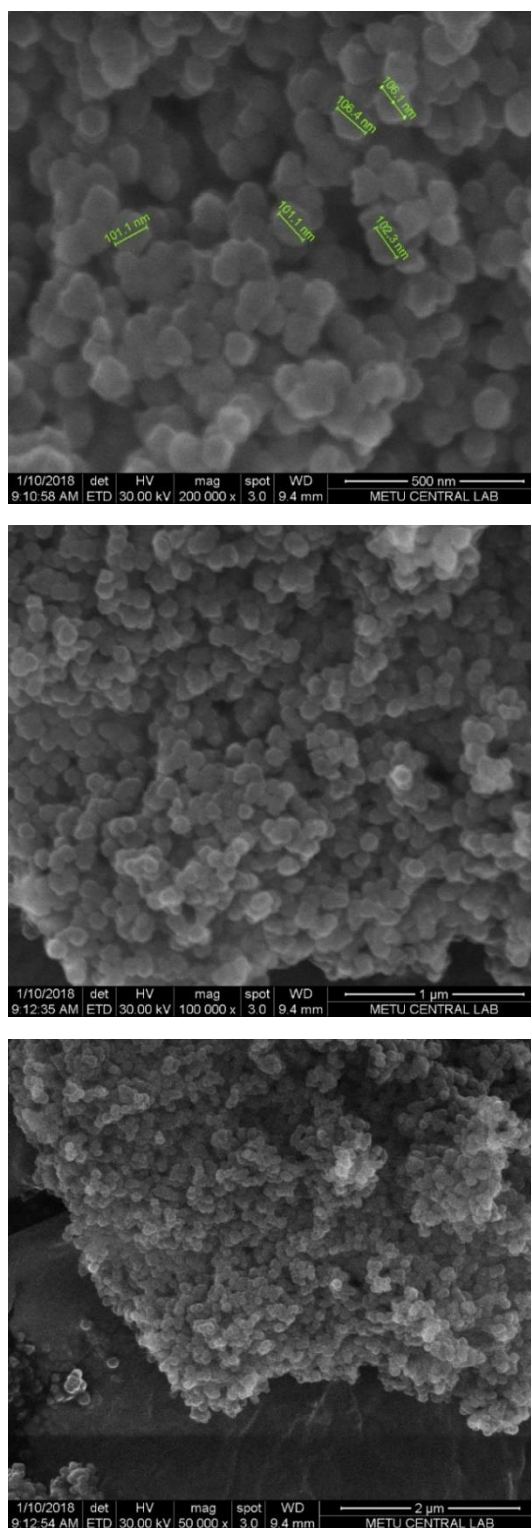


**Figure F. 5** SEM micrographs for 30 min. later NaOH added ZIF-8

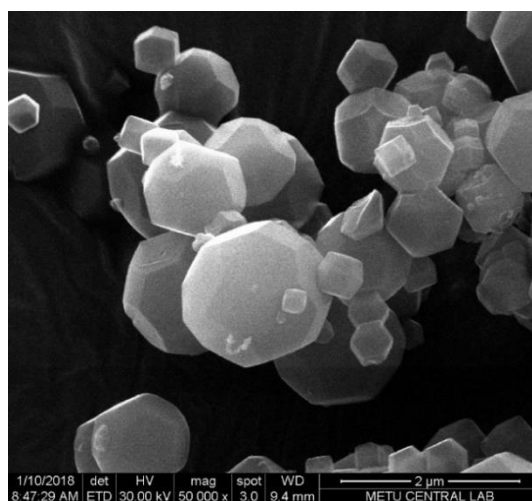
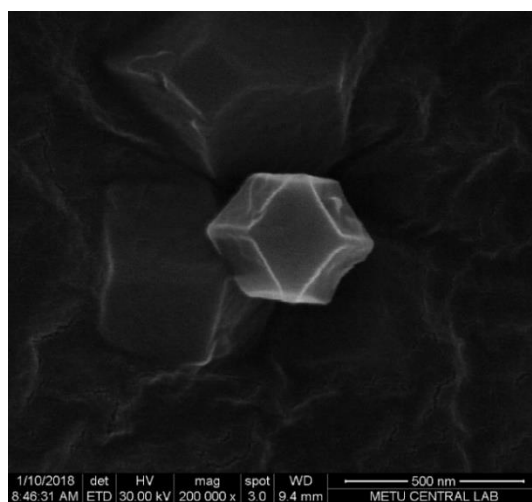
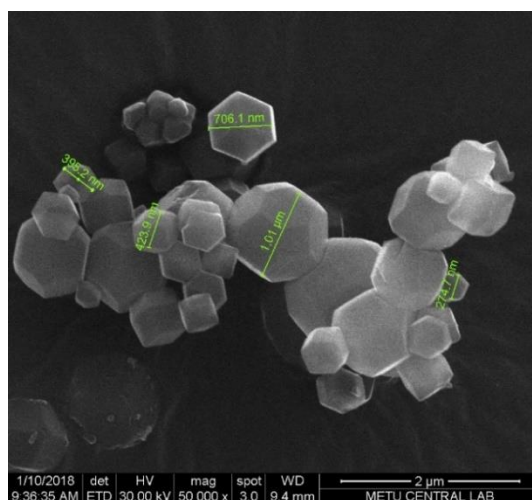


**Figure F. 6** SEM micrographs for 1-MI-ZIF-8



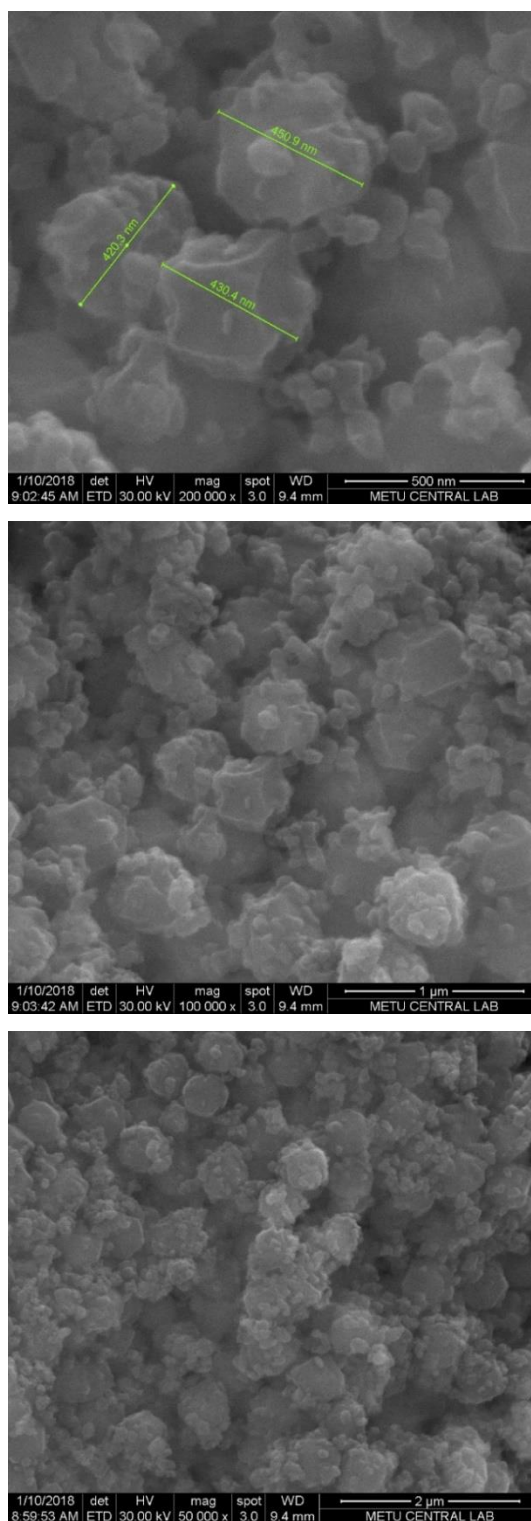


**Figure F. 7** SEM micrographs for 1-hour later NaOH added 1-MI-ZIF-8



## G. SEPARATION AND PURIFICATION CALCULATIONS

$$\begin{aligned} & \text{Amount of rGCSF Concentration (mg/L)} \\ &= \frac{\text{Reactor Supernatant OD} * \text{Amount of rGCSF in Standard} * \text{Dilution Factor}}{\text{Standard OD}} \end{aligned}$$

$$\begin{aligned} & \text{Amount of rGCSF (Eluent) added on ZIF (mg)} \\ &= \text{Amount of rGCSF Concentration in Reactor Supernatant} \\ & \quad * \text{Volume of Added Reactor Supernatant (Eluent) on ZIF} \end{aligned}$$

### Percentage of Each Step wrt. Reactor Supernatant

$$\begin{aligned} & \text{Percentage of Remained rGCSF in Incubation Liquid} \\ &= \frac{\text{Amount of rGCSF in Incubation Liquid}}{\text{Amount of rGCSF added (Eluent) on ZIF}} * 100 \end{aligned}$$

### Percentage of Each Step wrt. Separated Protein

$$\begin{aligned} & \text{Percentage of Separated rGCSF in Washing 1} \\ &= \frac{\text{Amount of Separated rGCSF in Washing 1}}{\text{Amount of Separated rGCSF from Incubation Liquid}} * 100 \end{aligned}$$

### Conservation of Mass

$$\begin{aligned} & \text{Amount of rGCSF in 1000 } \mu\text{L (Added or Eluent) Reactor Supernatant on ZIF} \\ &= \text{Amount of rGCSF in Incubation Liquid} \\ & \quad + \sum \text{Washing Fractions} + \sum \text{Eluates} + \text{Remained rGCSF on ZIF} \end{aligned}$$

$$\begin{aligned} & \text{Percentage of Remained rGCSF on ZIF} \\ &= \frac{\text{Remained rGCSF on ZIF}}{\text{Amount of rGCSF added on ZIF}} * 100 \end{aligned}$$



## H. FTIR COMPARISON OF ZIF-8 AND NH<sub>2</sub>-ZIF-8

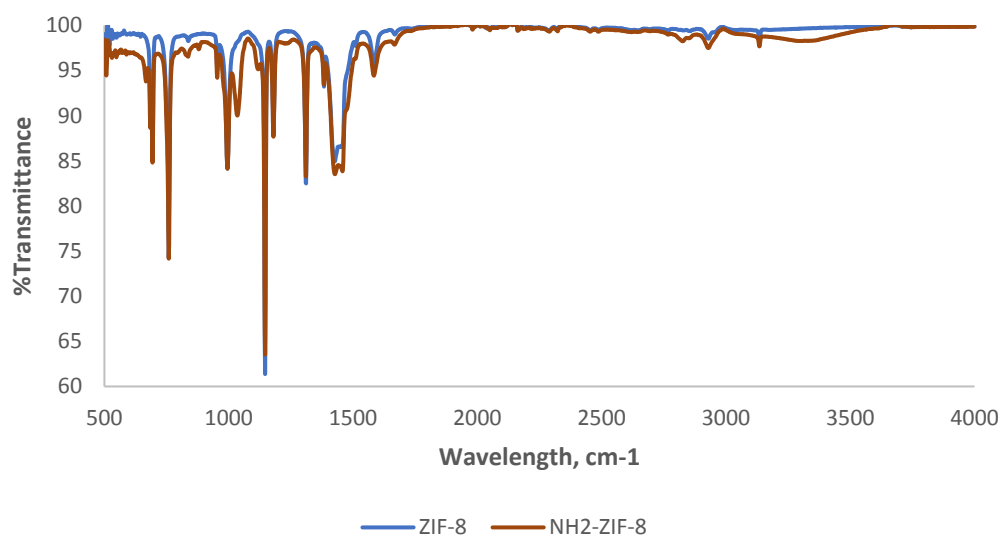


**Figure H. 1** FTIR comparison of ZIF-8 and NH<sub>2</sub>-ZIF-8

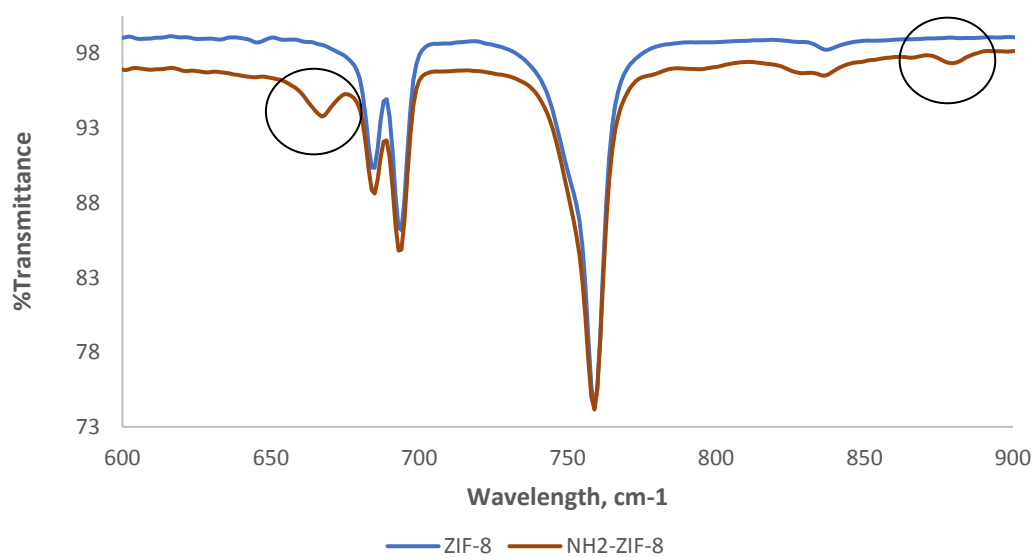


**Figure H. 2** FTIR comparison between 600-900 cm<sup>-1</sup> of ZIF-8 and NH<sub>2</sub>-ZIF-8

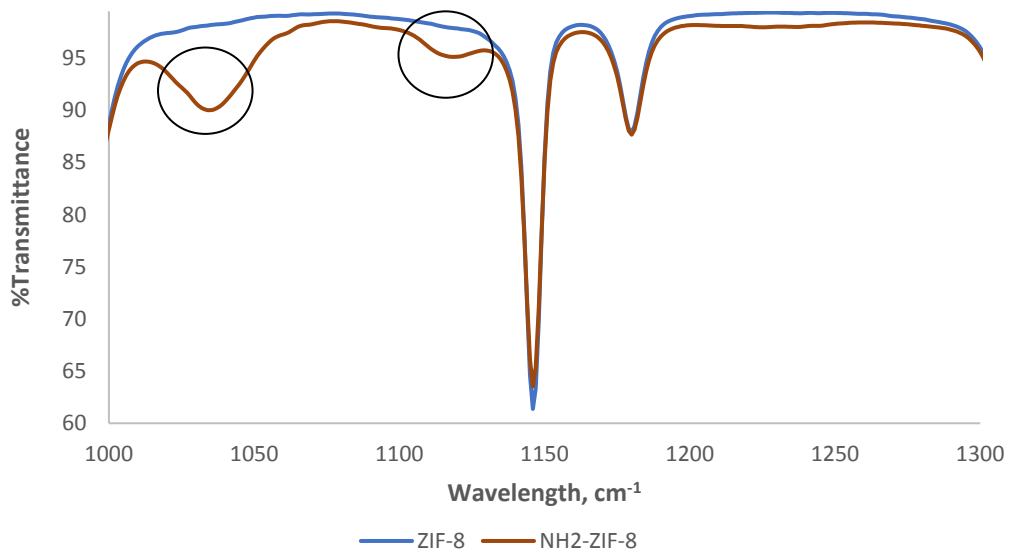


**Figure H. 3** FTIR comparison between 1000-1300  $\text{cm}^{-1}$  of ZIF-8 and  $\text{NH}_2$ -ZIF-8

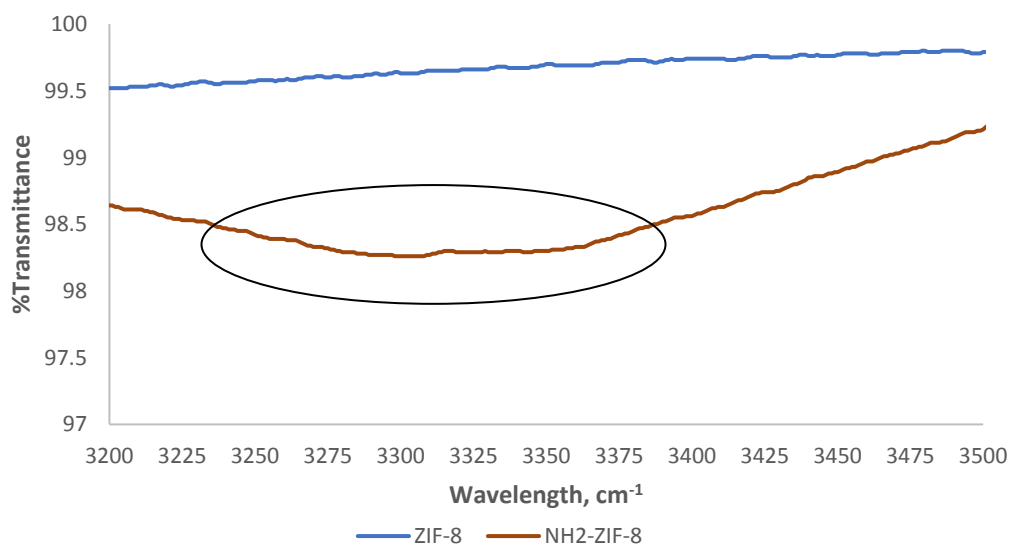


**Figure H. 4** FTIR comparison between 3200-3500  $\text{cm}^{-1}$  of ZIF-8 and  $\text{NH}_2$ -ZIF-8